UNIVERSITY OF SOUTHAMPTON

SCHOOL OF ENGINEERING SCIENCES

Bioengineering Sciences Research Group

SIMULATION OF THE PASSIVE AND ACTIVE MOTIONS OF THE REPLACED KNEE – EFFECT OF MALALIGNMENT AND LIGAMENT STRAINS

Neil Curtis

Thesis for the degree of

Doctor of Philosophy

May 2004

UNIVERSITY OF SOUTHAMPTON

ABSTRACT

FACULTY OF ENGINEERING AND APPLIED SCIENCES
BIOENGINEERING SCIENCES RESEARCH GROUP

Doctor of Philosophy

SIMULATION OF THE PASSIVE AND ACTIVE MOTIONS OF THE REPLACED KNEE – EFFECT OF MALALIGNMENT AND LIGAMENT STRAINS

By Neil Curtis

After total knee replacement (TKR) there are many factors that can affect the survivorship of the knee; these include knee replacement design, the component positioning and the soft tissue structures around the joint. Poor surgical technique can cause ligament imbalance or component malalignment, which could lead to instability and early implant failure. Intra-operative stability is deemed important towards the long-term success of the knee replacement, and can be assessed using simple passive stability tests. Although it is thought that passive stability is related to active stability, direct comparisons between the two have not been reported in the literature. The purpose of the present research was to assess the effects of ligament imbalance and component malalignment on both the passive and active stability of various total knee designs.

A fully mechanical test rig was developed to simulate a series of passive stability tests; the rig allowed the strains of the primary knee ligaments to be altered as well as coronal plane alignment. In addition, the rig was used to conduct contact pressure measurements using Tekscan instrumentation. It was shown that implant design played a significant role in the passive stability of the replaced knee, and that each design was affected differently by altered ligament strains and component alignment. Assessment of stability in a certain plane was able to highlight specific surgical inaccuracies; for example, ligament imbalance was best detected by varus-valgus stability testing.

In phase two of the research, computational finite element (FE) models were created for validation against the experimental test results. Using explicit FE analysis the experimental passive stability testing was simulated. There was a good agreement between the FE simulations and the experimental results in terms of displacements, rotations and contact pressures.

The final stage of the research focused on simulating normal gait using the FE models. After recording the kinematics and contact pressures for the idealised knees, gait was assessed with altered ligament strains and component malalignment. Results from the present study showed that imbalanced ligaments did not significantly affect the gait kinematics or contact pressures; however the force distribution across the knee was altered. It has been reported that post-operative malalignment may be due to imbalanced ligament strains; this correlates with the present research, which showed that immediate post-operative malalignment could occur due to an uneven force distribution caused by imbalanced ligaments. Slight malalignment did not however significantly alter the kinematics during gait, but did affect the contact pressure distribution. The present research also correlates with studies that have suggested that 10° of malalignment could cause catastrophic failure of TKRs. Each knee type reacted differently to excessive malalignment, however for all knees contact pressures were significantly altered. The results highlighted the fact that varus malalignment should be avoided in particular.

List of Contents

List of Figures

List of Tables

List of Abbreviations

A-P - Anterior-Posterior
ACL - Anterior Cruciate Ligament
ANOVA - Analysis of Variance

CAD - Computer Aided Design
CH line - Condylar Hip line
CP angle - Condylar Plateau angle

FE - Finite Element
FEA - Finite Element Analysis
FEM - Finite Element Method

HCC - High Conformity Curve-on-Curve
HFF - High Conformity Flat-on-Flat
HKA angle - Hip Knee Ankle angle

I-E - Internal-External
IGES - Initial Graphics Exchange Specification

L - Lateral
LBA - Load Bearing Axis
LCL - Lateral Collateral Ligament
LPDT(s) - Linear Potentiometric Displacement Transducer(s)

M - Medial
M-L - Medial-Lateral
MCC - Medium Conformity Curve-on-Curve
MCL - Medial Collateral Ligament

PA line - Plateau Ankle line
PC - Posterior Cruciate
PC-RF - PC-Retaining Fixed-Bearing Knee
PC-RR - PC-Retaining Rotating-Bearing Knee
PC-SF - PC-Substituting Fixed-Bearing Knee
PC-SR - PC-Substituting Rotating-Bearing knee
PCL - Posterior Cruciate Ligament
PG(s) - Proteoglycan(s)
PID - Proportional Integral Differential

RSA - Radiostereometric Analysis

S.D. - Standard Deviation

TKA(s) - Total Knee Arthroplasty(ies)
TKR(s) - Total Knee Replacement(s)

UHMWPE – Ultra-High Molecular Weight Polyethylene
USL - Ultra Super Low

V-V - Varus-Valgus

Units:

KN - Kilo-Newton
mm - Millimetre(s)
mm^2 - Millimetre(s) squared
MPa – Mega Pascal(s)
ms - Millisecond(s)
N – Newton(s)
Nm - Newton Metre
PSI - Pounds per Square Inch
secs - Seconds

Introduction

The knee is a biomechanically complex joint [1], [2], [3], [4] that can be subjected to loads of up to six times body weight during normal daily activities; thus over time it is prone to injuries and degeneration through conditions such as rheumatism and osteoarthritis. At a certain level of degeneration extreme pain and reduced motion will occur in the joint, resulting in the need for the articular surfaces to be replaced by prosthetic components, in a process known as total knee arthroplasty (TKA). Ideally after TKA the knee joint will be subjected to the same forces as in the normal knee, however sometimes the loading patterns on the replaced knee are altered, resulting in eccentric loading that could cause possible complications. The type of prosthesis, component positioning and the balancing of soft tissue structures around the knee are all factors that contribute to the performance and survivorship of the implanted components.

Many studies have been performed to evaluate the performance of the knee after TKA, including the assessment of implanted knees *in vivo* [12], [13], [14], *in vitro* [15], [16], [17], [18], and via computer simulations [19], [20], [21]. Fully mechanical simulations of the replaced knee have been developed for wear studies using complex knee wear simulators [22], [23], in which the soft tissue structures are represented by the use of springs, and the prosthesis is put through a test pattern that applies loads and/ or forces similar to the normal gait cycle. Rigs have been developed to assess the stability of different knee replacements on cadaveric specimens [24] and also non-biological rigs are available to assess contact pressures [25]. However, a fully mechanical model of a replaced knee that will allow the assessment of component positioning and ligament balancing on the passive stability of the joint is not currently available. This study will develop such a rig and record the changes in knee stability caused by altering ligament strains and component position. A surgeon can assess the stability of the knee joint during a total knee procedure through a series of passive stability tests; these tests will be adopted in the present study and reproduced on a mechanical knee model. Active motion is more complex, and would be to difficult to reproduce in the proposed experimental setup; however computer simulations of active stability will be modelled and initially validated against the experimental results, using both the motion and pressure data.

Chapter 1 Anatomy and Mechanics of the Knee

1.1 General Knee Anatomy

The knee joint is a complex structure consisting of bone and soft tissue that form the largest, and one of the most biomechanically complex joints in the body. External observation of the knee gives the impression that it is a simple hinge joint, especially when compared to a joint such as the hip, which can swing in many directions. However, instead of just flexion and extension, a mixture of gliding, rolling and rotational motions occur [1], [2]. The knee is known as a tri-articular synovial joint, with two articulations occurring between the medial and lateral femoral/ tibial condyles, and one articulation due to tracking of the patella on the patellofemoral groove (Figure 1.1).

1.1.1 Bones of the Knee Joint

The knee joint involves the interaction of three bones, the distal end of the femur, the proximal tibia and the patella.

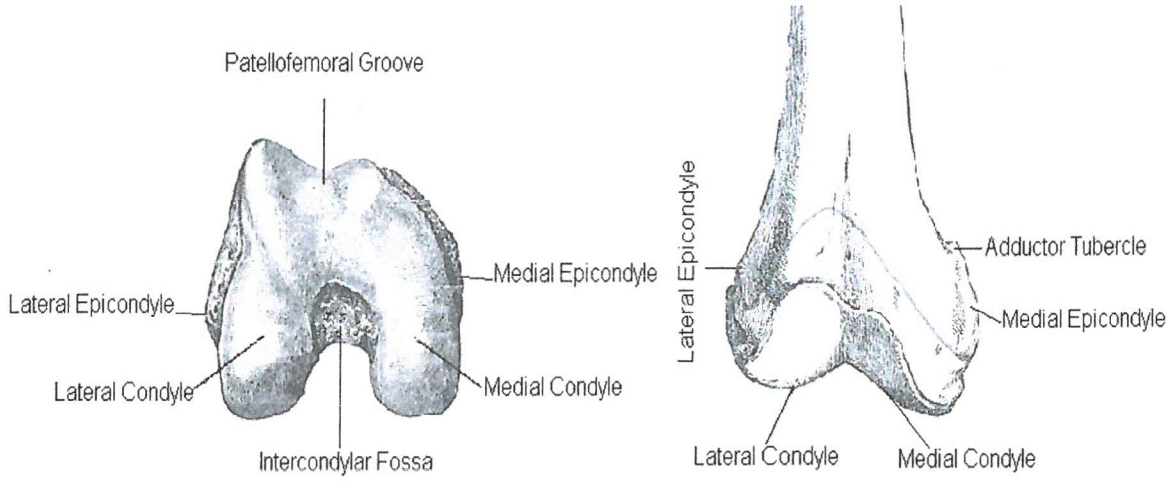

Figure 1.1 Distal femur (Modified from Gray's Anatomy [142])

The fibula (Figure 1.2) is an important structure for the integrity of the knee joint, since it acts as a location for muscle/ ligament attachment (also see section 1.3.3). The fibula does not actually form part of the articulating knee joint however, since it has no interaction with the bearing surfaces.

On the proximal surface of the tibia there are a number of different areas that assist with the motions of the joint and with the attachment of important soft tissue structures. The two main areas are the tibial plateaux, on which the femoral condyles articulate. Between the plateaux is a roughened region called the intercondylar area, which provides a surface for soft tissue attachment, as well as housing the intercondylar eminence, which adds greater stability to the joint by resisting medial and lateral gliding movements (Figure 1.3).

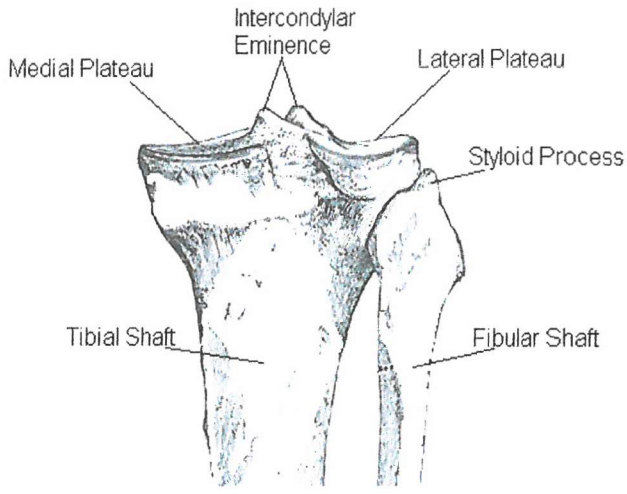

Figure 1.2 Posterior view of the proximal tibia (Modified from Gray's Anatomy [142])

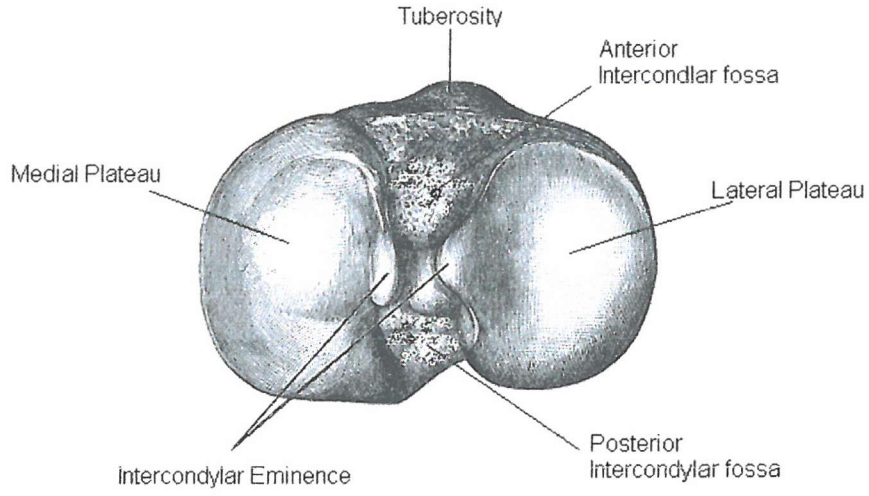

Figure 1.3 Bearing surface of the tibia (Modified from Gray's Anatomy [142])

All bearing surfaces of the knee joint are completely covered in articular cartilage; its rubbery texture and low friction properties offer protection and smooth motions between bones. As well as the articular cartilage there are menisci, which are fibro-cartilaginous structures that are situated between the femoral and tibial bearing surfaces of the knee

joint. The menisci sit over the medial and lateral tibial plateaux, and act as shock absorbers, reducing the impact forces taken by the bony surfaces. The medial side of the medial meniscus is firmly attached to the tibia via the posterior margins of the medial collateral ligament (MCL); its anterior horn is attached to the intercondylar area of the tibia in front of the anterior cruciate ligament (ACL), while its broader posterior horn is similarly attached on the intercondylar area in front of the posterior cruciate ligament (PCL). The lateral meniscus is attached to the intercondylar area of the tibia immediately in front of and behind the intercondylar eminence. There is no fusion with the lateral collateral ligament (LCL).

1.1.2 Alignment of the Knee Joint

The alignment of the knee joint is important as malalignment could cause excessive loading to be applied to one area of the knee joint, and also alter the performance of the soft tissue structures. The distribution of load across the knee is of interest particularly when operations are performed that modify the alignment in the coronal plane, for example such corrections may be required when there are extensive valgus or varus deformities within the knee. The significance of valgus and varus deformities in the coronal plane has been recognised as an important factor in the development of osteoarthritis of the medial or lateral compartments of the knee [3]; this is more prevalent in patients over 50 years [26]. If the load is applied eccentrically to one compartment in the knee this will lead to articular cartilage degeneration and eventually bone will be uncovered within the load bearing regions of the knee, causing pain and restricted movement. The natural correct alignment of the knee (from hip to ankle) is shown in Figure 1.4. The alignment can be referred to in terms of the mechanical axis, or load bearing axis (LBA) of the knee, and can be subdivided into the axis of the femur and tibia. The mechanical axis can be seen as a straight line that starts from the centre of the femoral head and passes through the centre of the ankle at the distal end of the tibia, and is on average 3° off vertical. The two sub-axes, the long axis of the femur and the long axis of the tibia are represented by a line from the centre of the femoral head to the centre of the intercondylar notch of the knee, and a line originating from the centre of the intercondylar notch and passing down through the centre of the ankle respectively (Figure 1.4).

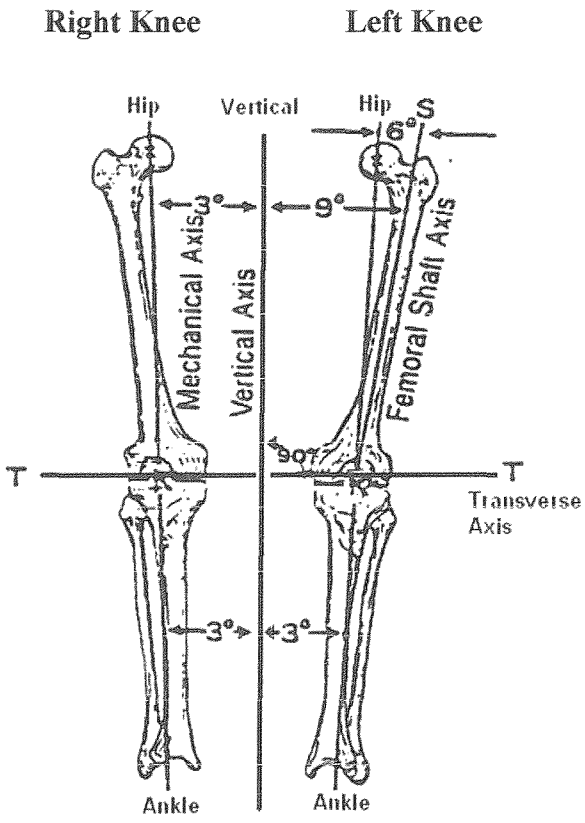

Figure 1.4 Alignment of the anatomic knee.

The mechanical axis in healthy knees is closely aligned to the mechanical long axis of each bone, such that the hip, knee and ankle approach co-linearity in extension. The angle formed by the cross over of the mechanical axis of the femur and tibia can be noted as the hip-knee-ankle angle (HKA angle), see Figure 1.5(a), with a positive angle representing valgus alignment and a negative angle representing varus alignment. A HKA angle of zero represents co-linearity. A line across the condyles of the distal femur (condylar-hip, CH line) and another line across the medial and lateral plateaux (plateau-ankle, PA line) of the proximal tibia in the coronal plane can be used to work out the HKA angle of the lower limb (Figure 1.5(b)).

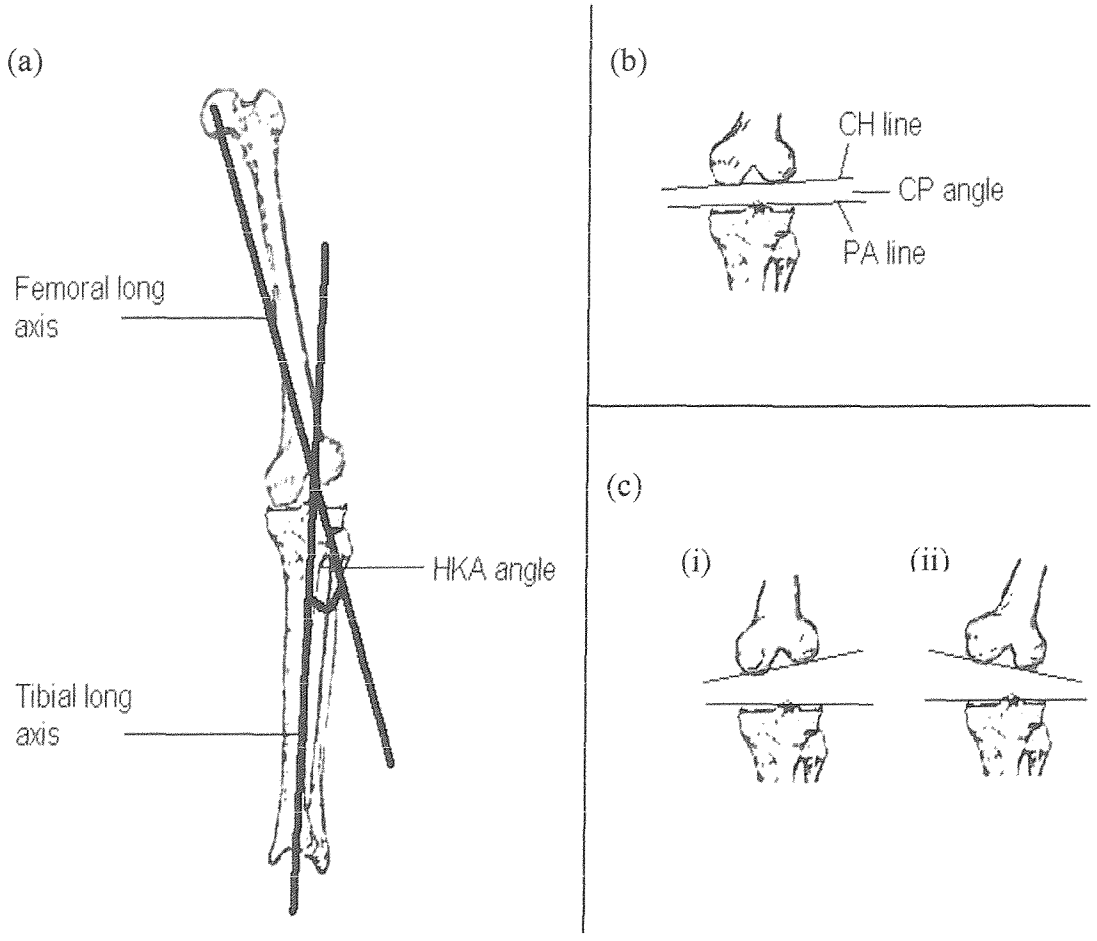

Figure 1.5 (a) An exaggerated HKA angle of the lower limb, (b) the CH & PA lines and the CP angle of the knee and (c) the (i) medially and (ii) laterally converging CH and PA lines.

The CH and PA lines are represented as deviations from 90°, with a negative (< 90°) angle representing varus and a positive (>90°) angle representing valgus. The angle between the knee joint surfaces is known as the condylar-plateau angle (CP); if the CH and PA lines converge medially a negative angle is formed, and if they converge laterally a positive angle is formed (Figure 1.5(c)). Geometrically the four angles that define coronal plane limb alignment are related by the expression HKA= CH + PA + CP. In healthy adults the average CH angle is 3-4° valgus, while the average PA angle is 3-4° varus. The mean CP angle is –1.7°, which is almost parallel and accounts for an HKA angle of around 0°. However variations do exist in healthy knees and even more so in arthritic knees.

Two other axes that should be mentioned are the transverse axis, and the shaft axis of the femur. The transverse axis is a horizontal axis, which is positioned at right angles to the vertical axis. When the thigh and leg are positioned in such a way, as shown in Figure 1.4, the femoral condyles and tibial plateaux line up straight across the transverse axis. The shaft axis can be seen as a line that travels down the shaft of the femur, normally being 6° off the mechanical axis of the knee and 9° off the vertical.

1.2 The Ligaments

During TKA, soft tissue balancing is deemed to be crucial for the long-term survivorship of the implant. Thus, in producing a mechanical simulation of the motions of a replaced knee consideration of the ligaments are essential. The primary ligaments of the knee contribute considerably to the integrity and movement of the joint, and any alteration in their position or strain will affect the joint's performance.

Ligaments are cord-like structures made up of dense, highly orientated connective tissue. The majority of ligaments are made from pure type 1 collagen (see over page for a brief description), with fibres arranged along the length of the ligament in the direction of direct load. In the unloaded state a 'crimped' effect can be seen within the ligament (Figure 1.6); upon loading, in what is referred to as the 'toe-in' region, the fibre orientation straightens out. A relatively linear region follows this, and then at their limit the fibres begin to tear apart until final failure. A typical load-extension curve of a ligament takes on the shape of a 'J' (see Figure 1.6). From Figure 1.6 the crimped effect can be seen at point A, with the ligament fibres straightening out at point B. The fibres begin to tear at point C up to final failure at point D. At the end of the toe-in region as the fibres straighten out (beginning of point B) the strain value has been reported to be between 1.5 and 4% [27], [28], with the strain reaching about 15 to 17% upon final failure (point D) [11], [5].

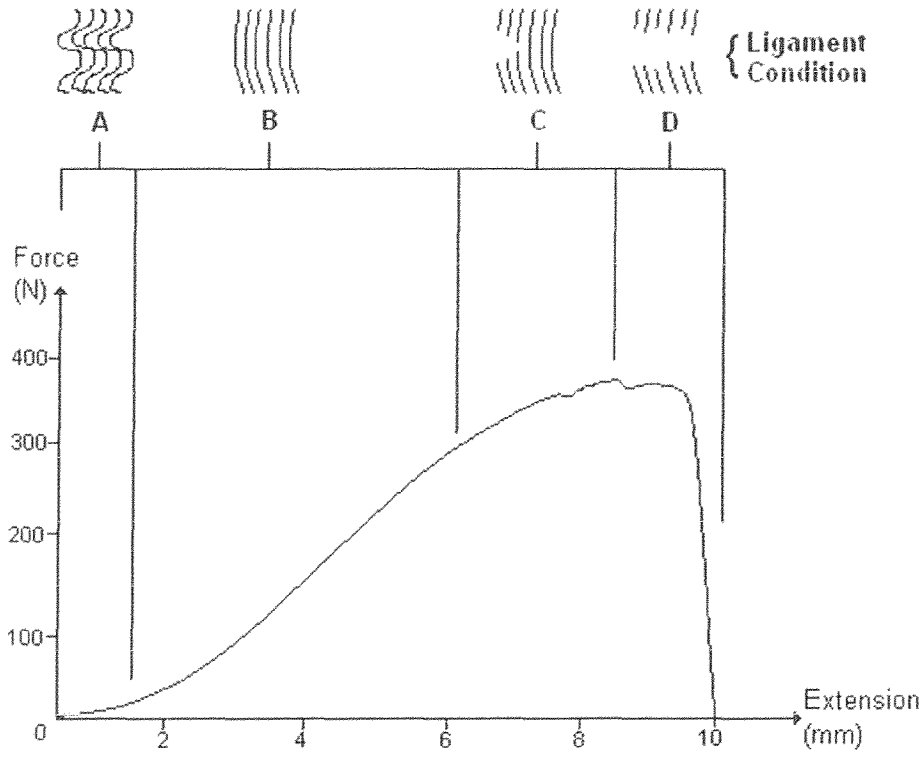

Figure 1.6 A typical force/ extension curve for a ligament.

It should be noted however, that even though the direction of direct load is normally applied down the length of the ligament, ligaments are sometimes loaded in other directions. Ligaments are subjected to shear loading and compressive forces over bony structures, allowing them to transfer load to the bone surface far from the insertion sites.

1.2.1 Composition of Ligaments

In general, the cellular material of ligaments occupies about 20% of the total tissue volume, while the extracellular matrix accounts for the remaining 80%. Of this matrix, water contributes around 70%, with a mixture of solids, collagen, ground substance and elastin making up the remaining 30% of the matrix. Type 1 collagen contributes roughly 70%-80% of the dry weight of normal ligaments.

Collagen: Collagen is a triple helix formed by three polypeptide chains (α chains), each coiled in a left-handed helix with approximately 100 amino acids, two of which are identical (called α-1 chains), with one that differs slightly (the α-2 chain). The three α chains are combined in a right-handed triple helix, which gives the collagen molecule a

rod-like shape. The length of the molecule is about 280nm, and its diameter is about 1.5nm [29], [30]. The key to the ligament's tensile strength and resistance to chemical or enzymatic breakdown is the ability of the collagen molecule to form covalent intramolecular (aldol) and intermolecular (Schiff base) cross-links [31], [32], [33].

Elastin: The proportion of elastin within the ligament determines its mechanical properties. The protein elastin is scarcely present in extremity ligaments (e.g. knee joint ligaments), but in elastic ligaments such as the ligamentum flavum (ligaments that connect the laminae of adjacent vertebrae) the proportion of elastic fibres is substantial.

Ground Substance: In ligaments the ground substance consists of proteoglycans (PG's) (up to about 20% of the solids) along with structural glycoproteins, plasma proteins and a variety of small molecules. The PG units are macromolecules composed of various sulphated polysaccharide chains (glycosaminoglycans) bonded to a core protein, which bind to a long hyaluronic acid chain to form an extremely high-molecular weight PG aggregate, similar to that found in the ground substance of articular cartilage. The ground substance of ligaments make up only a small percentage of the dry tissue weight, but nevertheless it is quite important because of its association with water, which represents 60%-80% of the total wet weight (the water content in the human ACL varies between 65%-70% [34]). Dense connective tissue contains a very small amount of ground substance; loose connective tissues contain a lot.

The PG aggregates bind most of the extracellular water of the ligament, making the matrix a highly structural gel-like material rather than an amorphous solution. Furthermore, by acting as a cement-like substance between the collagen microfibrils they may help in stabilising the collagenous skeleton of ligaments and contribute to the overall strength of these composite structures. The water and PGs provide lubrication and spacing crucial to the gliding function at intercept points where fibres cross in the tissue matrix. The movement of water in the system is inhibited by its entrapment between large PG molecules. These molecules are highly negatively charged and possess a large number of hydroxyl groups, which attract water through hydrogen bonding. A more extensive review of these components is available in Basic Orthopaedic Biomechanics [35].

1.2.2 Function of Ligaments

Today it is known that ligaments play a very important role in the stability of the knee joint, acting as restraints against excessive movements which could cause damage to the joint, including disruption of other soft tissue and dislocation. In the past, it was thought that the ligaments did not play a significant role as far as constraining properties were concerned, and it was claimed the medial-lateral motions were prevented by "definite bone contact" [36]. As more complex studies have been performed, the stabilising role of specific ligaments has been highlighted. A study by Piziali *et al.* [37] showed that medial tibial displacement was restricted primarily by the LCL and the ACL, whereas lateral tibial displacements were obstructed primarily by the MCL and PCL. The major function of the MCL is as a primary valgus restraint [38], [39], [40] with the LCL providing varus restraint [39], [41]. The MCL is relaxed during varus rotations and the LCL relaxed during valgus rotations; the effects on varus-valgus rotations are maximised when the MCL and LCL are tight (in extension). Harfe *et al.* [42] applied a 3° valgus rotation to the tibia and noted that it significantly increased the strain in the MCL for flexion angles of 15°-120°, and a 3° varus rotation significantly increased the strain in the LCL for flexion angles of 15°-120°.

Another factor affecting how the different ligaments work is the contribution of the surrounding ligaments. For example Wroble *et al.* [43] hypothesized that the LCL is a secondary restraint to both internal rotation and external rotation, however the amount of restraint is dependent on the effectiveness of other knee structures. There is considerable debate in the literature concerning the MCL response to internal and external tibial axial rotation. Depending upon the investigation, the MCL has been shown to resist external rotation, internal rotation, both rotations or neither rotation [44], [45]. However, the majority of studies note the MCL as a restraint to external rotation only [42]. Harfe *et al.* [42] also noted that a 10° external tibial axial rotation significantly increased the strain within the MCL for flexion angles of 30°-120°, whereas the LCL did not show a consistent strain response to internal or external rotation.

The anterior and posterior cruciate ligaments play a dominant role in the restriction of anterior and posterior tibial motions respectively [37]. Noyes *et al.* [46] noted that for a 5mm anterior tibial displacement with the knee flexed at 30° the ACL carried 87% of the

shear load, and for a 5mm posterior tibial displacement the PCL carried about 94% of the shear load. Bratigan and Voshell [36] noted an increased A-P gliding of the tibia of 1mm-2mm when the cruciates were cut, and an increase in anterior laxity in excess of 200% has been reported after ACL removal [37], [44]. Table 1.1 shows the primary and secondary functions of the ACL, PCL, MCL and LCL [10]. In order for a ligament to be considered a primary restraint to a particular load direction, it must show consistent behaviour across all the specimens tested.

Ligament	ACL	PCL	MCL	LCL
Primary Restraint to	Anterior drawer	Posterior drawer	Valgus bending	Varus bending
Secondary Restraint to	Internal rotation Varus bending	Internal rotation Valgus bending	Internal rotation Anterior drawer	External rotation Posterior drawer

Table 1.1 The functions of the primary ligaments of the knee joint [10].

As well as restraining properties, ligaments also possess sensory properties that allow them to act as the first link in the 'kinetic chain' [47]. Impulses arising in ligaments are transmitted through the central nervous system back to the effector muscles, allowing for the maintenance of normal, smooth, coordinated motion of the joint. Thus when ligaments are overstretched they produce abnormally high impulses, resulting in the contraction of allied muscle groups, which helps prevent further injury and subluxation of the knee. Tests carried out by Attfield *et al.* [47] lead them to state that soft tissue imbalance after a total knee replacement (TKR) would have a negligible effect on the position of the resultant force vector through the knee during dynamic activity but could be perceived proprioceptively as a varus or valgus deviation of the bony alignment. This could then produce a reflex antagonistic action from the muscles, resulting in a large corrective load being applied to the replaced knee. Such loading may affect the direction of dynamic force vector through the knee, and move it medially or laterally so that it is applied solely through one condyle.

The discussion in this thesis has been limited to the so-called primary ligaments of the knee: There are of course other ligaments and soft tissue structures around the knee, and one other important structure is the joint capsule, which is composed of fibrous connective tissue on the outside and the synovial membrane on the inside. The joint capsule is firmly attached around the femur just proximal to the articulating surfaces, and

to the tibia immediately distal to the articulating surfaces. The outer fibrous tissue assits in holding the bones together, and the synovial lining produces the synovial fluid that lubricates and nourishes the articulating surfaces. The knee possesses other soft tissue structures, such as bursae, which are not actually involved in the movement. Bursae are sac like structures lined with synovial membrane and filled with joint fluid; they can be found within the joint or they can be completely separate to it. The bursae act as cushions, and are generally found between bone and skin, muscle, tendons, or ligaments, helping to reduce the pressure and friction between moving parts.

1.2.3 Attachment of Ligaments

The points of attachment of the ligaments are also important to the way they work within the knee joint. The MCL runs from the medial aspect of the medial femoral condyle and attaches to the medial side of the tibia (Figure 1.7). The total length of the MCL is about 80mm-100mm, and can be broken down into 2 parts: the superficial and deep portions. The superficial portion is attached 40mm-50mm distal to the joint, and can itself be further subdivided, into anterior and posterior portions. The posterior fibres blend with the medial meniscus of the joint capsule while the anterior fibres are separate from the joint capsule. The deep portion of the MCL is anatomically the third (deep) layer of the medial compartment, and is separated from the superficial MCL by a bursa. The LCL is a strong, rounded cord-like ligament about 50mm long and runs from the outer surface of the lateral condyle to the head of the fibula (Figure 1.8). The cruciate ligaments lie inside the joint capsule, and for this reason can be known as intracapsular ligaments, however they are extrasynovial. The cruciates are largely contained within the intercondylar notch and when viewed from the anterior-posterior (A-P) aspect they cross each other, hence their name. The ACL has a length ranging from 25mm-41mm with a mean width of 10mm and is attached to the anterior intercondylar fossa of the tibia. It runs obliquely, superiorly and laterally and is attached to a narrow patch on the internal aspect of the lateral condyle of the femur (Figure 1.9). The PCL is shorter and stronger than the ACL, with a length of approximately 38mm and a width of 13mm. The PCL can be separated into anterolateral and posteromedial bundles, although the anterolateral bundle represents 95% of the total PCL substance. The PCL is attached to the posterior part of the posterior intercondylar fossa of the tibia, overlapping the posterior rim of the upper surface of the tibia. The PCL runs obliquely, medially, anteriorly and superiorly, and is attached into

the depths of the intercondylar notch and also to a patch on the edge of the lateral surface of the medial condyle along the line of articular cartilage (Figure 1.9). The exact orientations and insertion sites of the different ligaments cannot be stated since they are patient dependent, but the general areas of attachment can be outlined. The anatomical differences of the insertion sites and the reference lengths of knee ligaments were noted in a study of knee ligament recruitment by Blankevoort *et al.* [48], and accounted for the quantitative differences of the ligament length patterns that they reported.

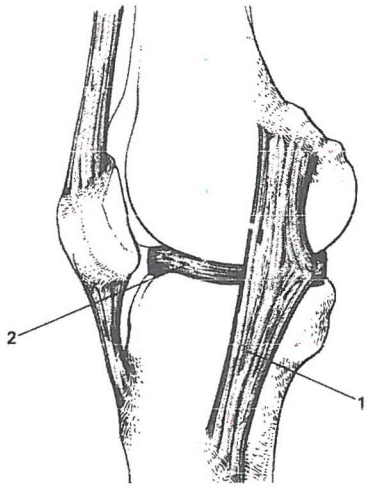

Figure 1.7 The medial collateral ligament (1) and medial meniscus (2) [141].

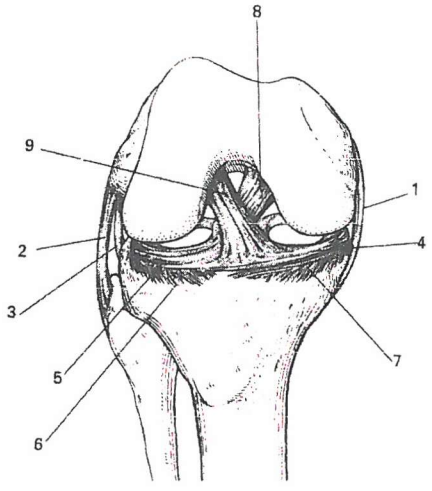

Figure 1.8 Anterior view of the coronary ligaments, with the knee in flexion: (1) medial collateral ligament; (2) lateral collateral ligament; (3) popliteus tendon; (4) medial meniscus; (5) lateral meniscus; (6) lateral coronary ligament; (7) medial coronary ligament; (8) posterior cruciate ligament; (9) anterior cruciate ligament [141].

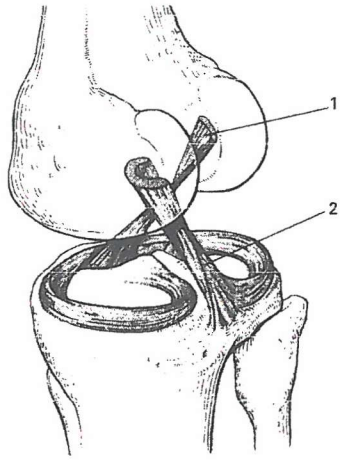

Figure 1.9 Posteromedial view of the cruciate ligaments: anterior (1), posterior (2) [141].

The insertion of the ligaments to the bone is another important feature, with two possible types, direct and indirect. The insertions of the ligaments to bone are functionally adapted to dissipate forces by passing through fibrocartilage to bone. As documented by Matyas *et al.* [49], it appears that there is a correlation between the shape of the cells in the ligament-bone insertion zone and the mechanical stresses.

Direct insertion consists of 4 zones. At the end of the ligament (zone 1), the collagen fibres intermesh with fibrocartilage (zone 2). This fibrocartilage gradually becomes mineralized fibrocartilage (zone 3) and then merges into cortical bone (zone 4). The change from more ligamentous to more bony material produces a gradual alteration in the mechanical properties of the tissue (i.e. increased stiffness), which results in a decreased stress concentration effect at the insertion of the ligament into the stiffer bone.

Indirect insertion is less common than direct insertion, and occurs when the ligament inserts directly into bone relative to the periosteum (a membrane several cell layers thick that covers almost all of every bone). The superficial layers attach to the periosteum with deeper layers that anchor to the bone via Sharpey's fibres (tiny attachment fibres). The MCL is unique in that it has direct femoral insertion and an indirect tibial insertion [50].

1.2.4 Ligament Characteristics and Properties

Ligaments display time- and history-dependent viscoelastic properties that reflect the complex interactions of collagen and the surrounding proteins and ground substance. Due to internal energy losses, the loading and unloading curves of ligaments do not follow the same path, thereby forming a hysteresis loop. During walking or jogging, the applied strains and strain rates are nearly constant [51]. Cyclic stress relaxation will effectively soften tissue substance resulting in a continuous decrease in peak stress as cycling proceeds. This phenomenon may help prevent fatigue failure of the ligaments. Two important viscoelastic properties of ligaments (and tendons) are creep, an increase in elongation of the tissue under a repeated or constant load, and stress relaxation, a decline in load under repeated or constant elongation, see Figure 1.10. Deformation increases slightly during cycles at a constant load, demonstrating the creep behaviour of ligaments. These changes have been noted clinically with temporary softening of all these tissues and thus increases of test excursion (laxity) in exercised joints [35]. After a short recovery period there is a return to normal joint stiffness and apparent length.

It is however speculated that creep is fundamentally more nonlinear than relaxation and that the microstructural processes taking place in a material undergoing creep could be quite different from those taking place in a material undergoing relaxation. On the basis of the known behaviours of ligaments, which have been shown to feature recruitment of collagen fibres at increasing loads, it can be speculated that recruitment would occur during creep, although such recruitment would be unlikely to occur during stress relaxation. As static stress relaxation occurs at a constant elongation it can be speculated that a discrete group of fibres (or fibre bundles) are recruited at the prescribed constant elongation. However, in static creep tests a constant load is applied, which allows elongation of the ligament, therefore more and more fibre bundles are recruited as the specimen elongates. The question therefore arises as to how much is due to the creep of the fibres, and how much is due to the recruitment of the fibres that contribute to the time-varying function of a tissue under a constant load. This query does not however affect the end fact that creep and relaxation occur within ligaments.

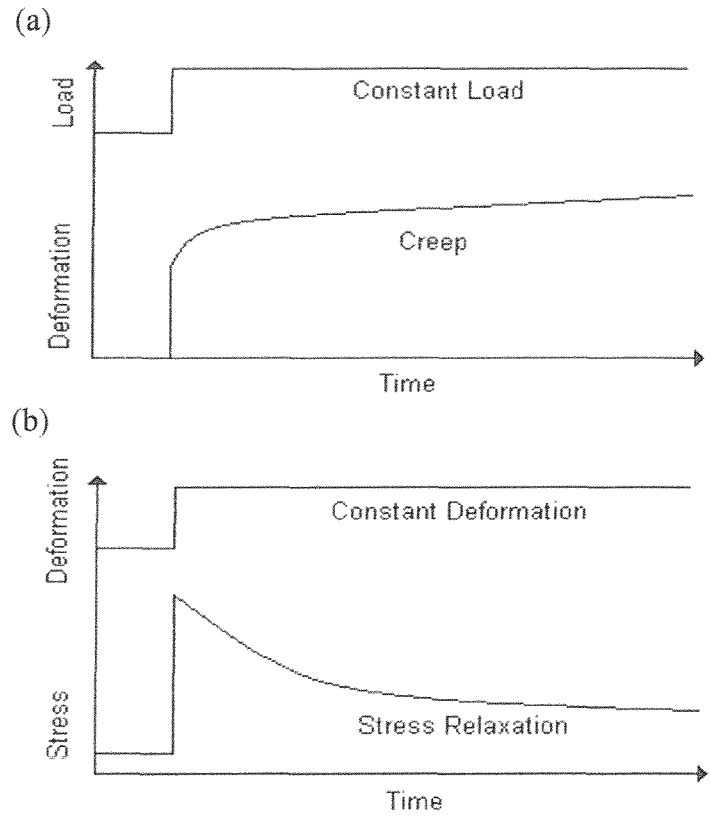

Figure 1.10 (a) Schematic representation of creep behaviour (increasing deformation over time under a constant load). (b) Stress relaxation (decreasing stress over time under a constant deformation).

Ligaments are however not always strained in a uniform manner. The flexion angle affects the strains in the ligaments considerably. At certain angles particular ligaments restrict the majority of motion, but at other angles they may have a negligible effect. Many experiments have concluded that in general the MCL and LCL are tightest (or longest) at full extension and most relaxed (shortest) at full flexion [42], [48], [52]. Fox *et al.* [53] studied the PCL and concluded that the *in situ* forces increased from 36± 13N at full extension to 112± 29N at 90° of flexion under a 110N posterior tibial load.

The three-dimensional orientation of particular ligaments also affects their contribution to knee stability. For example, the anterior bundle of the PCL can be expected to sustain the highest tension in full extension; however, it will not restrain motion but will merely act to compress the joint surfaces, since its orientation will be nearly parallel with the tibial axis. Restraining rotations, such as internal and external rotation of the tibia with respect to the femur, also depends on the relative positions of the restraining ligaments, of which the tensions contribute to the restraining moment through the moment arm. The

restraining function of the cruciate ligaments to internal and external rotation is probably limited by the small moment arm between both ligaments, or between a ligament and the rotation axis for axial rotations [54]. Another restraining mechanism should then assist. In external rotation the collateral ligaments are the restraining structures, in which case the moment arm is relatively large.

The properties of the individual ligaments determine their unique behaviour. A few studies into the properties of ligaments have been carried out, with the ACL, PCL and LCL being studied the most. Butler *et al.* [11] tested the ACL, PCL and LCL in a saline buffer solution at 37°C and recorded the average modulus, maximum stress and strain at maximum stress for these ligaments (Table 1.2). The study also showed that the ligaments failed by a strain-dependent mechanism, with the tissues achieving maximum stress at about the same maximum strain value (~15%).

Ligament Characteristic	Ligaments (ACL, PCL, LCL)
Modulus (MPa)	345.0
Max. Stress (MPa)	36.4
Strain at max. Stress (%)	15.0 n= 23

Table 1.2 Reported Ligament properties [11].

Quapp and Weiss [5] tested the MCL in both the longitudinal and transverse directions, and showed that the ligament was stronger when loaded in the direction of the collagen fibres (Table 1.3). These results were comparable to those of Butler *et al.* [11] for the ACL, PCL and LCL.

	Longitudinal	Transverse
Ave. Tensile Strength (MPa)	38.6± 4.8	1.7± 0.5
Ave. Ultimate Strain (%)	17.1± 1.5	11.7± 0.9
Ave. Modulus (MPa)	332.2± 58.3	11.0± 3.6

Table 1.3 Reported MCL properties [5].

Author	Stiffness (N/ mm)± S.D.				
	n	ACL	PCL	MCL	LCL
Noyes and Grood [55]	20	129± 39 (O)			
	9	182± 56 (Y)			
Woo *et al.* [56]	9	242± 28 (Y)			
	9	180± 25 (O)			
Trent *et al.* [57]	4-6	141± 99	183± 65	72± 17	61± 43
Momersteeg *et al.* [58]	2-4	210± 102	258± 62	134± 1	114± 29

Table 1.4 Measured stiffness values (N/ mm) ± standard deviation (S.D.) of the ACL, PCL, MCL and LCL. 'O' implies old donors were used, 'Y' represents younger doners and 'n' indicates the number of donors.

Due to the non-uniform stress-strain values of ligaments their exact modulus cannot be predicted, instead some authors have estimated the tangent modulus in the relatively linear region of the ligaments stress-strain curve (Tables 1.3 and 1.4). The general stiffness of the entire ligament may be a better representation, especially if replacement ligament prostheses are needed. Several authors have calculated stiffness values of the knee ligaments, with the ACL being the most extensively tested (Table 1.4). The recorded stiffness values of the knee ligaments varied from author to author, and there are a few possible reasons for this. Momersteeg *et al.* [58] looked into the effect of the tilt of the femoral insertion site on the recorded stiffness values of human knee ligaments. They noted that the recorded stiffness was significantly affected by the tilt and translation of the femoral bone relative to the tibial bone, and it was also noted that the effect was greater on the cruciate ligaments compared to the collateral ligaments. The primary reasons for this are probably due to (i) the more complex fibre orientation and lengths within the cruciates, and (ii) the fact that the cruciate ligaments are relatively short and wide compared to the longer and thinner collateral ligaments, meaning that tilting the collateral ligaments will have less of a shortening effect. Other possible reasons for the variations in recorded stiffness values could be due to measurement techniques, i.e. RSA (Radiostereometric Analysis) or vernier caliper displacement measurements, or possibly due to donor age, which has been noted to have a significant effect on ligament structural properties [55]. Osteoarthritis has also been shown to modify knee ligament stiffness [59], [60] with a threefold increase in MCL stiffness being noted [15] in an arthritic knee.

1.3 Knee Biomechanics

The biomechanical behaviour of the knee is complex, with flexion and extension providing the catalyst for internal-external rotation and anterior-posterior rolling-gliding motions. The range of motion of the normal knee is around 130°, and is dependent upon the hip position and whether the movement is performed actively or passively. Around 140° of flexion can be reached when the hip is actively flexed (Figure 1.11(a)), however this is reduced by 20° if the hip is extended (Figure 1.11(b)). The amount of movement in the knee is ultimately limited by the presence of muscles and ligaments, with the limiting factor in this case being the hamstrings, which lose some of their efficiency during hip extension.

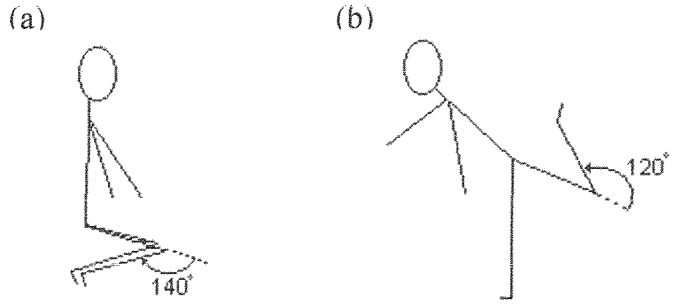

Figure 1.11 The influence of hip position on the movement of the knee joint, both with (a) the hip flexed and (b) the hip extended.

Axial rotation of the knee joint occurs during flexion, this is caused by rotations of the medial and lateral femoral condyles on their respective tibial plateaux. The lateral femoral condyle has a greater posterior sliding distance over the tibia compared to the medial condyle as the knee is flexed. As the knee travels through the entire range of flexion the contact point between the medial femoral condyle and the tibia moves posteriorly by about 1mm-2mm, whereas the contact point between the lateral femoral condyle and the tibia moves posteriorly by about 6mm-7mm, and sometimes as much as 9mm. This mechanism causes gradual lateral rotation of the femur over the whole range of flexion and is known as automatic rotation. This motion is viewed as a special aspect of knee rotation and is produced due to the joint geometry, allowing the knee to have on one hand a stable, solid state and on the other a more relaxed, mobile state. As flexion begins the femur rotates externally, as described above, and is sometimes referred to as 'unlocking'. As the knee extends the opposite occurs, with medial rotation to once more

'lock' the joint firmly in place for stance. This medial locking rotation is often referred to as a "screw home" mechanism. At 110°-120° flexion, lateral rotation of femur with respect to the tibia becomes so great that the lateral femoral condyle will almost, if not completely lift off the meniscus, resulting in virtually all the load passing through the medial condyle. The "screw home" mechanism has been described as characteristic of healthy knee motion and its absence is often noted as an indication of instability or joint damage, such as meniscal tears [2], [61], [62]. Although the balance of evidence supports the existence of the screw home mechanism in the knee, there are arguments about its actual significance or perhaps even occurrence [63]. Several measurements have apparently been made of screw home, with values ranging from 7°-15° during passive and active testing [64]. Other authors did not measure any screw home during their studies [65], [66], although axial rotation was always noted. One possible explanation for these discrepancies is "kinematic crosstalk", which is an error that arises when the chosen joint coordinate system is not aligned with the axis about which rotations are assumed to occur (e.g., the flexion-extension axis is not aligned in the mediolateral direction). This misalignment can cause screw home motion to be measured where none exists and can prevent a true screw home motion from being measured [63].

Movement of the femoral condyles over the tibial plateaux is achieved by a combination of rolling and gliding motions. As the knee flexes from full extension the femoral condyles begin to roll without sliding, then as flexion increases the sliding movement is prevalent and the motion becomes almost all sliding at the end of flexion. The medial and lateral condyles have different rolling-gliding ratios at different angles of flexion and extension, which causes the axial rotation of the knee. Figure 1.12 shows the point of the contact of the femoral condyles on the tibial plateaux as the knee rotates from full extension to 90° of flexion. As the knee joint moves beyond 20° flexion it becomes looser, the ligaments loosen and the radii of the condyles are reduced; this prepares the joint for a wider range of axial rotation. The amount of axial rotation noted during the normal gait cycle is around 10° [67], [68], [69], with the peak external rotation seen at heel strike [64].

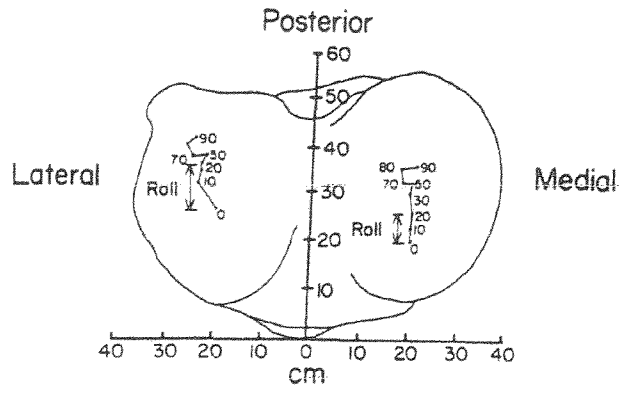

Figure 1.12 The tibial-femoral contact points as the knee flexes from 0° to 90° [1].

The active motions of the knee are ultimately controlled by muscle forces and are guided by the interaction of muscles, ligaments and the geometry of the knee. The forces produced at the joint vary depending on the activity. Normal walking produces forces of between two to four times body weight across the femorotibial joint, and about half body weight across the patellofemoral joint. Table 1.5 shows the compressive forces across the tibiofemoral joint for various activities. It has been noted that the distribution of loads across the knee are generally more medial for a normal valgus tibiofemoral alignment. When the alignment becomes more varus the load on the medial plateau rapidly approaches 100% of the total load on the joint. For valgus deformities however, the load generally remains medial [70].

In addition to compressive forces, anterior and posterior shear forces act on the tibiofemoral joint. The posterior shear forces tend to be greater than the anterior shear forces; for example, walking up and down stairs produces a posterior force ranging between 0.4-1.7 times body weight, whereas for the same activity the anterior shear force ranges between 0.04-0.2 times body weight. Table 1.6 shows posterior and anterior shear forces for several activities.

Author	Activity	Force (times body weight)
Ericson and Nisell	Cycling	1.2
Morrison	Walking	3.0
Harrington	Walking	3.5
Morrison	Downstairs	3.8
Morrison	Upstairs	4.3
Dahlkvist *et al.*	Squat-rise	5.0
Dahlkvist *et al.*	Squat-decent	5.6

Table 1.5 Compressive tibiofemoral forces during different activities [6].

Author	Activity	Posterior force (times body weight)	Anterior force (times body weight)
Ericson and Nisell	Cycling	0.05	0.05
Morrison	Walking	0.4	0.2
Morrison	Downstairs	0.6	0.1
Morrison	Upstairs	1.7	0.04
Dahlkvist *et al.*	Squat-rise	3.0	-
Dahlkvist *et al.*	Squat-decent	3.6	-

Table 1.6 Shear forces on the tibiofemoral joint during different activities [6].

Chapter 2 Surgical Aspects: Total Knee Replacement

Osteoarthritis is a major cause of knee problems, with the most common outcome being varus deformity that results in medial compartment degeneration. Severe pain and restricted motion will occur if degeneration progresses, resulting in the need for a joint replacement. Results of TKA are among the best of any orthopaedic procedure, but failures do occur, and tend to fall into recognisable groups. Correct alignment of the joint, alignment of the prosthesis and the balancing of the soft tissue structures are important for the long-term survival of a replaced knee. Goldberg *et al.* [71] identified loosening and instability pre-operatively as the most common reasons leading to revision surgery in their series of 65 consecutive revision TKAs. Other frequent causes of failure include infection, patellofemoral complications and periprosthetic fractures [72], [73], [74].

2.1 Alignment

Alignment of the knee prosthesis in the coronal plane is particularly important, where an error of 5° can be significant and 10° is often catastrophic [75]. Some authors do not fully agree with this statement [76] and believe that some degree of malalignment will not necessarily cause catastrophic failure. It is generally agreed however that the optimum tibiofemoral alignment of the knee is between 5°-8° of valgus, with the components orientated perpendicular to the mechanical axis [76], [77] (see Figure 2.1).

Specifically, instability is closely related to malalignment and loosening, and is difficult to study in isolation [72]. Over time the abnormal mechanical forces associated with axial malalignment can produce chronic incompetence of the collateral ligaments, resulting in instability [78], [72].

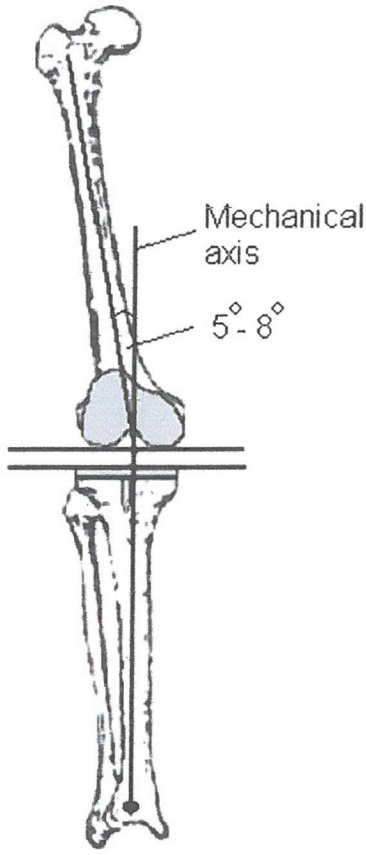

Figure 2.1 Position of a standard right TKR. The femoral component is orientated within 5°-8° of valgus relative to the anatomic axis of the femur. Both components are perpendicular to the mechanical axis of the extremity.

Varus rotation of the femoral component tends to increase stresses on the tibial component, leading to wear or loosening. Loosening can contribute to subsidence of the prosthesis resulting in joint instability. Gait analyses approximates that in the normal knee 60% of the total joint load is transferred through the medial part of the knee [79]. Johnson *et al.* [70] stated that with varus alignment there is a further shift of load to the medial side, rapidly approaching 100%. Contrary to the predictions of static analysis [64], valgus alignment does not have the opposite effect, with more than 50% of the load still transferred medially [70] during dynamic motions.

Malalignment of the knee components is the most common cause of isolated rotational instability. When present, rotational instability usually occurs in the posteriolateral direction. In a cadaver study by Nagamine *et al.* [80] it was found that external femoral component rotation causes internal tibial rotation instability at a flexion angle of more than 45°. This phenomenon is exacerbated further with internal rotation of the tibial

component. Bargren [81] concluded that internal tibial component rotation was the main cause of posterior dislocations, a finding supported by Lecuire and Jaffar-Bndjee [82]. On analysing retrieved tibial polyethylene components, Wasielewski *et al.* [83] reported that polyethylene from patients with tibiofemoral subluxation showed abnormal rotational wear patterns, indicating that rotational instability was a major motion pattern. Cameron and Hunter [73] also noted that placing the tibial component into excessive internal rotation could cause failure due to rotatory subluxation.

It is understood that during TKA the surgeon tries to place the tibial component at an angle of 0° in the coronal plane (i.e. a tibial cut angle of 90°), thus cutting the femoral surfaces in such a way as to cause an overall tibiofemoral angle of around 7° of valgus. Coull *et al.* [84] examined the tibial angles of 79 consecutive total knee arthroplasties to determine the prevalence of tibial component malposition. Their findings showed the mean tibial component angle to be 86.9° (S.D.± 2.8°), 7.6% had an angle of ≤83°, 48% had an angle <87°, and 84% had an angle <90°. Most surgeons choose a femoral cutting guide with an angle between 5°-7°, and if the tibial angle is less than 87° the overall alignment will be less than 4° of valgus. As mentioned the recognised ideal position of the knee prostheses is between 5°-8° of valgus. In a study of TKR failures Cameron and Hunter [73] noticed that problems were generally evident on the tibial side rather than the femoral side. Lateral subluxation of the tibia resulted in tibial component loosening, with posterior, anterior and direct sinkage observed. Analysis showed that in a high proportion of the knees in this study the tibial components were initially inserted obliquely, and subsequently tilted further. Reasons for the malpositioning of tibial components may be due to the reluctance of the surgeon to remove sufficient bone from the lateral condyle, which is needed in the more common varus knee. A larger lateral condyle resection accentuates collateral ligament laxity, requiring a more extensive medial release. In addition, using the standard medial parapatellar arthrotomy, the patella tendon obscures the lateral condyle and may prevent the tibial cutting block sitting flush with the proximal tibia. Whilst extramedullary jigs attempt to minimise error in the tibial cut, there remains an element of subjectivity in determining the correct sitting of the jig.

Further research indicates that producing an ideal valgus alignment in knees is an issue that needs to be addressed. In a review of 442 revision total knee procedures performed at the Centre for Hip and Knee Surgery from 1975-1990, it was found that 56% of knees

were in varus, 31% were in neutral and only 13% were in valgus [85]. Thus, the ideally aligned knee appears to be the exception rather than the rule.

2.2 Ligament Balancing

Residual tension in the knee may exist if the soft tissues are not adequately released. This can cause the femur to internally rotate during flexion and any residual tension during extension will tend to maintain a varus alignment. Tibiofemoral instability can be directly related to the failure of the collateral ligaments, which can often be found in cases of frontal deformity in both the varus and valgus knee, and also with rheumatoid arthritis. This kind of instability has been reported to be a reason for failure of knee replacements in 10%-30% of all cases, and is a problem that can be avoided by precise pre-operative planning.

Reilly [86] described aspects of varus deformity and the soft tissue surgical techniques necessary for the solution. He states that firstly the deep portion of the MCL is released; this is carried posteriorly to include the semimembranous insertion on varus knees but not valgus knees. The second phase of the release procedure involves the removal of osteophytes that obstruct the MCL. With severe deformities the posterior medial capsule must be released from the tibia to allow correction of the deformity. Insall [75] also states an approach for varus and valgus corrections. For a varus deformity balanced ligaments are achieved by progressively releasing the medial soft tissues until they reach the length of the lateral ligamentous structures. Use of a laminar spreader and an alignment rod allows the extent of the release to be monitored. Insall states that the cruciate ligaments must be completely excised before starting the release because their presence will often inhibit correction as their length is not altered and will not allow the stretching required in the medial release procedure.

For valgus deformities the principles for the correction are the same as for varus deformities. There are however differences due to the anatomy. The popliteal nerve passes on the lateral side of the knee and along with the other structures is stretched beyond its original length (there is no corresponding structure on the medial side of the knee). Other differences mean that the release must be done from the femur rather than the tibia.

Several studies have been performed to assess the effect of collateral ligament imbalance on knee stability and general knee performance after TKR. Sambatakakis *et al.* [87] carried out a radiographic study to evaluate the prevalence of malaligned tibial components. Their findings showed that an inconsistent bone cement thickness beneath the tibial component was sometimes seen, with a wedge of bone cement formed. Further evaluation consistently showed that the thinnest area of bone cement was noted on the side of maximum pre-operative bone loss, that is, towards the 'tight' side of a deformed knee. Sambatakakis *et al.* [87] suggested that cement inconsistencies could be due to persistent soft tissue imbalance following TKR, and is associated with the development of radiolucent lines during follow-up. They also believed that more extensive ligament release is necessary in a large proportion of knee replacements, and that the Insall method [75] should be followed to improve the overall alignment of the limbs and lessen the incidence of radiolucent lines.

Cameron and Hunter [73] showed that failure to accurately balance the ligaments mediolaterally contributed to poor results, with the general view that adequate release of the medial ligament is important to obtain a stable knee with good congruence over the whole tibiofemoral joint. If the contact forces are not balanced then under load-bearing and motion conditions, loosening and increased polyethylene wear may occur [88]. In deformed arthritic knees, contractures of the ligaments and articular capsule may require progressive release of the MCL and other medial soft tissue structures (e.g. per anserinus and posteromedial capsule) during a TKA. This is a procedure that is difficult to judge and excessive release may lead to joint instability and failure of the operation. Wasielewski *et al.* [83] confirmed that the adequacy of ligament release during the operation is closely related to polyethylene wear and wear patterns seen after revision. The recognition of pre-operative ligament incompetence, intra-operative ligament incompetence, intra-operative collateral ligament damage, or trauma in the immediate post-operative period is vitally important. Failure to achieve adequate medial-lateral soft tissue balance intra-operatively is probably the most common cause for early failure. Takahashi *et al.* [89] stated that the intra-operative measurement of contact forces is a useful means of detecting imbalance at the tibiofemoral joint, and can be done by using simple passive motion tests. The information gained can then be used in assessing the proper release of soft tissues of the knee joint.

2.3 The Knee Prosthesis

Although there are numerous individual designs of TKR available today, there are only a limited number of design forms or types. Knee prostheses consist of a metallic femoral component (e.g. cobalt chrome), a polyethylene tibial insert (Ultra-high molecular weight polyethylene - UHMWPE) and a metallic tibial tray. If needed a prosthetic patella can be implanted (UHMWPE bearing surface).

When deciding on which knee type to implant the general choice is between a fixed or rotating-bearing design, and a posterior cruciate-retaining or posterior cruciate-substituting design. There are specialist modifications available but ultimately the choices are limited to those mentioned above. Fixed-bearing TKRs represent the major clinical usage today. The term 'fixed-bearing' applies to the bearing between the metallic tibial tray and the polyethylene tibial insert, in this case the two are rigidly attached so that there is no significant movement between them. Rotating-bearing knees allow the insert to axially rotate on the tibial tray, thus reducing the sliding of the femoral component on the insert and increasing the sliding of the insert on the tray. The ACL is almost always sacrificed during TKA, leaving only the choice of whether to retain or sacrifice the PCL.

Conventional fixed-bearing knee prostheses have proven to be clinically successful, but with some reservations. In a study of 101 knees, 96% had good-to-excellent clinical results, and the rate of survival where revision was the end point was 96.4% after ten to fifteen years follow-up [90]. However, these good results are viewed with some caution, most of the patients in this kind of study are elderly with low activity levels and the physical demand on the prosthesis is relatively low. This consideration aside, there is always the problem of wear associated with fixed-bearing designs that can lead to either catastrophic failure or osteolysis around the joint. As the femoral component articulates over the insert problems such as delamination may occur in low conformity designs, with high contact pressures causing fixation failure in more constrained designs. Undersurface wear caused by micro-motion between the polyethylene insert and the metallic tibial tray may also occur, leading to osteolysis around the joint and ultimately joint failure.

The mobile-bearing prosthesis shifts the rotational emphasis away from tibiofemoral articulations and places it onto the tibial insert to tibial tray interface. This is achieved by allowing the insert to rotate about a central shaft, which fits within the tibial tray and allows the conformity between insert and femoral component to be higher since it will not restrict the axial rotations of the knee. This increases the contact area between the femoral and tibial components from approximately 200mm^2 in a good fixed-bearing design, to 1000mm^2 or more for the mobile-bearing design. This increase in contact area consequently reduces the contact stresses from approximately 25MPa in the fixed-bearing to 5MPa or less in the rotating-bearing [91]. The use of a mobile-bearing does however mean that there is considerable movement between the polyethylene insert and the metallic tibial tray, which is normally made from a hard metal such as cobalt-chromium alloy. The metallic tray can be highly polished to allow the polyethylene component to move freely over it with negligible resistance. With a mobile-bearing knee problems such as dislocation due to 'spin-out' [92] may occur in designs without a mechanical stop, and when a stop is present, wear may occur as the polyethylene bearing strikes against it.

As well as the choice between the fixed- and rotating-bearing designs, there is the choice as to whether to retain or sacrifice the posterior cruciate ligament. Whether it is better to retain or sacrifice the PCL is still not proven, but in general it is agreed that resection of the PCL requires some sort of mechanism to substitute for its function in the implant design.

Most posterior cruciate-substituting (PC-substituting) designs work on the same basic principle, which is based on interactions between a tibial spine and femoral cam (see Figure 2.2). The spine-cam interaction causes femoral rollback as the knee is flexed, translating the femorotibial contact area posteriorly and creating a net compression force at the proximal tibial interface. As the arc of motion produced is controlled, it is therefore predictable, meaning that the femorotibial articulation could be designed with the maximum conformity compatible with this motion, reducing the stresses on the polyethylene component as much as possible. Results have been encouraging for this kind of prosthesis [90], however problems have been noted with the use of a spine-cam mechanism due to the large volume of bone resection and dislocation. Dislocations occur as the femoral cam translocates anteriorly over the tibial spine, resulting in an acute

dislocation with the knee locked in a flexed position. It has been suggested that most dislocations occur in flexion and are caused by laxity of the ligaments and other soft tissues when the knee is flexed. One way to reduce the possibility of dislocation is to increase the distance from the top of the tibial spine to the bottom of the femoral cam. A study by Delp *et al.* [93] showed that the chance of dislocation was higher at large knee flexion angles, therefore a ligament substituting mechanism is less effective in compensating for excessive soft tissue laxity, emphasizing the important role of the surgeon in balancing the ligaments with the knee in flexion. The findings by Delp *et al.* [93] indicate that increasing the tibial spine height and placing the cam posteriorly are effective means of reducing the chance of dislocation. However, the amount of flexion produced does decrease, therefore the spine-cam mechanism in PC-substituting prosthetic knees may be best suited to prevent knee subluxation and dislocation and not as a mechanism to maximise flexion.

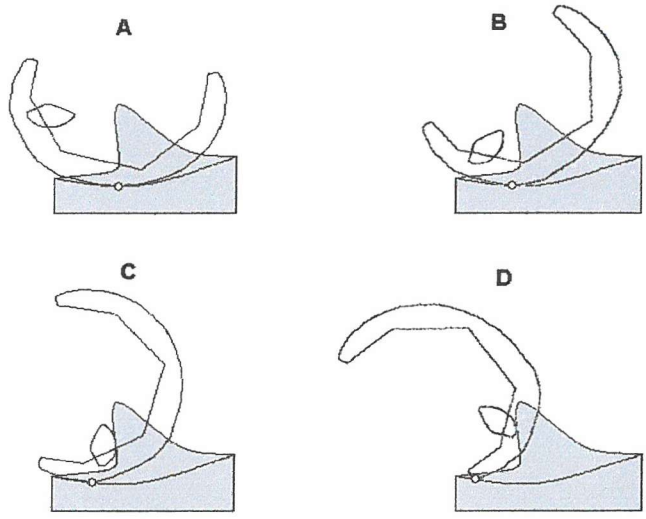

Figure 2.2 Illustration of the function of the spine-cam mechanism in the PC-substituting knee replacement. The components are shown in (A) full extension, (B) 40°, (C) 80° and (D) 120° flexion. The white circles represent the contact point between the femoral and tibial components.

As discussed, it still remains controversial as to whether the PCL should be resected or not, and although this question has not been fully answered retention of the PCL is a popular choice. Today almost two thirds of the knees used worldwide are of the posterior cruciate preserving type, although there is a trend emerging towards the posterior cruciate-substituting designs. Advocates of PCL retention have argued that an intact PCL provides many advantages, including improved knee function, preservation of femoral

rollback, increased range of motion, increased knee stability, decreased stresses at the bone-prosthesis-cement interface, and decreased prosthetic wear patterns. Care must be taken however to accurately strain the PCL during TKA, otherwise the aforementioned advantages will be replaced by detrimental effects. Increased posterior stresses, excessive rollback of the femur and pain in the ligament itself could occur if over strained, and may be rendered nonfunctional if it is too slack.

Several studies have shown that PC-retaining designs do provide a greater passive range of motion over PC-sacrificing designs [94], [95], [96], however other authors have shown that relatively little femoral rollback occurs in PCL-retaining designs [97]. A study by Stiehl *et al.* [98] raised several important questions regarding existing PC-retaining TKR. Physiological rollback was not seen and it was thought that the resection of the ACL, alteration of the normal joint line or other subtle changes that modify kinematics were major factors contributing to the lack of rollback. In addition abnormal translation was noted, which could cause an excessive degree of shear forces at the articulation. Even though increased rollback has been noted in *in vitro* studies, it cannot be clearly stated that it occurs on a consistent basis *in vivo*. Although the evidence of improved performance of PC-retaining TKR is not conclusive, it is hard to say which kind of prosthesis is best; patients who have undergone bilateral arthroplasties (one PC-retaining and one PC-sacrificing) have not noticed any difference in terms of performance between the two [99].

2.4 Passive and Active Knee Motions: Review of the Literature and Clinical Procedures

2.4.1 Passive Motions

Knee stability in the sagittal, coronal and transverse planes can be assessed to highlight the condition of a particular ligament or to view the general stability of the joint. Similar passive stability tests to those performed clinically by a physician or surgeon have been reported in the published literature, assessing knee joint stability before and after total joint replacement. A review of the literature has led the present research towards three passive stability tests. Over the page is a brief description of clinical procedures and similar investigations reported in the literature.

Clinical Procedures:

- ***Varus-Valgus (V-V) Rotational Stability:*** A strong, laterally/ medially directed force is applied at the ankle with counter-pressure at the lateral femoral condyle; this tests the MCL and LCL. Testing is normally carried out at full extension, however minor instability may be better identified if the test is carried out at 30° of flexion.

- ***Internal-External (I-E) Rotational Stability*:** This test puts stress on the medial coronary ligament and the posterior fibres of the MCL. The knee is flexed to a right angle, and the heel is placed on the couch. The foot is pushed upwards into dorsiflexion, thus I-E rotation is easily performed by using the foot as a lever.

- ***Anterior-Posterior (A-P) Translation Stability***: The knee is flexed to a right angle, the examiner sits on the patients foot and one hand is placed on the patella/ tibial tuberosity while the other is placed on the back of the upper tibia (rests on the back of knee in the posterior test). The upper tibia is strongly jerked forwards/ backwards to test the ACL/ PCL. Conducting the anterior drawer test at 30° can be more precise in disclosing elongation or rupture of the ACL; also known as the 'Lachman test'. The Lachman's test applies an anterior force of 68N or 90N to the upper tibia, and the end tibial displacement and feel is noted. The end feel specifies whether an abrupt (hard) or a more dampened (soft) end point is felt. The displacement and end feel help the surgeon understand the state of the ACL, and to a lesser extent the MCL.

Review of the Literature:

The literature was reviewed to gain an insight into the testing that was performed previously; this will allow comparable and realistic testing to be carried out in the present research. The following section only details the methodologies employed by the various researchers. The results of these tests are compared with the present study in the Section 5.9.

Varus-Valgus (V-V) Rotational Stability Testing:

Lundberg and Messner [12] carried out manual passive motion testing following the standard method described by Oliver and Coughlin [100]. V-V rotational stability was assessed at full extension (zero position) and 20° flexion by applying a 20Nm valgus torque followed by an immediate varus torque. Results of the study by Lundberg and Messner were assessed at 12Nm. Mills and Hull [101] applied similar torques during their V-V stability testing while assessing the joint at 15° and 60° flexion. The studies by Lundberg and Messner and Mill and Hull were performed prior to TKR. However Mitts [102] examined a Miller-Gallante II, (Zimmer Corporation, Warsaw, IN, US) posterior cruciate-retaining TKR with minimally conforming tibial inserts. V-V stability testing was performed in full extension and 20°-30° flexion and a grading system was incorporated in the analysis of results: grade 0= 0°-5°, grade 1= 6°-10°, and grade 2= 11°-15° of total V-V rotation. Saeki *et al.* [103] also carried out V-V stability testing after TKR (Profix total knee system - Smith & Nephew, Inc, Memphis, TN), applying a 10Nm torque at flexion angles of 0°, 30°, 60° and 90°. Whiteside and Amador [104] assessed V-V laxity after TKA (posterior stabilised TKR) at 0°, 45° and 90° flexion in response to a 15Nm torque under a 70N compressive load, and in a different study by Whiteside *et al.* [105] (assessment of a rationally unconstrained TKA - Ortholoc, Dow Corning Wright) the same testing protocol was applied. Shoemaker *et al.* [18] carried out V-V stability testing on a posterior cruciate-substituting knee that had been modified to allow the retention of the PCL. A 10Nm torque was applied and testing was performed at 0°, 10° and 20° flexion under compressive loads of 0N and 920N.

Internal-External (I-E) Rotational Stability Testing:

Lundberg and Messner [12] assessed the I-E stability at 20° and 80° flexion by applying a 10Nm torque. However they analysed the results at a point of 8Nm. Mills and Hull [101] recorded I-E rotations at 15° and 60° flexion, applying a lower torque of 5Nm when assessing knees before total joint replacement. Under a 1.5Nm torque Saeki *et al.* [103] carried out an I-E rotation investigation on a Profix total knee system (Smith & Nephew, Inc, Memphis, TN), testing at 0°, 30°, 60° and 90° flexion. A slightly larger torque of 2.5Nm was applied by Whiteside *et al.* [105], who carried out I-E stability testing at 0°, 45° and 90° flexion on a rotationally unconstrained TKA (Ortholoc, Dow Corning Wright). In another cadaveric study by Whiteside and Amador [104] the effect of a posterior stabilising mechanism on rotational stability in TKA was investigated while applying a 2.5Nm torque. Shoemaker *et al.* [18] applied a 10Nm torque to a modified PC-substituting knee, under a 0N and 920N compressive load.

Anterior-Posterior Translation Stability:

In an *in vivo* study, Mitts [102] assessed the A-P stability at 90° flexion of a Miller-Gallante II posterior cruciate-retaining TKR (Zimmer Corporation, Warsaw, IN, US). Five grades of laxity were highlighted, with grade 0= 0mm-5mm, grade 1= 5mm-10mm, grade 2= 11mm-15mm, grade 3= 16mm-20mm and grade 4 for >20mm of total A-P motion. Matsuda *et al.* [106] investigated a flat-on-flat TKR design (Miller Galante I - posterior cruciate-retaining TKR), testing at 30° and 75° flexion under an anterior force of 133N and a posterior force of 89N. In a cadaveric study by Whiteside and Amador [104] the effect of a posterior stabilising mechanism on rotational stability in TKA was investigated, applying a 45N A-P force at 0° flexion. Yamakado *et al.* [107] applied a 133N A-P force at 30° flexion to knees that had undergone cruciate-retaining TKA; Saeki *et al.* [103] assessed A-P stability (Profix total knee system - Smith & Nephew, Inc, Memphis, TN) at 0°, 30°, 60° and 90° flexion, under a lower A-P force of 35N. Shoemaker *et al.* [18] applied a 100N A-P force to a modified posterior cruciate-substituting TKR, recording A-P displacements with and without the PCL.

Regardless of whether malalignment of the components or laxity of the ligaments caused instability, it was agreed that manual testing provided the most meaningful information

to the practicing orthopaedist. Mitts *et al.* [102] suggested that clinical measurements of knee laxity should be part of a routine periodic evaluation of patients that were implanted with certain knee types. The applied forces and flexion position must be known when evaluating the joint stability, as different ligament groups restrain motions to a greater extent at certain flexion positions [108], [109], [110], with stability generally increasing under higher compressive forces [18].

2.4.2 Active Motions

In the present research the effect of passive stability on the active motions after TKR will be assessed, therefore gaining knowledge of similar studies that had been performed previously was important. Analysis of the kinematics during gait can be assessed using cadaveric, mechanical simulation, *in vivo* studies (e.g. fluoroscopy) and computer simulations [9], [8], [23], [111], [112], [113]. Initially, the most relevant information will come from the mechanical and computational simulations; however, the *in vivo* studies will become useful in the assessment of the results.

Using a four-station TKR wear simulator (as described by Walker *et al.* [23] - Stanmore/ Instron, Model KC Knee Simulator) DesJardins *et al.* [8] assessed the kinematics during gait of eight implant designs. Six-degrees-of-freedom articulation was permitted; one femoral flexion angle waveform and three tibial force waveforms were applied to the components to simulate level walking; this data was comparable to published work by Morrison [114]. Completely mechanical simulations, like the one used by DesJardins *et al.* [8] allow relatively easy and reproducible testing of knee replacements, this can be extended in computational simulations. Sathasivam *et al.* [113] developed computer models with different bearing surface geometries, and analysed the effect these differences had on the contact stresses and kinematics of two knees. Again, data derived from Morrison [114] was used to simulate level walking. Godest *et al.* [112] developed a computational knee model using CAD (Computer Aided Design) models, which were used to predict movements in the sagittal plane; the models were based on the mechanical Stanmore Knee Simulator [23]. Another study by Godest *et al.* [9] simulated both the kinematics and the internal stresses during a single gait analysis. A three-dimensional explicit finite element model of a PFC Sigma total knee (DePuy International, Leeds, UK) was developed. Four springs were modelled to simulate the

action of the soft tissues around the knee on both the medial and lateral sides. The same gait data as with the other simulations was inputted to produce active motions [114].

Simulating gait relies on freedom of movement and applied forces similar to that of the anatomic joint. Data published by Morrison [114] tends to be adopted to drive the simulations, with mechanical and computational results being comparable.

2.5 Aims and Objectives

The aim of the present research was to assess how alterations in ligament strains and component alignment affect the stability of the knee after total joint replacement. Passive and active stability conditions would be assessed, and direct comparisons between the two would be made.

To achieve these aims a mechanical test rig needed to be developed to allow passive motion tests to be carried out. The rig had to allow soft tissue structures to be attached and different knee designs to be assessed. The next stage of the research involved developing computational finite element (FE) models of the replaced knee. The FE models would primarily be used to compare/ validate against the experimental testing, and then used to simulate active motions (gait).

With this in mind the present research has the following objectives:

- Assess the effect of altered ligament strains on passive knee stability.
- Assess the effect of altered component alignment on passive knee stability.
- Highlight which passive stability test provides the most relevant stability information.
- Assess the effect of altered ligament strains on active knee stability.
- Assess the effect of altered component alignment on active knee stability.
- Make a direct comparison of passive stability and active stability.
- Determine whether individual implant design has a significant effect on joint stability during both passive and active motions.

Chapter 3 Experimental Passive Stability Testing Rig

3.1 Mechanical Test Rig

The aim of this study was to develop a fully mechanical test rig needed that would allow the passive stability of total knee replacements to be simulated. In order to construct such a rig the exact specifications needed to be assessed; these are detailed below.

3.1.1 Rig Specifications

- *Simulation of Passive Stability Testing:* a comprehensive literature review was conducted to quantify the methods adopted by other authors to assess knee stability after total joint replacement. *In vivo* and *in vitro* investigations were assessed and the simulation of anterior-posterior translation (A-P), internal-external rotation (I-E) and varus-valgus rotation (V-V) to be built into the present mechanical test rig.

- *Representation of Soft Tissue Structures:* representing all soft tissue structures surrounding the knee joint would have proved extremely problematic; thus the primary ligaments of the joint were chosen for the present research. The primary restraints towards knee motion are the cruciate ligaments and collateral ligaments [10], [37-43]. The ACL is virtually always sacrificed during TKA and therefore it was not considered in the present mechanical rig, however the PCL, MCL and LCL were all incorporated.

- *Component Malalignment:* The literature highlighted alignment in the coronal plane as being significant towards implant stability, and the rig was developed to cater for this. It was suggested that achieving coronal alignment of 7° off the femoral shaft axis was desirable; however between 4°-10° acceptable.

- *Assessment of several Total Knee Designs:* One of the original aims of the research was to assess the sensitivity of total knee design towards surgical inaccuracies (e.g. imbalanced ligaments, malalignment). Four versions of the PFC Sigma knee system (DePuy, UK) were provided and therefore the mechanical test rig was required to allow interchangeable total knee designs.

- *Natural Movements:* Ultimately the mechanical test rig had to represent the natural anatomic knee joint after TKR. To achieve this the motions of the natural joint were reviewed from the literature and the freedom of each prosthetic component (i.e. femoral component, tibial tray, tibial insert) was noted. To enable more natural motions an x-y motion table and a tibial section varus-valgus pivot were incorporated into the design.

3.1.2 Rig Design and Development

Following the specifications of the mechanical test rig the design and construction took place. The primary consideration was that all testing was to take place on a servo-hydraulic bi-axial (tension/compression & rotation) actuator (Instron Ltd, Bucks, UK), onto which the rig had to be fitted. A separate mini-actuator was also available for applying external forces. It was decided that the femoral component would be attached to the main actuator arm of the Instron test machine and the tibial section would be attached to the base of the test machine.

Initially, a method had to be devised for holding the prosthetic components in the test rig. The inner angles of the femoral component were provided by the TKR manufacturers (DePuy, UK); these were used to design a block onto which the femoral component could fit. Using a computer-modelling package (Ideas Master Series 7.00.000) three-dimensional (3-D) models were constructed to help visualise the shape and size of the required blocks (see Figure 3.1). Characteristics that were unique to each block were included so that the individual femoral components could be fitted, as shown in Figure 3.2. These images were used to allow the Engineering Design and Manufacturing Centre (EDMC) at the University to construct the components. Aluminium was of chosen as the block material as it was light, relatively cheap and easy to cut into the required shape. A similar procedure was followed for the tibial block development (see Figure 3.3), which incorporated a fixation hole corresponding to the geometry of the tibial tray (see Figure 3.4)

The next stage of the rig development addressed the need for passive stability testing. Taking into account that the Instron had the capability of applying tension/ compression and internal/ external rotation it was decided that I-E rotational stability testing would be applied to the femoral component, as this section would be fitted to the main actuator

arm. After considering all other aspects such as ligament attachment and varying flexion positions a jig was developed to hold the femoral block on the main actuator arm. This jig would not restrict ligament attachment and would permit rotation (flexion: 0° - 90°) of the femoral block. In order to allow varying flexion positions specially designed femoral arms were developed. These femoral arms were universal for all femoral blocks and left the sides of the femoral blocks free for ligament attachment. As stated in the rig specifications coronal malalignment of the femoral component was to be simulated. A method of lowering and raising an alignment plate using grub screws was developed for this procedure. Figure 3.5 shows the 3-D images that were constructed of the jig to allow attachment to the main actuator arm.

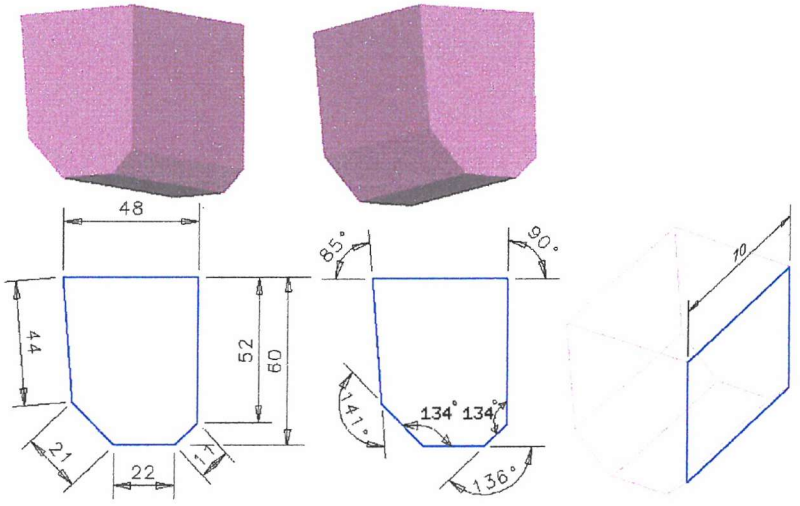

Figure 3.1 3-D images of a standard femoral block to help with the visualisation and construction. Dimensions in mm.

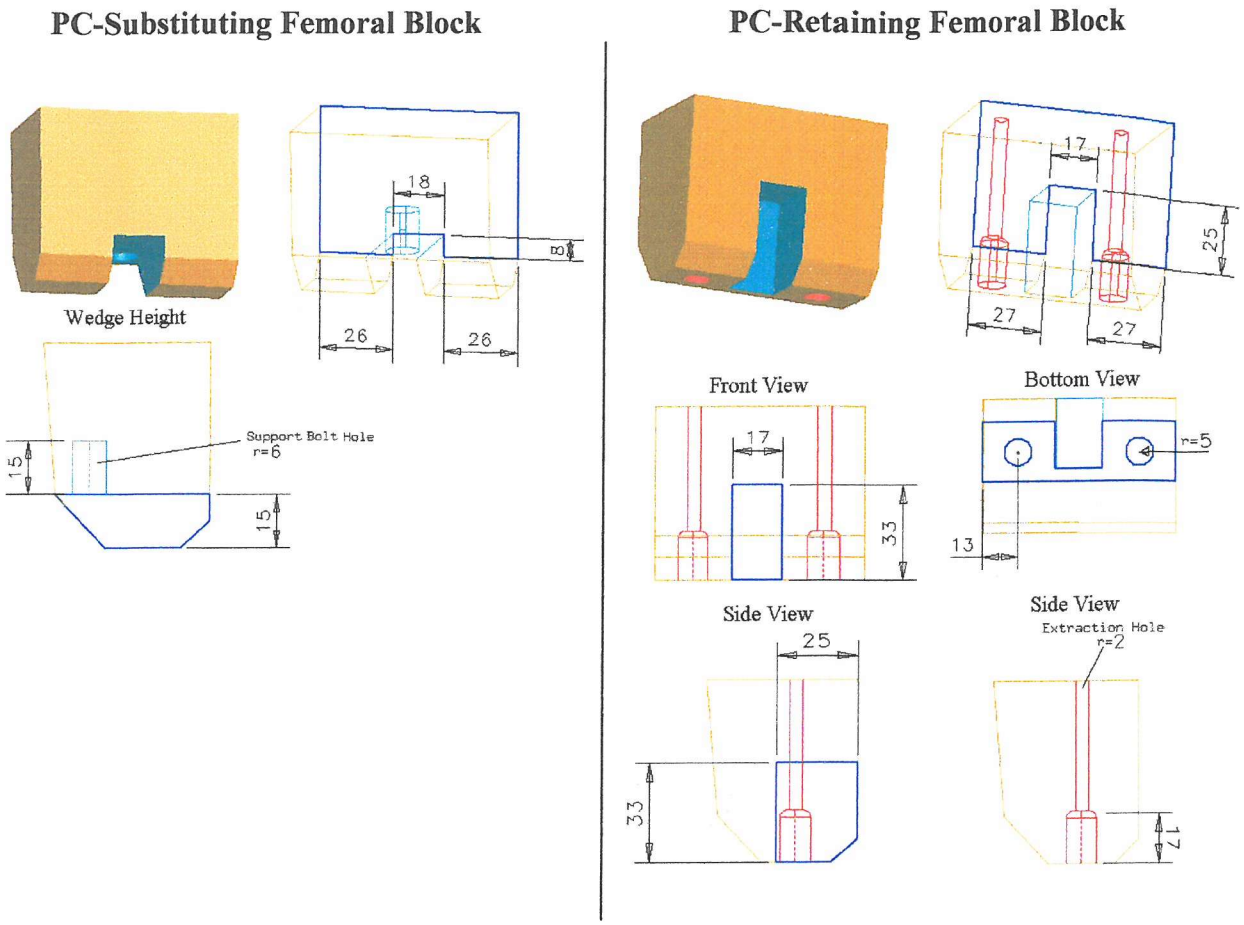

Figure 3.2 Individual femoral blocks were modelled so that the specific components could be fitted. Dimensions in mm.

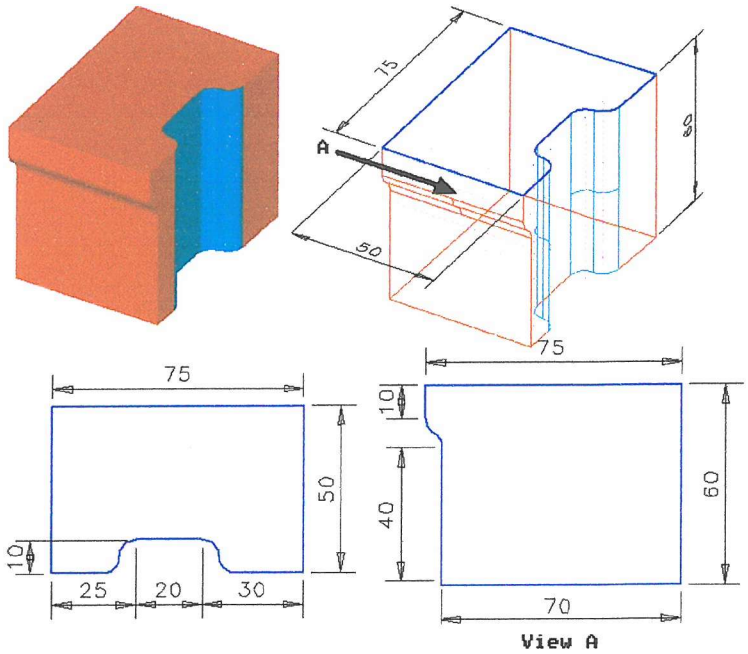

Figure 3.3 3-D images of a standard tibial block to help with the visualisation and construction. Dimensions in mm.

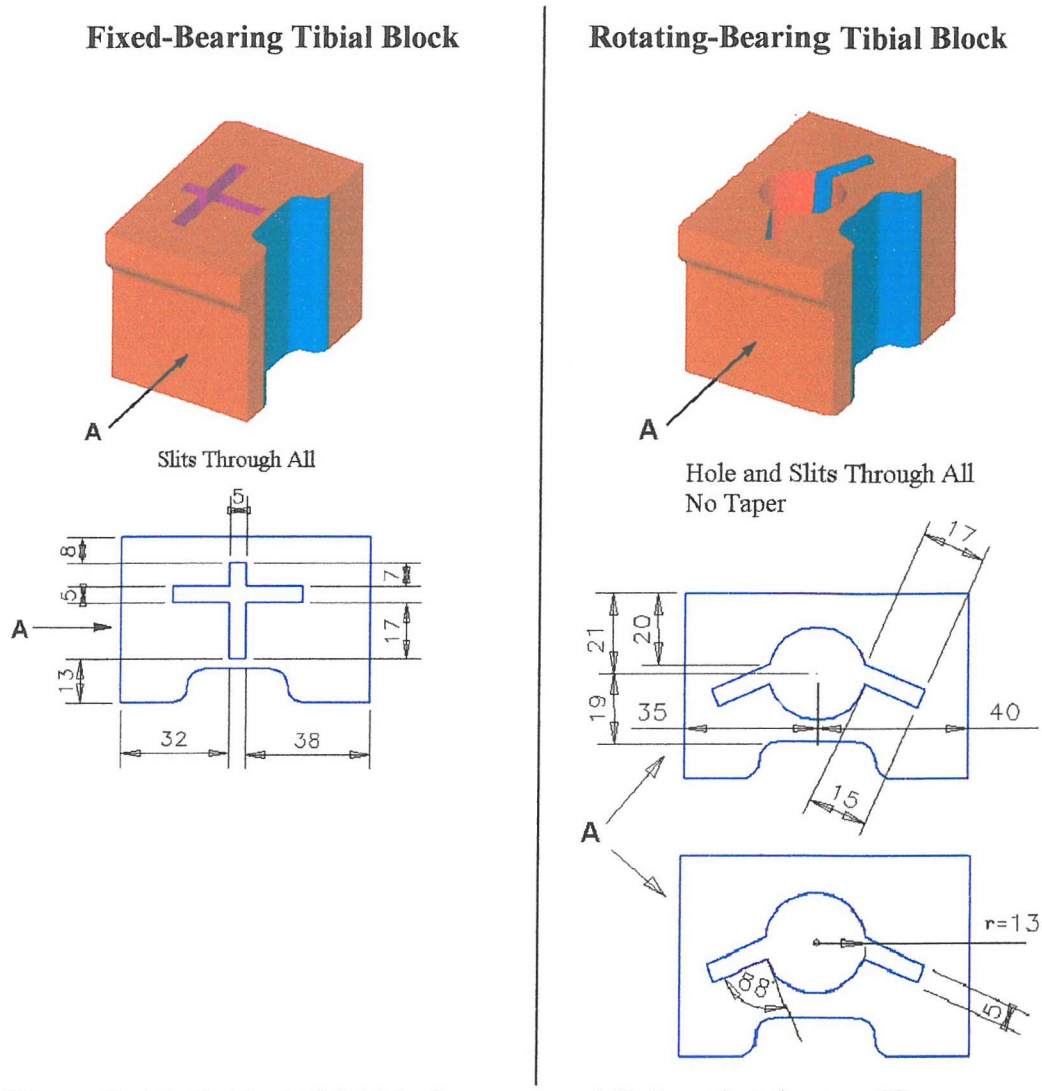

Figure 3.4 Individual tibial blocks were modelled so that the specific components could be fitted. Dimensions in mm.

Once the attachment and movements of the femoral section had been developed attention was turned to the tibial section of the rig. A search of the literature highlighted two factors that needed to be addressed: The first was the requirement for relatively frictionless motion in the A-P and M-L directions, and the second was to allow V-V rotations of the tibial section. After consideration it was decided that using a specialist x-y motion table would provide the best means of simulating frictionless A-P and M-L motions. When choosing the table the dimensions of the top surface, the amount of travel and the maximum load that the motion table could carry were important specifications. A suitable x-y motion table was chosen from Parker Automation (Poole, UK). A central pivot on to which the motion table would fit would provide the best means of simulating V-V rotations. A 20mm diameter silver steel bar was chosen and passed through two self-lubricating bearings to allow frictionless V-V rotations.

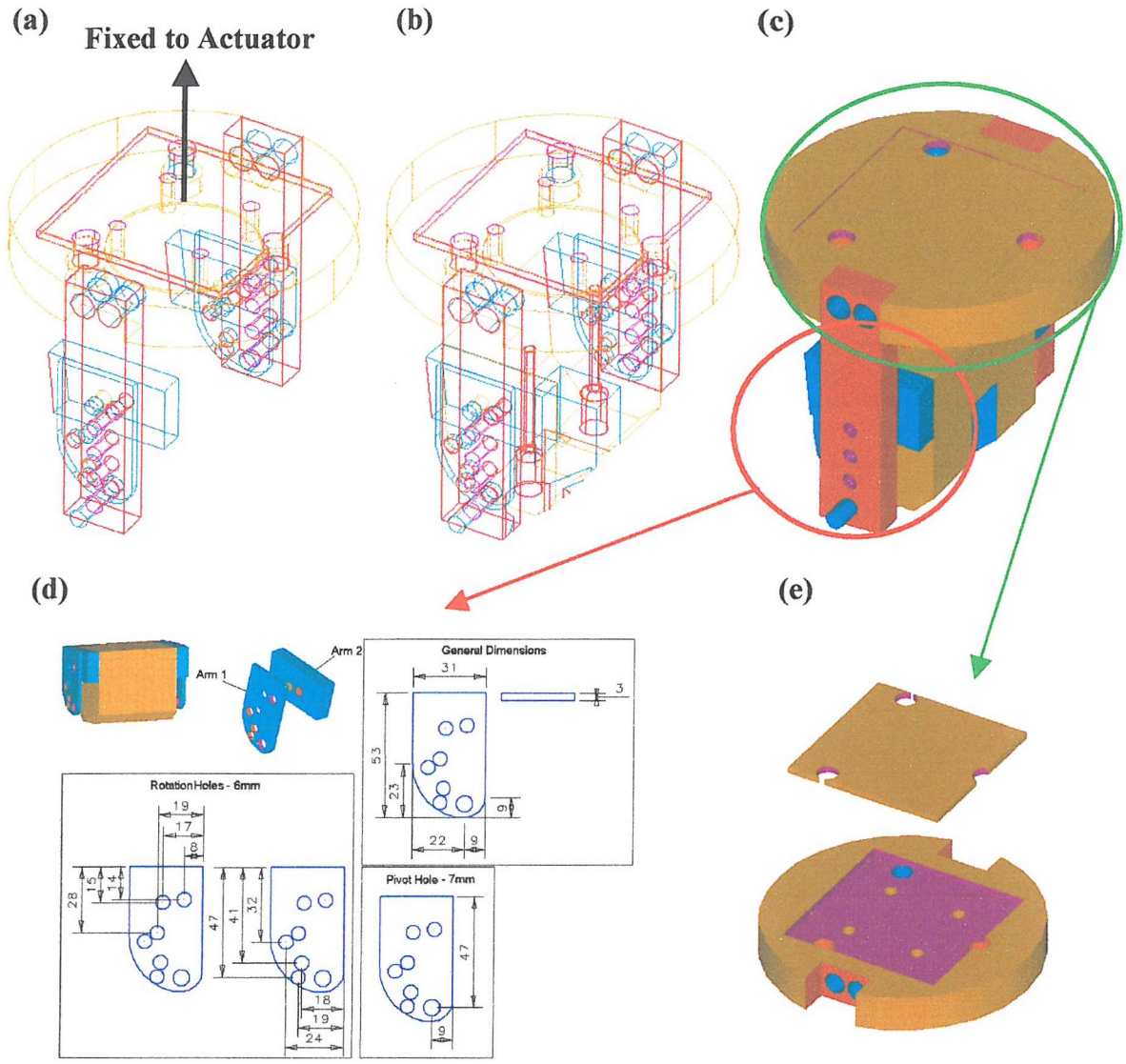

Figure 3.5 3-D representation of (a) the fixation jig, (b) the fixation jig with femoral block attached, (c) solid image of the fixation jig with femoral block attached, (d) flexion permitting femoral arms and (e) alignment plate. Dimensions in mm.

3.1.3 Finalised Test Rig

The majority of the final rig was made from aluminium, with the more heavily loaded structures such as the base plate, V-V pivot and femoral actuator attachment plate constructed from steel. Figure 3.13 shows the fully completely mechanical test rig.

Femoral Main Frame (Attachment to Test Machine and Fixation of Femoral Block):

As shown in Figure 3.13 the main frame of the test rig was attached to the Instron actuator arm and holds the femoral block, onto which the femoral component is fitted. It consisted of a rigid circular section that fixed to the test machine, and had two support posts attached to its sides (Figure 3.6). On the top surface of the main frame was the alignment plate, which could be raised and lowered by grub screws. Depending on the position of the alignment plate the femoral section could be placed in a neutral or malaligned position.

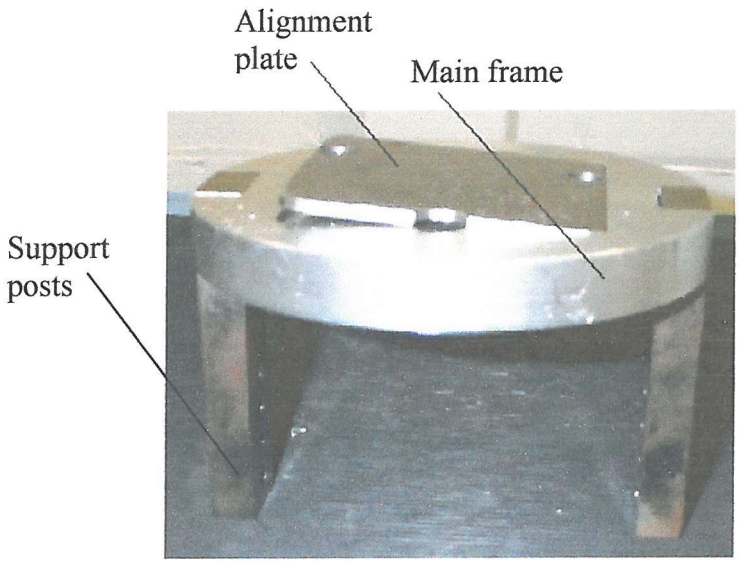

Figure 3.6 Main frame, showing a raised alignment plate.

Femoral Block and Femoral Arms:

The standard shape of all femoral blocks was universal, however specific characteristics were formed in each block to allow the individual femoral component to be fixed. The femoral block was unique to each knee design; thus interchanging the femoral block in the knee rig allowed different knee designs to be tested. The femoral arms could be used with any femoral block design. The outer section of each femoral arm had a series of holes that lined up with holes in the main frame support posts; this allowed the femoral block to be rotated and fixed in several flexion positions. Figure 3.7 shows an example of a femoral block with attached femoral arms and femoral component.

Figure 3.7 Femoral block with the femoral arms and femoral component attached.

Tibial Block:

The purpose of the tibial block was to hold the tibial component. The design of each block was universal, however the fixation hole in each block was specific to the individual tibial tray design. Figure 3.8 shows a tibial block with a component attached.

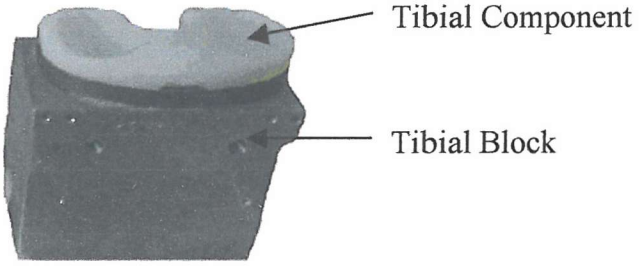

Figure 3.8 Tibial block with the tibial component attached.

Extra Tibial Structures:

A-P and V-V stability testing needed to be performed with the test rig, thus additional structures needed to be fitted to the tibial section of the rig to allow forces to be applied. The tibial block was fixed onto an x-y motion table (Parker Automation, Poole, UK), which in turn was fixed to a 20mm diameter metal rod (varus-valgus pivot). Connection structures were fixed to the tibial block to allow the attachment of a mini actuator, which was used to apply external forces to the test rig. Figure 3.9 shows the attachment of the mini actuator to the front of the tibial block via a linear bearing.

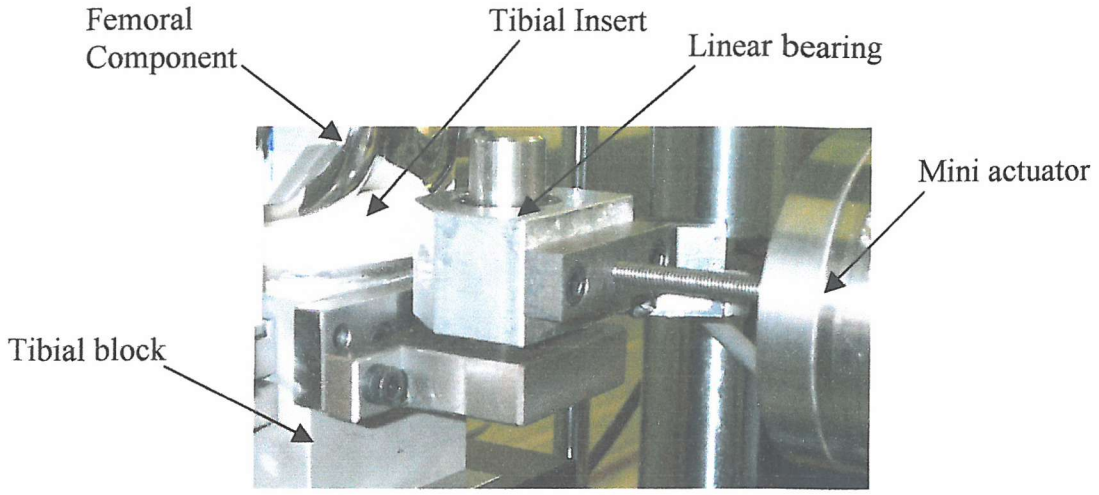

Figure 3.9 Tibial block with connection to the mini actuator.

Ligament Attachment:

Section 3.1.4 will discuss the material choice considerations, however this section will discuss the attachment of the material to the rig. The collateral ligaments were attached to the femoral section of the rig via a pin, which passed through the proximal section of the ligament and screwed into the femoral block. The same method was adopted for the femoral attachment of the PCL, with the addition of a washer to help secure the ligament and reduce the chance of the pin pulling through the PCL material. A clamp was used to attach the PCL to the tibial block (Figure 3.10). The collateral ligaments were attached to the tibial block through specially designed clamps. The clamps could displace distally and proximally up the sides of the tibial block; this allowed the addition of pre-strain or laxity to the ligaments prior to testing (Figure 3.11). A clamping method was not used for the femoral attachment of the ligaments since the relatively high stiffness of the substitute ligament material made flexion difficult. The femoral attachment of the collateral ligaments permitted rotation about the attachment pins, allowing easy knee flexion to occur.

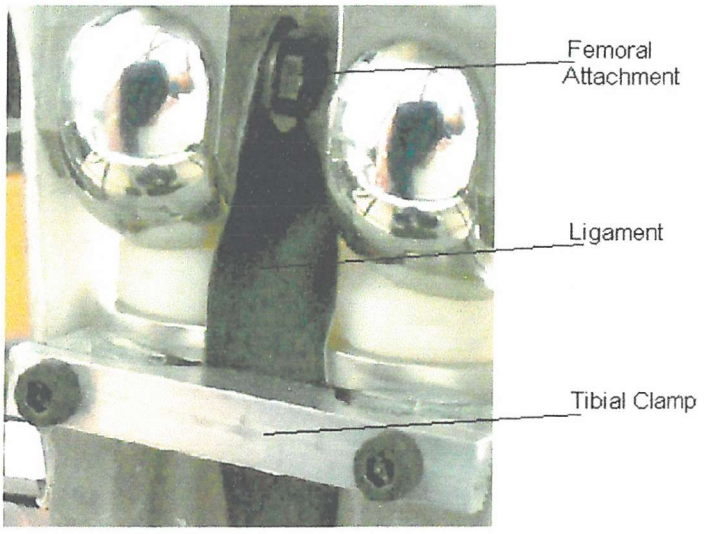

Figure 3.10 Femoral and tibial attachment of the PCL.

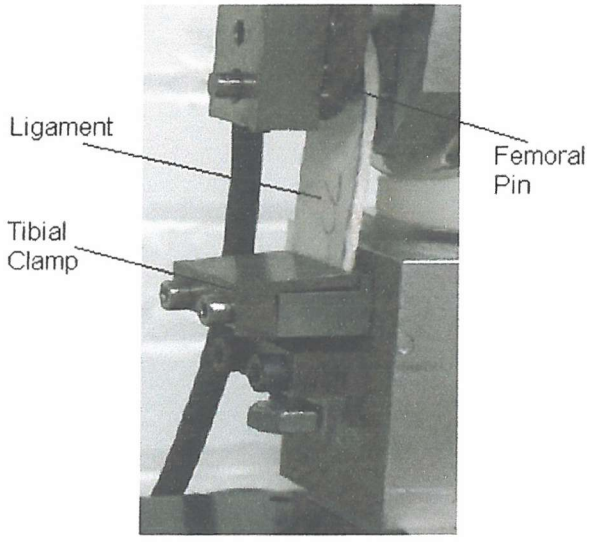

Figure 3.11 Femoral and tibial attachment of the collateral ligaments.

Displacement Measurement:

The vertical displacement and axial rotation of the femoral component could be directly recorded by the testing machine (Instron Ltd., Bucks, UK). A-P displacements, M-L displacements and insert rotations were measured by external LPDTs (Linear Potentiometric Displacement Transducer: Techni-Measure, Warwickshire, UK) (see Figure 3.12).

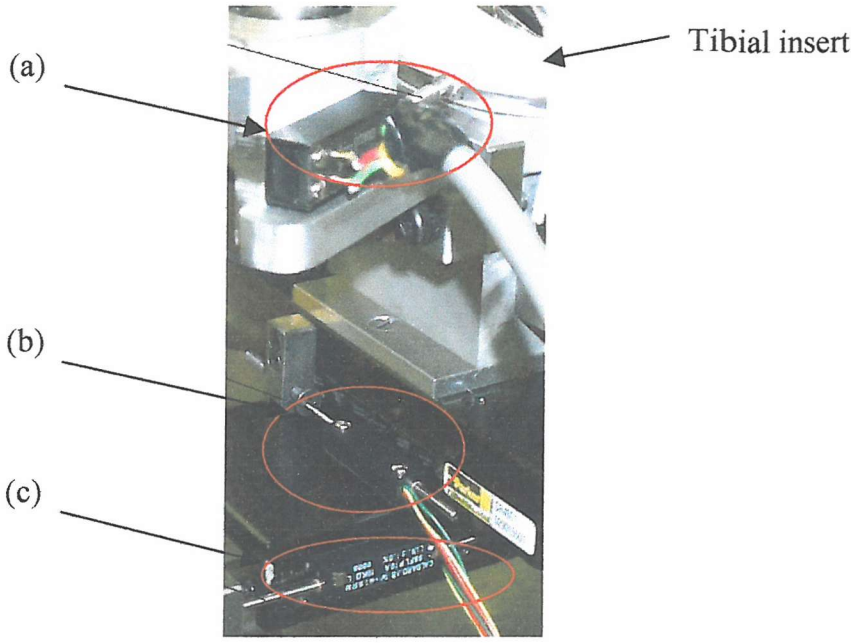

Figure 3.12 Attachment of the (a) insert rotation LPDT; (b) M-L displacement LPDT and (c) A-P displacement LPDT.

Voltage outputs were recorded on a laptop computer using Windaq data acquisition software (DATAQ Instruments, Akron, US). Voltage readings were calibrated against rotational angles and horizontal displacements prior to testing; this allowed changes in voltage to be directly related to changes in displacement or rotation.

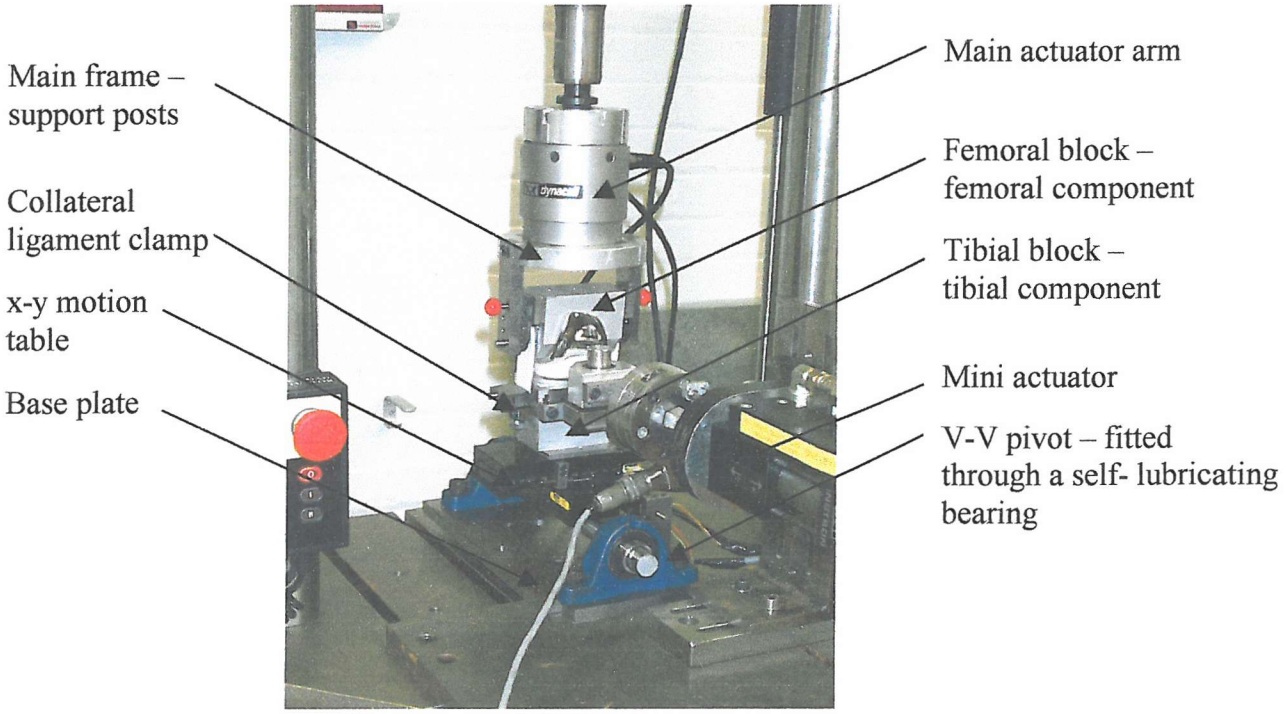

Figure 3.13 Complete setup of the new knee rig.

3.1.4 Substitute Ligament Material

Natural ligaments are very complex structures (see Section 1.2) and finding an exact material to simulate them proved problematic. It was decided that the stiffness properties of the ligaments would be the most useful characteristic to replicate in the synthetic substitute; after consideration of the literature, materials with a stiffness of about 200N/ mm, 100N/ mm and 80N/ mm were chosen to replicate the PCL, MCL and LCL respectively [57], [58]. Finding a material with these stiffness properties was a very time consuming process, particularly as there were relatively strict constraints on material dimensions (mainly due to the size of attachment zone on the rig). It was decided to use a rubber type material as it was more readily available; several sheet rubber suppliers were contacted and samples were obtained.

The samples were prepared as tensile test specimens and strained past their yield point using in house tensile test machines. Force/ extension curves were generated for all the rubber samples, and those with stiffness values relatively close to that required were checked to see if they had a suitable stiffness when using more restricted dimensions. Out of all the specimens tested the material that most closely represented the stiffness properties of the collateral ligaments was White Hypalon (synthetic rubber). This material was supplied by DRC Polymer Products Limited (Cambridgeshire, UK) and commercially one of its general applications is for waterproofing on roofs. The Hypalon was supplied in 0.5mm thick sheets, and from the tensile test data a sample 2mm thick was most appropriate to represent the ligaments. This therefore required the adhesion of four Hypalon sheets, which was a relatively simple process and required the heating of the Hypalon and pressing together to form a strong bond. From the advice of DRC (Hypalon suppliers) this process is a standard approach used for adhering sheets together, and is a process adopted by themselves. A sample 30mm wide corresponded to a stiffness of 100N/ mm and a 25mm wide sample corresponded to a stiffness of 80N/ mm. The material used to represent the PCL was also supplied by DRC Polymer Products Limited (Cambridgeshire, UK). It was a composite material (DR2079a/ DR2078a) 1mm thick, of which a sample 20mm wide possessed a stiffness of 200N/ mm. The general purpose of this material is for heat/ fireproofing. No adhesion was necessary in this case. The tensile test curves of the LCL, MCL and PCL are shown in Figure 3.14.

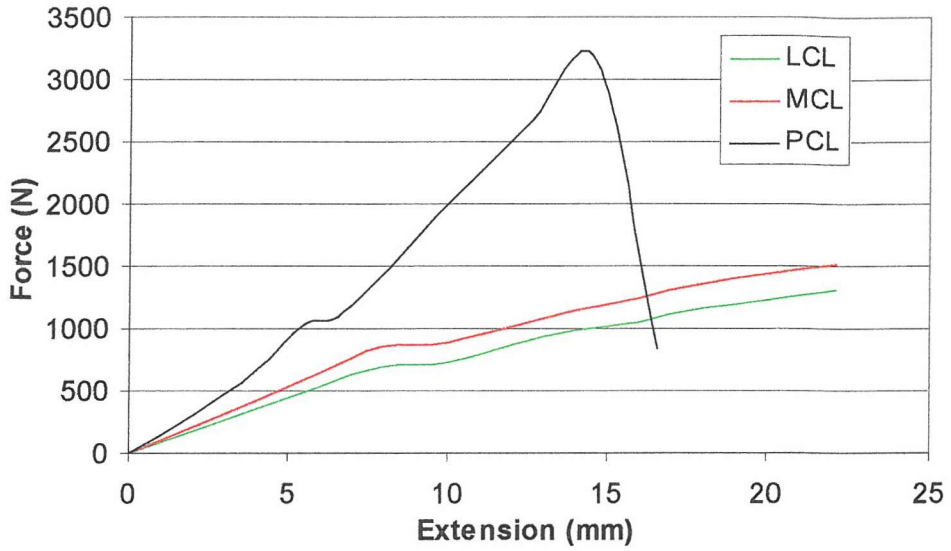

Figure 3.14 Force/ extension curves for the LCL, MCL and PCL.

When attached to the test rig the initial 0% strain length of the MCL, LCL and PCL was 58mm, 43mm and 37mm respectively. From the force/ extension curves we can see that the yield points of the MCL, LCL and PCL were 15.5%, 21.0% and 15% strain respectively.

3.2 Overview of Mechanical Testing

All testing was carried out using a servo-hydraulic bi-axial actuator (Instron Ltd, Bucks, UK), with a ±20kN tension/ compression and a ±10Nm rotational capacity. In addition a separate 1kN actuator could be fitted to provide extra testing options. This system was entirely computer controlled. Three sets of passive stability tests were performed: (i) Anterior-posterior (A-P) translation, (ii) internal-external (I-E) rotation and (iii) varus-valgus (V-V) rotation. The tests were chosen because they assess the knee in three different planes and were also well documented in the literature [12], [18], [101], [115]. In each of these separate investigations certain parameters were either kept constant or varied according to the type of test: i.e. effect of ligamentous structures on TKR stability, effect of component malpositioning on TKR stability and the sensitivity of component design to ligament strains and alignment. Four versions of the PFC Sigma knee system (DePuy, Leeds, UK) were assessed: (i) PC-retaining rotating-bearing knee (PC-RR), (ii) PC-substituting rotating-bearing knee (PC-SR), (iii) PC-retaining fixed-bearing knee (PC-

RF) and (iv) PC-substituting fixed-bearing knee (PC-SF). For a comprehensive review of the different knee designs see section 2.3.

3.2.1 Ligament Investigation

All strains in the ligaments were representative of the initial ligament strain and not the varying strain throughout testing. A 0% strain equated to the normal anatomic ligament strain in these studies. To the best of the author's knowledge, no data was available stating the exact initial strain values of knee ligaments, thus the initial 0% strain value used represents a preliminary investigation and may be subject to alteration as data becomes available. Applying 5% strain to the collateral ligaments represented a tight ligament, –5% strain represented a lax ligament. 5% strain corresponded to about a third of the ultimate strain of collateral ligaments [11]. There were two states assessed for the PCL, either a normal PCL at 0% strain or a non-functioning PCL, represented by complete removal of the ligament. All ligaments were released and then restrained after each test, and all initial strain values were calculated with the knee in the fully extended (0° flexion) position. Table 3.1 shows the different MCL/ LCL ligament strain combination tests carried out in this study when the knee components were ideally positioned (femoral and tibial component parallel to each other).

Ligament Strain	
MCL	**LCL**
Normal	Normal
Tight	Tight
Normal	Tight
Tight	Normal
Slack	Normal
Normal	Slack
Slack	Slack
Tight	Tight
Normal	Tight
Tight	Normal
Slack	Normal
Normal	Slack
Slack	Slack

Table 3.1 Ligament strain combinations assessed when the components were ideally positioned.

3.2.1.1 Straining Methods

Posterior Cruciate Ligament:

The PCL was attached to the femoral section of the rig and pulled until any slack was removed. Then, taking care not to strain the material significantly, it was clamped to the tibial section of the rig, as shown in Figure 3.5. This gave a nominal initial strain value of 0% in the PCL.

Collateral Ligaments:

0% strain in the collateral ligaments was achieved by positioning the substitute ligament into the fixation device (Figure 3.6), and removing any visible slack by displacing the tibial clamp distally. From this position any additional ligament strain was applied by further distal displacement of the tibial clamp.

3.2.2 Malalignment Investigation

In the present research the normal ideal alignment of the TKR corresponds to the femoral component being parallel to the tibial component and the tibial component at 90° to the tibial shaft axis (as shown in Figure 2.1). Testing was carried out in the neutral, 3° of varus and 3° of valgus alignment positions. A varus position was achieved by rotating the femoral component in the coronal plane so that the lateral side of the knee lowered, resulting in an overall varus position (see Figure 3.15). A valgus position was achieved by rotating the femoral component in the coronal plane so that the medial condyles lowered.

Malalignment testing was conducted with normally strained collateral ligaments and with a variety of altered ligament strains. Table 3.2 shows the different ligament strain combination tests carried out in this study when the knee components were malaligned.

Ligament Strain	
MCL	**LCL**
Slack	Slack
Normal	Normal
Tight	Tight
Slack	Normal
Normal	Slack
Tight	Slack
Slack	Tight
Tight	Normal
Normal	Tight

Table 3.2 Ligament strain combinations assessed when the components were malaligned.

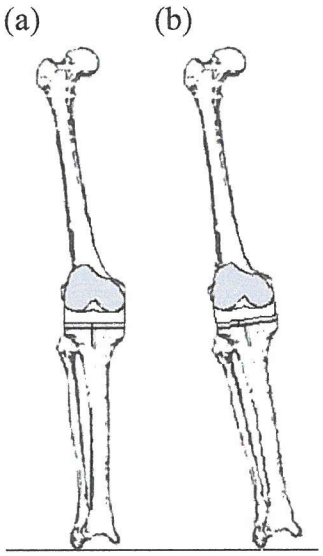

Figure 3.15 The lower extremity after TKR with (a) neutral alignment and (b) varus alignment.

3.3 Stability Testing Methods

All stability testing was performed under a 50N vertical compressive load, which was applied through the femoral section of the knee via the main actuator arm. This load was chosen since it was similar to that used in other stability tests [103], and initial testing showed it was sufficiently high to not be significantly affected by background noise (machinery vibrations etc.). Additionally, the load was relatively small; this was an important consideration since the rig was simulating passive stability testing, which would be carried out intra-operatively, when muscle forces were low.

Each test was conducted independently, i.e. the anterior test was performed separately to the posterior test, the internal test was performed separately to the external test and the varus test was performed separate to valgus test. All testing was repeated three times.

3.3.1 Anterior-Posterior Translation Stability Testing

The "Lachman test" is a common method used to investigate the integrity of the joint in the sagittal plane (A-P direction), thus it was adopted in these studies. With both collateral ligaments at 0% strain (i.e. the normal state), testing was performed over a range of knee flexion positions; these included full extension (0° flexion), 30°, 60° and 90° flexion, while applying a ±90N force. Altered ligament strain and femoral malalignment tests were carried out at 0° and 90° flexion only.

Figure 3.16 shows the experimental setup for A-P stability testing. Testing involved applying a horizontal force to the tibial section of the rig, via a mini actuator. The force ranged from 0N-90N and was applied over a one second period. A-P displacements could be measured directly from the mini actuator output, or from the A-P LPDT recording.

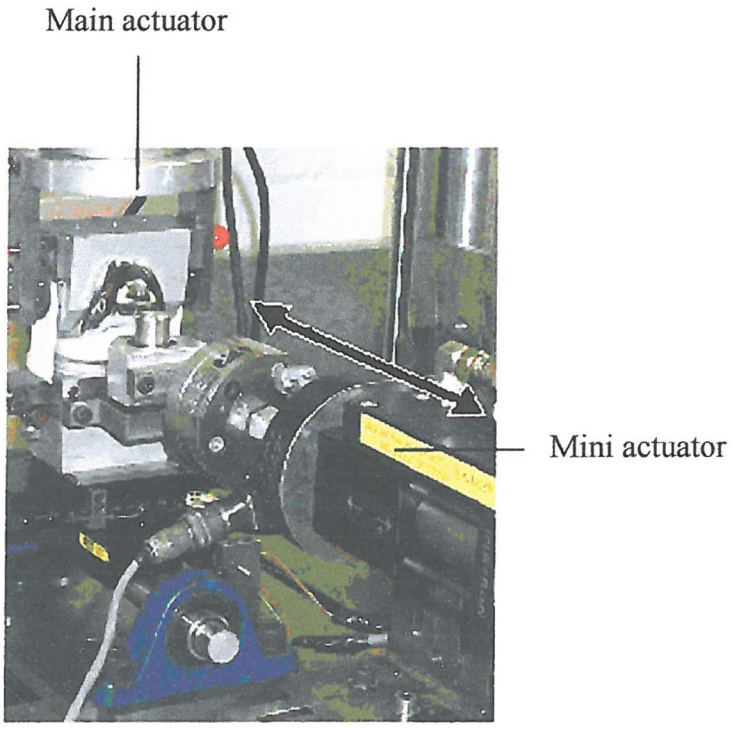

Figure 3.16 A-P translation stability testing. The arrows indicate the direction of the mini actuator movement, producing either an anterior or posterior displacement.

3.3.2 Internal-External Rotational Stability Testing

An ±8Nm torque was applied through the femoral component via the main actuator, producing internal and external rotations. The torque was applied from 0Nm-8Nm over a three second period, with a positive torque producing an internal femoral rotation and a negative torque producing an external femoral rotation. 8Nm was chosen as it was comparable to testing in the literature [12]. In the neutral position with both collateral ligaments normally strained, testing was performed at 0°, 15°, 60° and 90° flexion. I-E stability testing is normally performed with the knee flexed to 20° and 80°; however 15° and 90° flexion were chosen in the present study as they were the closest flexion angles available with the knee rig. All other tests, including ligament imbalance and femoral malalignment were carried out with the knee flexed at 15° and 90° only. Figure 3.17 shows the experimental setup for I-E rotational stability testing.

Figure 3.17 I-E rotational stability testing. The arrows show the rotations produced through the main actuator.

For the rotating-bearing knee designs, tibial insert rotations and femoral rotations were recorded. Femoral rotations were recorded on the Instron computer software while the tibial insert rotations were calculated from the LPDT readings (see section 3.1), which

were logged onto a laptop computer using Windaq data acquisition software (DATAQ Instruments, Akron, US).

3.3.3 Varus-Valgus Rotational Stability Testing

A system was devised so that a medial and lateral force could be applied to the tibial section of the rig via a mini actuator to produce varus and valgus tibial rotations (Figure 3.11). A ±100N horizontal force, which equated to about a 7Nm rotational torque with the present rig setup, was applied to the tibial section of the knee. Initially a 12Nm torque was chosen, as it was comparable to that used in other studies reported in the literature [12]; however, testing with certain knee prostheses produced excessive medial-lateral movements, thus a lower 7Nm torque was chosen. Testing was performed at full extension only due to restrictions in the valgus-varus measurement techniques. An LPDT was positioned to record the opening of either the medial or lateral side of the knee during testing, which could then be used to calculate the varus-valgus rotations. The LPDT was positioned to push against a post attached on the femoral block (see Figure 3.18). However, when the knee was placed at other flexion angles the LPDT could not function correctly, which this limited testing to one flexion position.

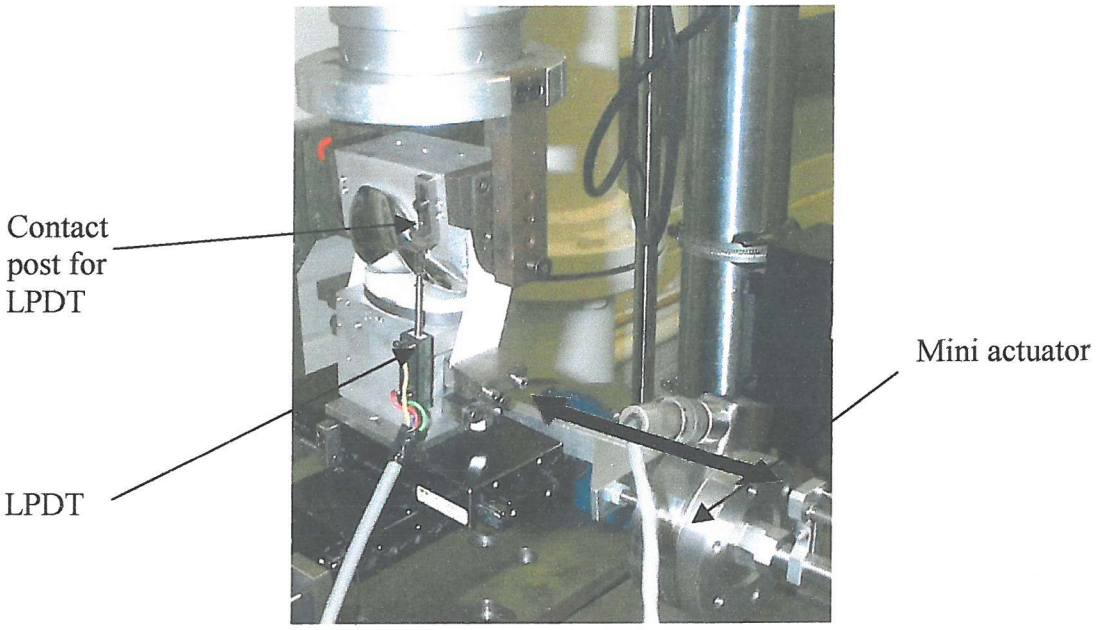

Figure 3.18 V-V rotational stability testing. The arrow indicates the direction of applied force.

3.3.4 Total Knee Designs Investigated

Figure 3.19 shows the four different knee designs that were tested in this research. Two femoral components were used, a PC-retaining design and a PC-substituting design. Each femoral component could be used with two tibial inserts, either a fixed- or a rotating-bearing. All knees were subjected to the same testing protocols so that direct comparisons could be made between the four different designs.

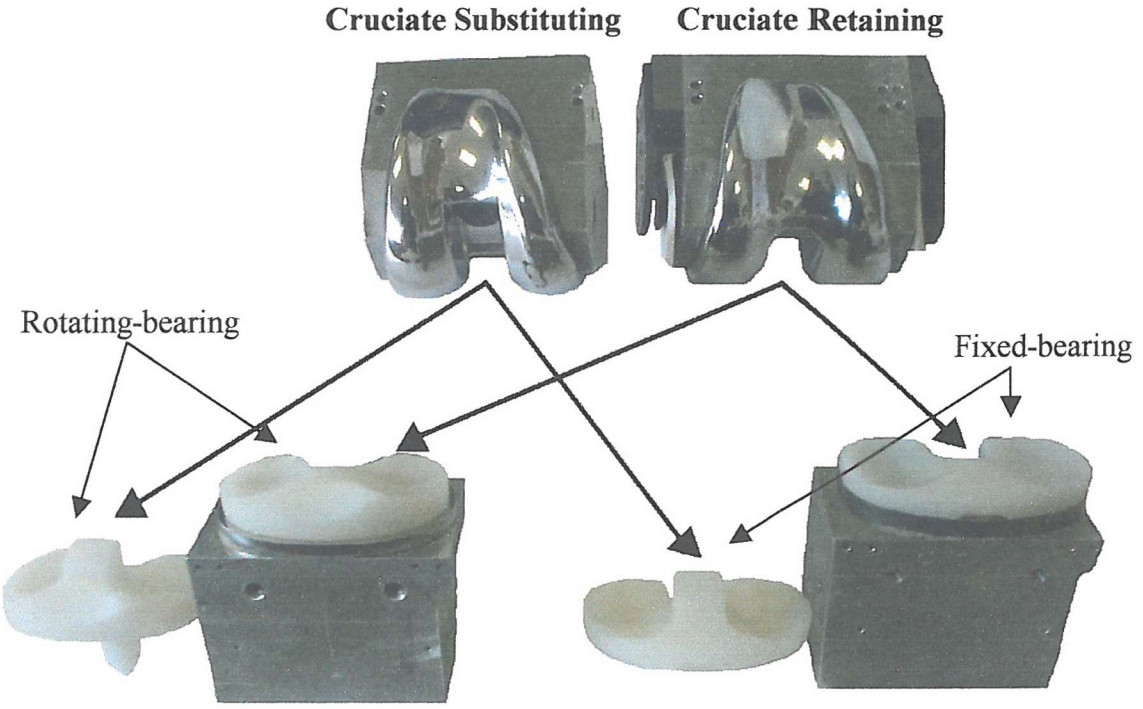

Figure 3.19 Knee designs tested during the passive stability study.

The PC-retaining fixed-bearing knee has a low conformity design with the tibial insert firmly attached to the tibial tray. The low conformity permits axial rotation of the femoral component with reduced restriction, however it also promotes small contact areas and therefore potentially higher contact stresses. The knee is designed to allow the retention of the PCL. The PC-retaining rotating-bearing knee also allows the PCL retention; however the tibial insert can axially rotate on the tibial tray, therefore shifting the rotation point from the insert/ femoral component and onto the insert/ tray. This change allows the insert and femoral component to have a much higher conformity, which in turn significantly increases the contact areas and reduces the contact pressures. The PC-substituting knees follow the same design issues as the PC-retaining knees but are designed to be used without the PCL, and with this in mind they have a tibial spine

protruding from the tibial insert. The function of this spine is to control femoral rollback during flexion, which is thought to be controlled by the PCL in anatomic knee; in addition it also provides increased A-P and M-L stability. The reader is referred to section 2.3 for more information on the different knee types.

3.3.5 Repeatability and Reproducibility of the Knee Rig

The purpose of the knee rig was to provide anatomically realistic simulations of passive stability testing after TKA. In this research large quantities of tests were to be carried out over a significant period of time, and therefore the repeatability and reproducibility of the rig were important issues. To quantify these characteristics the results of testing from Chapter 4 were assessed as they provided information on repeat tests and also testing that had taken place after the rig had been removed from the test machine and replaced for further evaluation. Three tests were conducted for each individual simulation, thus an average and standard deviation could be calculated along with the average % variation among the results. For the representation of repeatability/ reproducibility an ideally conditioned PC-RR was assessed at 0° flexion over each passive stability test. Table 3.3 shows the repeatability and reproducibility findings. The repeats represent testing carried out on one day and the reproducibility represents testing that was carried out on two separate occasions when the rig had been removed and replaced for further testing.

The results shown in Table 3.3 highlight that the rig possessed good repeatability and reproducibility characteristics, and all individual results lay within 6% of each other.

Stability Test	Repeat Test	Standard Deviation	Average % variation	Reproducibility Tests (Average(S.D.))	Standard Deviation	Average % variation
A-P (mm)	4.6	0.2	4	4.6(0.2)	0.1	2
	4.4			4.9(0.3)		
	4.8					
I-E (°)	54.1	1.7	3	54.1(1.7)	2.0	4
	55.8			56.9(2.0)		
	52.4					
V-V (°)	5.0	0.3	6	5.0(0.3)	0.3	6
	5.3			4.6(0.3)		
	4.7					

Table 3.3 Repeatability and reproducibility of the mechanical test rig. (S.D.=standard deviation)

3.4 Experimental Contact Pressure Measurement

Contact pressures were recorded experimentally to provide another means of validation against the finite element models in the present research (see Chapters 5 and 6). Motions of the different knee designs were assessed experimentally (see Chapter 4) and could be compared to the finite element models; however, with the addition of contact pressure measurements a conclusive comparison could be made between the experimental and computational simulations (see Chapter 6). In the present research a Tekscan pressure measurement system† (K-scan sensor: Tekscan Inc., Boston, US) was used to measure the contact pressures across the tibial bearing surfaces.

Justification for the use of Tekscan:

The Tekscan system was operator friendly and allowed continuous data monitoring during testing; this was an immediate advantage over other pressure recording systems, such as Fuji film. Harris *et al.* [25] compared the Tekscan sensor equipment (K-Scan 4000) to several grades of Fuji film, including 'Ultra Super Low' (USL), 'Super Low', 'Low' and 'Medium' levels, which recorded from 0.2MPa-0.6MPa for USL to 9.8MPa-49MPa for Medium. It was shown that the Fuji film had limitations when determining the contact areas, and this has also been reported in other studies [116]. Compared to the K-Scan findings by Harris *et al.* [25], the Fuji method underestimated the contact areas by between 11%-30%. Harris also noted that the Tekscan system enabled easy, reproducible and reliable measurements of contact areas at different loads and flexion angles. In the present research repeatability was demonstrated in terms of similar contact areas and pressures. From Tests 1 to 3 (Appendix 2) the paths of the dynamic simulations were very similar, with contact areas and magnitudes comparable in each test.

However, the Tekscan system does have some limitations. The sensor, though thin (0.1mm), had a finite thickness that may have altered the contact area and pressure measurements by altering the topography of the bearing surfaces [117]. The Tekscan sensors are affected by temperature; therefore in the present research the sensors were calibrated in the laboratory directly before testing was conducted. One possible source of

† The Tekscan pressure system was kindly loaned by DePuy Orthopaedics (Warsaw, IN, US)

error may have been the fact that creep of the sensor material could occur with prolonged loading, therefore testing was conducted as quickly as possible to avoid such an occurrence. Another possible drawback of the Tekscan system was that the sensor had to be attached to a computer via a coupler (which could make it awkward to position), and the testing apparatus had to allow access for this connection.

The Tekscan system used in the present research consisted of thin sensor films that could be placed between the bearing surfaces of the implants; Iscan software was used to record and analyse the results. Figure 3.20 shows the Tekscan system sensor pads. The remainder of the Tekscan system kit consisted of a sensor handle (S/ N 2197), which housed the sensor; this was connected to an IBM ThinkPad laptop computer with docking station. Iscan software was used to visually display the contact pressure outputs in real-time. Options were available to take a snapshot recording at a particular moment in time, or to record over a period of time. Figure 3.21 shows the whole system setup; care was taken not to damage the sensors during testing, particularly at the ligament attachment areas.

The Tekscan system sensors (CH/ 4001/ 0997Y1/ 35 000 150@10k) measured from 198PSI-17 000PSI (~1.4MPa-117MPa). The sensors had two separate sensing areas measuring 33mm x 22mm and 0.1mm thick and consisted of 26 rows x 22 columns with intersection points that formed the sensing location. Each sensing area therefore comprises 572 individual sensors or "sensels".

Some slight difficulties arose due to the curvature of the insert on which the sensors were fitted. Even though the sensors were relatively thin (0.1mm) and flexible they did not retain their shape and continuously tried to return to their original flat state. Fixation was achieved by positioning the sensors over the tibial condyles and applying a low load through the femoral component (10N-20N). This load brought the femoral and tibial components together and caused the sensors to deform into the tibial condyles. At this point care was taken to adjust the sensors so that no folding or crimping was present. The next step involved securing the anterior and posterior sensor flaps to the tibial block, as shown in Figure 3.22, and applying tape to hold the sensors in position. The axial load was then removed so that no polyethylene creep occurred (a potential error source). Due to time and setup logistics the PC-retaining fixed-bearing knee was chosen for this study.

This implant possessed the lowest geometric constraint and condylar curvature of all the knees in this study, meaning that the sensors could be placed relatively easily onto the tibial bearing surfaces. Ideally the contact pressures of all four knee types would be measured experimentally; however this could have been problematic, particularly with the PC-substituting knees where the tibial spine would interfere with the sensor positioning and attachment.

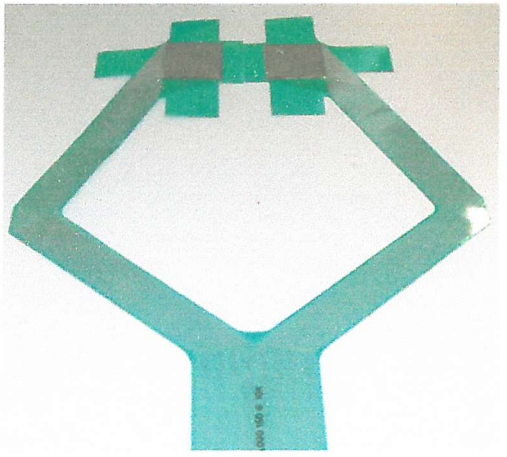

Figure 3.20 Tekscan system pressure sensor pads.

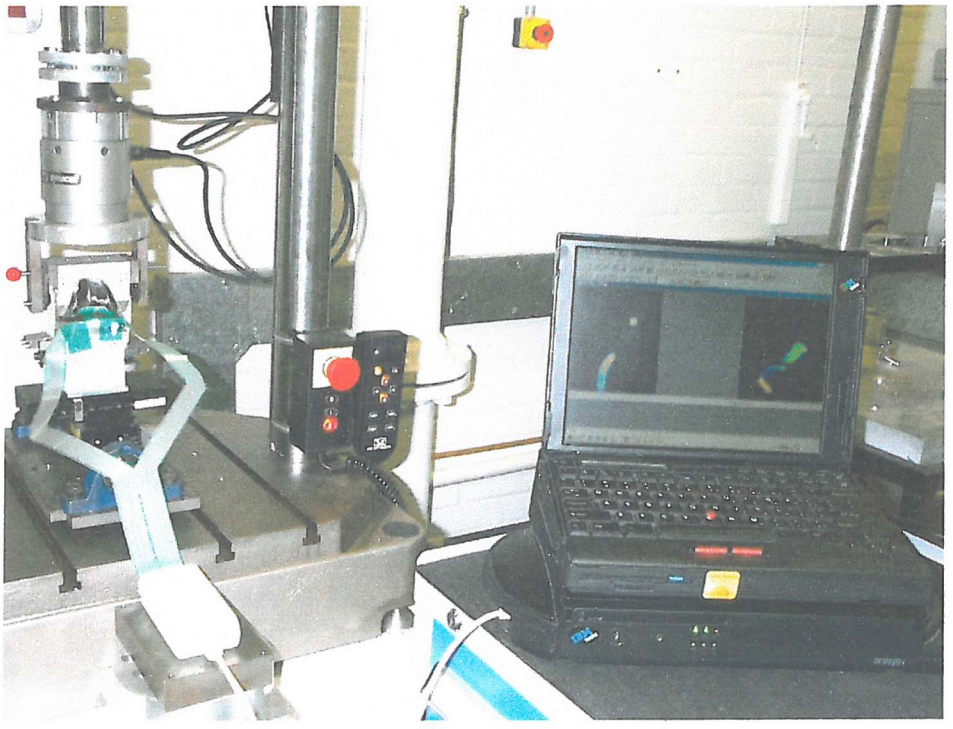

Figure 3.21 Tekscan system setup, showing the placement of the sensors and the attachment to the IBM laptop with a visual read out.

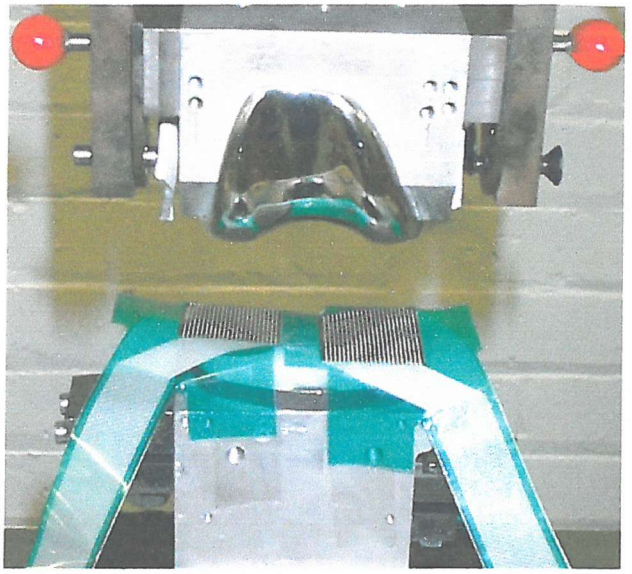

Figure 3.22 Positioning and fixation of the sensor pads.

Sixteen tests (some of which were repeats) were conducted, which simulated scenarios such as ligament imbalance and malalignment (see Table 3.4). Positioning and attachment of the sensors on the test rig only allowed I-E rotational stability testing to be conducted, as both A-P and V-V stability testing would require extra rig attachments that would impede the sensors. Calibration of the sensors was required before testing, and this was achieved by applying a 200N (ramped) vertical load to the sensors via the femoral component. Once the calibration process was complete the compressive load was removed, minimising the risk of polyethylene creep. Calibration was performed at the beginning of each testing session.

Repeatability of the pressure measurements:

The raw contact pressure data is shown in Appendix 2. All repeat tests demonstrated comparable contact areas and contact pressures. Of the repeat contact pressure measurements the maximum deviation was 1.7MPa between the three sets of results, however the average standard deviation was just 1.2MPa. During the dynamic motion paths the contact pressures recorded were ~13MPa, and the repeat measurements lay within 6% of each other. Tests 10 and 11 were repeats of tests 1 to 3 with the addition of Vaseline as a lubricant. This was applied to the sensor pads and femoral component to minimise any possible effects of friction. It was shown that results with and without lubrication were similar, and that lubrication was not necessary during the experimental

contact pressure measurements. The effect of shear forces may have been an issue and could have contributed to possible inaccuracies; however, these tests addressed this concern.

		Ligament State				
Test	**Femoral Alignment**	**MCL**	**LCL**	**Flexion Angle (°)**	**Applied Load (N)**	**Description of Test (duration 3secs)**
1	***Neutral***	Normal	Normal	0	50	-8Nm torque applied, causing external femoral rotation
2		Repeat of Test 1				
3		Repeat of Test 1				
4		Slack	Tight	0	50	-8Nm torque
5		Slack	Tight	15	50	-8Nm torque
6		Tight	Slack	0	50	-8Nm torque
7		Tight	Slack	15	50	-8Nm torque
8		Normal	Normal	0	50	+8Nm torque applied, causing internal femoral rotation
9		Repeat of Test 8				
10		Repeat of Test 1 except lubrication (Vaseline) was applied to bearing surfaces				
11		Repeat of Test 10				
12	***Varus***	Normal	Normal	0	50	-8Nm torque
13		Repeat of Test 12				
14		Slack	Normal	0	50	-8Nm torque
15	***Neutral***	No Ligaments		0	100	15° internal femoral rotation
16	***Valgus***	No Ligaments		0	200	Snapshot of pressure distribution

Table 3.4 Experimental contact pressure investigations carried out.

3.5 Possible Experimental Uncertainties

As with all experimental testing there were instances where experimental error may have arose. The exact effect of each possible error source could not be represented, however a ranking system has been devised to show the circumstances that may have provided a more significant effect. The rank of 1 represents the greatest possible effect.

1 - Ligament factors:

Accurate ligament straining: When applying pre-strain or laxity to the ligaments there was a possibility of over- or under-straining. Care was taken to firstly apply normal strain to the ligaments, and then from this position care was taken to avoid over-strain or under-strain. Rotating the screw connected to the distal portion of the ligament allowed the ligament to be stretched or compressed, and since the thread size of the screw was known accurate straining could be achieved. Due to the large amount of testing that was conducted there may have been slight variations across the tests; however, these would be minimal.

Specimen degeneration: Over many tests fatigue or over-straining of the ligaments may occur. The visual effect may not be obvious; however, the performance of the material may be compromised. To avoid specimen degeneration the ligament material was replaced at regular intervals. The same procedure was adopted if there was concern about the ligament's performance. The replacement ligament material came from a common batch, and was prepared in an identical manner.

Temperature variations: Cooler environments caused the ligament material to become stiffer in appearance, with the opposite occurring in warmer environments. Testing was performed over long periods of time and regulation of temperature in the laboratory was not possible. To minimise temperature effects the ligaments were warmed before testing to a constant temperature. Again, due to the long testing times and the number of investigations carried out slight variations in ligament temperature may have occurred; however the overall effect on the results was anticipated to be low.

Ligament preparation: The ligaments consisted of four 0.5mm thick sheets adhered together. During the adhesion process there was the possibility of air bubbles, deformation, or poor adhesion across the samples. To avoid these detrimental effects the same methodology was adopted when compiling the ligaments, and if the ligament properties were suspected of being compromised they were discarded.

2- LPDT Measurements:

LPDTs were used to record various motions during the passive stability testing. Errors may occur due to the sensitivity of voltage change in relation to rotation/ displacement outputs. For example during V-V rotational testing motions of ~1° are recorded, therefore slight alterations in voltage change could result in slight alterations in recorded angles, which would have been significant. All LPDT were carefully calibrated and all voltages were carefully recorded to minimise this possible error source.

3- Alignment of the Components:

During malalignment simulations slight variations in coronal femoral alignment may have occurred. Grub screws were raised and lowered on the underside of the femoral alignment plate to achieve femoral malalignment (see Chapter 3). Alignment was measured accurately using a technician's protractor (with guide arm attached).

4- Consistent Apparatus Performance:

All forces and torques applied during the experimental testing were controlled by the main test machine (Instron, Bucks, UK). Over time changes in oil condition and pressure may alter the accuracy in performance; this can result in slow response times to load and displacement changes, or inaccurate loading patterns. At the beginning of each testing session the force output curves generated by the Instron actuator were compared to the ideal loading curves. If deviations between the two curves were present the PID (Proportional, Integral, Differential) settings were checked and tuned to give the most accurate response. An auto-tune option was available to allow large deviations to be corrected, and manual alterations were conducted for small differences.

Although all of these error sources were possible, care was taken during each phase of testing to minimise their effects. Each individual investigation was conducted as close as possible to the previous one, and if there was any evidence of an error the test was discarded in favour of a new test.

Chapter 4 Passive Stability Testing: Results and Discussion

The number of results obtained in this study is such that a presentation and discussion of each individual result would be exhaustive and beyond the scope of the present thesis. For the reader however, select results have been chosen and presented in Chapters 4, 6 and 8 of this thesis to demonstrate trends and highlight the most significant effects of component alignment and ligament strains on the specific knee types.

Sections 4.1 to 4.4 discuss the A-P, I-E and V-V stability of each knee design in the idealised condition (neutral alignment position when both collateral ligaments normally strained). Section 4.5 then compares the general stability of all idealised knee types.

4.1 Analysis of the PC-Retaining Rotating-Bearing Knee (PC-RR)

Anterior-Posterior Translation Stability

All A-P stability results are presented in Tables 1 and 2 in Appendix 1. These show the neutrally aligned knee and malaligned knee results respectively. The idealised knee findings are discussed below.

As the knee was flexed the conformity between the components reduced, resulting in increased translations. At 30° flexion a slight gap was formed posteriorly between the tibial and femoral components, which gave rise to the increased displacements. Further flexion shifted the contact position between the components posteriorly on the insert; this reduced the component restraint to posterior tibial translations, hence the increased posterior movements noted at 90° flexion (see Figure 4.1). Figure 4.2 illustrates the changing conformity and component restraint at different flexion angles.

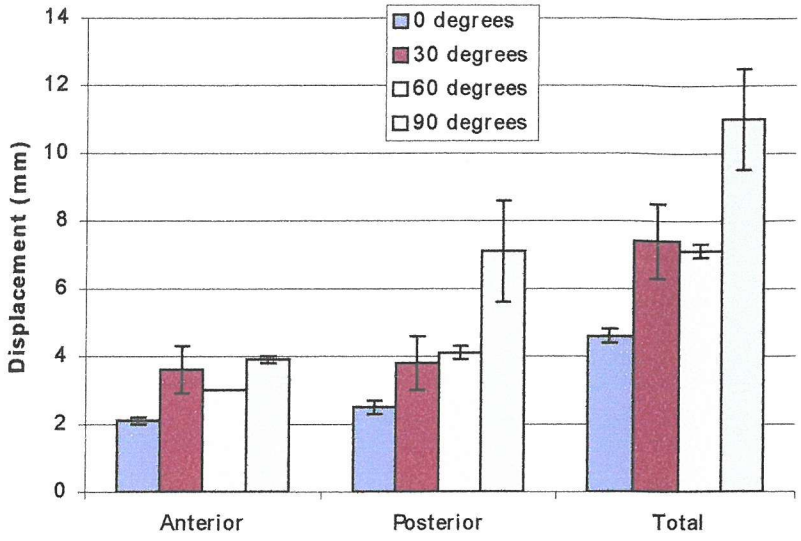

Figure 4.1 A-P translations over the flexion range of the PC-RR. Displacements refer to the tibial component with respect to the femoral component.

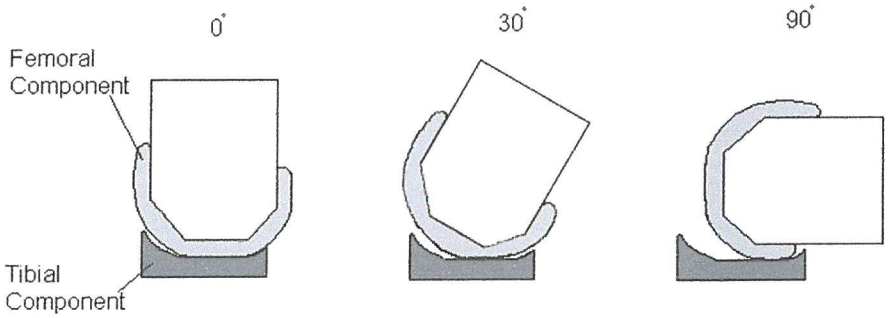

Figure 4.2 Illustration of how the component conformity/ restraint changed with flexion.

The flexion position statistically (ANOVA)[†] altered A-P stability ($F= 220.2_{3,8}$ $p<0.05$); total displacements ranged from 4.0mm to 9.2mm over the entire flexion range. This finding highlighted that care must be taken to ensure that the flexion angle was constant when assessing A-P stability.

[†] ANOVA (analysis of variance) can look for an overall difference between the mean scores in two or more samples. Degrees of freedom are calculated and a critical F-statistic value (normally 95% chance that samples are different, $p<0.05$) is chosen from an F-distribution table. The F-statistic value is calculated for a particular set of samples (F= average sum of squares due to group differences / average sum of squares due to subject differences), and if it is larger than the critical value then the samples can be viewed as statistically different. The data is normally represented as $F= X_{a,b}$, $p<0.05$, where X is the value of F-statistic, a is the number of sample groups minus 1, and b is the total number of samples minus the number of sample groups. For example, if there are 4 flexion positions (groups) and 3 sets of results for each position (samples), then a= 4 - 1= 3, and b= (3 x 4) – 4= 8.

Internal-External Rotational Stability

All I-E stability results are presented in Tables 3 and 4 in Appendix 1. These show the neutrally aligned knee and malaligned knee results respectively. The idealised knee findings are shown below.

A change in flexion angle did not cause I-E laxity to alter significantly ($F= 1.1_{3,8}$, $p<0.05$); however there was a slight increase in femoral rotations noted from 0° to 90° flexion (see Figure 4.3). The high conformity between the tibial insert and femoral component at full extension caused the insert rotations to follow those of the femoral component; however, as flexion increased the component conformity reduced, resulting in greater sliding between the components and a reduction in insert rotation (see Figure 4.3).

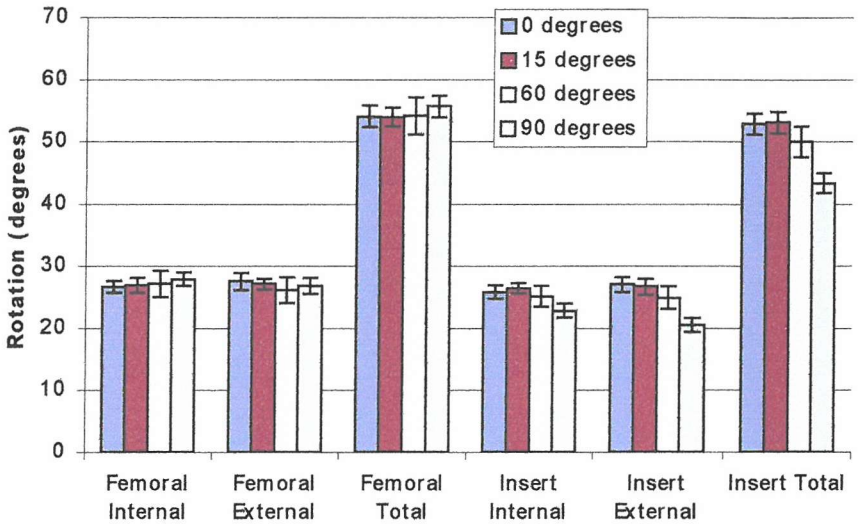

Figure 4.3 Femoral and insert I-E rotations of the PC-RR over the flexion range.

Varus-Valgus Rotational Stability

All V-V stability results are presented in Tables 5 and 6 in Appendix 1. These show the neutrally aligned knee and malaligned knee results respectively. The idealised knee findings are shown below.

A varus rotation relates to the lateral side of the knee and valgus relates to the medial; for example a 4° varus rotation equates to the lateral side of the knee opening by 4°.

It was observed that varus rotations were significantly larger than valgus rotations. Varus rotations of 4.3± 0.2° and valgus rotations of 0.7± 0.2° were recorded (see Figure 4.4).

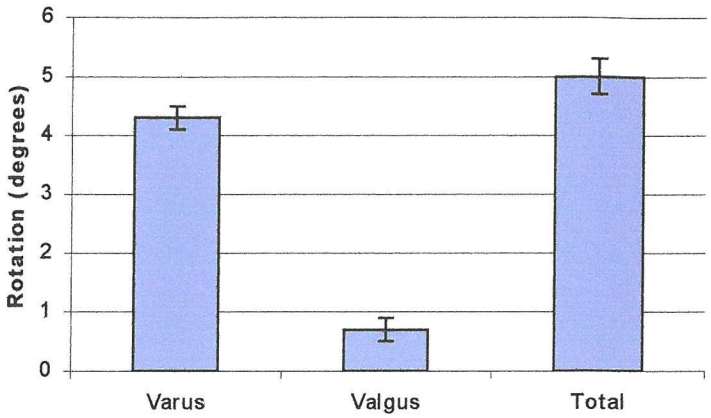

Figure 4.4 V-V stability of the PC-RR. Rotations refer to the tibial component with respect to the femoral component.

4.2 Analysis of the PC-Substituting Rotating-Bearing Knee (PC-SR)

Anterior-Posterior Translation Stability

All A-P stability results are presented in Tables 7 and 8 in Appendix 1. These show the neutrally aligned knee and malaligned knee results respectively. The idealised knee findings are shown below.

Total A-P translation was constant over the flexion range, differing by just 1.6mm from 0° to 90° flexion (see Figure 4.5). Anterior displacements increased steadily with flexion, which was most likely due to the changing component conformity. Posterior translations fluctuated slightly from 0° to 60° flexion, then dropped significantly at 90° ($F= 46.1_{1,4}$ $p<0.05$ from 60° to 90°). The sudden reduction in posterior displacements was caused by the interaction of the tibial spine and femoral cam. At 90° flexion the initial contact position between the components placed the spine of the insert close to the cam of the femoral component; thus, posterior motion was immediately hindered by their interaction.

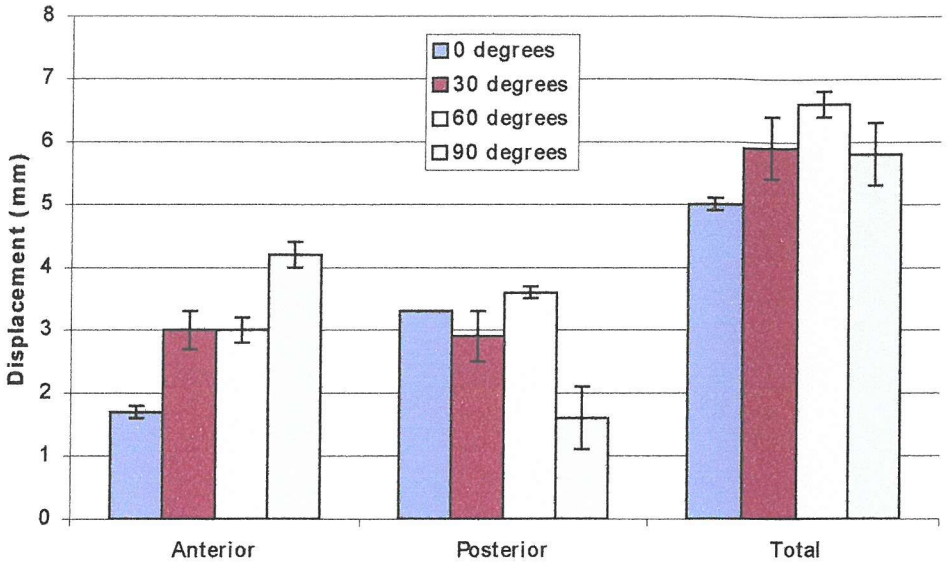

Figure 4.5 A-P stability of the PC-SR. Displacements refer to the tibial component with respect to the femoral component.

Internal-External Rotational Stability

All I-E stability results are presented in Tables 9 and 10 in Appendix 1. These show the neutrally aligned knee and malaligned knee results respectively. The idealised knee findings are shown below.

When both collateral ligaments were normally strained flexion position did not significantly affect I-E stability ($F= 3.4_{3,8}$, $p<0.05$). In general there was an incline in total rotations from 0° to 90°; however, due to the relatively large standard deviations this was not significant (see Figure 4.6). In general the tibial insert rotations did not significantly change over the flexion range; however, at 15° flexion the insert rotations were noticeably larger. The larger femoral rotations at 15° flexion and the lower insert rotations at 60° flexion make this result more prominent.

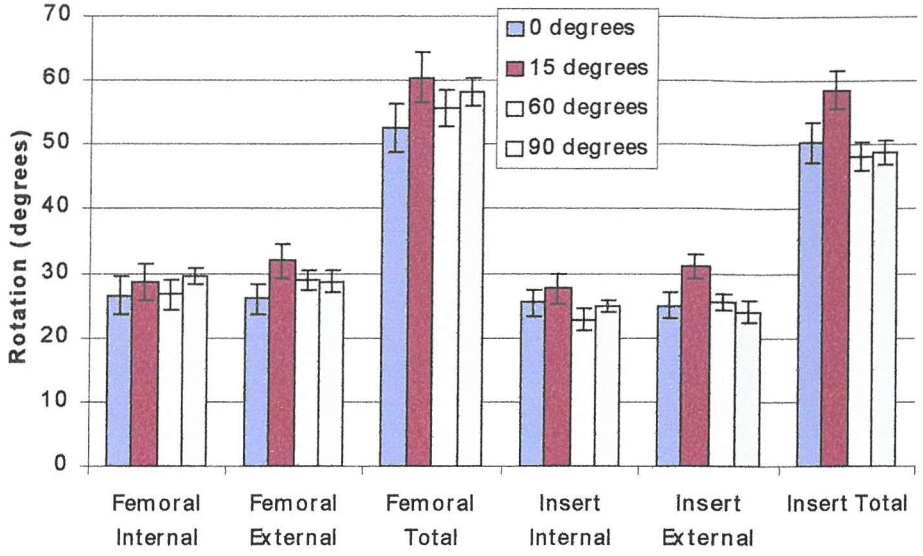

Figure 4.6 Femoral and insert I-E rotations over the flexion range for the PC-SR.

Varus-Valgus Rotational Stability

All V-V stability results are presented in Tables 11 and 12 in Appendix 1. These show the neutrally aligned knee and malaligned knee results respectively. The idealised knee findings are shown below.

Total V-V rotations of 5.9± 0.6° were recorded with the PC-SR (see Figure 4.7); varus rotations were significantly larger than valgus rotations (4.3± 0.6° and 1.6± 0.2° respectively).

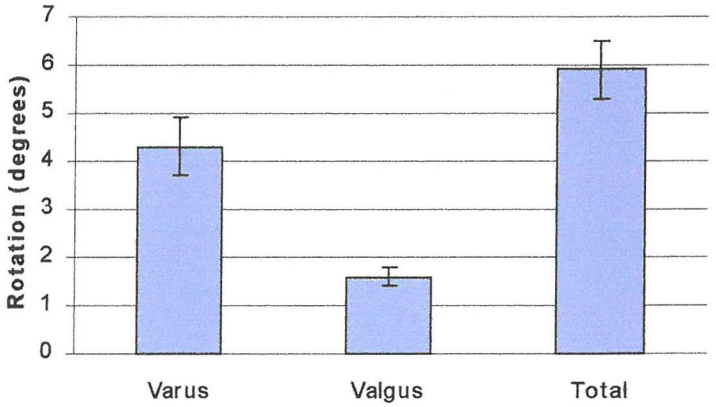

Figure 4.7 V-V stability for the PC-SR. Rotations refer to the tibial component with respect to the femoral component.

4.3 Analysis of the PC-Retaining Fixed-Bearing Knee (PC-RF)

Anterior-Posterior Translation Stability

All A-P stability results are presented in Tables 13 and 14 in Appendix 1. These show the neutrally aligned knee and malaligned knee results respectively. The idealised knee findings are shown below.

The anterior translations were relatively constant over the flexion range, with posterior translations increasing from 0° to 30° flexion, then remaining constant at 60° and 90° flexion. The total A-P displacements increased steadily from 0° to 90° flexion (see Figure 4.8).

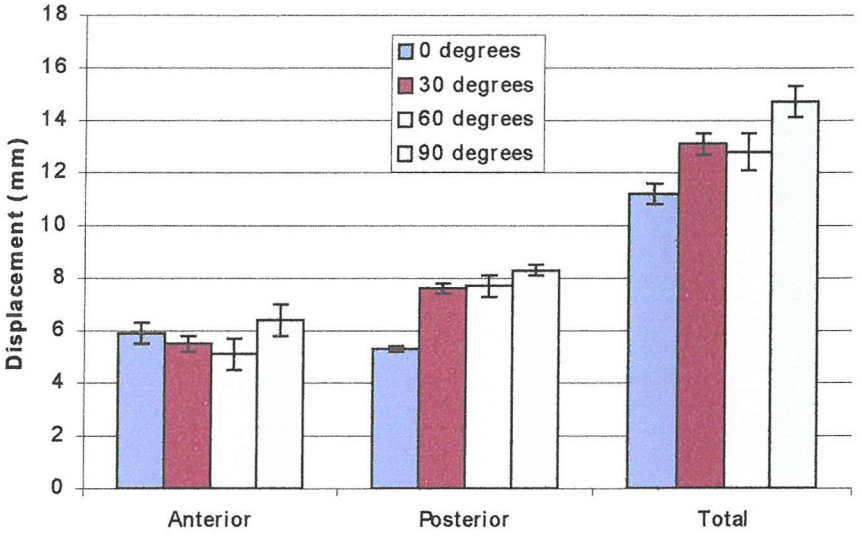

Figure 4.8 A-P stability over the flexion range for the PC-RF. Displacements refer to the tibial component with respect to the femoral component.

Internal-External Rotational Stability

All I-E stability results are presented in Tables 15 and 16 in Appendix 1. These show the neutrally aligned knee and malaligned knee results respectively. The idealised knee findings are shown below.

Flexing from 0° to 60° did not significantly alter the I-E stability of the PC-RF; however from 60° to 90° flexion the rotations significantly increased (~6°). Internal and external rotations were similar across the flexion range, as shown in Figure 4.9.

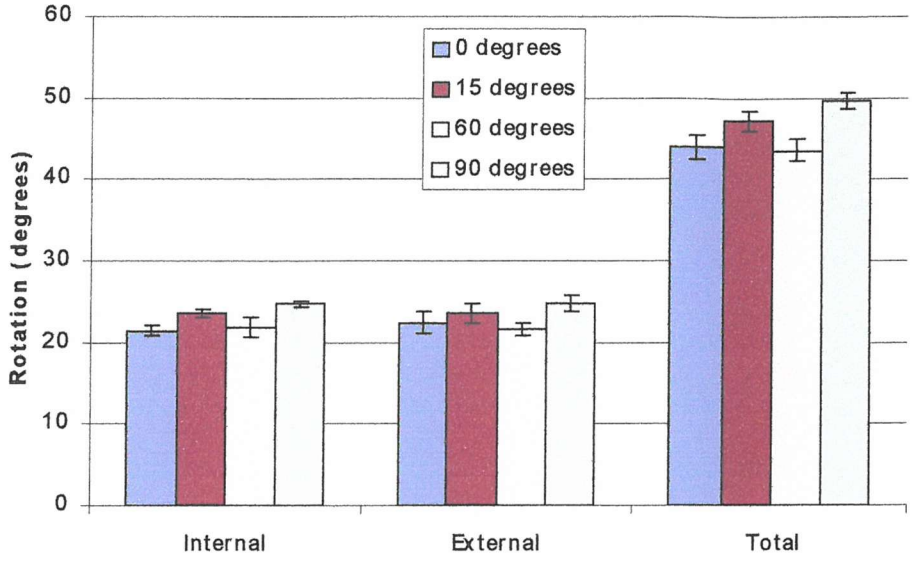

Figure 4.9 I-E stability of the PC-RF over the flexion range. Rotations refer to the femoral component with respect to the tibial component.

Varus-Valgus Rotational Stability

All V-V stability results are presented in Tables 17 and 18 in Appendix 1. These show the neutrally aligned knee and malaligned knee results respectively. The idealised knee findings are shown below.

The V-V stability of the PC-RF was similar to the V-V stability of the other knees tested in this study; varus rotations were significantly larger than valgus rotations (4.4± 1.5° and 1.3± 0.5° respectively) (see Figure 4.10). The amount of medial-lateral (M-L) tibial displacement that accompanied the varus and valgus rotations was larger in the PC-RF than with any of the other knees. An M-L displacement limit that was set to avoid excessive movement, possibly leading to M-L dislocation, was tripped during varus stability testing; this meant that an average torque of 6Nm was applied (target torque of 8Nm) during varus stability testing.

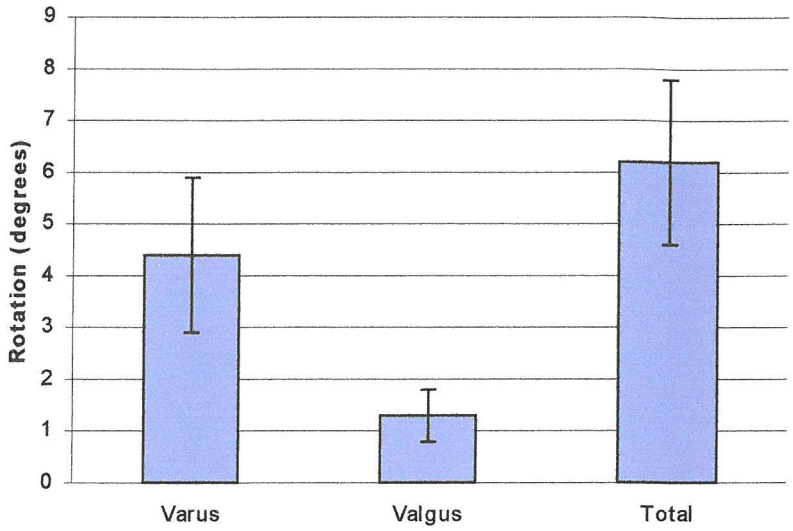

Figure 4.10 V-V stability of the PC-RF. Rotations refer to the tibial component with respect to the femoral component.

4.4 Analysis of the PC-Substituting Fixed-Bearing Knee (PC-SF)

Anterior-Posterior Translation Stability

All A-P stability results are presented in Tables 19 and 20 in Appendix 1. These show the neutrally aligned knee and malaligned knee results respectively. The idealised knee findings are shown below.

From 0° to 30° flexion there was no significant alteration in A-P translations, thereafter they reduced; most significantly at 90° flexion (see Figure 4.11). At 60° and 90° flexion the posterior tibial displacements were significantly reduced by the interaction of the tibial spine and femoral cam.

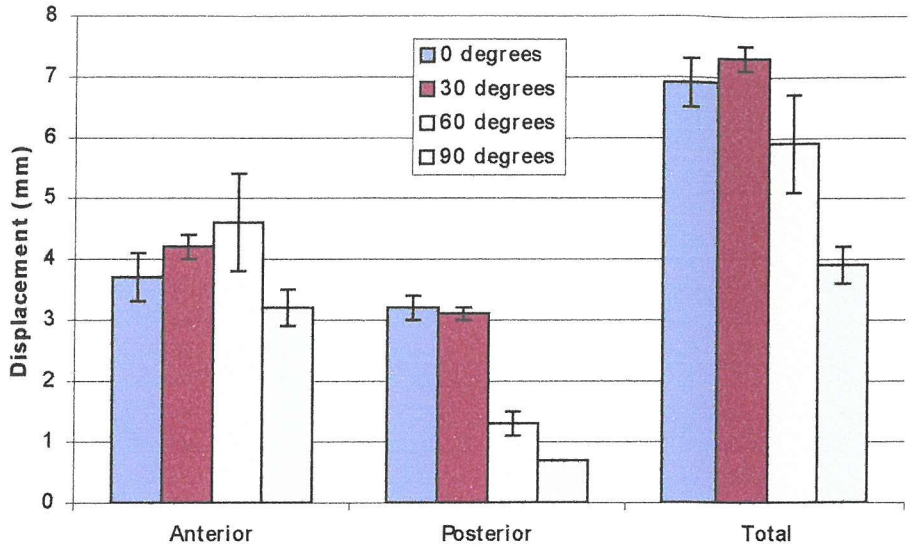

Figure 4.11 A-P stability of the PC-SF over the flexion range. Displacements refer to the tibial component with respect to the femoral component.

Internal-External Rotational Stability

All I-E stability results are presented in Tables 21 and 22 in Appendix 1. These show the neutrally aligned knee and malaligned knee results respectively. The idealised knee findings are shown below.

From 0° to 15° flexion there was a large increase (~6°) in I-E laxity which reduced as flexion increased to 90° (see Figure 4.12). This large increase in rotations was probably caused by the altered ligament strains and component conformity at 15° flexion. The strains in the collateral ligaments varied with flexion position (see Figure 4.13); this showed that at 15° flexion the ligaments were in a lax state.

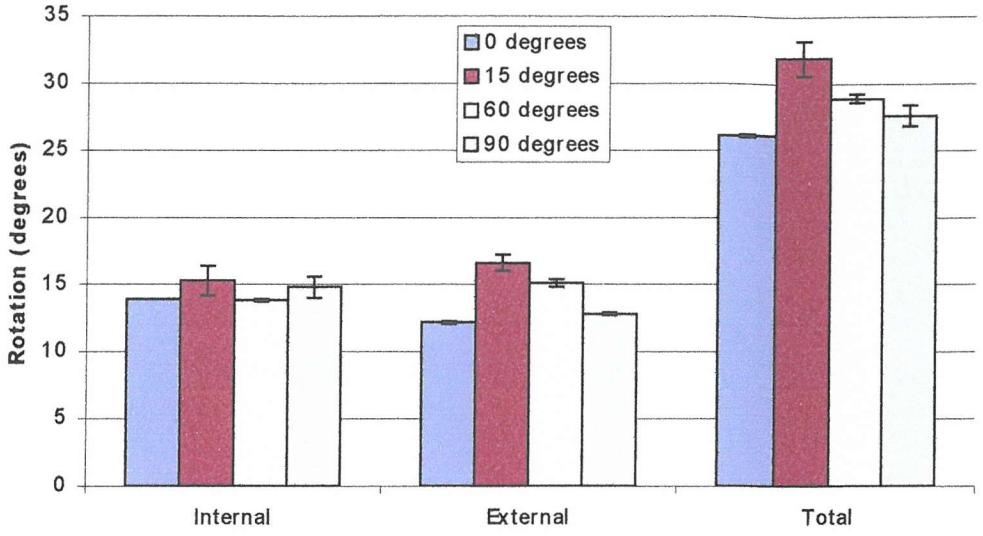

Figure 4.12 I-E stability of the PC-SF over the flexion range. Rotations refer to the femoral component with respect to the tibial component.

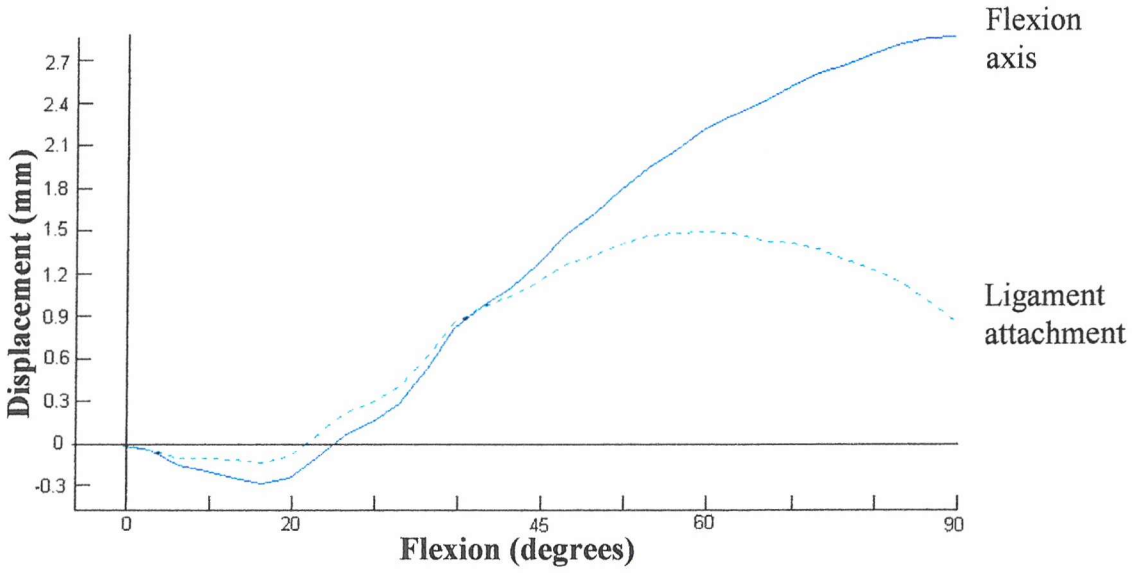

Figure 4.13 Change in vertical position of the flexion axis and the collateral ligament attachment point during flexion.

Varus-Valgus Rotational Stability

All V-V stability results are presented in Tables 23 and 24 in Appendix 1. These show the neutrally aligned knee and malaligned knee results respectively. The idealised knee findings are shown below.

As with the other knees tested in the present research, varus rotations were significantly larger than valgus rotations (5.3± 0.9° and 1.4± 0.2° respectively) (see Figure 4.14).

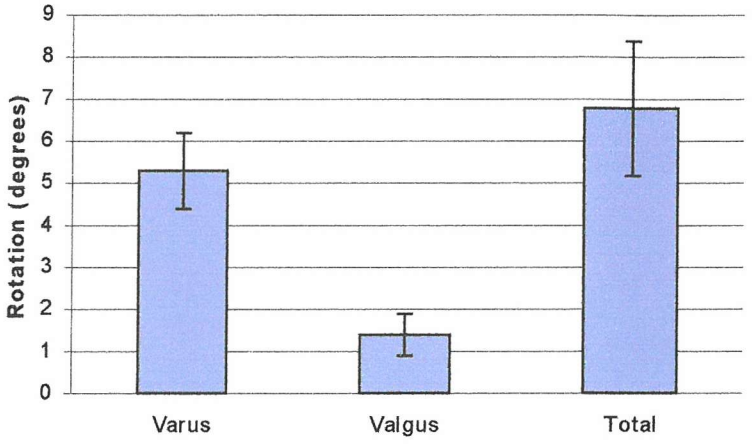

Figure 4.14 V-V stability of the PC-SF. Rotations refer to the tibial component with respect to the femoral component.

4.5 Summary of the Passive Stability Results

This section of the results will directly compare the different knee designs in the idealised condition.

4.5.1 A-P Stability

Figure 4.15 shows the total A-P displacements for all knees over the flexion range.

The PC-RF offered the lowest restraint towards A-P translations at all flexion positions. At lower flexion angles the rotating-bearing knees had the highest stability due to their greater component conformity; however, as flexion increased the conformity between the insert and the femoral component reduced and caused the displacements to increase in

the PC-RR. In the PC-SR the displacements were relatively constant over the flexion range due to the interaction of the tibial spine and femoral cam. The PC-SF produced relatively consistent translations from 0° to 60° flexion, reducing at 90° flexion. This total reduction at 90° flexion was due to the virtually zero posterior insert displacement that occurred; this was again caused by the interaction of the tibial spine and femoral cam.

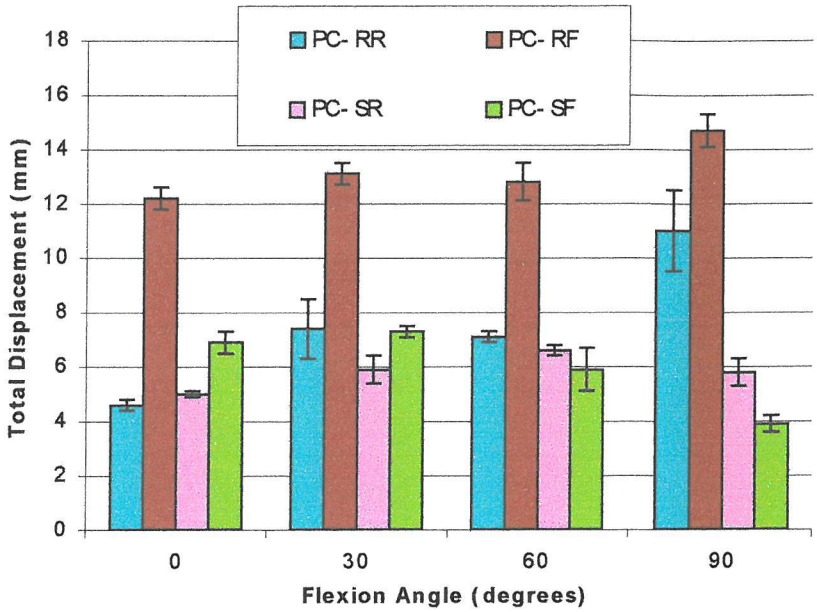

Figures 4.15 Total A-P translations of all four knees over the flexion. Displacements refer to the tibial component with respect to the femoral component.

4.5.2 I-E Stability

Figure 4.16 shows the I-E rotations for all knees over the flexion range.

Both rotating-bearing knees had similar rotations over the flexion range. At 15° flexion the PC-SR had increased total rotations compared to the PC-RR. This was possibly due to the different insert geometries, which could alter the contact position or ligament strains (see Figure 4.13). The PC-RF had lower rotations than the rotating-bearing knees; however, due to the low component conformity the rotations were still relatively high. The PC-SF offered substantially higher axial stability than the other designs due to the tibial spine restricting the axial rotations of the femoral component.

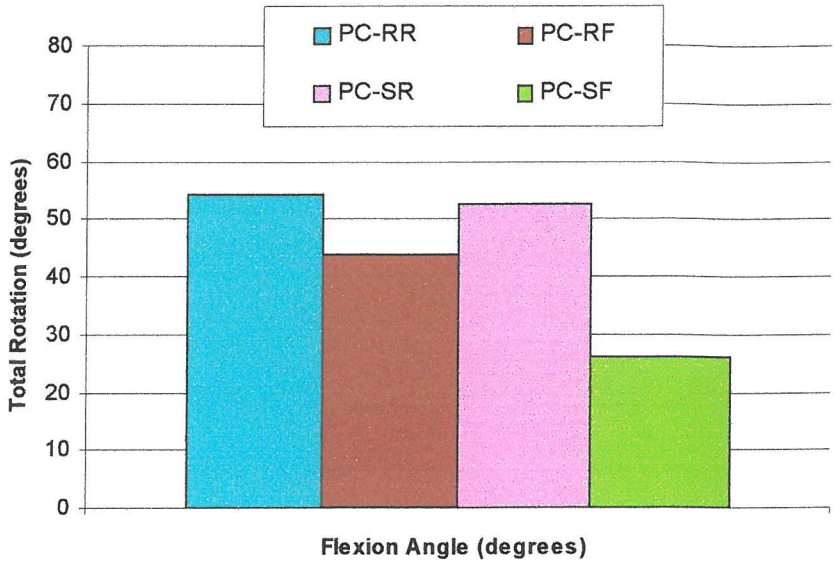

Figure 4.16 I-E rotations of all knees tested in the present research. The same trend was followed at all flexion positions. Rotations refer to the femoral component with respect to the tibial component.

4.5.3 V-V Stability

Figure 4.17 compares the V-V stability of all knees.

All knees had similar stability in the coronal plane; this would be expected, as there was no obvious difference in V-V restraint between the different knees.

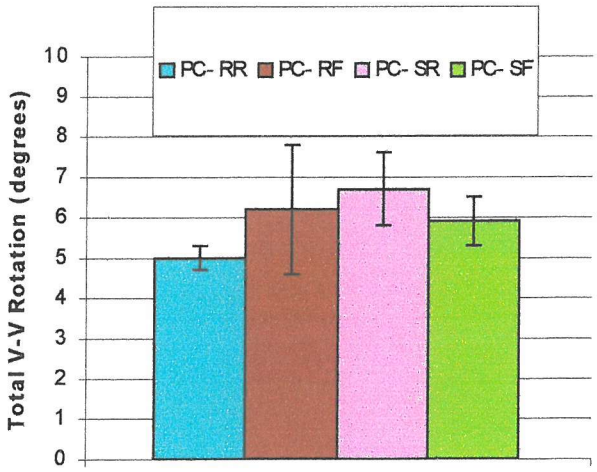

Figure 4.17 V-V stability of all four knees tested in the present research. Rotations refer to the tibial component with respect to the femoral component.

Overall, the general stability of the PC-SF was the greatest of all knees tested in the present research, in particular A-P and I-E stability. Both types of rotating-bearing knee had the lowest I-E stability, highlighting the fact that good soft tissue structures are required if this knee was to be implanted to reduce the risk of axial instability. Good ligaments were also required in the PC-RF due to the increased chance of M-L dislocation and low A-P stability.

4.9 Comparison with the literature

As discussed in Section 2.4.1 several other studies had investigated the passive stability of the replaced knee. This section will compare their findings to those in the present research.

A-P Stability Testing:

A-P laxity ranging from 0mm to >15mm was noted in a cadaver study Mitts *et al.* [102] who assessed a posterior cruciate-retaining prosthesis with minimally conforming tibial inserts. His study identified eleven knees with A-P translations of between 0mm-5mm, twenty knees with displacements of between 6mm-10mm, eighteen between 11mm-15mm and two knees with A-P translations in excess 15mm. Testing was performed at 90° flexion and all knees had a functioning PCL; however the force applied was not specified. A-P displacements of 14.7± 0.6mm were recorded in the present research for the PC-RF (most comparable knee to that assessed by Mitts *et al.*), this fell into the higher end of results from Mitts *et al.* The slightly higher translations could be due to a number of factors, including the possibility of a higher A-P force being applied, or the fact that no other soft tissue structures apart from the collateral ligaments were present. In the study by Mitts *et al.* all soft tissues around the joint were present.

Matsuda *et al.* [106] carried out *in vivo* A-P testing by applying a 133N anterior force and an 89N posterior force to PC-retaining knees (fixed-bearing with flat tibial inserts). Testing was performed at 30° flexion and total A-P displacements of 13.2± 4.2mm were recorded. Again, the PC-RF in the present research was most comparable to the TKR assessed by Matsuda *et al.* A total displacement of 13.1± 0.4mm was recorded with the

PC-RF at 30° flexion in the present research, which compared well to the displacements recorded by Matsuda *et al.*

In a cadaveric study with a PC-retaining knee (Profix total knee system: Smith & Nephew), Saeki *et al.* [103] applied a 35N force to produce A-P translations under a constant compressive load of 45N. A-P displacements of ~5mm were observed at both 30° and 90° flexion. The PC-retaining knees in the present research were chosen for comparison. At 30° and 90° flexion A-P translations of 7.4± 1.1mm and 11.0± 1.5mm respectively were recorded for the PC-RR, and 13.1± 0.4mm and 14.7± 0.6mm respectively for the PC-RF. Both these knees had larger displacements than in the study by Saeki *et al.*, however a 90N A-P force was applied in the present research compared to a 35N force in Saeki's work, which would most likely account for this difference.

Shoemaker *et al.* [18] applied a 100N A-P force to a modified PC-substituting knee, in which a section of the insert was removed to allow the retention of the PCL. Testing was conducted with and without the PCL, under a 0N and a 920N compressive load. A comparison to the PC-substituting knees used in the present study would be more relevant; thus the results without the PCL in Shoemaker's study are analysed. The 920N compressive load applied by Shoemaker *et al.* was considerably larger than the 50N compressive load used in the present study; therefore the results with a 0N compressive load are compared. Translations of 5.7± 1.5mm, 12.0± 1.0mm and 14.8± 0.9mm at 0°, 10° and 20° flexion were recorded by Shoemaker *et al.* [18]; this compared reasonably well with the 6.9± 0.4mm and 7.3± 0.2mm recorded for the PC-SF and 5.0± 0.1mm and 5.9± 0.5mm for the PC-SR at 0° and 30° flexion respectively in the present research. The effect of flexion position was not as significant as that demonstrated by Shoemaker *et al.*, possibly due to the individual knee design, which may offer a specific restraint at a specific flexion position.

V-V Stability Testing:

Mitts *et al.* [102] examined a Miller-Gallante II (Zimmer Corporation, Warsaw, IN, US) PC-retaining prosthesis with minimally conforming tibial inserts. A grading system was incorporated in the analysis of results using three grades: grade 0= 0°-5°, grade 1= 6°-10°, and grade 2= 11°-15° of total V-V rotation. Out of eight knees, four showed grade 2

coronal plane instability, two had grade 1 and two had grade 0. The prosthesis tested by Mitts *et al.* had a flat-on-flat design; therefore the PC-RF in the present research was a suitable comparator. Total V-V rotations of 6.2° were recorded with the PC-RF in the present research, this falls into the grade 1 classification of Mitts *et al.* (i.e. it showed a degree of laxity).

In a cadaver study by Romero *et al.* [121] the V-V laxity of a commercially available knee prosthesis (Duracon, Howmedica Inc) was assessed by applying a 10Nm torque. The knee was placed under a constant axial compressive load of 150N during these tests. Total V-V rotations of around 7°-8° were noted which were similar to the results in the present study (5.0°-6.2° for all knees). One observation from Romero's study was that the varus and valgus rotations were not statistically different from each other; this was not the case in the present research. This may be due to the extra soft tissue structures around the knee in the study by Romero *et al.*, which may even out the separate varus and valgus rotations. In the present research it was merely the LCL or the MCL restricting the motions.

Edwards *et al.* [122] assessed the V-V laxity of sixty-three knees, ten of which had 0°-5° of laxity, thirty had 6°-10° of laxity, twenty had 11°-16° of laxity and three had 16°-20° of laxity. All four knee designs in the present research fell into the 0°-5° or 6°-10° laxity groups of Edwards *et al.* Findings of Yamakado *et al.* [107] also compared well; twenty-one knees that had undergone cruciate-retaining TKA had varus rotations of 6.2± 0.9° and valgus rotations of 4.3± 0.5°, results ranged from 1° to 16° varus and 1° to 8° valgus. The varus rotations were very similar to those in the present research; however the 4.3° of valgus rotation was considerably larger. In the study by Yamakado *et al.* valgus rotations ranged from 1° to 8° across the knees assessed; this demonstrated that the 1.5° of valgus rotation recorded in the present research was feasible.

In a cadaveric study by Whiteside and Amador [104] the effect of a posterior stabilising mechanism on the V-V stability in TKA was investigated. Total V-V rotations of around 3° were recorded in response to a 15Nm torque, compared to the 5°-6° observed in the present research. Similar rotations to those of Whiteside and Amador were noted in a cadaveric study by Saeki *et al.* [103], who applied a 10Nm. The slightly lower rotations recorded in the cadaveric studies compared to those of present research could be due to

the extra soft tissue restraints around the cadaveric knees, as previously noted. In addition the individual implant design could also have a bearing on the results.

In a further cadaveric study by Whiteside *et al.* [105] a rotationally unconstrained TKA (Ortholoc, Dow Corning Wright) was assessed by applying a 15Nm torque. Total V-V rotations of 5.8± 2.2° were recorded in the knees with normal ligament strains; these were similar to those found in the present research. Whiteside *et al.* observed that a lax knee increased the rotations by ~3° and a tight knee reduced rotations by ~1.5°. In the present research slack ligaments increased total V-V rotations by ~1.5°, and tight ligaments reduced rotations by ~1.0°. Applying a 10Nm torque Shoemaker *et al.* [18] carried out cadaveric V-V stability testing on a PC-substituting knee that had been modified to allow the retention of the PCL. The findings by Shoemaker *et al.* without the PCL were most comparable to testing with the PC-substituting knees in the present research. Shoemaker *et al.* recorded V-V rotations of 4.7± 1.5°, which were slightly lower than the 6.7± 0.9° and 5.9± 0.6° recorded in the present research for the PC-SF and PC-SR respectively. As previously mentioned, extra soft tissue restraint and differences in component design could have accounted for this discrepancy.

I-E Stability Testing:

Compiling studies for the comparison of I-E stability was problematic due to the variation in applied torques. In a cadaveric study by Whiteside *et al.* [105] I-E testing was carried out on a rotationally unconstrained TKA (Ortholoc, Dow Corning Wright) using a 2.5Nm torque. At 0° flexion Whiteside *et al.* recorded total rotations of 4.9± 3.4°; this was considerably lower than the rotations of all the knees in the present study. The applied torque in the study by Whiteside *et al.* was over three times lower than that used in the present research, and combined with the extra soft tissue structures around the cadaveric knee could explain the lower rotations. In a separate cadaveric study by Whiteside and Amador [104] the effect of a posterior stabilising mechanism on rotational stability in TKA was investigated. A posterior stabilised TKA with either a rotationally constrained or an unconstrained articular surface was tested using a 2.5Nm torque. No significant difference between the two knee types was noted by Whiteside and Amador, with rotations of about 6°, 20° and 28° recorded at 0°, 45° and 90° flexion respectively. These findings were again considerably lower than those of the present research.

In a cadaveric study Shoemaker *et al.* [18] applied a 10Nm torque to a modified TKA, which took a PC-substituting knee and removed a section of the insert to allow the retention of the PCL. Under a 0N compressive load total I-E rotations of 24.5± 5.5°, 31.6± 7.0° and 36.5± 5.8° were recorded at 0°, 10° and 20° flexion respectively when the PCL was sacrificed. The knee assessed by Shoemaker *et al.* was closest to the PC-SF in the present research, which had rotations of around 26.1° and 31.9° at 0° and 15° flexion respectively. The torque applied by Shoemaker *et al.* was slightly larger than that in the present research; however, extra soft tissue restraint was present in the cadaveric knees and may have balanced this affect.

The present research only simulated the MCL and LCL. Thus, achieving a direct comparison with the literature proved difficult since cadaveric specimens possess a joint capsule, patella and other soft tissue structures. Varying forces/ torques and differences in individual prostheses design also made direct comparison difficult. Generally however, the motions noted in the literature lay within the same range as those in the present study, indicating that the knee rig developed for the present research realistically simulated the passive motions of the replaced knee.

4.10 Posterior Cruciate Ligament: Results and Discussion

Tables 4.1 to 4.4 shows the effects of the PCL on A-P and I-E stability for the PC-RR and PC-RF.

Flexion (°)	**Displacement without the PCL (mm)**			**Displacement with the PCL (mm)**			**Difference (mm)**		
	Anterior	Posterior	**Total**	Anterior	Posterior	**Total**	Anterior	Posterior	**Total**
0	2.1	2.5	**4.6**	1.8	2.2	**4**	0.3	0.3	**0.6**
30	3.6	3.8	**7.4**	2.8	2.5	**5.3**	0.8	1.3	**2.1**
60	3	4.1	**7.1**	3	3.7	**6.7**	0	0.4	**0.4**
90	3.9	7.1	**11**	3.8	5.4	**9.2**	0.1	1.7	**1.8**

Table 4.1 A-P stability with and without the PCL for the rotating-bearing knee.

Flexion (°)	Rotation without the PCL (°)			Rotation with the PCL (°)			Difference (°)		
	Internal	External	**Total**	Internal	External	**Total**	Internal	External	**Total**
0	26.6	27.5	**54.1**	24.9	25.1	**50**	1.7	2.4	**4.1**
30	26.9	27.1	**54**	25.8	25.6	**51.4**	1.1	1.5	**2.6**
60	27.1	26.1	**54.2**	25.9	25.4	**51.3**	1.2	0.7	**2.9**
90	27.9	26.8	**55.7**	26.8	25.9	**52.6**	1.1	0.9	**3.1**

Table 4.2 I-E stability with and without the PCL for the rotating-bearing knee.

Flexion (°)	Displacement without the PCL (mm)			Displacement with the PCL (mm)			Difference (mm)		
	Anterior	Posterior	**Total**	Anterior	Posterior	**Total**	Anterior	Posterior	**Total**
0	5.9	5.3	**11.2**	5.8	4.7	**10.5**	0.1	0.6	**0.7**
30	5.5	7.6	**13.1**	5.1	6.1	**11.2**	0.4	1.5	**1.9**
60	5.1	7.7	**12.8**	4.5	5.7	**10.3**	0.6	2	**2.5**
90	6.4	8.3	**14.7**	5.5	7.7	**13.2**	0.9	0.6	**1.5**

Table 4.3 A-P stability with and without the PCL for the fixed-bearing knee.

Flexion (°)	Rotation without the PCL (°)			Rotation with the PCL (°)			Difference (°)		
	Internal	External	**Total**	Internal	External	**Total**	Internal	External	**Total**
0	21.5	22.5	**44**	19.4	20.1	**39.5**	2.1	2.4	**4.5**
30	23.6	23.6	**47.2**	21.2	19.1	**40.3**	2.4	4.5	**6.9**
60	21.9	21.7	**43.6**	20.1	19.9	**40**	1.8	1.8	**3.6**
90	24.8	24.8	**49.6**	22.6	22.8	**45.4**	2.2	2	**4.2**

Table 4.4 I-E stability with and without the PCL for the fixed-bearing knee.

It is clear that the presence of a PCL affected the passive stability of the two knees tested. Maximum reductions of 2.5mm and 6.9° occurred when the PCL was attached, which indicates that stability was increased by the PCL. However, these results will not be discussed in great detail for the reasons outlined in Section 4.10.1.

After initial passive stability testing with the PCL the reliability and accuracy of the results were questioned. Visual plastic deformation of the synthetic PCL material occurred after relatively low usage, in particular around the femoral attachment point. It was feared that this deformation would alter the PCL stiffness characteristics, and if it occurred during an individual test the motions produced may not have been representative.

Testing the PC-retaining knees without the PCL in the present research would still be applicable as the actual relevance of the PCL after TKA has not been satisfactorily proven. Section 4.10.1 highlights this point and indicates that the motions and stability of the joint are possibly more due to the prosthesis design itself rather than the PCL.

4.10.1 PCL Retention or Sacrifice: Pros and Cons

The retention of the PCL after a TKR is still a source of debate [7], [55], [96], [123], [124], [125], [126]. Those supporting the retention of the PCL have maintained that following knee arthroplasty the ligament will continue to prevent posterior subluxation of the tibia and will provide increased knee flexion through physiological femoral rollback. Gait analysis studies have revealed that PCL sacrifice is associated with high flexion and varus moments across the knee. This will result in higher workloads required by the muscles and tendons around the knee, resulting in a less effective gait pattern. However, advocates of cruciate sacrifice argue that the ligament cannot be retained physiologically due to the chronic deformities and soft tissue deterioration present in the arthritic knee, and that during acute flexion increased tension in the PCL may result in unusually high joint contact forces [55], [96]. It was also thought that cutting the PCL allows maximal exposure of the proximal tibia during surgery and that as a result, improper seating and poor alignment of the components are much less likely [123]. It was argued that implant loosening and failure are much more likely to occur from prosthetic malalignment than from any increased shear stresses associated with PCL resection. The clinical performance of PC-retaining and -excising knees does not seem to yield any significant differences, as highlighted in a list of over 5000 TKAs compiled by Mahoney [124].

Finding information on the exact role of the PCL after TKA proved difficult, as most studies in the literature assessed knees that had been designed for use without the PCL. In addition these studies compared their findings against knees that had been designed to be used with the PCL. Other authors also noticed this, and a study by Straw *et al.* [7] has actually claimed to be the first clinical trial to examine the exact role of the PCL after TKA, using the same articular geometry for the tibial, femoral and patellar components for all groups of patients [7]. This investigation assessed a Genesis I prosthesis (Smith & Nephew), and looked at 237 knees implanted between 1996-2000. Patients were randomised for either PCL retention or excision, and those who were randomised to

excision were further randomised to receive either a standard tibial insert or a posterior stabilised tibial insert. For those patients with a retained PCL for whom it proved impossible to achieve satisfactory ligamentous balancing at surgery, the PCL was released from its insertion into the posterior aspect of the tibia until its tension was judged appropriate by digital palpation. From this study there were no differences in mean pain score, range of movement, knee score or function score between the excised, retained and posterior stabilised groups. The released group had significantly worse mean pain and knee scores than the other groups. The retained group had the least amount of knee flexion (mean 100°), with all other groups having at least 110° flexion. The posterior stabilised knees had the greatest overall stability (A-P and V-V stability), the excised knees possessed the lowest A-P stability, and the retained knees had the lowest V-V stability (see Table 4.5).

Knee	(%) less than 5mm A-P	(%) less than 5° V-V
Retained	54	78
Excised	51	84
Posterior Stabilised	71	88
Released	54	79

Table 4.5 Stability in PCL retained, excised, posterior stabilised and released knees [7].

In summary this study showed that release of the PCL can have a deleterious effect after knee replacement, and could result in poor performance with more postoperative pain and worse knee and function scores. Retention, excision and substitution of the ligament can all lead to favourable outcomes with little difference between pain, knee or function scores. It was also shown that if the PCL was excised it was not essential to use a PC-substituting insert, as long as reasonably conforming inserts were used. This study was however looking at the short-term results and not claiming to predict long-term performance (wear, loosening etc.).

Misra *et al.* [125] also assessed the role of the posterior cruciate ligament in replaced knees, randomising 129 knees into two groups of TKRs: those implanted with the PCL retained and those with the PCL resected. A standard cruciate retaining TKR (press-fit condylar, DePuy Orthopaedics Inc) was implanted in all knees. There was no statistical difference found between the amount of femoral rollback with the retained and resected PCL knees (21.6% and 24.1% in retained and resected knees respectively), and there was

also no increased loosening in the resected group after an average of 57 months (via the assessment of radiolucent lines). The findings by Misra *et al.* [125] and Straw *et al.* [7] suggest that the preservation of the PCL did not play a significant functional role in the PC-retaining TKR, and a knee with an excised PCL may not need a posterior stabilised implant.

Pereira *et al.* [126] assessed 163 TKAs performed by one surgeon using a Kinemax prosthesis (Howmedica). No cam or post was present in this design. It was theorised that the prosthesis could be used with or without the PCL due to the geometry of the implant. A mixture of PC-retaining and PC-sacrificing arthroplasties was performed. After one year no difference between pain results or ability to climb stairs was noted between the two groups, and there were no significant differences in quadriceps strength and V-V stability. This study suggests that there were no differences in clinical or early radiographic outcome caused by retaining or sacrificing the PCL, and seems to agree with other studies that say sacrificing the PCL was not a problem as long as a suitable prosthesis was implanted [7], [125].

Mahoney *et al.* [124] carried out a laboratory study to evaluate the effect of retention of the PCL on the biomechanical performance of TKAs (PCL-retaining prosthesis; Miller-Galante, Zimmer) during stairclimbing. A force of 110N was passed through an intact knee joint, and six cycles of ascending and descending (stairclimbing) configurations were applied. Testing was repeated with an implanted PC-retaining TKR and with a PC-sacrificing TKR, using a posterior cruciate-excising (Miller-Galante Anterior Lipped Component, Zimmer) and a posterior cruciate-substituting (Insall-Burstein Posterior Stabilised component, Zimmer) design. The recorded femoral rollback of the intact knee at 90° flexion was 12.3± 0.9mm while ascending and 11.9± 1.0mm while descending. This value decreased to 8.2± 0.7mm (ascending) and 7.4± 0.7mm (descending) for the PC-retaining knees, and decreased further in the PC-excised prosthesis (3.9± 0.7mm ascending and 3.4± 0.7mm descending - a reduction of 68% and 71% compared to the intact knee). In the PC-substituting knee the cam was activated at an average of 69.2± 2.4° flexion; this resulted in 11.0± 1.0mm rollback while ascending and 10.2± 1.6mm while descending, which was 10% and 14% lower than the normal knee. This study appears to support the use of a PC-substituting implant over both retaining and excising designs. The sensitivity of the strain within the PCL to relatively small changes in tibial

tray thickness was also recognised, and even when care was taken to achieve a good PC-retaining TKR the normal strain patterns in the PCL were difficult to achieve.

From the literature it appears that the retention of the PCL was not necessary after TKR. If retention of the PCL was not possible then using a PC-substituting knee design provided acceptable knee stability [7]; however, if component conformity was relatively high, and the geometry of the implant helped restrain A-P, M-L and V-V motions, then there was no real need to use a PC-substituting knee design [7], [125], [126].

4.11 Experimental Contact Pressure Results

Table 3.4 in Section 3.4 shows all the experimental contact pressure investigations conducted on the PC-RF. The visual raw contact pressure data is presented in Appendix 2; Table 4.6 shows the maximum contact pressures initially, and during dynamic testing. The initial contact pressure was the pressure produced under compressive loading only, before I-E rotations occurred. The dynamic pressures were recorded throughout the whole test and divided into the pressures formed at the extremes of the motion and those formed within the sliding path. The pressures at the extremes of motion were formed as the femoral component pushed against the internal rim of the insert, and the pressures during sliding were formed on the bearing surfaces of the insert (see Figure 4.18 - the recorded contact pressure results have been superimposed onto an image of a tibial insert to help with visual interpretation).

The purpose of the experimental contact pressure investigation was to provide additional information for validation with the computational finite element models (see Chapter 6). For this reason only general observations will be discussed in this section; however, the contact areas and contact pressures of all knees assessed in this research will be discussed in more detail in Chapters 7 and 8, where they occur during gait.

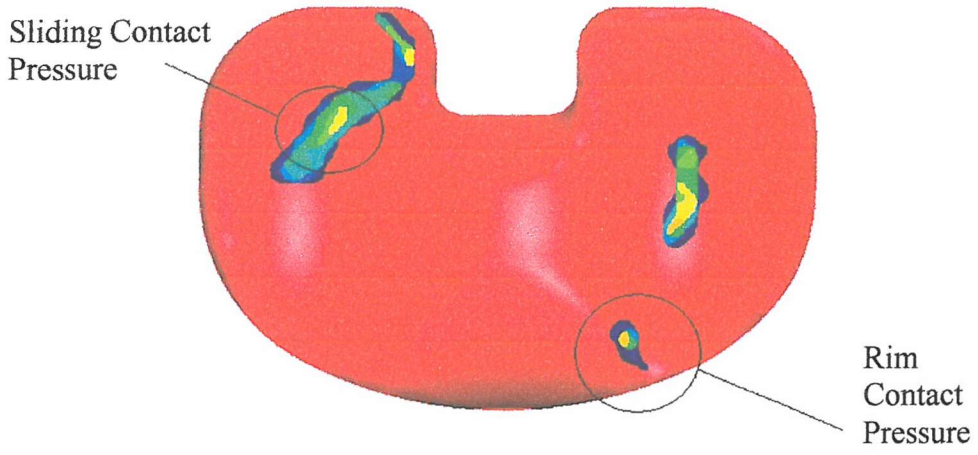

Figure 4.18 Example of rim and sliding contact pressures.

Test	Maximum Contact Pressure (MPa)					
	Initial (compressive load only)		Dynamic Motion (compressive load + rotation)			
			Rim Contact		Sliding Path	
	Medial Condyle	Lateral Condyle	Medial Condyle	Lateral Condyle	Medial Condyle	Lateral Condyle
1	7 – 9	7 – 9	17	4	11 – 12.5	11 – 12.5
2	9 – 11	6 – 7.5	17	11 – 12.5	12.5 – 14	12.5 – 14
3	11 – 12.5	4.5 – 6	17	17	12.5 – 14	11 – 12.5
4	-	12.5 – 14	17	11	-	14 – 15.5
5	-	9 – 11	17	15.5	11 – 12.5	9.5 – 12.5
6	9.5	-	15.5	12.5	14 – 15.5	3 – 4.5
7	4.5 – 6	-	15.5	6 – 7.5	14 – 15.5	-
8	9 – 11	3 – 4.5	12.5	15.5	14 – 15.5	9 – 11
9	7.5	3	17	17	14 – 15.5	9 – 11
10	7.5 – 9	11	15.5	15.5	14 – 15.5	11
11	6 – 7.5	6 – 7.5	14	15.5	14 – 15.5	12 – 14
12	7.5	7.5	11	15.5	12 – 14	11 – 12
13	7.5	7.5 – 9	14	15.5	12 – 14	11 – 12
14	-	9	4.5	9	-	12 – 14
15	7.5	7.5	11	11	12 – 14	9 – 11
16	12.5 – 15.5	4.5	-	-	-	-

Table 4.6 Maximum contact pressures recorded experimentally for the PC-RF (- indicates where no contact pressure was recorded).

General Observations:

In the idealised knee initial contact pressures were slightly larger on the medial side of the insert; however, during dynamic motion the contact pressures and contact areas were similar on both the medial and lateral bearing surfaces. Rim contact pressures were larger

on the medial side, however this measurement was prone to change since the longer the pressures were recorded the more the femoral component would push against the inner insert rim, causing the peak pressures to increase. On this basis the most valuable results were those produced during sliding. During Test 4 (MCL= slack, LCL= tight @ 0° flexion) there were no recorded contact pressures on the medial condyle apart from those at rim contact. This highlights the fact that the collateral ligaments play an important role in distributing the load across the knee under low load testing. When the knee was flexed to 15° (Test 5) the maximum recorded contact pressures were similar for the medial and lateral condyles, however the contact area on the lateral condyle was significantly larger than that on the medial condyle. Tests 6 and 7 (MCL= tight, LCL= slack) also show that the ligaments altered the way the pressures were distributed across the knee. There were no recorded contact pressures on the lateral condyle in Test 7, and only very low contact pressures in Test 6 (only rim contact recorded).

Chapters 7 and 8 discuss the contact pressures and contact areas in more detail for all knee types used in the present research.

4.12 Progression of the Research

Using the mechanical test rig developed in the present research restricts testing to the passive state. With the knee rig we can assess the passive stability of various total knee designs and quantify the effects of malalignment and altered ligament strains; however, the importance or even relevance of the passive stability data can not be fully understood in terms of the effect on active motion. Reproducing active motions such as gait on the test rig would be extremely difficult and beyond the scope to the project. Virtual simulations using finite element analysis (FEA) would allow active motions to be simulated more easily, and was the approach adopted in the present research. Exact finite element (FE) simulations of the mechanical testing would be reproduced to validate all the computational results, then active data would be inputted into the FE models to simulate normal gait. This process would allow direct comparisons between passive and active motions, highlighting particular passive stability issues and their direct effect during gait.

Chapter 5 Finite Element Analysis (FEA): Construction of Computational Models

5.1 The Finite Element Method (FEM): A brief description

For a complete, or even just a suitably detailed explanation of the FEM a whole Chapter could be dedicated in itself. A partial description could cause some confusion, so it was the decision of this author to give a short summary of the FEM and to guide the reader to relevant texts, such as Zienkiewicz (1992) or Jacob and Goulding (2002) for a more detailed description. In brief, the FEM allows a problem with complex boundaries and properties to be broken down into series of common elements or volumes, each with finite dimensions and within which reasonable approximations can be made on the variation of parameters such as displacement, temperature, stress and strain. A global problem can then be represented by an array of common elements with known properties and a solution can then be found by ordered, but repetitive computational operations.

5.2 Construction of the Computational Models

5.2.1 Three-Dimensional Modelling and Meshing

Three-dimensional CAD (Computer Aided Design) models were provided in either IGES (Initial Graphics Exchange Specification) or Parasolid format by DePuy Orthopaedics Inc. (Warsaw, IN, US), and these were meshed using solid modelling programs (Ideas, Marc). The tibial (tray and insert) and femoral components were meshed as rigid shells, which meant that no internal stresses (Von Misses Stresses) within the components could be recorded. However, as only the motions and contact pressures were being assessed in the present research solid bodies were not required. Quadrilateral meshes with an average element edge length of approximately 2mm were assigned to all components, and a refined mesh of 1.2mm (average element edge length) was applied to the bearing surfaces of the tibial insert. An average element edge length of 1.2mm was shown to be sufficient to provide accurate contact pressure outputs [9]. Above this value recorded maximum contact pressures were seen to decrease, with a reduction of around 23% noted with an element edge length of 2mm; further refinement did not have a significant effect. The ligamentous structures were meshed as solid bodies, with a larger tetrahedral mesh (~8mm element edge length) assigned. The analysis would concentrate on the motions

and pressures of the prosthetic components, and thus detailed analysis of ligaments was not necessary.

In Pam-Crash-Generis (ESI Group, France) the separate implant components were defined as rigid bodies, the collateral ligaments as solid bodies and the PCL as a bar element. The PCL had a more complex shape compared to the collateral ligaments, which proved difficult to create as a solid structure, therefore a bar element was chosen. Figure 5.2 shows an example of a completely assembled computational FE model. Modelling the components as rigid bodies instead of solid bodies reduced the solver time considerably when running the simulations, which was an important consideration due to the large number of simulations necessary. Only the collateral ligaments were defined as solid bodies; this was necessary since they were assigned a particular material property (Material 37 in Pam-Crash) that would allow pre-strain and laxity to be simulated. Material 37 was an adaptation of a basic isotropic hyperelastic *Mooney-Rivlin* type "matrix" (Material 17 in Pam-Crash), with an additional anisotropic nonlinear hyperelastic contribution in the direction of the fibres. An exact description of the ligamentous properties and function of Material 37 was reported by Limbert [118]. The computational ligamentous structures simply needed to represent the rubber ligaments in the experimental rig and not natural anatomic ligaments, thus the complex workings of the above-mentioned material were not needed. The correct stiffness values of the computational ligaments are represented by eight lines (CARDS), which represent a number of constants and material properties, including Poisson's ratio and isotropic coefficients. However, ultimately the stiffness values were determined by performing a number of virtual trial and error tensile simulations and altering the material constants to achieve the desired values. Figure 5.2 shows the Pam-Crash code used to represent the normally strained MCL and LCL. The end value in CARD 3 of each ligament represents the initial pre-strain value (i.e. 1.05 in Figure 5.1); 1.05 equates to normally strained, 1.20 represents a tight ligament and 0.90 represents a slack ligament. As mentioned, the PCL was represented by a bar element due to its complex shape. The bar element was correctly positioned and assigned appropriate stiffness properties. All other components were modelled as rigid bodies, which meant that no deformation of the structures would occur during the simulations. Material properties of the TKR components are shown in Table 5.1, and were taken from the study by Godest *et al.* [9], who in turn received the information from the implant suppliers (DePuy International, UK).

```
CARD
        $---5---10----5---20----5---30----5---40----5---50----5---60----5---70----5---80
1       -MATER /     3    37        9e-5     0    2
2       -            8    9    10     7
        $ LCL
3       -  0.0027    0.0    0.450    0.0    0.0    0.0    1.000    1.05
4       -      1
5       -
6       -
7       -
8       -
```

```
        $
1       -MATER /     4    37        9e-5     0    2
2       -            8    9    10     7
        $ MCL
3       -  0.0047    0.0    0.450    0.0    0.0    0.0    1.000    1.05
4       -      1
5       -
6       -
7       -
8       -
        $
```

Figure 5.1 Section of Pam-Crash code used to represent the normally strained LCL and MCL in the FE simulations.

Component	Youngs Modulus (GPa)	Poissons Ratio
Femoral	211	0.3
Tray	211	0.3
Insert	0.7	0.3

Table 5.1 Material properties used in the finite element models.

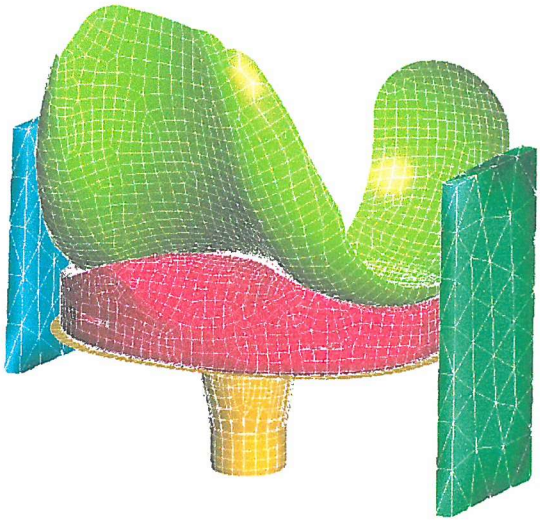

Figure 5.2 Computational model of the PC-retaining rotating-bearing knee.

5.2.2 Rigid Body Contact

Pam-Crash-Safe (ESI Group, France) was used to solve the explicit FE models in this study. This adopted a 'penalty' contact method when assessing the interaction of the prosthetic components. An advanced penalty method based contact algorithm (contact element 44 in Pam-Crash) was used to model the contact between two components. This algorithm required the geometric penetration of the slave nodes to be penalised by counteracting forces proportional to the penetration depth and penalty factor, which were chosen by the user. A second-order polynomial approximation of the master surface was used. This approach had been specifically developed to model contact between spherical surfaces and to avoid kinks in the contact surface, which may occur at the element boundaries. Basically, when two bodies contact each other there is an opposing (reaction) force acting against them. This force is a representative of the penalty factor and contact thickness parameters that are set by the user. If the reaction force is too small then the components will move through each other and the model will fail, and if the reaction force is too large the components well be forced apart, again resulting in a failed model. Achieving accurate contact parameters is essential for a successful and realistic FE simulation.

When constructing the FE models in Pam-Crash-Generis in the present research, slave nodes were assigned to the tibial insert and master nodes were assigned to the tibial tray (where present) and the femoral component. No contact occurred between the ligament

structures and any of the TKR components; therefore no contact nodes were assigned. A penalty factor of 0.001 and a contact thickness of 0.1mm were used in the present research. The contact thickness of 0.1mm was chosen as it was comparable to the thickness in a study by Godest *et al.* [9], who demonstrated that the kinematics of the specific knee model could accurately recreate those observed within the Stanmore knee simulator [23]. The penalty factor used in the study by Godest *et al.* was 0.01, however this value gave unrealistic contact areas and pressures in the present research, with localised pressure points occurring and patchy contact areas. Godest *et al.* meshed the tibial insert as a solid body, where small contact abnormalities would deform, giving lower and more evenly distributed contact pressures. However, in the present research the rigid body structures did not deform, thus any slight abnormalities caused localised peak pressure readings. The penalty factor of 0.001 in the present research allowed greater contact penetration between the structures and therefore ignored the small surface defects (which would be deformed in a solid body), providing more realistic contact areas and pressures.

The co-efficient of friction was another contact parameter that needed to be specified. Godest *et al.* [9] assessed the effect of altering the co-efficient of friction value between the femoral and tibial insert components. They found that A-P translations were affected, but I-E rotations and peak contact pressures were not significantly affected over a gait cycle. They decided on a value of 0.04, which gave motions within a few percent of the experimental data, and lay between the values of 0 and 0.15 which had previously been reported in the literature [119], [120]. Using this value for the contact between the femoral and tibial insert also provided good correlation with A-P, I-E and V-V stability measurements recorded in the present research (see Chapter 6). The frictional value for the contact between the tibial insert and tibial tray was increased to 0.15, which still lay between the values observed in other studies [113]. This value was chosen since it produced results comparable to those found experimentally in the present research (Chapters 4 and 6); the value of 0.04 caused I-E rotations in the rotating-bearing knees to be larger than those recorded experimentally (Appendix 1).

5.2.3 Simulation of the Experimental Passive Stability Testing

In order to allow the computational simulations to replicate the experimental stability tests (A-P, I-E and V-V) accurately, comparable forces were applied to select nodes, and specific boundary conditions were set for each investigation (see Table 5.2). Free nodes were created and attached to the various rigid bodies (tibial section, femoral component etc.), with forces directly applied to these nodes, producing the required motions. All other conditions were replicated to exactly simulate the experimental testing, and forces, attachment points, relative movements and all other variables were kept constant. The only condition that was not replicated exactly was the application of I-E torques. Experimentally, a torque was applied through the centre of the femoral component; this however proved difficult to replicate in the computational simulations. Simulating the required torque was achieved by applying a known force to a free node (of known position) that was attached to the femoral component, as shown in Figure 5.3. The rotations that occur were fixed about the centre of gravity of the femoral component, which was also represented by a free node that has been assigned this characteristic. Boundary conditions were set to the femoral component to restrict translations in the medial-lateral and anterior-posterior directions, thus only allowing axial rotation to occur. The boundary conditions applied to the separate components were altered depending on which test was being simulated. Table 5.2 shows all configurations used, including those applied during normal gait, which is discussed later in this section. Note that the rotating-bearing insert was free to move in all planes, however, its motions were greatly restricted by the tibial tray.

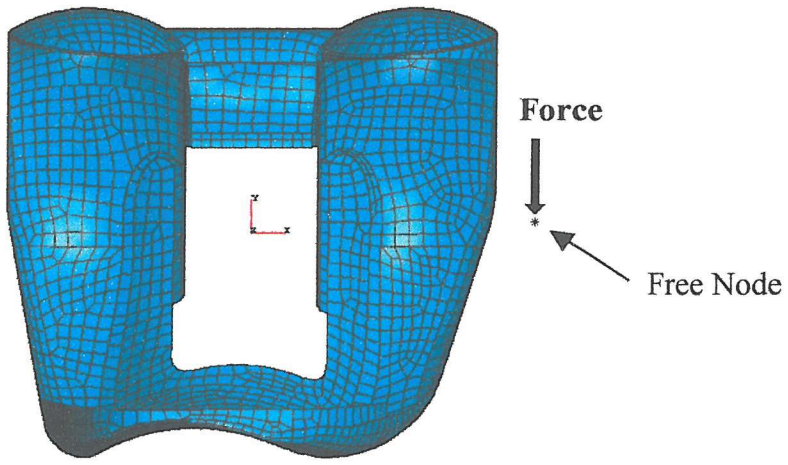

Figure 5.3 Proximal view of the femoral component showing the free node (*) onto which forces were applied to produce I-E femoral rotations.

Component	Test	Boundary Conditions					
		A-P displacement	M-L displacement	Inferior-Superior displacement	V-V Rotation	I-E Rotation	Transverse Axis Rotation
Femoral	A-P	Fixed	Fixed	Free	Fixed	Fixed	Controlled
	I-E	Fixed	Fixed	Free	Fixed	Free	Controlled
	V-V	Fixed	Fixed	Free	Fixed	Fixed	Controlled
	Gait	Fixed	Fixed	Free	Fixed	Free	Controlled
Tibial Tray & Fixed Insert	A-P	Free	Free	Fixed	Free	Fixed	Fixed
	I-E	Free	Free	Fixed	Free	Fixed	Fixed
	V-V	Free	Free	Fixed	Free	Fixed	Fixed
	Gait	Free	Free	Fixed	Free	Fixed	Fixed
Rotating Tibial Insert	A-P	Free	Free	Free	Free	Free	Free
	I-E	Free	Free	Free	Free	Free	Free
	V-V	Free	Free	Free	Free	Free	Free
	Gait	Free	Free	Free	Free	Free	Free

Table 5.2 Boundary conditions applied for each simulated test.

5.2.4 Gait Simulation

Axial loads, I-E torques, A-P forces and flexion angles comparable to those used in the study by Godest *et al.* [9] were applied to the computational models to achieve active gait simulations (Figure 5.4). These values came from the data used to drive the Stanmore knee simulator [23], which in turn used data derived by Morrison [114]. The gait cycle was run over 1000ms, as shown in Figure 5.4, starting from heel strike (hence the large posterior force applied to tibial section), through the stance phase (~100ms-300ms), followed by toe-off (~300ms-600ms), and then the swing phase (~600ms-1000ms).

A-P forces were applied to the tibial section of the model, and I-E torques, axial loads and flexion values were applied to the femoral component. I-E torques were applied to two free nodes on opposite sides of the femoral component, which produced I-E rotations without any other motions, such as M-L translations. In the literature [9] the I-E torques were applied to the tibial component, which could therefore axially rotate, with the femoral component restrained. In the present research the tibial component (either the insert or tray depending on which model was used) was restricted in this motion and the femoral component was free to axially rotate in the I-E direction. Allowing I-E rotations of the tibial component caused the models to become unstable but no instability was noted with femoral I-E rotations. Initial ligament strain oscillations could be a possible explanation for tibial I-E instability. As the tibial component could not displace in the

inferior-superior direction these strain oscillations could produce I-E rotations. In contrast, the femoral component could displace in the inferior-superior direction, thus the oscillations could have been transmitted in this plane. Other reported models of the replaced knee have used horizontal springs to represent the soft tissue structures [9], [23], [112], therefore no initial ligament strain oscillations would occur.

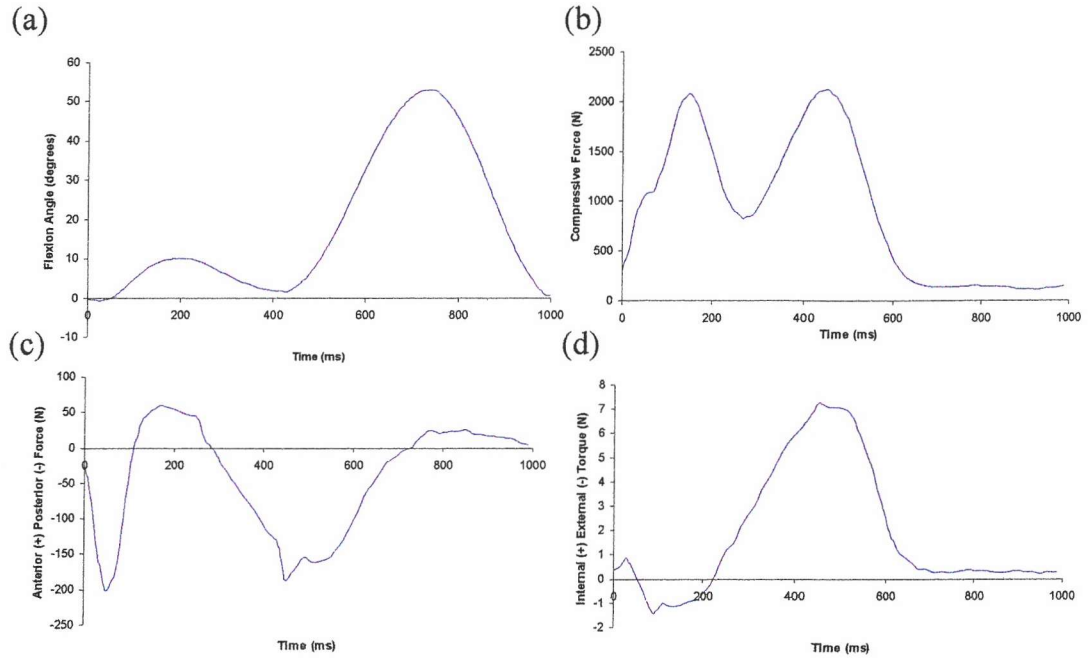

Figure 5.4 Visual representations of (a) Flexion angle; (b) axial compressive force; (c) A-P force and (d) I-E torque applied to the FE models to produce level gait.

One other difference from the models reported in the literature [9] was that V-V rotations were fixed in the femoral component and free to occur in the tibial component. Initially, the models were setup as in the literature (V-V rotations free in the femoral component and fixed in tibial component), however further testing showed that any alteration in ligament strains or component alignment did not cause a significant change in the contact pressure distribution across the medial and lateral sides of the knee. Extreme varus malrotation of the femoral component was simulated (10° of varus rotation), and analysis of the results showed equal and unaltered force distribution across the knee. The models were then altered to allow tibial V-V rotations. Comparable testing showed the pressure distribution to change with femoral malpositioning and altered ligament strains, as would be expected.

Chapter 6 Validation/ Comparison of Experimental & Computational Models

6.1 Motion Validation

A full set of computational passive stability test results are presented in Appendix 3.

6.1.1 Confidence in A-P Stability

Figure 6.1 shows the computational and experimental A-P stability results for all idealised knees (neutral alignment and normally strained collateral ligaments).

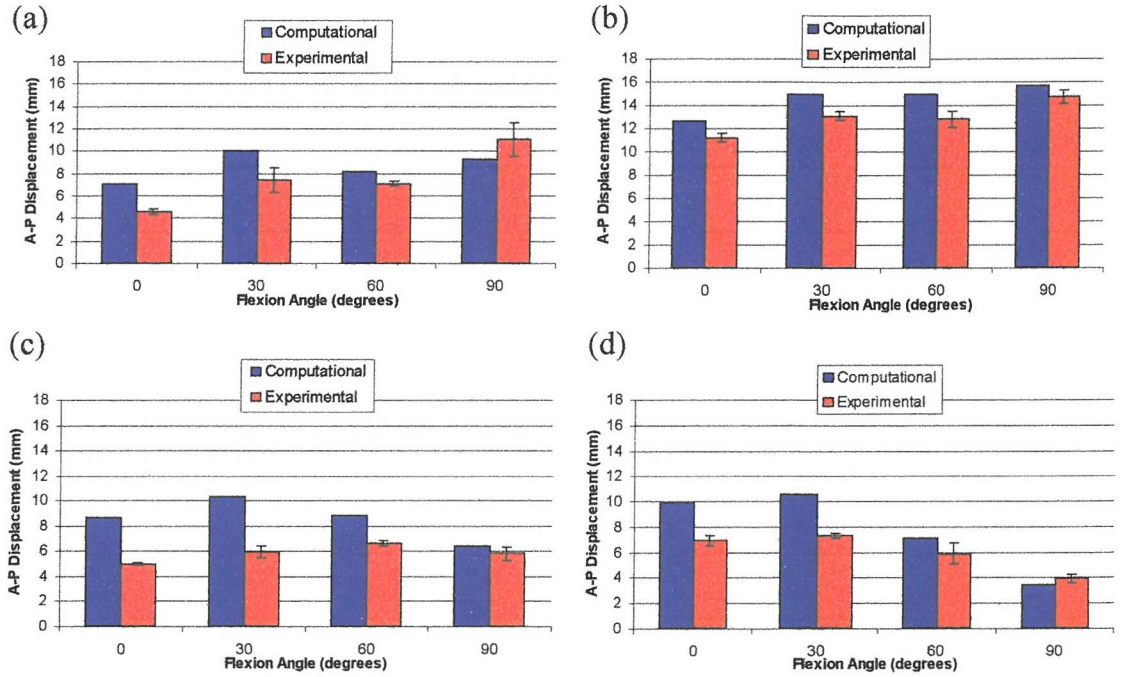

Figure 6.1 Comparison of the computational and experimental A-P translation results of the (a) PC-RR; (b) PC-RF; (c) PC-SR and (d) PC-SF. Displacements refer to the tibial component with respect to the femoral component.

The computational A-P translations tended to be slightly larger than those measured experimentally; however, in all but one test (PC-SR at 30° flexion) the maximum deviation between the computational and experimental results was below 4mm. The trends over the flexion range were similar in all knees, and the overall stability provided by each knee was comparable to that observed experimentally.

6.1.2 Confidence in I-E Stability

Figure 6.2 shows the computational and experimental I-E stability results for all idealised knees.

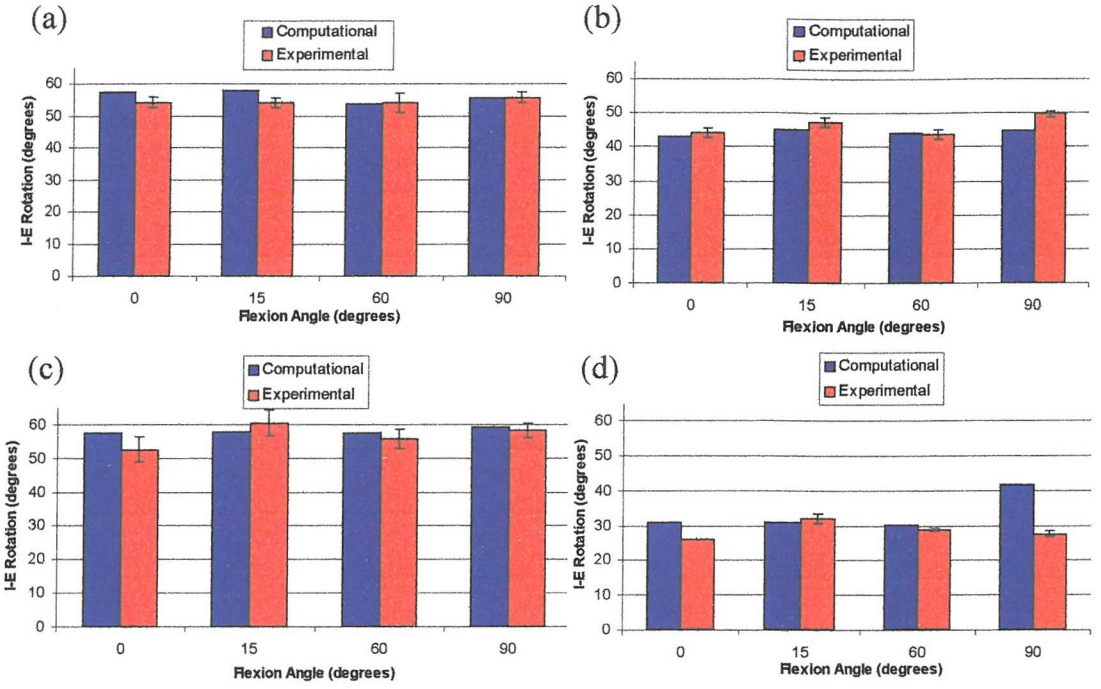

Figure 6.2 Comparison of the computational and experimental I-E stability results of the (a) PC-RR; (b) PC-RF; (c) PC-SR and (d) PC-SF. Rotations refer to the femoral component with respect to the tibial component.

The I-E stability of the computational simulations were very similar to the experimental models. The only significant deviation occurred at 90° flexion in the PC-SF, where rotations differed by 14.1°. In the experimental testing there was definite contact between the tibial spine and the femoral component during I-E rotations at all flexion positions, contact occurred on both the medial and lateral aspects of the tibial spine. For example, during external femoral rotation the femoral component would contact the inferior-to-mid anterior region on the medial side of the tibial spine, and also the superior-posterior aspect on the lateral side of the tibial spine; this interaction restricted external rotations (see Figure 6.3). However, in the computational simulations at 90° flexion, contact only occurred at the mid-anterior position on the medial side of the tibial spine, with the lateral femoral condyle missing, or just brushing the lateral side of the tibial spine (see Figure 6.3 at 90° flexion) causing increased femoral rotations compared to the

experimental results. The discrepancy between the experimental and computational contacts may have been caused by slight differences in initial contact position, or the ligaments may have caused the femoral component to rotate slightly differently in the FE simulations, altering interaction of the tibial spine and femoral component.

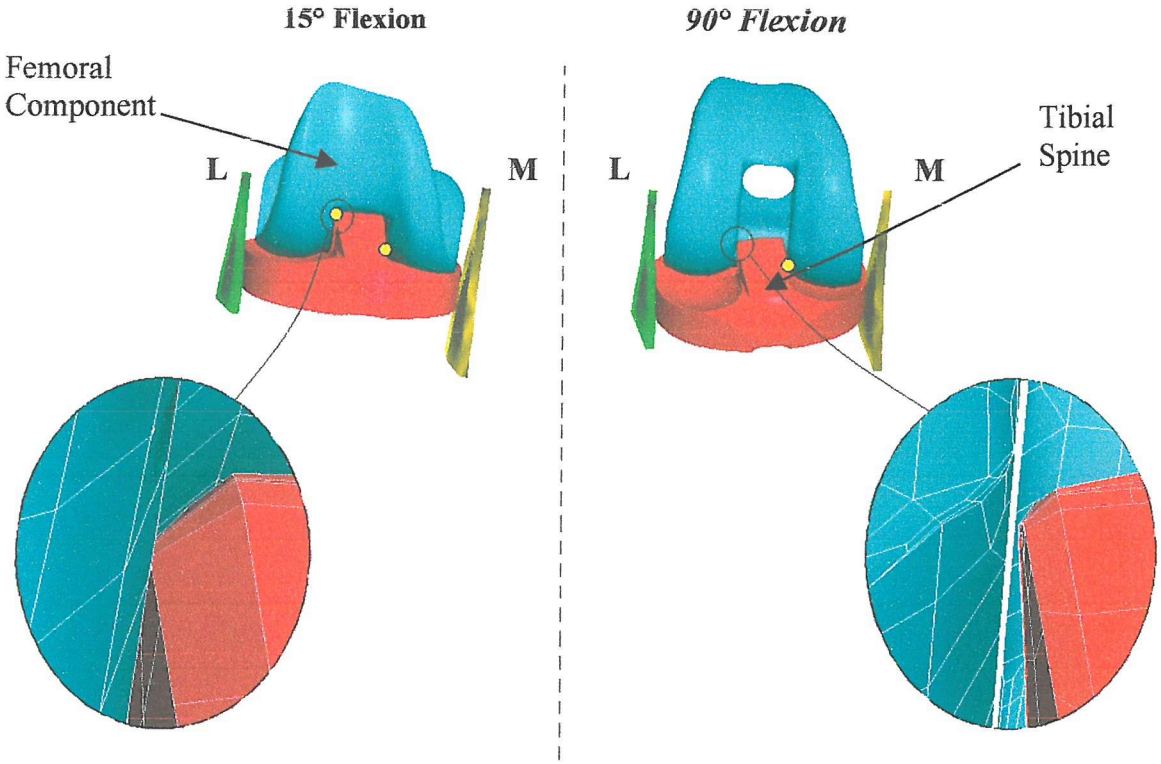

Figure 6.3 Computational model of the PC-SF, showing the contact between the femoral component and the tibial spine at 15° and 90° flexion during external femoral rotation. The yellow areas highlight the contact points: M= Medial side, L= lateral side.

At 0°, 15° and 60° flexion the computational simulations differed from the experimental results by 4.8°, 1.0° and 1.4° respectively; significant differences were only noted at 90° flexion. During the gait cycle (see Chapter 5) the knee does not flex beyond 60°, thus the results produced with the computational PC-SF can be viewed with confidence during normal gait.

In the rotating-bearing knees the rotations of the tibial insert need to be taken into account. Figure 6.4 [(a) & (b)] shows the insert rotations for the idealised PC-RR and PC-SR respectively.

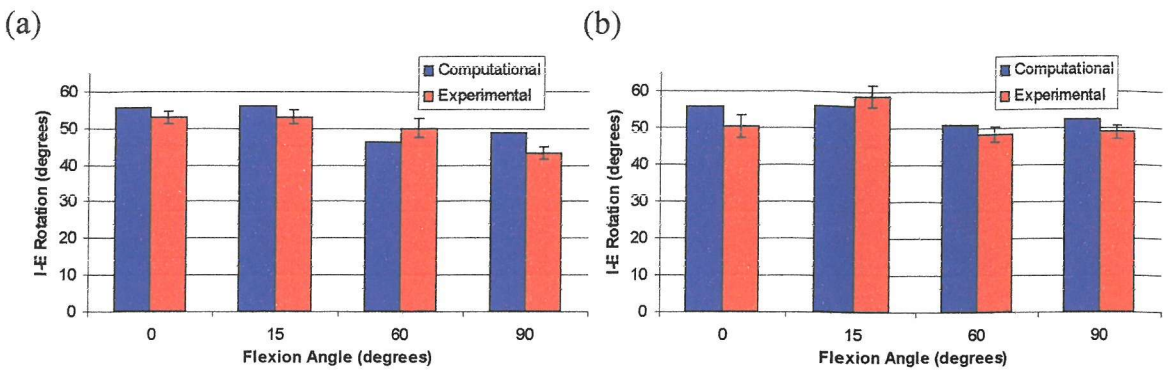

Figure 6.4 Tibial insert rotations with respect to the tibial tray in the idealised (a) PC-RR and (b) PC-SR over the flexion range.

The computational and experimental insert rotations agree well. The only slight deviations occurred at 60° and 90° flexion in the PC-retaining knee where, unlike the experimental results, the computational rotations at 90° flexion were slightly larger than at 60° flexion. Overall however, the same general trend of rotations was followed in the computational simulations and experimental simulations over the flexion range.

6.1.3 Confidence in V-V Stability

V-V stability testing was conducted at 0° flexion only (as discussed in Chapter 3). Figure 6.5 shows the V-V stability of the idealised computational and experimental knees.

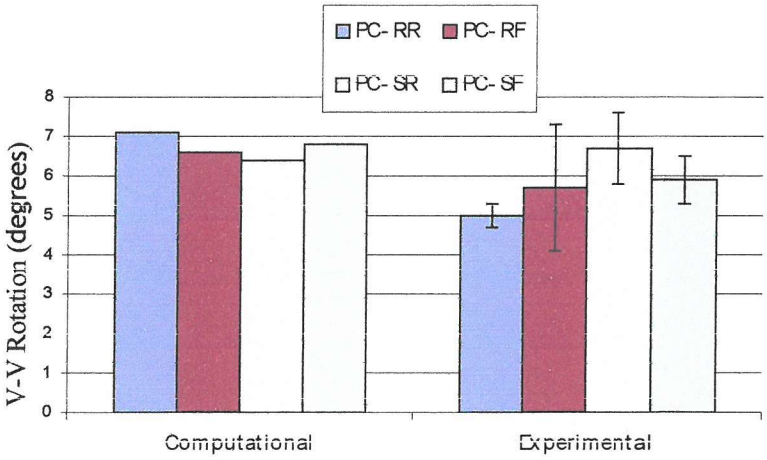

Figure 6.5 Comparison of the computational and experimental V-V stability. Rotations refer to the tibial component with respect to the femoral component.

The V-V stability of the computational and experimental models were comparable. The largest deviation between the computational and experimental rotations occurred in the

PC-RR; this deviation was due to the very small valgus rotations recorded experimentally. The measurement of V-V rotations experimentally may have been prone to slight deviations due to the voltage-to-rotation ratio of the LPDT. The change in voltage recorded by the LPDT during experimental testing was calibrated to correspond to varus or valgus tibial rotations; however because rotations were relatively small (1°-2°), slight alterations in voltage could cause significant changes in recorded rotations. Experimentally the valgus rotations were in the region of 1.5° across all knees, with varus rotations being 60%-80% larger than the valgus rotations. Valgus rotations in the computational simulations were closer to 2.6°, with the varus rotations being 30% larger than the valgus rotations in the rotating-bearing knees, 36% larger in the PC-SF and 52% larger in the PC-RF. The computational findings were more in line with those reported in the literature (see Section 5.9), where the difference between the varus and valgus rotations were not as significant as in the experimental testing. For example, in an *in vivo* study by Yamakado *et al.* [107] the varus rotations were about 30% larger than the valgus rotations; this was comparable to the computational results in the present research.

6.1.4 Confidence in Altered Ligament Strains

Overall the computational simulations of altered ligament strains were consistent with the experimental findings. The change in total I-E rotations caused by altered ligament strains in the experimental and computational work generally lay within 2° of each other. The experimental and computational PC-SF models at 90° flexion differed more significantly than any of the other knees. As discussed in Section 6.1.2 the interaction of the tibial spine and femoral component differed between the experimental and computational models with normally strained collateral ligaments, producing different I-E rotations. Altered ligament strains intensified this difference.

The effect of altered ligament strains on experimental and computational A-P stability was similar. In general the experimental and computational results differed by between 1.0mm-1.4mm for all knee and ligament strain combinations. The effects of altered ligament strains on V-V stability in the computational and experimental models were generally within 0.5°-1.0° of each other. The largest deviation between the computational and experimental results was 1.5° and occurred with a slack-slack MCL-LCL combination in the PC-RF; the experimental simulation did not apply the full force

during testing due to excessive M-L displacements, and this is likely to have produced this discrepancy.

6.1.5 Confidence with Femoral Malalignment

Selected tests were carried out with the computational models for comparison. The knee was malaligned (by 3° of varus or 3° of valgus) and testing was carried out at both 15° and 90° flexion with normally strained collateral ligaments. Under valgus malalignment testing was also performed with a tight MCL and a slack LCL, and under varus malalignment with a slack MCL and a tight LCL. Tables 6.1 and 6.2 present the change in I-E stability when the ligaments are normally strained and imbalanced respectively.

Alignment	Knee	Flexion (°)	Computational (°)			Experimental (°)		
			Internal	External	**Total**	Internal	External	**Total**
Valgus	PC-RR	15	0.6	-0.1	**0.5**	1.2	1.0	**2.2**
		90	4.4	-1.9	**2.5**	3.8	-2.0	**1.8**
	PC-RF	15	0.5	-0.7	**-0.1**	-1.3	-2.7	**-4.0**
		90	4.7	-4.8	**-0.1**	0.5	-4.0	**-3.5**
	PC-SR	15	0.6	-0.1	**0.5**	0.8	-1.6	**-0.8**
		90	4.1	-3.0	**1.0**	1.5	-0.4	**1.1**
	PC-SF	15	2.5	1.3	**3.8**	2.9	0.0	**2.9**
		90	5.1	-2.5	**2.6**	6.6	3.6	**10.2**
		Flexion (°)	Internal	External	**Total**	Internal	External	**Total**
Varus	PC-RR	15	-0.4	0.5	**0.2**	1.7	0.0	**1.7**
		90	-3.7	5.2	**1.5**	-3.4	0.9	**-2.5**
	PC-RF	15	-0.9	0.8	**0.0**	-2.9	-1.9	**-4.8**
		90	-4.9	4.7	**-0.2**	-4.5	1.9	**-2.6**
	PC-SR	15	-0.5	0.7	**0.2**	-0.4	-3.1	**-3.5**
		90	-3.5	4.8	**1.2**	1.7	2.8	**4.5**
	PC-SF	15	0.2	2.6	**2.8**	1.0	2.0	**3.0**
		90	1.1	1.3	**2.4**	1.0	8.9	**9.9**

Table 6.1 Change in I-E rotational stability caused by malalignment. MCL-LCL normally strained. A positive value represents an increase in rotation.

Alignment	Knee	Flexion (°)	Computational (°)			Experimental (°)		
			Internal	External	**Total**	Internal	External	**Total**
Valgus	**PC-RR**	15	0.8	-1.0	**-0.1**	3.1	3.7	**6.8**
		90	4.6	0.2	**4.8**	5.4	-2.4	**3.0**
	PC-RF	15	1.0	0.4	**1.5**	1.2	-2.7	**-1.5**
		90	5.5	-4.4	**1.2**	-1.1	-4.7	**-5.8**
	PC-SR	15	0.8	-0.8	**0.0**	2.9	-1.1	**1.8**
		90	4.0	1.2	**5.1**	-0.3	-2.3	**-2.6**
	PC-SF	15	4.4	-0.3	**4.1**	5.5	0.6	**6.1**
		90	5.9	-3.0	**2.9**	8.3	3.4	**11.7**
		Flexion (°)	Internal	External	**Total**	Internal	External	**Total**
Varus	**PC-RR**	15	-1.5	0.3	**-1.1**	2.5	2.7	**5.2**
		90	-3.7	4.4	**0.7**	-0.8	1.1	**0.3**
	PC-RF	15	-1.3	-1.2	**-2.4**	-4	-1.3	**-5.3**
		90	-5.6	4.2	**-1.3**	-5.2	1.5	**-3.7**
	PC-SR	15	-2.1	0.4	**-1.7**	3.2	-1	**2.2**
		90	-0.8	3.7	**2.8**	-1.1	3.2	**2.1**
	PC-SF	15	0.6	2.7	**3.3**	-0.1	2.4	**2.3**
		90	2.0	2.0	**4.0**	1.3	11.4	**12.7**

Table 6.2 Change in I-E rotational stability caused by malalignment with imbalanced ligaments. A positive value represents an increase in rotation.

Internal and external rotations followed the same trend in the computational and experimental models with normally strained collateral ligaments. Valgus malalignment tended to cause internal rotations to increase and external rotations to decrease, and the opposite occurred in the varus knees. At 15° flexion the effects of malalignment were not as great as at 90° flexion. With altered ligament strains (Table 6.2) the experimental effects of malalignment did not match the computational effects as closely as with normally strained ligaments. In about 50% of the results the findings were comparable, and in a further 20% the same general trend was followed in both the computational and experimental results. However, 30% of the findings were not close enough to be viewed as comparable. A possible reason for the discrepancies between the computational and experimental findings may be due to complications in ligament straining in the malaligned knees due to the experimental setup procedure; as discussed in Section 5.8. In brief, the tibial component did not fully rotate in the coronal plane due to the malaligned femoral component and made accurate ligament straining difficult.

In the neutrally aligned computational model of the PC-SF at 90° flexion, the tibial spine did not restrict femoral rotations as significantly as in the experimental model, as discussed in Section 6.1.2. Malalignment of the computational model did not further alter

the tibial spine and femoral component interaction; however, in the experimental model malalignment altered the tibial spine and femoral component interaction more significantly, hence the greater deviation between the computational and experimental results in the PC-SF with malalignment.

The overall affect of malalignment on the A-P stability was relatively minor, with differences of ~1.5mm were noted for all knees (see Tables 6.3 and 6.4). Similar effects were noted in the experimental and computational models. The computational results were within 2mm of the experimental results in all but one case (PC-SR at 90° flexion; valgus alignment; tight-slack MCL-LCL: 2.7mm difference).

Alignment	**Knee**	**Flexion (°)**	**Computational (mm)**			**Experimental (mm)**		
			Anterior	Posterior	**Total**	Anterior	Posterior	**Total**
Valgus	**PC-RR**	0	0.0	0.1	**0.1**	0.7	0.6	**1.3**
		90	-0.2	-0.1	**-0.3**	0.4	-1.9	**-1.5**
	PC-RF	0	-0.1	0.0	**0.0**	-0.9	0.2	**-0.7**
		90	-1.3	-0.5	**-1.7**	-0.5	-1.4	**-1.9**
	PC-SR	0	-0.5	-0.1	**-0.7**	0.3	-1.4	**-1.1**
		90	-0.3	0.1	**-0.2**	-0.7	0.5	**-0.2**
	PC-SF	0	0.0	0.0	**0.0**	0.0	-1.4	**-1.4**
		90	0.2	0.0	**0.2**	0.2	0.3	**0.5**
		Flexion (°)	Anterior	Posterior	**Total**	Anterior	Posterior	**Total**
Varus	**PC-RR**	0	0.0	0.0	**-0.1**	-0.8	-0.5	**-1.3**
		90	-0.2	-0.2	**-0.4**	0.4	-2.7	**-2.3**
	PC-RF	0	-0.1	-0.1	**-0.1**	-1.3	-0.5	**-1.8**
		90	-1.0	-0.4	**-1.3**	-0.9	-0.7	**-1.6**
	PC-SR	0	-0.3	-0.1	**-0.5**	0.5	-1	**-0.5**
		90	-0.4	0.1	**-0.4**	0	0.7	**0.7**
	PC-SF	0	0.0	0.0	**0.0**	-0.4	-1.4	**-1.8**
		90	0.2	0.0	**0.2**	0.1	0.1	**0.2**

Table 6.3 Effects of malalignment on A-P translations with normally strained collateral ligaments. A positive value represents an increase in translation.

Alignment	Knee	Flexion (°)	Computational (mm)			Experimental (mm)		
			Anterior	Posterior	**Total**	Anterior	Posterior	**Total**
Valgus	**PC-RR**	0	-0.3	0.4	0.1	0.7	0.7	**1.4**
		90	-0.7	1.0	0.3	0.2	-1.7	**-1.5**
	PC-RF	0	-0.1	0.2	0.2	-0.8	0.3	**-0.5**
		90	-1.7	-0.3	-1.9	-0.2	-1.5	**-1.7**
	PC-SR	0	0.4	0.4	0.7	0.4	-0.6	**-0.2**
		90	-2.1	0.1	-2.0	-0.2	0.9	**0.7**
	PC-SF	0	0.1	0.3	0.4	0.2	-0.7	**-0.5**
		90	-0.2	0.0	-0.2	-0.3	0.0	**-0.3**
		Flexion (°)	Anterior	Posterior	**Total**	Anterior	Posterior	**Total**
Varus	**PC-RR**	0	-0.3	-0.2	-0.5	-0.4	-0.6	**-1.0**
		90	-0.7	0.1	-0.6	0.0	-1.1	**-1.1**
	PC-RF	0	-0.1	-0.1	-0.1	-1.1	0.5	**-0.6**
		90	-1.8	-0.3	-2.1	-1.0	-0.7	**-1.7**
	PC-SR	0	-0.7	-0.4	-1.2	0.6	-1.3	**-0.7**
		90	-0.4	0.0	-0.5	-0.7	1.1	**0.4**
	PC-SF	0	0.0	-0.2	-0.2	-0.2	-1.1	**-1.3**
		90	0.1	0.0	0.1	0.2	0.0	**0.2**

Table 6.4 Effects of malalignment on A-P translations with imbalanced ligaments. A positive value represents an increase in translation.

With normally strained collateral ligaments the effect of malalignment on V-V stability in the computational models was minimal; however, during experimental testing there was an increase in varus rotations of up to 1.9°. As with I-E stability, the difference between the computational and experimental results was possibly caused by inaccurate ligament straining (see Section 5.8). From Table 6.5 it can be clearly seen that the computational results were more consistent across all knees and that malalignment had little effect on V-V stability. These findings were more realistic as in theory when both collateral ligaments are normally strained malalignment should not significantly affect stability in the coronal plane under low loads.

Overall the computational passive stability testing compared well with the experimental testing, forming a good basis for further test simulations. Additional confidence in the results was gained in the contact pressure validation section of this thesis (Section 6.2).

Alignment	Knee	Computational (°)			Experimental (°)		
		Varus	Valgus	Total	Varus	Valgus	Total
Valgus	PC-RR	0.0	0.0	0.0	1.6	0.2	1.8
	PC-RF	-0.1	0.1	0.0	-1.1	0.8	-0.3
	PC-SR	-0.1	0.1	0.0	0.0	1.1	1.1
	PC-SF	-0.1	-0.1	-0.2	1.1	0.0	1.1
Varus	PC-RR	0.1	-0.1	0.0	1.6	-0.6	1.0
	PC-RF	0.1	0.0	0.1	0.6	-0.5	0.1
	PC-SR	0.1	0.0	0.1	0.9	-0.9	0.0
	PC-SF	0.1	-0.2	-0.1	1.9	-1.0	0.9

Table 6.5 Effects of malalignment on V-V stability with normally strained ligaments. A positive value represents an increase in rotation.

6.1.6 PCL Comparison

As discussed in Section 5.10 testing with the PCL would not form part of the overall analysis of the present research. The experimental PCL was reproduced in the computational simulations for a simple comparison, however the findings will not be analysed in detail. Tables 6.6 and 6.7 show the change in I-E and A-P motions respectively caused by the attachment of the PCL in both the experimental and computational simulations.

Knee	Model	Flexion Angle (°)	Change in Rotation (°)	Difference between Experimental & Computational (°)
PC-RR	Experimental	0	4.1	**1.8**
	Computational	0	2.3	
	Experimental	15	2.6	**0.3**
	Computational	15	2.9	
	Experimental	60	2.9	**1.4**
	Computational	60	4.3	
	Experimental	90	3.1	**0**
	Computational	90	3.1	
PC-RF	Experimental	0	4.5	**2.3**
	Computational	0	2.2	
	Experimental	15	6.9	**4.8**
	Computational	15	2.1	
	Experimental	60	3.6	**0.1**
	Computational	60	3.7	
	Experimental	90	4.2	**1.8**
	Computational	90	2.4	

Table 6.6 Reduction in I-E laxity caused by the PCL in the experimental and computational simulations.

Knee	Model	Flexion Angle (°)	Change in Translation (mm)	Difference between Experimental & Computational (mm)
PC-RR	Experimental	0	0.6	**0.5**
	Computational	0	1.1	
	Experimental	30	2.1	**0.8**
	Computational	30	2.9	
	Experimental	60	0.4	**0.4**
	Computational	60	3.2	
	Experimental	90	1.8	**0.6**
	Computational	90	2.4	
PC-RF	Experimental	0	0.7	**1**
	Computational	0	1.7	
	Experimental	30	1.9	**3.1**
	Computational	30	5	
	Experimental	60	2.5	**2.7**
	Computational	60	5.2	
	Experimental	90	1.5	**2.1**
	Computational	90	3.6	

Table 6.7 Reduction in A-P laxity caused by the PCL in the experimental and computational simulations.

The reduction in I-E and A-P laxity caused by the PCL was relatively similar for the experimental and computational simulations. The greatest deviations between the experimental and computational results occurred with the fixed-bearing knee (maximum deviation of 4.8° in I-E stability at 15° flexion and 3.1mm in A-P stability at 30° flexion). In general the experimental and computational results differed by 0°-2° and 0mm – 3mm across all flexion positions in both the PC-RR and PC-RF.

6.2 Contact Pressure Validation

Table 3.4 in Section 3.4 described the various experimental contact pressure tests performed. In the images below the experimental contact pressure results have been superimposed onto a tibial insert to show the contact positions more clearly. All results show the path of the peak pressures over the duration of the test performed. Red inserts represent the experimental results and blue inserts represent the computational results, the colour contour scale was constant. Table 6.8 shows the maximum contact pressures during sliding recorded experimentally and by the FE simulations. All tests were for the PC-RF.

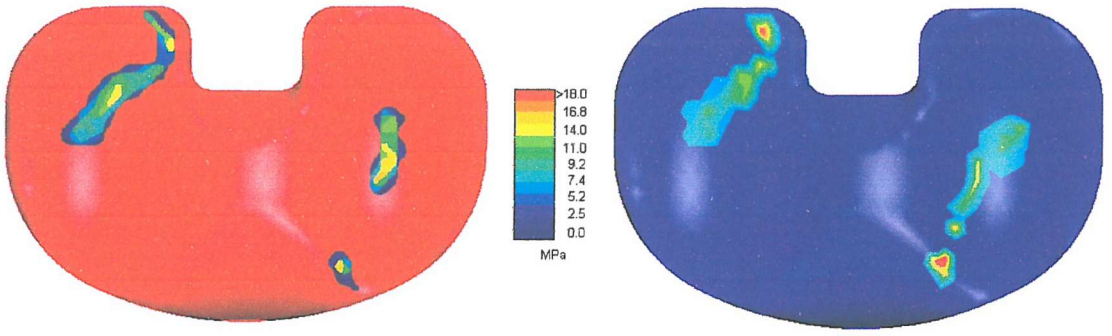

Experimental Computational

Validation Tests 1-3, 10 & 11: -8Nm torque applied through the femoral component (external rotation). Neutral alignment, 0° flexion, MCL-LCL= Normal strain, 50N compressive load, 3 second test.

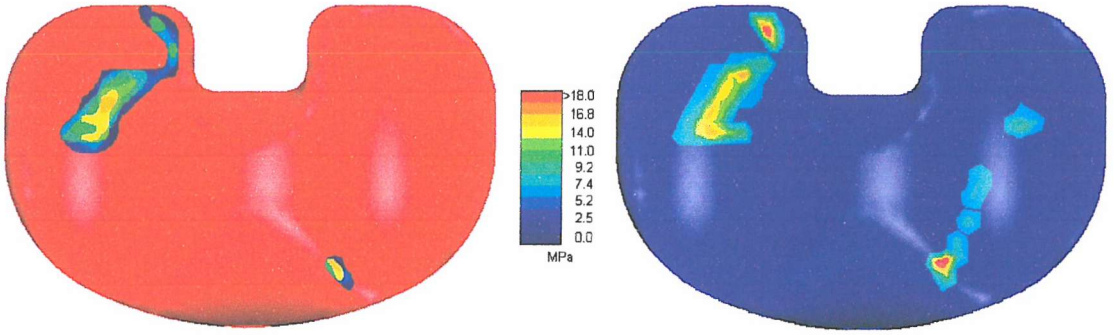

Experimental Computational

Validation Test 4: -8Nm torque applied through femoral the component (external rotation). Neutral alignment; 0° flexion, MCL= Slack LCL= Tight, 50N compressive load, 3 second test.

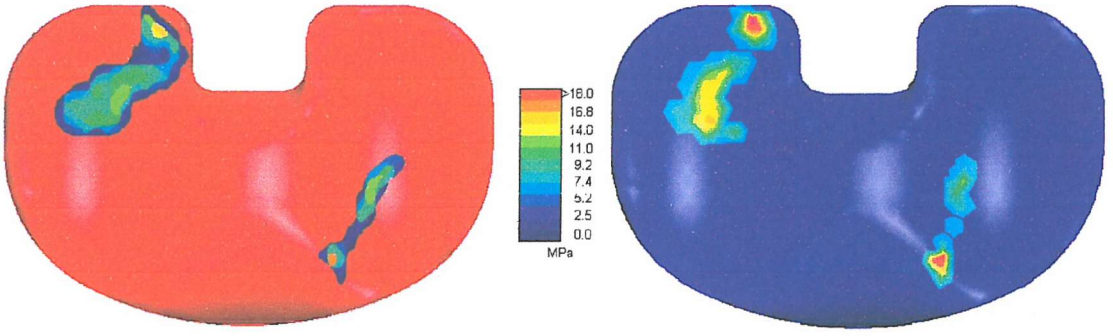

Experimental Computational

Validation Test 5: -8Nm torque applied through the femoral component (external rotation). Neutral alignment, 15° flexion, MCL= Slack LCL= Tight, 50N compressive load, 3 second test.

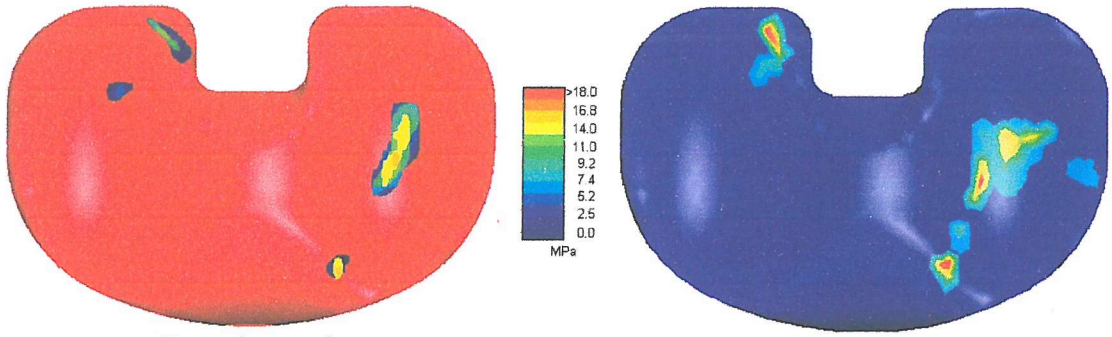

Experimental Computational

Validation Test 6: -8Nm torque applied through the f ernal rotation). Neutral alignment, 0° flexion, MCL= Tight LCL= slack, 50N compressive load, 3 second test.

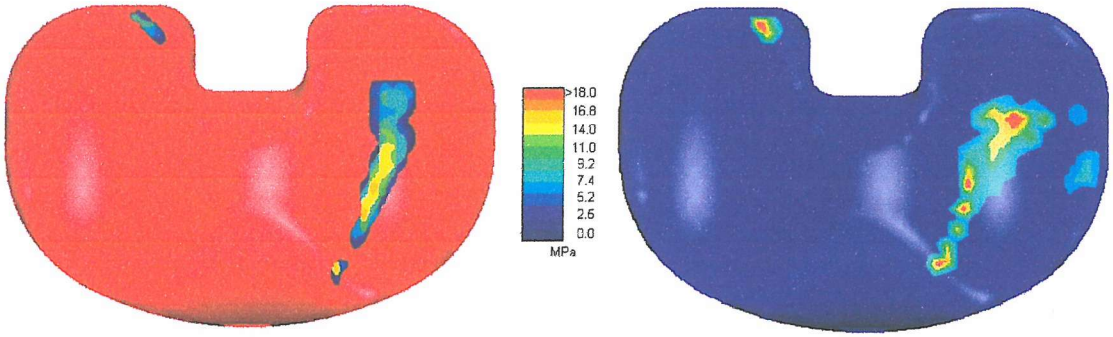

Experimental Computational

Validation Test 7: -8Nm torque applied through the femoral component (external rotation). Neutral alignment, 15° flexion, MCL= Tight LCL= slack, 50N compressive load, 3 second test.

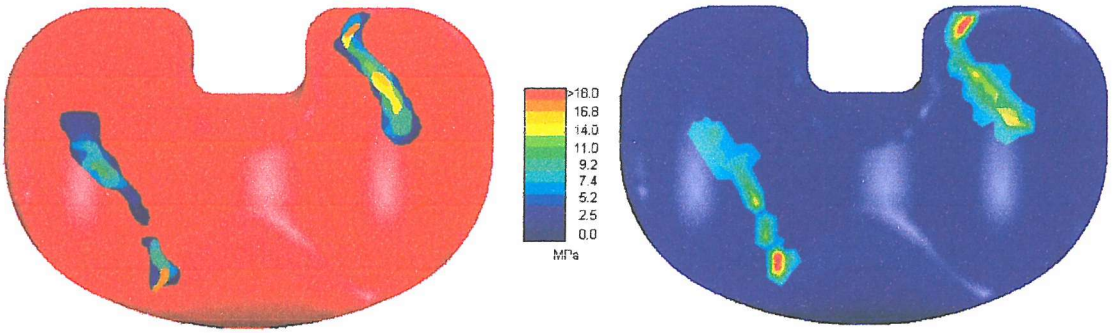

Experimental Computational

Validation Tests 8 & 9: +8Nm torque applied through the femoral component (internal rotation). Neutral alignment, 0° flexion, MCL-LCL= Normal strain, 50N compressive load, 3 second test.

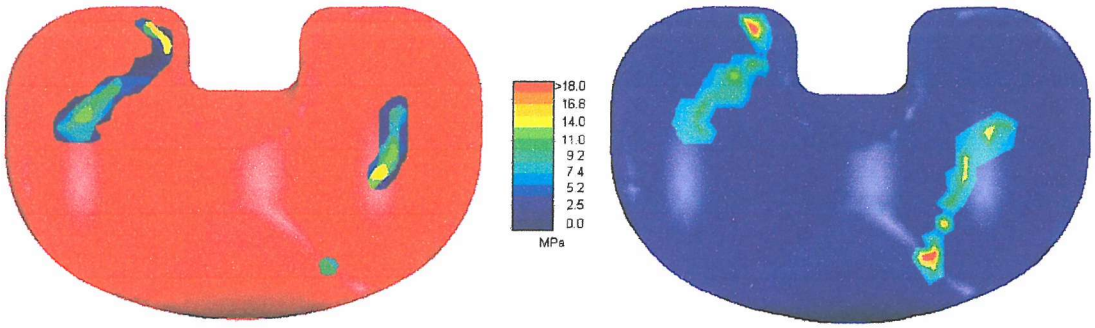

Experimental Computational

Validation Tests 12 & 13: -8Nm torque applied through the femoral component (external rotation). Varus alignment, 0° flexion, MCL-LCL= Normal strain, 50N compressive load, 3 second test.

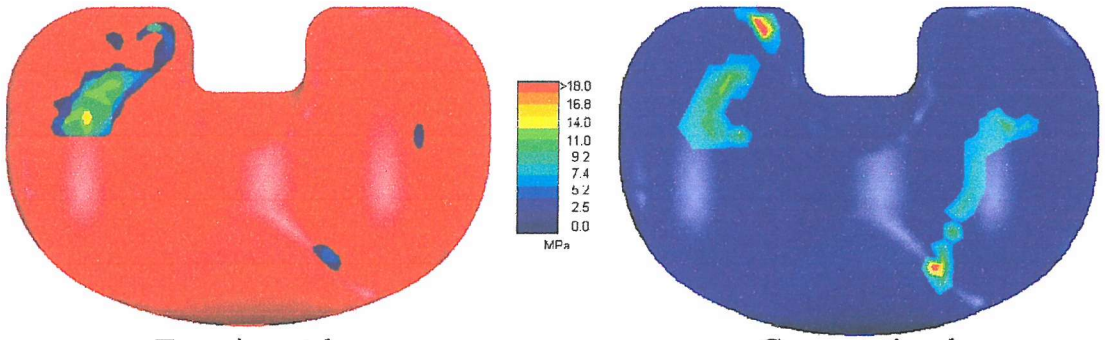

Experimental Computational

Validation Tests 14: -8Nm torque applied through femoral component (external rotation). Varus alignment, 0° flexion, MCL= Slack LCL= Normal, 50N compressive load, 3 second test.

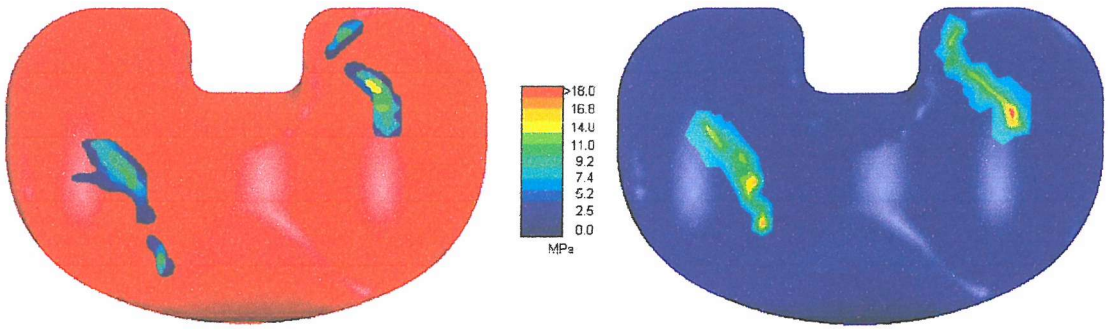

Experimental Computational

Validation Tests 15: 15° internal femoral rotation. Neutral alignment, 0° flexion, no ligaments, 100N compressive load, 3 second test.

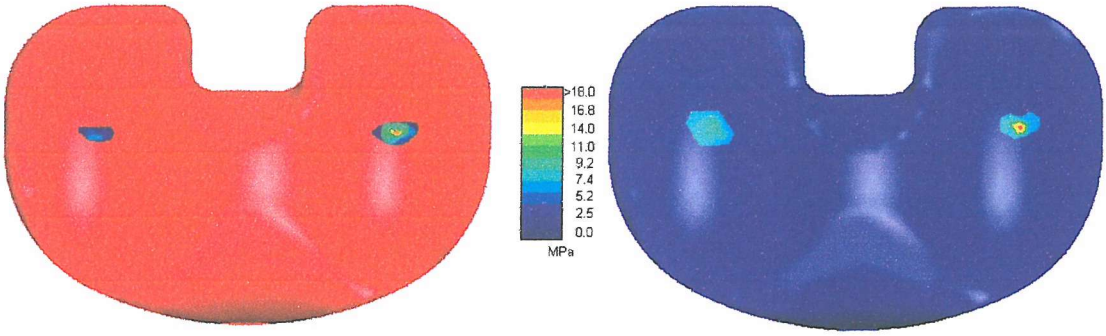

Experimental Computational

Validation Tests 16: Valgus alignment, 0° flexion, no ligaments, 200N compressive load, 3 second test.

Good visual and numerical comparisons between the experimental and FE models were evident. The computational results tended to show larger overall contact pressure areas, however this was most likely due to the computational models recording the lower contact pressures more accurately. As briefly noted in Section 3.4 the low contact pressure threshold of the Tekscan sensors was about 1.5MPa, thus any contact pressures below this would not be recorded. Examples of this phenomenon are shown in Tests 4, 7 and 14, where there were considerably more blue regions (low contact pressure areas) in the computational models. The higher contact pressure regions in the computational and experimental images were however very similar in both magnitude and area, and conclusively show that the computational simulations were accurate and reliable. It was notable that the rim contact pressures in the computational models tended to be higher (red rim regions). This could be due to the frictional forces produced by the sensors reducing the force of the femoral component as it contacts the insert rim, or the sensors may have cushioned the initial high impact force. For the validation in the present study this was not viewed as an important issue as experimentally measured rim contact pressures may have varied depending on the length of the test or the duration of the recording (as discussed in Section 5.11).

The experimental results were an average approximation as the original contact pressures were recorded as a range; thus, the mid value of this range was taken, and then an average was calculated when repeats were performed. In Tests 4, 7 and 13 the computational models recorded contact pressures where the experimental testing did not, however these were low values, and as mentioned may not have been recorded

experimentally due to the minimum threshold value of the sensors. In general, the FE and experimental results were within 1MPa-2MPa of each other, and were closely matched in terms of contact areas.

Test	Peak FE Contact Pressure (MPa)		Peak Experimental Contact Pressure (MPa)	
	Medial Side	Lateral Side	Medial Side	Lateral Side
1-3	11.3	12.6	12.8	12.3
4	2.3	15.8	-	14.8
5	9	11.5	11.8	11
6	13.5	2.3	14.8	3.8
7	15.8	-	14.8	-
8-9	13.5	9	14.8	10
12-13	14.3	9.1	13	11.5
14	3.5	11.3	-	13
15	11.3	11.3	13	10

Table 6.8 Peak contact pressures recorded during passive stability testing for the PC-RF. – indicates that no pressures were recorded.

In summary, the motions and contact pressures produced in the computational simulations closely matched those produced experimentally. Some motion variations did occur, particularly in the V-V stability and malalignment investigations; possibly caused by difficulties in experimental ligament straining and recording of V-V rotations, however, the experimental and computational motions closely agreed. The findings of any future computational simulations with the models of the present research can be viewed with confidence, with all results comparable to those found *in vitro*.

Chapter 7 Active Stability: Normal Gait

As mentioned in Chapter 5 gait data was inputted into the finite element models to simulate active motions (normal gait). The motions were produced by force-controlled input values; this meant that the kinematics of the different knee designs were dictated by the individual component geometries and soft tissue restraints.

7.1 Kinematics during Normal Gait

Figure 7.1 [(a & b)] shows the I-E rotations (femoral) and A-P translations (tibial) for the four knees designs assessed. Testing was conducted in the idealised knee (neutral alignment with normally strained collateral ligaments).

I-E stability:

I-E rotations over the gait cycle could be divided into two groups, those with rotating-bearing inserts and those with fixed-bearing inserts. The rotating-bearing inserts offered a considerably reduced restraint towards I-E rotations (as shown in the passive stability testing in Chapter 4), thus both the PC-RR and PC-SR had significantly larger I-E rotations compared to the fixed-bearing knees. Peak internal rotations of about 24.1° were recorded for the PC-SR, which was slightly larger than the 23.5° produced in the PC-RR (peak internal rotation was recorded between 50%-60% of the gait cycle). The PC-SR also had a slightly larger peak external rotation (~5.8°) compared to the PC-RR (~4.1°) (peak external rotation was recorded between 10%-20% of the gait cycle). In general however, both rotating-bearing knees had comparable I-E rotations throughout the gait cycle (see Figure 7.1(a)).

As the fixed-bearing inserts did not axially rotate, the geometry of the insert dictated I-E rotations more than in the rotating-bearing knees. The peak internal rotation of the PC-RF was reduced by over 50% (peak internal rotation of 10.6°) compared to the rotating-bearing knees; the peak external rotation was ~2° smaller. As highlighted in the passive stability testing (Chapter 4), the PC-SF had a significantly increased geometric restraint towards I-E rotations and caused lower peak internal and external rotations of 6.0° and 1.1° respectively (see Figure 7.1(a)).

(a)

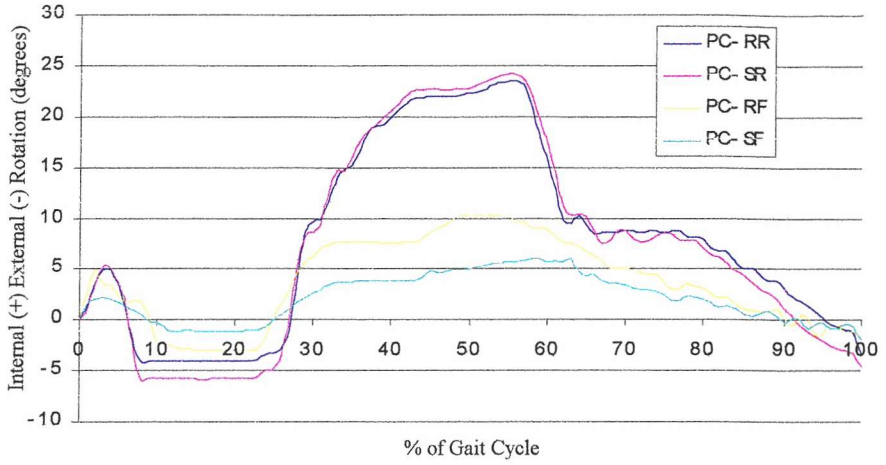

(b)

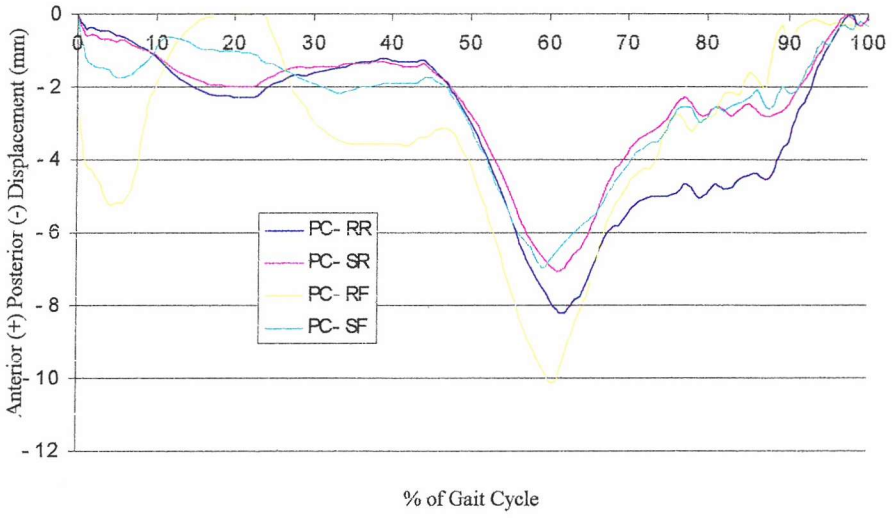

Figure 7.1 (a) I-E femoral rotations and (b) A-P tibial displacements over the gait cycle for the four knee designs tested.

A-P Stability:

A combination of the rolling motions of the femoral component during flexion and the applied A-P forces dictated the A-P displacements during gait. From the passive stability data (Chapter 4) we know that the PC-RF had the lowest A-P stability, which was further highlighted in the gait results. At heel strike (beginning of gait cycle) there was an abrupt posterior displacement of the PC-RF insert of about 5.2mm; this was significantly larger than all other knee designs (see Figure 7.1 (b)). At ~60% of the gait cycle all knees showed a peak posterior displacement, again the PC-RF had the greatest translation (~10.0mm). For the first 50% of the gait cycle both rotating-bearing knees had similar A-P translations; however, the peak posterior translation was ~1.2mm larger in the PC-RR.

From the peak posterior translation position until the end of the gait cycle the PC-RR was more posteriorly positioned compared to the PC-SR. The PC-SF had relatively similar A-P translations to the rotating-bearing knees (see Figure 7.1 (b)).

7.2 Maximum Contact Pressures and Contact Areas

Peak contact pressures were plotted on both the medial and lateral sides of the insert at selected positions during the gait cycle. The contact pressures were noted from visual contact pressure images that were displayed in Pam-Crash-View. Readings were taken at positions of interest across the gait cycle, which were chosen from a contact pressure over % gait cycle plot presented in work published by Godest *et al.* [9] (see Figure 7.2). Select data points were taken at 1%, 10%, 30%, 50%, 80% and 99% of the gait cycle and corresponded to areas of interest, including initial pressures, peak pressures and final pressures. The contact pressures over the entire gait cycle were not assessed since it would be too expensive in terms of time and effort. Pam-Crash-View did not provide a pressure over time plot, but instead showed the peak pressure at a certain point during the gait cycle. Manually recording the peak pressure values at each position across the gait cycle (over 100 positions) and typing them into a spreadsheet would be time consuming in itself, and to add complexity Pam-Crash-View did not specify between the medial and lateral contact pressures, only providing the peak pressure value across the entire insert at the particular moment in time. Therefore the only way to record the peak pressures on the medial and lateral condyles was to visually assess the pressure distributions and compare them against a colour contour pressure scale.

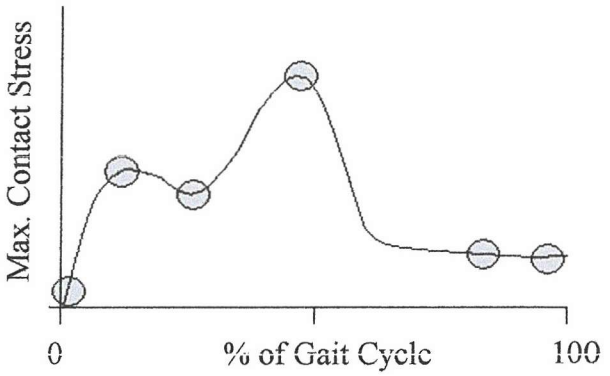

Figure 7.2 Representation of the trend of maximum contact pressures over a gait cycle [9]. Shaded areas indicate where data readings were taken in the present research.

The goal of the rotating-bearing knee was to reduced I-E restraint, increase component conformity (increasing contact areas) and consequently reduce the contact pressures across the insert bearing surfaces. This was shown to occur in the present research, with both rotating-bearing knees possessing significantly larger contact areas and lower peak contact pressures throughout the gait cycle compared to the fixed-bearing knees. The PC-RF, which had the lowest component conformity of the four knees tested, produced the largest maximum contact pressures. The PC-SF had slightly lower peak contact pressures (see Figure 7.3). The peak contact pressures were generally greater on the medial side of the knee, however one exception to the rule was the PC-RF which had larger lateral contact pressures at 50% of the gait cycle. This position corresponded to the point of maximum internal femoral rotation causing a pressure build up on the medial aspect of the lateral insert condyle, where the geometry of the insert restricted internal femoral rotations (see Figure 7.5 at 50% of gait). Both rotating-bearing knees had relatively even medial and lateral contact pressure distributions.

(a)

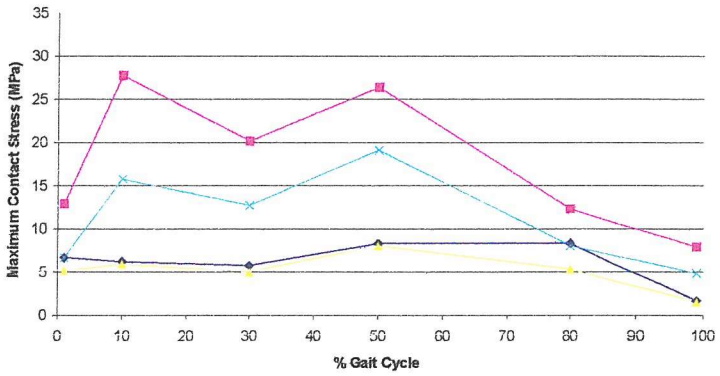

(b)

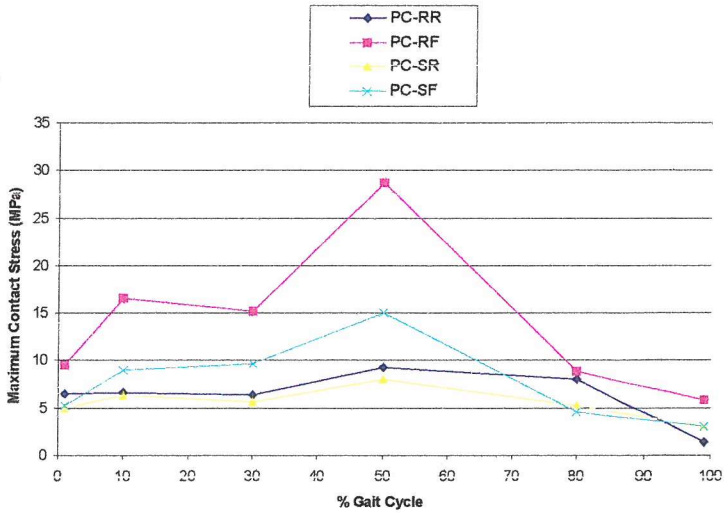

Figure 7.3 Peak contact pressures over the gait cycle on (a) the medial insert bearing surface and (b) the lateral insert bearing surface.

Contact pressures in the region of 5MPa-9MPa were formed in the rotating-bearing knees throughout the entire gait cycle. Peak contact pressures reached ~19MPa in the PC-SF and 29MPa in the PC-RF. The maximum contact pressures occurred at ~50% of the gait cycle; this corresponded to a position where forces were at their greatest. The size of the contact area could be directly related to the magnitude of the contact pressures formed, and both the rotating-bearing knees had significantly larger contact areas than the fixed-bearing knees. Contact areas at each of the recorded positions are shown Figure 7.4, and fixed pressure limits of between 0.1MPa and 30MPa were set in each case. Contact areas were estimated by counting the number of elements covered by the pressure field in Pam-Crash-View, and since the approximate size of the elements were known (average edge length of 1.2mm) the contact areas could be calculated.

In general the medial contact areas were larger than the lateral contact areas throughout the gait cycle. With the exception of the PC-SF the medial contact area was ~1.6 times larger at 50% of the gait cycle (maximum peak contact pressures) for all knees. The medial contact area of the PC-SF was 2.4 times larger. A larger contact area would be expected to lower the peak contact pressure, but Figure 7.3 illustrates that this was not always the case, suggesting the forces across the knee were not evenly distributed (see Figure 7.6).

Both rotating-bearing knees had similar vertical contact forces and both fixed-bearing knees had similar vertical contact forces throughout the gait cycle (see Figure 7.6). For the first 30% of the gait cycle, and between 60%-100% of the gait cycle the medial and lateral contact force distribution in the rotating-bearing knees was relatively even (maximum of 52% through lateral side). However, between 30%-60% of the gait cycle as much as 59% of the load passed through the medial side of the knee, which corresponded to an extra 397N. This altered force distribution had minor effects on the peak contact pressures due to the large medial contact areas.

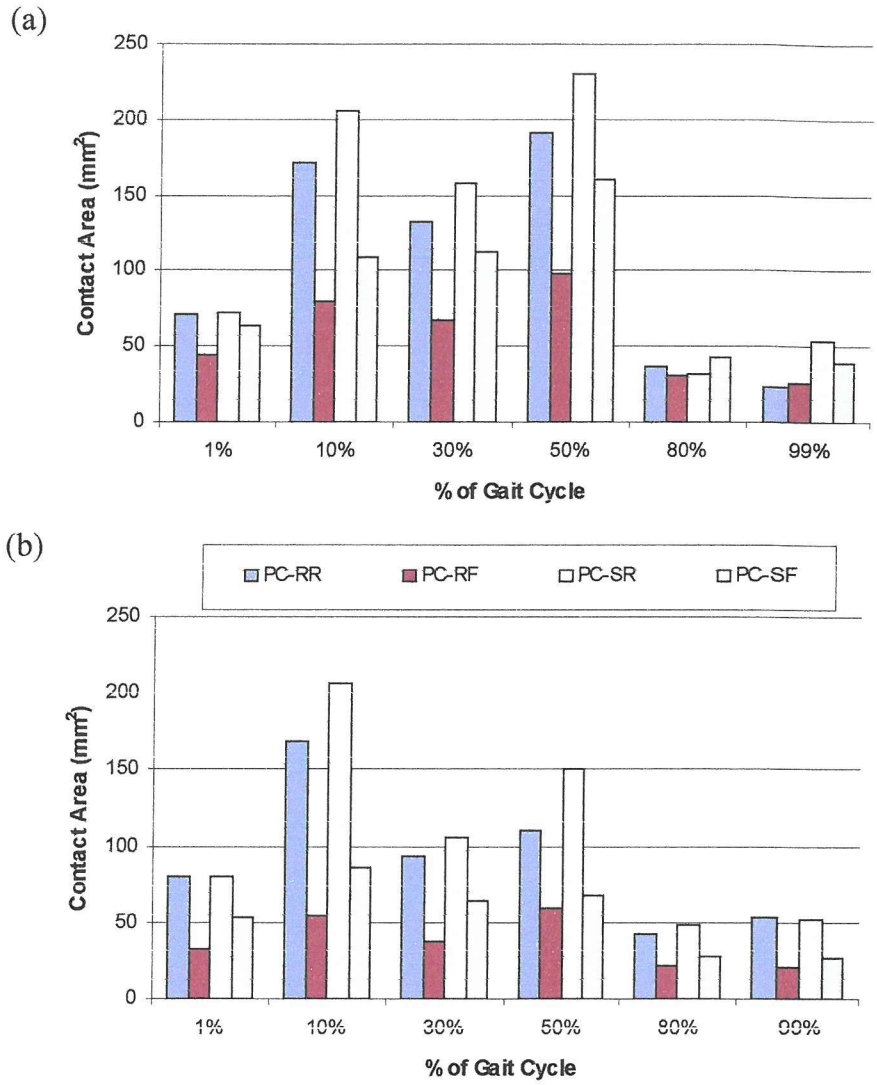

Figure 7.4 Contact areas on (a) the medial side and (b) the lateral side of the knee throughout the gait cycle.

The contact force distribution was not so evenly distributed in the fixed-bearing knees, with a maximum of ~75% of the total vertical force being applied through the medial bearing surface. This significant difference in loading patterns between the rotating-bearing and fixed-bearing knees may be due to the I-E rotational restraint of the knees, or the strains within ligaments. I-E torques were opposed to a greater extent in the fixed-bearing knees, which may then cause the increased medial forces observed during the gait cycle. Another possible explanation could be that the force distribution may be disrupted by the initial pull of the ligaments, and the effect may not be as significant in the rotating-bearing knees due to the fact that the insert could rotate. However, no initial rotations were observed in the rotating-bearing knees.

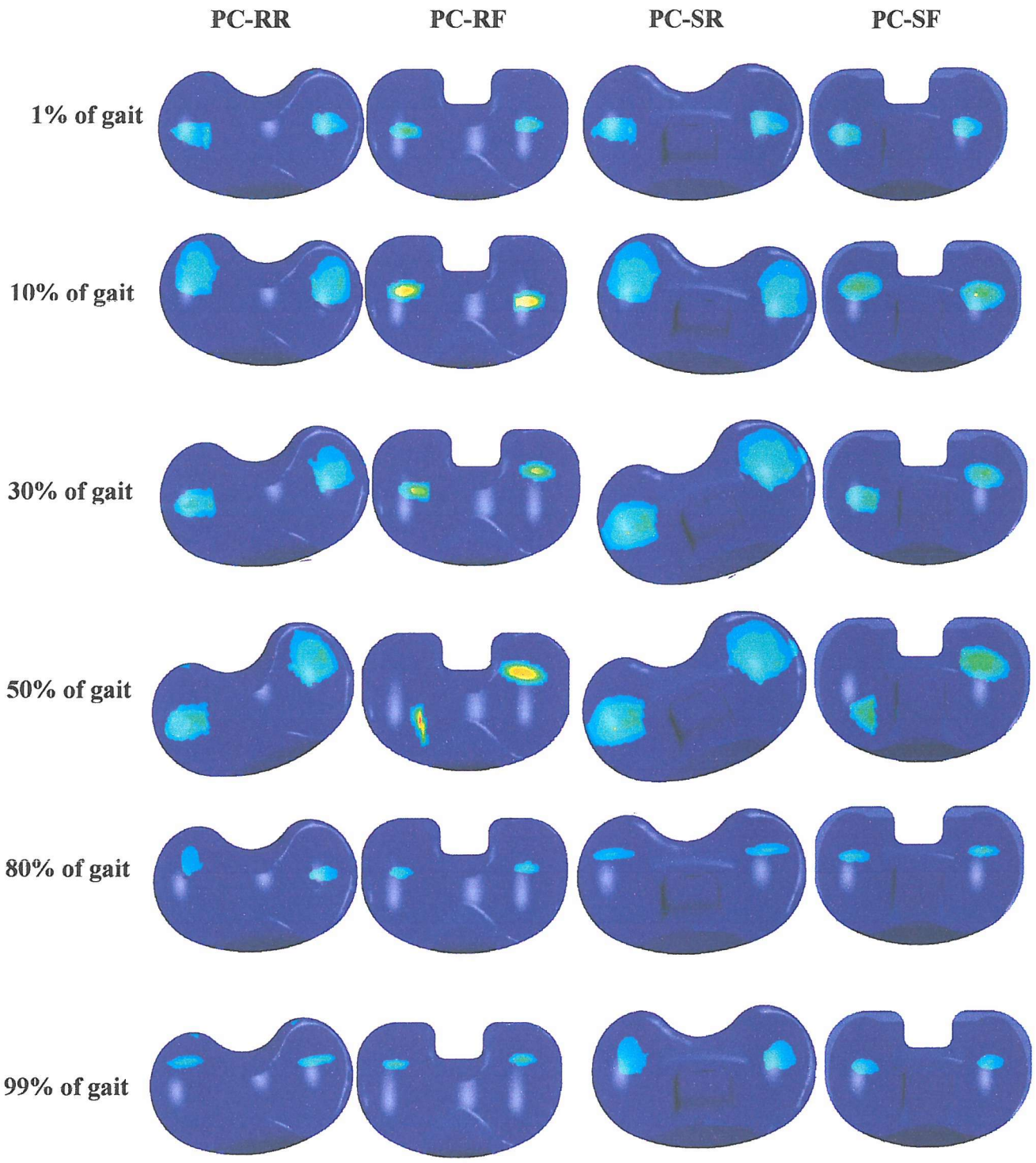

Figure 7.5 Contact pressures and contact areas throughout the gait cycle for all knees tested in the present research. Figure for visual comparison not direct measurement.

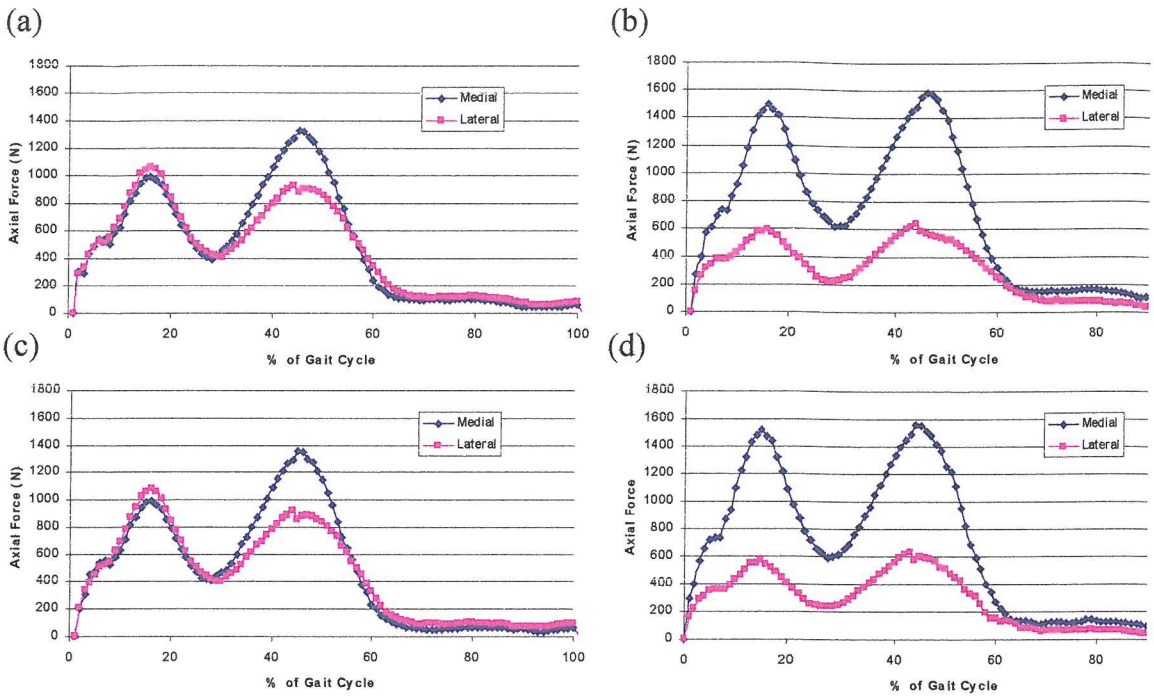

Figure 7.6 Medial and lateral axial load distribution throughout the gait cycle in the idealised (a) PC-RR, (b) PC-RF, (c) PC-SR and (d) PC-SF.

The difference in kinematics/ axial loading and contact pressures of the difference knee designs could have an effect on the long-term behaviour of the prosthesis. The increased sliding and contact pressures noted in some knees may increase wear rates, the chance of insert fracture and implant loosening. Circumstances that could lead to these failure modes are discussed in more detain in Chapter 9, which provides a global review of all work carried out in this thesis.

7.3 Possible role of the PCL during Gait

Despite previously stating that the results with the PCL will not be assessed in detail (Chapter 4), a comparison test was conducted to view the possible role of the PCL during gait. One gait cycle was performed on the idealised PC-RR and PC-RF. Figure 7.7 [(a & b)] compares the I-E and A-P motions with and without the PCL for both knees.

The I-E rotations were relatively unaffected by the PCL; peak internal rotations were very similar and external rotations varied by a maximum of ~1° for both knees. The PCL restricted the rate at which the rotating-bearing knee returned from the peak internal

rotation position; however, ultimately all rotations ended at the same value (see Figure 7.7(a)).

A-P stability was affected to a greater extent by the presence of the PCL, particularly in the fixed-bearing knee (a maximum reduction of ~2.5mm). However, in general A-P translations were not significantly altered.

(a) (b)

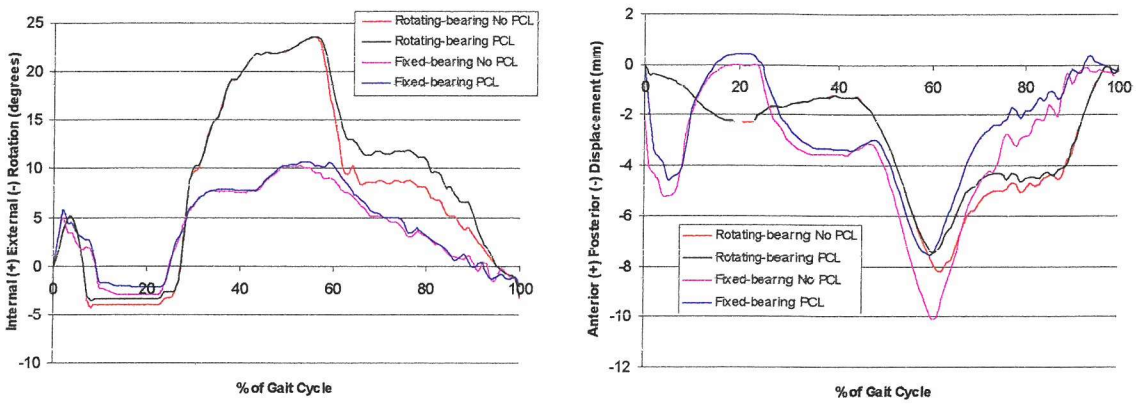

Figure 7.7 (a) I-E femoral rotations and (b) A-P tibial translations with and without the PCL during gait.

7.4 Literature Comparison

7.4.1 Contact Pressure and Contact Area

The contact area at 0° flexion of a size 3 Advanced semi-congruent TKA was assessed using Tekscan pressure equipment (K-Scan) [25]. On a specially devised rig Harris *et al.* [25] recorded a 350mm^2 contact area, produced under a 3600N compressive load. Total contact areas (medial + lateral) in the present research at the point of maximum axial load (~ 2200N @ 50% of the gait cycle) were 301mm^2 and 158mm^2 for the PC-RR and PC-RF respectively, and 380mm^2 and 229mm^2 in the PC-SR and PC-SF respectively. The knee in the study by Harris *et al.* was semi-congruent, and was likely to have a lower conformity than the rotating-bearing knees in the present research, but a greater conformity than the PC-RF. The PC-SF in the present research was therefore likely to be the most comparable to the knee assessed by Harris *et al.* The 229mm^2 total contact area of the PC-SF in the present research was smaller than the 350 mm^2 in the study by Harris

et al.; however, the compressive load was lower (2200N compared to 3600N), and may account for the smaller contact area. Also, the exact geometries of each individual knee design will vary somewhat, which will have a bearing on the size of the contact area.

Using Tekscan sensors Colsman *et al.* [127] measured the contact pressures during dynamic motions. An *in vitro* technique was developed to simulate isokinetic knee flexion and extension, recording the contact pressures and contact areas of fixed- and rotating-bearing inserts. Maximum peak contact pressures of ~27MPa and ~9MPa occurred at 50° flexion in the standard fixed-bearing insert and the rotation-bearing insert respectively in Colsman's study. The average contact areas at these positions were 119mm^2 and 215mm^2 for the fixed- and rotating-bearing knee respectively. These findings compared well to those in the present research, where the maximum contact pressure of the PC-RF was ~30MPa with a contact area of 158mm^2, and the contact pressure of the PC-RR was ~9MPa with a contact area of 301mm^2. The contact areas in the present research were slightly larger than those reported by Colsman *et al.*, which could be due to differences in applied contact forces or component conformities. In general the medial contact pressures tended to be slightly larger than the lateral contact pressures in the study by Colsman *et al.*; this agreed with the present research.

Using three-dimensional finite element models of three TKR designs, Liau *et al.* [128] recorded the contact areas and pressures under a 3000N compressive load at 0° flexion. The knees assessed were high conformity flat-on-flat (HFF), high conformity curve-on-curve (HCC) and medium conformity curve-on-curve (MCC) designs of the U-knee (United Orthopaedic, Taipei, Taiwan). The contact areas of the HFF, HCC and MCC knees were 167.8mm^2, 162.2mm^2 and 147.4mm^2 respectively, with corresponding maximum contact pressures of 32.6MPa, 31.6MPa and 37.5MPa. The HCC knee would best compare to the rotating-bearing knees in the present research. The contact area of 162.2mm^2 reported by Liau *et al.* was lower than the 301mm^2 and 380mm^2 recorded for the PC-RR and PC-SR respectively in the present research. The individual component conformity, compressive load and knee position can all affect the contact area, and may help explain the differences between the results. Liau *et al.* recorded contact pressures of 31.6MPa for their highest conforming curve-on-curve design, which was significantly larger than the 9MPa recorded for the rotating-bearing knees in the present research. This pressure magnitude and the size of the contact area in Liau's study were more

comparable to the PC-RF, which was the lowest conforming TKR in the present research. One observation by Liau *et al.* was that contact pressures were generally larger on the medial side of the knee, which was also noted in the present research.

Sathasivam and Walker [129] used finite element analysis to determine the contact pressures of various knees over the gait cycle. Maximum pressures of ~16MPa were recorded with the lowest conforming components, and ~8MPa in the most conforming designs. These findings were comparable to the present research where maximum contact pressures of ~9MPa were noted in the rotating-bearing knees (most conforming), 30MPa in the PC-RF (least conforming) and 20MPa in the PC-SF (low conformity). The findings also agreed with work by Godest *et al.* [9], where a three-dimensional computational model, which had been validated against the Stanmore Knee wear simulator [23], was used to simulate a gait cycle after total knee joint replacement. The maximum contact pressures of a posterior cruciate-retaining fixed-bearing prosthesis reached ~25MPa at 40%-50% of the gait cycle. The PC-RF in the present research produced a maximum contact pressure of ~30MPa, which was comparable to Godest's findings. Also, the PC-RF in the present research had a slightly lower insert curvature than that in the study by Godest *et al,* which helps explain the slightly larger peak contact pressure. During the swing phase where axial forces were low, pressures in the region of ~7MPa were produced in the study by Godest *et al.*; this was also noted in the present research.

7.4.2 Kinematics

An *in vivo* study was carried out by Komistek *et al.* [111] comparing the kinematics of three conforming posterior cruciate-sacrificing knee implants during gait. 40 subjects were studied under fluoroscopic surveillance during the stance phase and the gait cycle. The AMK Congruency posterior cruciate-substituting (DePuy, Warsaw, IN, US), IB-II posterior cruciate-substituting (Zimmer, Warsaw, IN, US) and the LCS rotating-platform knee (DePuy, Warsaw, IN, US) were studied. For the AMK and the IB-II peak rotations during gait were 8.5° internal and 8.6° external, and for the LCS were 10.9° internal and 15.1° external; these referred to rotations of the tibial component with respect to the femoral component. The AMK and IB-II knees were most comparable to the PC-SF in the present research, and the LCS knee was most comparable to the PC-RR. Internal tibial rotations reported in the literature corresponded to external femoral rotations in the

present research. Peak internal and external femoral rotations in the present research for the PC-SF were 6.0° and 1.1°, which were lower than the rotations reported by Komistek *et al.* However the cruciate-substituting mechanism in the AMK and IB-II knees was a more conforming insert, whereas in the present research a tibial spine was employed, which offered increased I-E stability (as noted in Chapter 4). The rotating-bearing knees in the present research had significantly larger internal and external rotations than those in the LCS knee, possibly due to the fact that only the MCL and LCL were simulated in the present research. In the study by Komistek *et al.* other knee structures such as the PCL, joint capsule, patella and skin were present.

Using a four-station TKR wear simulator (Stanmore/ Instron, Model KC Knee Simulator), DesJardins *et al.* [8] examined eight different knee designs over a simulated gait cycle. Maximum and minimum A-P and I-E motions from this study are shown in Table 7.2. The I-E rotations of the fixed-bearing knees in the present research compare well to all knees tested by DesJardins *et al.*, with the IB and SML knees being more comparable to the PC-SF. The IB was a high conforming TKR, which meant that its I-E restraint would be relatively high, thus comparing well to the PC-SF in the present research, and the SML was a rotating hinged joint, also providing increased I-E stability. All other knees except the MBK were moderate to low conforming fixed-bearing designs, hence their good correlation to the PC-RF in the present research. A-P translations recorded by DesJardins *et al.* also showed good agreement with the results in the present research. The PC-RF had similar anterior translations to all knees in DesJardins' study, however the peak posterior displacement was about 5mm larger than most of the knees tested by DesJardins *et al.* This finding was not surprising since the A-P stability of the PC-RF was very low, as shown in the passive stability testing in Chapter 4.

Godest *et al.* [9] used explicit finite element models to simulate the kinematics of a PFC Sigma fixed-bearing knee. The maximum range of A-P displacements and I-E rotations was 4.3mm and 6.0° respectively. The PC-RF in the present research had a slightly lower conformity that that used by Godest *et al.*, which may account for the higher range of I-E rotations and A-P translations. Also, horizontal springs were used to simulate soft tissue restraint in Godest's study, whereas a rubber type material was used in the present research, attached to the femoral and tibial sections of the knee. The soft tissues in the

present research are vertically positioned, and may also explain the differences in A-P and I-E motions.

Knee Type	Max/ Min A-P Disp. (mm) (+ ant/ - post) [8]	Max/ Min I-E Rotation (°) (+ int/ - ext) [8]	Comparable Knee in Present Research	Present Knee A-P Disp. (°) (+ ant/ - post)	Present Knee I-E Rotation (°) (+ int/ - ext)
IB	-0.6/ -4.1	8.1/ 1.0	PC-SF	-0.6/ -7.0	6.0/ -1.1
NGL	-0.4/ -4.2	11.1/ -0.5	PC-RF	0.0/ -10.0	10.1/ -2.9
MBK	0.2/ -2.5	10.5/ -2.3	PC-RR/ PC-SR	~-1.4/ -7.5	~24.0/ -5.0
SML	0.3/ -0.1	5.5/ 0.3	PC-SF	-0.6/ -7.0	6.0/ -1.1
HOWD	-0.1/ -6.3	13.4/ -2.9	PC-RF	0.0/ -10.0	10.1/ -2.9
NGCR	0.3/ 4.7	11.6/ -2.3	PC-RF	0.0/ -10.0	10.1/ -2.9
SPRO	0.5/ -6.4	14.1/ -6.0	PC-RF	0.0/ -10.0	10.1/ -2.9
JJPFC	0.8/ -5.0	11.3/ -2.7	PC-RF	0.0/ -10.0	10.1/ -2.9

Table 7.1 Kinematic results as reported by DesJardins *et al.* [8]

In summary, the fixed-bearing knees of the present research had comparable kinematics to those recorded in the literature, but the I-E rotations of the rotating-bearing knees were significantly larger. No computational simulations of a rotating-bearing knee could be found in the literature for a direct comparison, and the rotation-bearing knees assessed *in vivo* or *in vitro* possessed extra soft tissue restraints (PCL, joint capsule, patella etc.), which may explain the lower I-E rotations.

Chapter 8 Comparisons of Passive and Active Stability

The aim of this Chapter was to identify the main effects of specific knee conditions (altered ligament strains and malalignment) on both passive and active stability. The work in this Chapter of the thesis deals solely with the computational FE simulations. The FE models of the different knee types were deemed realistic and reliable after they were validated against equivalent experimental testing (see Chapter 6).

8.1 Effects of Altered Ligament Strains:

As mentioned in Chapter 4, the number of results obtained in this study is such that a presentation and discussion of each individual result would be exhaustive and beyond the scope of the present thesis. Passive and active stability comparisons were conducted using tight-slack, slack-tight, slack-slack and tight-tight MCL-LCL strain combinations. All results were compared against the neutrally aligned knee with normally strained collateral ligaments. Passive A-P stability testing was conducted with the knee at full extension and 90° flexion; passive I-E stability testing was conducted at 15° and 90° flexion and V-V stability testing was conducted at full extension only.

8.1.1 Passive Stability

Tables 8.1 to 8.4 show the affects of altered ligament strains on I-E, A-P and V-V stability.

Knee	Flexion Angle (°)	A-P Stability (mm)			I-E Stability (°)			V-V Stability (°)		
		A	P	Total	I	E	Total	Varus	Valgus	Total
PC-RR	0/ 15	-0.3	0.4	0.1	-0.2	-0.4	-0.6	2.1	-1.6	0.5
	90	0.6	-0.1	0.5	-0.8	0.5	-0.3	-	-	-
PC-RF	0/ 15	-0.1	0.2	0.1	1.2	2.5	3.7	2.2	-1.7	0.5
	90	-0.4	0.3	-0.1	-0.3	1.4	1.2	-	-	-
PC-SR	0/ 15	-0.4	-0.2	-0.7	0.3	-0.5	-0.1	1.8	-1.1	0.8
	90	-0.3	0.1	-0.2	-1.2	1.5	0.2	-	-	-
PC-SF	0/ 15	-0.1	0.3	0.2	0.6	1.7	2.3	1.6	-1.2	0.4
	90	-0.4	0.0	-0.4	6.2	-6.8	-0.6	-	-	-

Table 8.1 Change in passive stability due to a tight-slack MCL-LCL combination. A positive value represents an increase in laxity.

Knee	Flexion Angle (°)	A-P Stability (mm)			I-E Stability (°)			V-V Stability (°)		
		A	P	Total	I	E	Total	Varus	Valgus	Total
PC-RR	0/ 15	-0.3	-0.1	-0.5	-1.3	-0.3	-1.6	-1.9	1.3	-0.6
	90	-0.1	-0.3	-0.3	-0.3	-1.3	-1.6	-	-	-
PC-RF	0/ 15	-0.1	0.0	-0.1	0.2	-0.7	-0.5	-2.0	1.4	-0.6
	90	-0.6	0.2	-0.4	0.3	-1.8	-1.4	-	-	-
PC-SR	0/ 15	-0.4	0.5	0.1	-0.8	-0.5	-1.3	-1.5	1.0	-0.5
	90	0.2	0.0	0.2	1.0	-2.1	-1.1	-	-	-
PC-SF	0/ 15	0.0	-0.2	-0.2	-0.2	-0.5	-0.7	-1.6	0.9	-0.7
	90	0.0	0.0	0.0	-0.4	-1.8	-2.2	-	-	-

Table 8.2 Change in passive motions due to a slack-tight MCL-LCL combination. A positive value represents an increase in laxity.

Knee	Flexion Angle (°)	A-P Stability (mm)			I-E Stability (°)			V-V Stability (°)		
		A	P	Total	I	E	Total	Varus	Valgus	Total
PC-RR	0/ 15	3.2	1.1	4.3	3.0	2.2	5.2	1.0	0.2	1.2
	90	0.5	1.7	2.2	2.5	2.3	4.8	-	-	-
PC-RF	0/ 15	2.1	1.1	3.3	4.2	4.2	8.4	1.2	0.0	1.2
	90	0.0	2.1	2.2	1.9	2.1	4.1	-	-	-
PC-SR	0/ 15	3.6	1.2	4.7	3.4	1.9	5.4	1.6	0.5	2.1
	90	2.2	0.1	2.3	2.5	2.6	5.0	-	-	-
PC-SF	0/ 15	2.1	1.1	3.1	4.4	2.6	7.0	1.0	0.4	1.4
	90	1.8	0.1	1.9	5.2	3.4	8.5	-	-	-

Table 8.3 Change in passive motions due to a slack-slack MCL-LCL combination. A positive value represents an increase in laxity.

Knee	Flexion Angle (°)	A-P Stability (mm)			I-E Stability (°)			V-V Stability (°)		
		A	P	Total	I	E	Total	Varus	Valgus	Total
PC-RR	0/ 15	-3.0	-0.8	-3.8	-3.4	-2.5	-5.9	-1.1	-0.6	-1.6
	90	-1.0	-1.1	-2.0	-3.5	-2.1	-5.6	-	-	-
PC-RF	0/ 15	-0.3	-0.6	-0.9	-3.2	-2.3	-5.6	-1.0	-0.4	-1.4
	90	-1.7	-0.7	-2.4	-2.8	-2.0	-4.7	-	-	-
PC-SR	0/ 15	-3.4	-0.9	-4.2	-2.6	-2.9	-5.5	-0.8	-0.5	-1.3
	90	-2.1	0.0	-2.1	-2.6	-3.3	-5.9	-	-	-
PC-SF	0/ 15	-1.2	-0.9	-2.1	-1.9	-1.4	-3.3	-1.1	-0.7	-1.8
	90	-2.1	0.0	-2.1	-4.4	-3.4	-7.8	-	-	-

Table 8.4 Change in passive motions due to a tight-tight MCL-LCL combination. A positive value represents an increase in laxity.

In all knees a tight-slack MCL-LCL combination did not have a significant effect on A-P stability (a maximum alteration of 0.7mm was recorded, see Table 8.1). The I-E stability of the PC-SF was dictated by the interaction of the tibial spine and femoral component, and at 90° flexion the PC-SF was particularly sensitive towards altered ligament strains; internal rotations were increased by 6.2° and external rotations reduced by 6.8°. The

effect on V-V stability was relatively uniform in all knees; varus rotations increased by ~1.9° and valgus rotations decreased by ~1.4°.

Similar findings were noted for a slack-tight MCL-LCL. The A-P stability of all knees was relatively unaffected; a maximum deviation of 0.5mm was noted (see Table 8.2). I-E laxity at 15° flexion increased by ~1.5° in the rotating-bearing knees and ~0.6° in the fixed-bearing knees. At 90° flexion internal rotations were slightly reduced in the PC-RR and the PC-SF, and slightly increased in the PC-RF and PC-SR; external rotations were reduced in all knees (see Table 8.2). Varus rotations were reduced by ~1.7° and valgus rotations increased by ~1.3° in all knees.

At 0° flexion slack collateral ligaments increased A-P translations by ~3.5mm in all knees, and at 90° flexion translations increased by ~2.0mm (see Table 8.3). I-E rotations in the fixed-bearing knees were increased by ~7.5° and ~6.0° at 15° and 90° flexion respectively, and rotations in the rotating-bearing knees increased by ~5.0° at both 15° and 90° flexion. In general valgus laxity increased by ~0.5° and varus laxity increased by ~1.3° in all knees (see Table 8.3).

At 0° flexion tight ligaments reduced A-P laxity by ~4.0mm in the rotating-bearing knees and 1.5mm in the fixed-bearing knees (see Table 8.4). At 15° flexion I-E rotations were reduced by ~5.7° and at 90° flexion I-E rotations were reduced by ~5.5° in all knees except the PC-SF (see Table 8.4). Total V-V stability was increased by ~1.5° across all knees; varus rotations were generally reduced by 0.5° more than valgus rotations.

8.1.2 Active Stability

All results in this section were compared against the idealised knee, which in the present research relates to neutral component alignment with normally strained collateral ligaments (Chapter 7 discussed the kinematics and contact pressures recorded in the idealised knees).

Gait Kinematics:

In general, regardless of knee type, altered ligament strains did not significantly affect the kinematics during gait (Figure 8.1 shows an example of the effect of a tight-slack MCL-LCL combination on I-E rotations). With a slack-tight MCL-LCL combination the insert of the PC-SR did not externally rotate with the femoral component between 60%-85% of the gait cycle (see Figure 8.2); however, at the end of the cycle all rotations were similar.

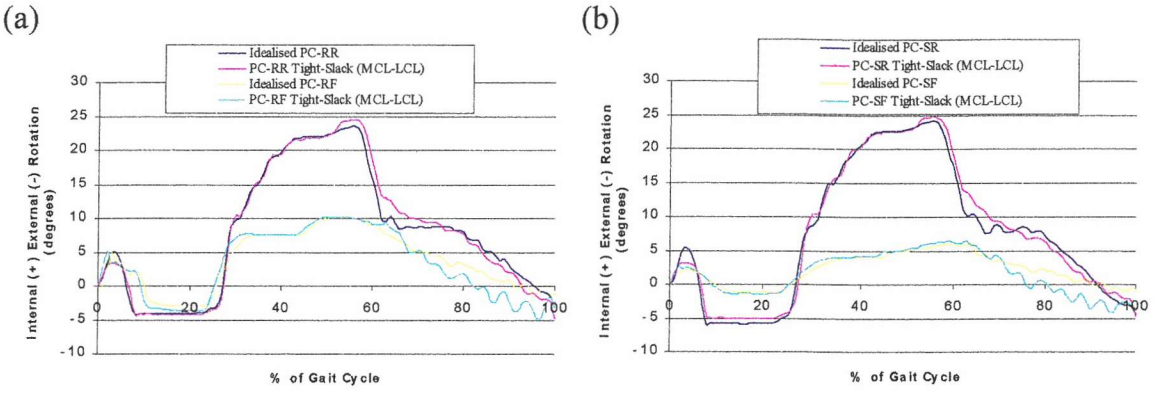

Figure 8.1 I-E rotations in the (a) PC-retaining and (b) PC-substituting knees during gait in the idealised knee and with a tight-slack (MCL-LCL) combination. Rotations refer to the femoral component with respect to the tibial component.

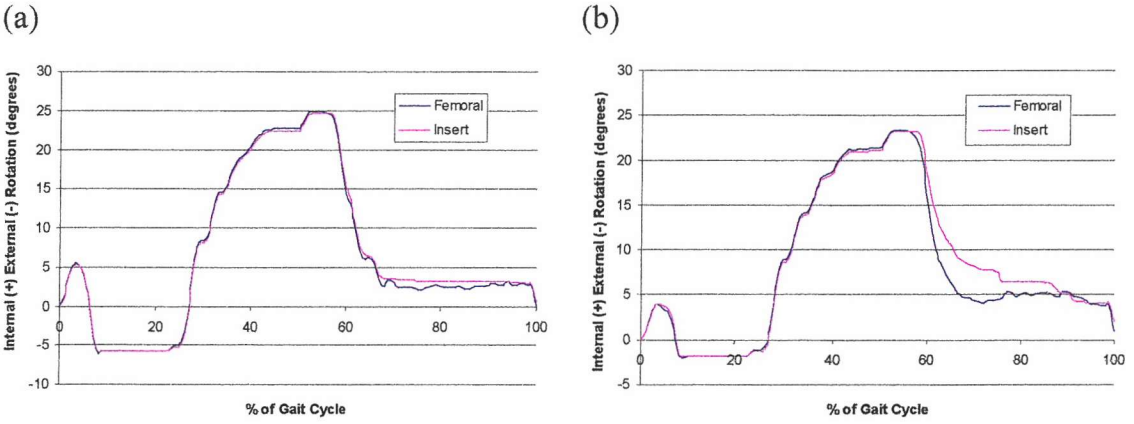

Figure 8.2 Femoral and insert rotations of the PC-SR in (a) the idealised knee and (b) with a slack MCL and a tight LCL.

Contact Force and Contact Pressure:

The larger contact pressures occurred at 10% and 50% of the gait cycle (see Figure 8.3), particularly in the fixed-bearing knees. Imbalanced ligaments altered the vertical force distribution across the knees; for example, a slack-tight MCL-LCL combination increased the force through the lateral side of the knee by a maximum of 80N, and reduced the force through the medial side by the same amount.

In the rotating-bearing knees a maximum reduction in peak contact pressure of 3.2MPa was recorded (PC-SR); however this occurred between 80%-99% of the gait cycle, where forces and contact areas were at a minimum. At the high axial force regions of the gait cycle (10% and 50% of gait) a maximum change in peak contact pressure occurred in the PC-RF (medial reduction of 3.9MPa at 50%; slack-tight MCL-LCL combination). This value was still relatively low since contact pressures in the normally strained knee reached over 26MPa at this position. A large reduction at 1% of the gait cycle was noted in the PC-RF (9.5MPa); however, at this stage of the gait cycle only, slight oscillations in the ligament strains may have occurred due to the pre-straining process, resulting in initially inaccurate contact pressure readings.

Overall, altering the ligament strains did not significantly alter the contact pressures across the knee during gait, particularly during the greater axial load phases of the cycle. At the low load regions of the gait cycle, where contact areas were relatively small, the greatest changes in contact pressures were noted.

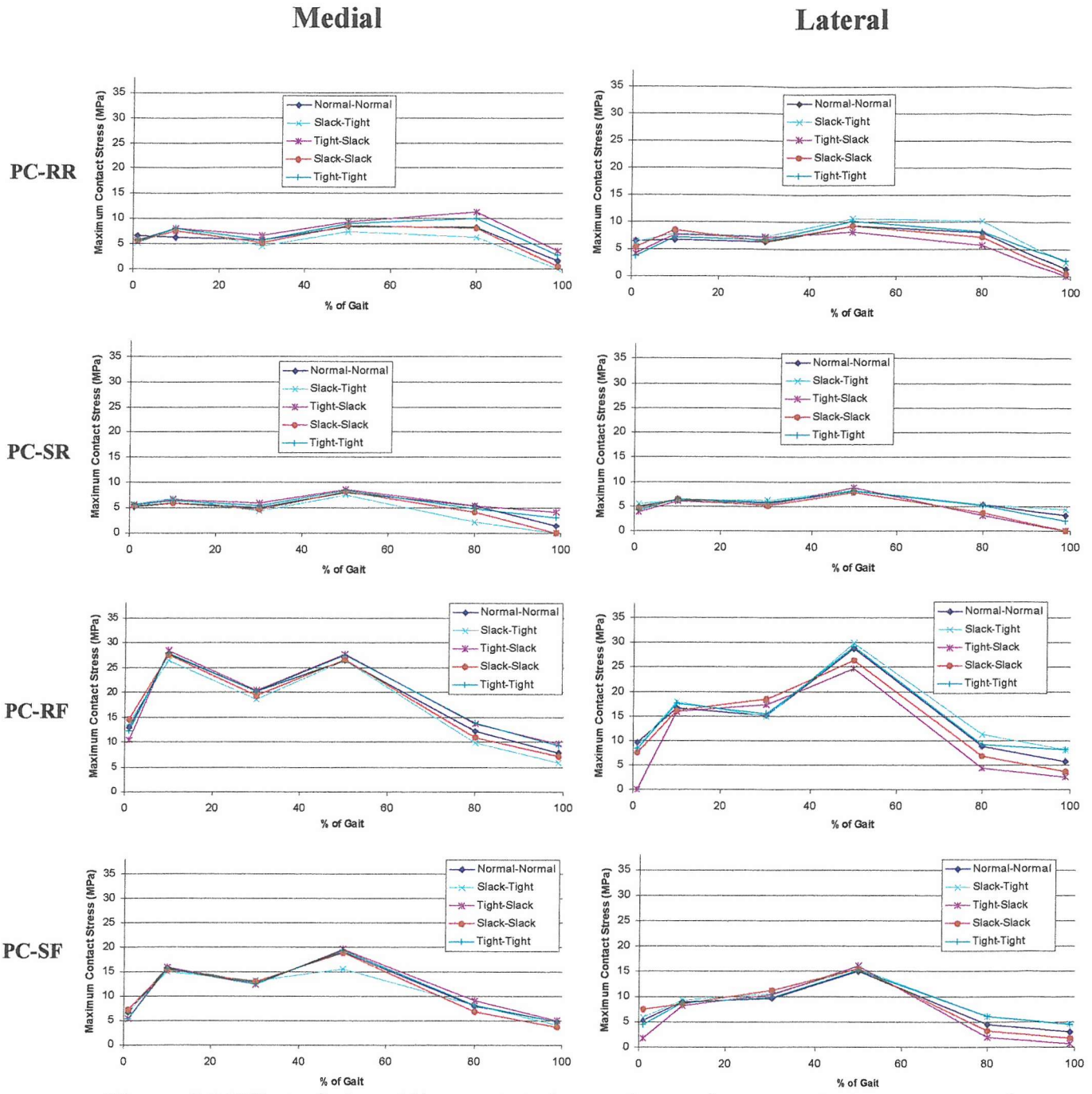

Figure 8.3 Effect of altered ligament strains on the maximum contact pressures on the medial and lateral sides of the knee during the gait cycle. Legend refers to MCL-LCL strain respectively.

8.2 Effects of Malalignment

The effects of 3° varus/ valgus malalignment on the passive stability of all knees are shown in Tables 8.5 and 8.6. These show the results with normally strained and imbalanced ligaments respectively. Ligament imbalance with varus alignment refers to a tight MCL and a slack LCL, and imbalance with valgus alignment refers to a slack MCL and a tight LCL. All testing was carried out at 90° flexion as previous work had indicated that greater changes in stability occurred at this position (see Chapter 4). All results were compared against the idealised knee.

Knee	Alignment	A-P Stability (mm)			I-E Stability (°)			V-V Stability (°)		
		A	P	Total	I	E	Total	Varus	Valgus	Total
PC-RR	*Varus*	-0.2	-0.2	**-0.4**	-3.7	5.2	**1.5**	0.1	-0.1	**0.0**
	Valgus	-0.2	-0.1	**-0.3**	4.4	-1.9	**2.5**	0.0	0.0	**0.0**
PC-RF	*Varus*	-1.0	-0.4	**-1.3**	-4.9	4.7	**-0.1**	0.1	0.0	**0.1**
	Valgus	-1.3	-0.5	**-1.7**	4.7	-4.8	**0.0**	-0.1	0.1	**0.0**
PC-SR	*Varus*	-0.4	0.1	**-0.4**	-3.5	4.8	**1.2**	0.1	0.0	**0.1**
	Valgus	-0.3	0.1	**-0.2**	4.1	-3.0	**1.0**	-0.1	0.1	**0.0**
PC-SF	*Varus*	0.0	-0.2	**-0.2**	1.1	1.3	**2.4**	0.1	-0.2	**-0.1**
	Valgus	0.2	0.0	**0.2**	5.1	-2.5	**2.6**	-0.1	-0.1	**-0.2**

Table 8.5 Change in stability caused by malalignment with normally strained collateral ligaments. A positive value represents an increase in laxity.

Knee	Alignment	A-P Stability (mm)			I-E Stability (°)			V-V Stability (°)		
		A	P	Total	I	E	Total	Varus	Valgus	Total
PC-RR	*Varus*	0.8	-0.4	**0.4**	-4.8	4.6	**-0.1**	2.1	-1.5	0.6
	Valgus	0.1	-0.7	**-0.6**	3.5	-4.9	**-1.3**	-1.9	1.3	-0.6
PC-RF	*Varus*	-0.3	-0.4	**-0.6**	-4.2	5.2	**1.1**	2.1	-1.4	0.7
	Valgus	-1.0	-0.7	**-1.6**	4.0	-5.4	**-1.4**	-2.1	1.5	-0.6
PC-SR	*Varus*	-0.4	0.0	**-0.4**	-4.8	5.1	**0.3**	1.8	-1.1	0.7
	Valgus	-0.6	0.0	**-0.6**	4.1	-5.2	**-1.1**	-1.6	1.0	-0.6
PC-SF	*Varus*	-0.1	0.0	**-0.1**	-6.3	-3.7	**-10.0**	1.6	-1.3	0.3
	Valgus	0.0	0.0	**0.0**	-0.2	-10.0	**-10.2**	-1.6	0.8	-0.8

Table 8.6 Change in stability caused by malalignment with imbalanced ligaments. A positive value represents an increase in laxity.

8.2.1 Passive Stability with 3° of Varus Malalignment

A-P stability was relatively unaffected by varus malalignment when both collateral ligaments were normally strained (maximum alteration of 1.3mm – see Table 8.5). Total I-E stability also remained relatively unaltered when both ligaments were normally strained; however, the effects on the individual internal and external rotations were greater. Internal rotations reduced by over 3.5° and external rotations increased by a similar value in all knees except the PC-SF. As discussed previously, the interaction of the tibial spine and femoral component dictated significantly the I-E rotations of the PC-SF, meaning that malalignment affected this particular knee differently to the other knee designs. V-V rotations were virtually unaltered by malalignment when both ligaments were normally strained.

Only I-E stability of the PC-SF was significantly affected when imbalanced ligaments were combined with varus malalignment; internal and external rotations reduced by 6.3° and 3.7° respectively. Imbalanced ligaments caused varus rotations to increase by ~1.9° and valgus rotations to decrease by ~1.3° in all knees.

8.2.2 Active Stability with 3° of Varus Malalignment

Gait Kinematics:

When both collateral ligaments were normally strained the effect of varus malalignment on A-P and I-E motions during gait was minor. When the ligaments were imbalanced, I-E rotations were altered slightly, however this was not significant.

Contact Force and Contact Pressure:

When the collateral ligaments were normally strained, 3° of varus malalignment caused medial axial forces to increase by a maximum of about 100N (an increase of ~4%); this occurred at the high axial load positions of the gait cycle (10% and 50% of the gait cycle). The effects were virtually mirrored on the lateral condyles, with reduced vertical contact forces on the lateral side of the knee during gait. Ligament imbalance combined with 3° of varus malalignment caused a maximum increase in medial vertical contact

force of 190N in all knees (an increase of ~8%), and a decrease of ~180N on the lateral side of the knee.

The effect on the contact pressures varied across the different knees types, however the general trend was for lateral contact pressures to reduce and medial contact pressures to increase with varus malalignment. At heel strike varus malalignment adds extra medial force through the joint as the knee resists further malrotation (buckling), and the force down the mechanical axis shifts medially (see Figure 8.4). A tight MCL and a slack LCL magnified this effect.

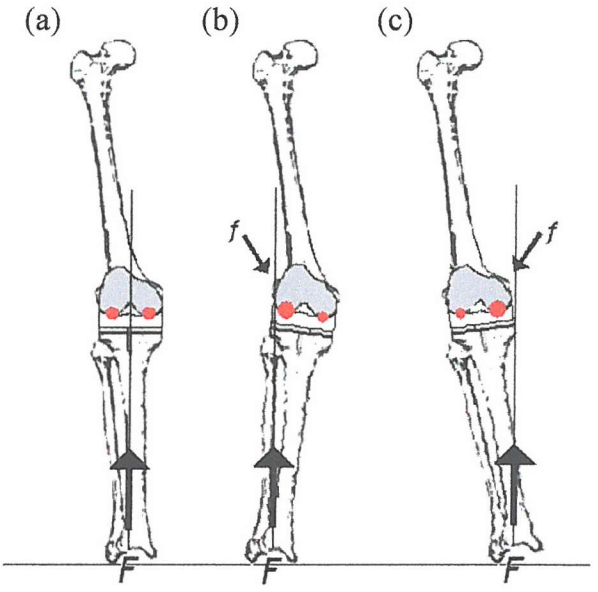

Figure 8.4 Forces applied with (a) neutral; (b) valgus and (c) varus alignment. ***F*** indicates the contact force in the direction of the mechanical axis, and ***f*** shows the extra force caused by the malalignment. The red areas represent the medial and lateral contact forces.

Overall, medial contact pressures in the rotating-bearing knees, and lateral contact pressures in the fixed-bearing knees were altered more significantly by 3° of varus malalignment. The combined effect of malalignment and imbalanced ligaments generally caused contact pressures to vary more significantly. The greatest increase in peak medial contact pressure occurred in PC-RR at 10% of the gait cycle (increase of 4.8MPa), and the greatest reduction in lateral contact pressure occurred in the PC-RF at 50% of the gait cycle (reduction of 5.4MPa).

8.2.3 Passive Stability with 3° of Valgus Malalignment

When the collateral ligaments were normally strained the effect of valgus malalignment on passive knee stability was very similar to varus malalignment; A-P and V-V stability were virtually unaltered for all knees. I-E stability was affected to a greater extent; internal rotations increased (maximum of 5.1° - PC-SF) and external rotations decreased (maximum of 4.8° - PC-RF) in all knees.

Valgus malalignment combined with imbalanced ligaments only significantly affected the I-E stability of the PC-SF; internal rotations reduced by 0.2° and external rotations reduced by 10.0°. During V-V stability testing varus rotations reduced by about 1.9° and valgus rotations increased by about 1.2° in all knees.

8.2.4 Active Stability with 3° of Valgus Malalignment

Gait Kinematics:

When both collateral ligaments were normally strained valgus malrotation did not significantly alter gait kinematics. A combination of valgus malalignment with a slack-tight MCL-LCL did however alter gait kinematics more significantly; the peak external rotations recorded in the neutrally aligned knee were replaced by internal rotations (Figure 8.5). A-P translations were not significantly affected by imbalanced ligaments (Figure 8.6).

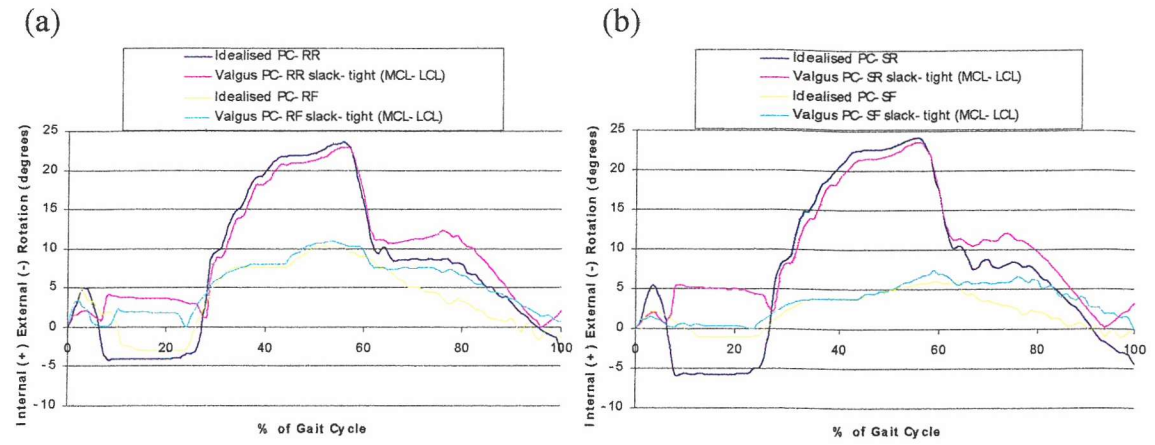

Figure 8.5 I-E rotations during gait for the idealised knee and malaligned knee with imbalanced ligament strains; (a) shows the PC-retaining knee translations and (b) shows the PC-substituting knee translations. Rotations refer to the femoral component with respect to the tibial component.

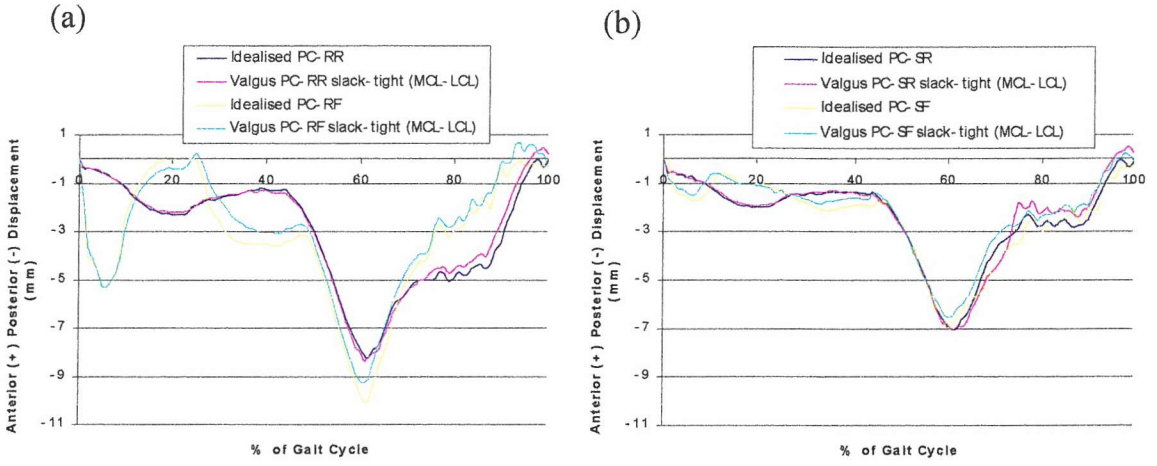

Figure 8.6 A-P translations during gait for the idealised knee and malaligned knee with imbalanced ligament strains; (a) shows the PC-retaining knee translations and (b) shows the PC-substituting knee translations. Displacements refer to the tibial component with respect to the femoral component.

Contact Force and Contact Pressure:

From Figure 8.4 valgus malalignment would be expected to cause an increase in lateral forces and a reduction the medial forces. At the positions of greatest axial load (10% and 50% of the gait cycle) a maximum lateral increase of 165N (~7%) was recorded; however, at positions of low axial load contact forces were relatively unaffected. The force distribution was consistently higher on the lateral side of the knee and reduced on

the medial side with a slack-tight MCL-LCL combination. At the low axial load stages of the gait cycle (70% onwards) there was an increase of ~65N on the lateral side of the knee and a reduction of ~55N on the medial side with imbalanced ligaments. The alteration in medial/ lateral contact force distribution had a minor effect on the peak contact pressures in all knees (a maximum increase of ~2MPa).

8.3 Effects of Extreme Malalignment

The effects of 10° femoral malalignment were assessed. Valgus malalignment testing was conducted with a slack MCL and a tight LCL, and varus malalignment testing was conducted with a tight MCL and a slack LCL. I-E and A-P passive stability was assessed at 90° flexion and V-V stability at 0° flexion with imbalanced ligaments. Active stability was assessed with imbalanced ligaments and normally strained ligaments.

8.3.1 Passive stability with 10° of Varus Malalignment

Table 8.7 shows the passive motions with 10° of varus malalignment, and Table 8.8 shows the difference between the malaligned knee and the idealised knee motions.

	A-P Translations (mm)			I-E Rotations (°)			V-V Rotations (°)		
Knee	Anterior	Posterior	**Total**	Internal	External	**Total**	Varus	Valgus	**Total**
PC-RR	3.3	3.1	**6.4**	12.7	43.9	**56.6**	6.7	1.0	**7.7**
PC-RF	5.3	3.7	**9.0**	5.8	38.2	**44.1**	7.0	0.5	**7.5**
PC-SR	4.4	0.1	**4.5**	14.6	45.4	**60.0**	6.0	1.2	**7.2**
PC-SF	1.5	0.1	**3.2**	1.4	33.7	**35.2**	5.9	1.3	**7.2**

Table 8.7 Passive stability with 10° of varus femoral malalignment; tight-slack MCL-LCL.

	A-P Translations (mm)			I-E Rotations (°)			V-V Rotations (°)		
Knee	Anterior	Posterior	**Total**	Internal	External	**Total**	Varus	Valgus	**Total**
PC-RR	-0.9	-2.0	**-2.9**	-15.6	16.6	**1.0**	2.3	-1.7	**0.6**
PC-RF	-3.0	-3.8	**-6.7**	-16.6	15.9	**-0.6**	2.5	-1.6	**0.9**
PC-SR	-2.0	0.1	**-1.9**	-15.1	15.8	**0.6**	2.2	-1.5	**0.8**
PC-SF	-2.0	0.1	**-1.9**	-17.6	11.1	**-6.5**	1.7	-1.4	**0.4**

Table 8.8 Difference between the malaligned knee and idealised knee results. A positive value represents an increase in laxity.

Flexion in the malaligned knee was accompanied by axial rotation of the femoral component. 10° of varus malalignment caused ~16° of external femoral rotation when

the knee was flexed from 0° to 90°. With the exception of the PC-SF, internal rotations were reduced by ~15.9° and external rotations were increased by ~16.5° in all knees during I-E stability testing (total I-E stability was altered by a maximum of ~1°). I-E stability of the PC-SF relied on the interaction of the tibial spine and femoral component. Malalignment altered the way these structures contacted during I-E rotations and this caused internal rotations to reduce by 17.6° and external rotations to increase by 11.1°.

A-P translations were reduced in all knees with 10° of varus malalignment, particularly in the PC-RF (a reduction of 6.7mm compared with a reduction of ~2.5mm for all other knees). During V-V stability testing varus rotations were consistently increased by ~2.2° and valgus rotations reduced by ~1.6° in all knees.

8.3.2 Active Stability with 10° of Varus Malalignment

Gait Kinematics:

For normally strained collateral ligaments the PC-RF was affected more significantly than the other knee designs during normal gait. At the point of maximum internal rotation (~50% of the cycle) stability was reduced in the transverse plane. This caused a sudden increase in internal rotation (see Figure 8.7). The contact position between the femoral component and the tibial insert was shifted from a mid-anteriomedial position on the lateral bearing surface (neutrally aligned knee) to the anterior insert rim (malaligned knee) at the point of maximum internal rotation (see Figure 8.8). With imbalanced collateral ligaments I-E rotations were not significantly affected during the first 40% of the gait cycle; however, internal rotations rose sharply to cause I-E instability beyond this point resulting in anterior dislocation of the lateral femoral condyle at 45%-50% of the gait cycle (see Figure 8.9).

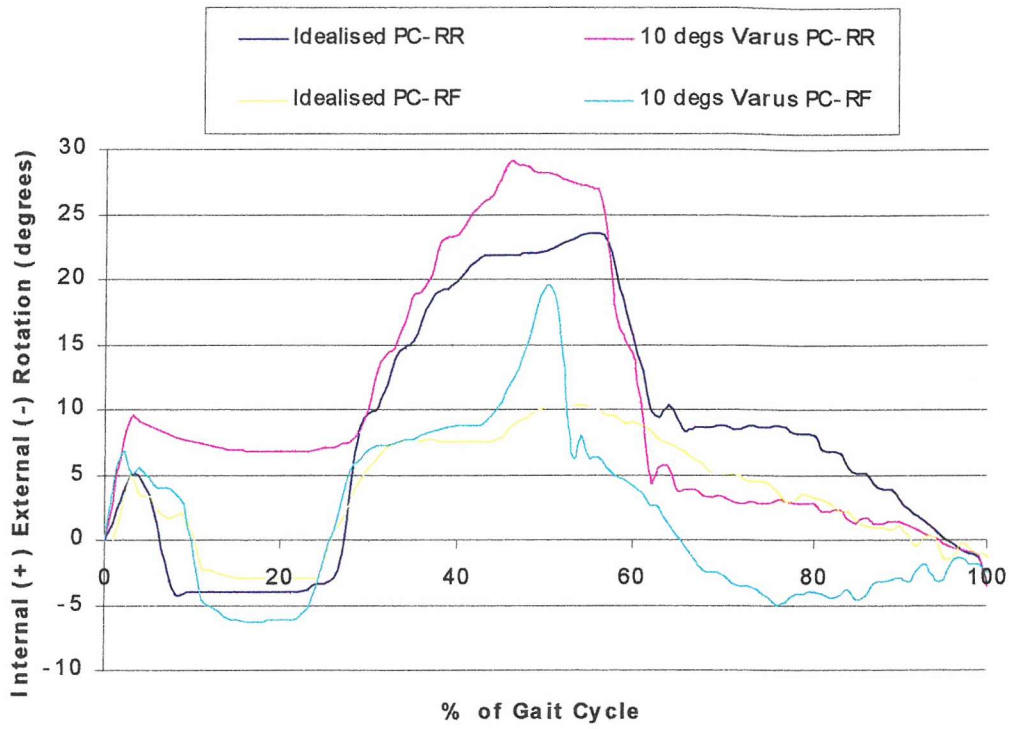

Figure 8.7 Comparison of I-E rotations in the idealised PC-RR/ PC-RF and malaligned PC-RR/ PC-RF with normally strained ligaments. Rotations refer to the femoral component with respect to the tibial component.

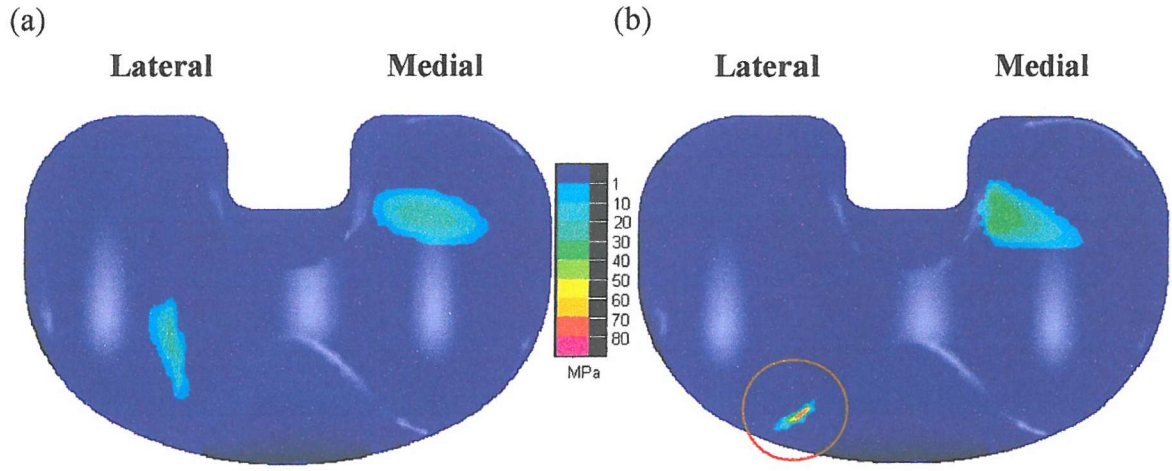

Figure 8.8 (a) Idealised knee contact pressures and (b) 10° varus malalignment contact pressures in the PC-RF at 50% of the gait cycle. Rim contact circled.

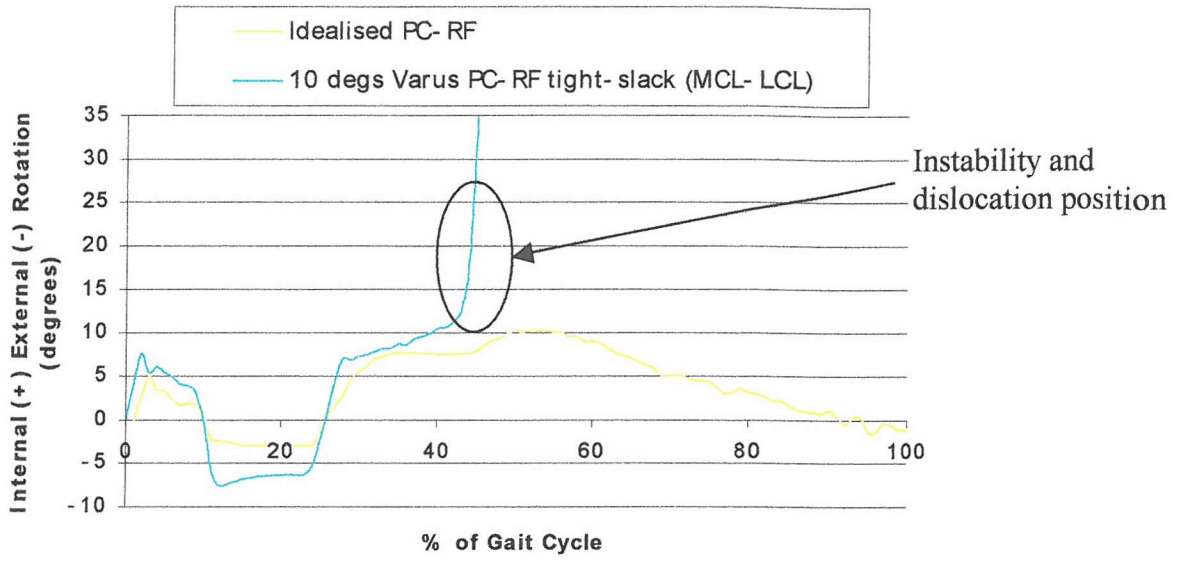

Figure 8.9 I-E rotations of the idealised PC-RF and malaligned PC-RF with imbalanced ligaments. Rotations refer to the femoral component with respect to the tibial component.

From ~50% to 100% of the gait cycle the PC-SF was in a more externally rotated position when both collateral ligaments were normally strained; a maximum deviation of over 9° was recorded (the neutral knee was internally rotated by 2.4° and the malaligned knee was externally rotated by 6.9°). Imbalanced ligaments produced I-E instability in the PC-SF at ~50% of the gait cycle, causing a sudden rise in peak internal rotations (maximum internal rotation of 16.2° - an increase of over 150%).

The rotating-bearing knees were not affected as significantly as the fixed-bearing knees. Irrespective of ligament strain the most significant effect of 10° varus malalignment was to eliminate initial external rotation, which occurred at ~20% of the gait cycle (see Figure 8.7), and to increase peak internal rotation. In general the A-P translations during gait of all knees were not significantly affected.

Contact Force and Contact Pressure:

The affect on the vertical contact forces was similar in all knees (see Figure 8.10); increasing on the medial side and reducing on the lateral side. Peak increases were noted at ~50% of the gait cycle (~450N), and peak reductions also noted at this position (~350N).

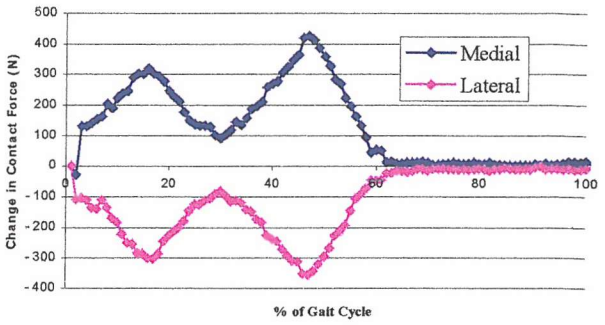

Figure 8.10 Change in contact force distribution due to 10° varus malalignment. The same trend was followed in all knees.

The effect of altered contact forces on the overall force distribution is shown in Figure 8.11. 75% of the total contact force was passed through the medial side of the rotating-bearing knees at the peak load position during the gait cycle. Approximately 90% of the total contact force passed through the medial side of the fixed-bearing knees at the peak load position during the gait cycle. This relates to a shift in force of ~15% towards the medial side of the rotating-bearing knees and ~20% in the fixed-bearing knees. Imbalanced ligament strains altered the force distribution by about another ±100N; medial forces increased and lateral forces decreased.

The effect of altered contact force distribution and gait kinematics on the peak contact pressures was significant. At the high load stages during gait, medial contact pressures increased by a maximum of 9.2MPa in the rotating-bearing knees, 12.0MPa in the PC-SF and 17.1MPa in the PC-RF (see Figure 8.12). The greatest pressure changes were produced with imbalanced ligaments.

(a) (b)

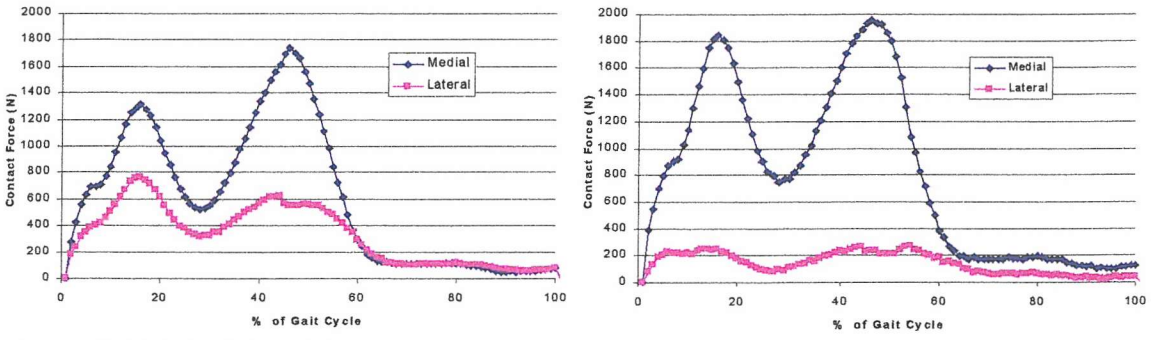

Figure 8.11 Medial and lateral contact force distribution in the (a) rotating-bearing and (b) fixed-bearing knee due to 10° varus malalignment.

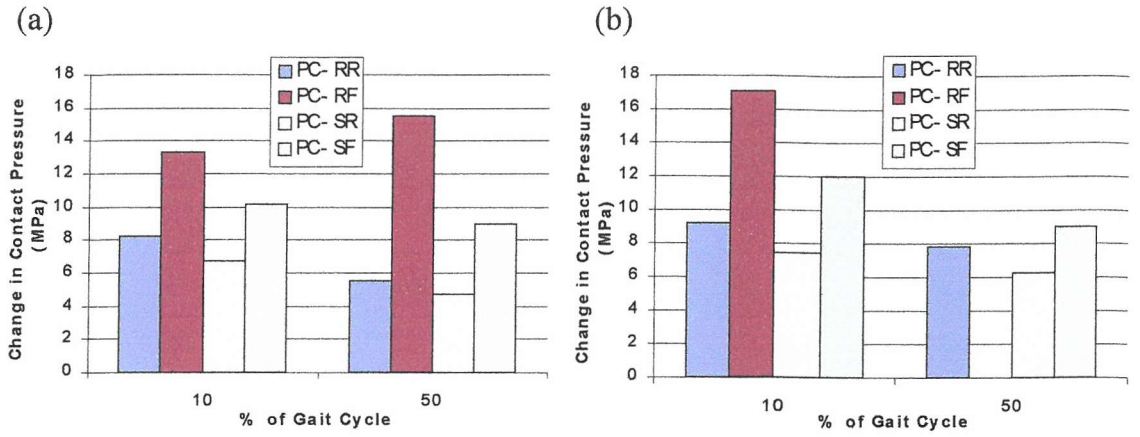

Figure 8.12 Increase in peak medial contact pressure with 10° varus malalignment; (a) normally strained collateral ligaments and (b) imbalanced collateral ligaments.

Lateral contact pressures were relatively unaffected in the rotating-bearing knees. However, due to anterior rim contact (see Figure 8.8) there was a significant increase in peak lateral contact pressure in the fixed-bearing knees (see Figure 8.13). Lateral pressures increased to 88MPa in the PC-RF when the collateral ligaments were normally strained. Peak contact pressures reached 57.5MPa in the PC-SF with normally strained collateral ligaments and 87.6MPa with imbalanced ligaments.

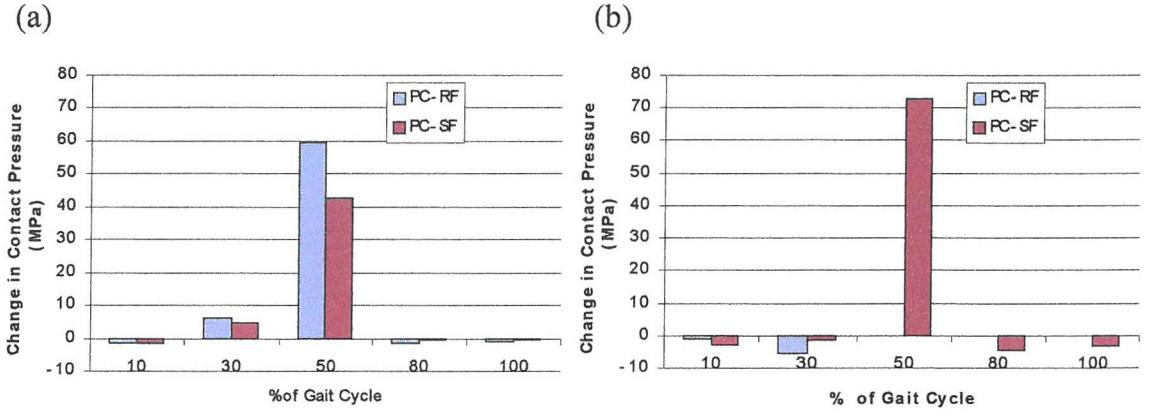

Figure 8.13 Change in peak lateral contact pressure with 10° varus malalignment; (a) normally strained collateral ligaments and (b) imbalanced collateral ligaments.

8.3.3 Passive Stability with 10° of Valgus Malalignment

Table 8.9 shows the passive motions with 10° of valgus malrotation, and Table 8.10 shows the difference between the malaligned knee neutral knee motions.

A-P translations were reduced in all knees, most significantly in the PC-RF (see Table 8.10). As the knee was flexed internal rotation of the femoral component was produced, reaching ~16° at 90° flexion. This initial rotation had a significant effect on I-E stability; internal rotations increased by ~15° and external rotation reduced by ~15.4° in all knees except the PC-SF (see Table 8.10). Total V-V stability increased by ~1° in all knees, due to reduced varus rotations and increased valgus rotations (see Table 8.10).

	A-P Translations (mm)			I-E Rotations (°)			V-V Rotations (°)		
Knee	Anterior	Posterior	**Total**	Internal	External	**Total**	Varus	Valgus	**Total**
PC-RR	3.0	3.2	**6.2**	43.7	11.6	**55.3**	2.1	4.0	**6.1**
PCRF	4.2	3.5	**7.7**	7.2	39.0	**46.2**	2.1	3.4	**5.4**
PC-SR	3.8	0.1	**3.9**	44.2	14.1	**58.3**	2.1	3.7	**5.8**
PC-SF	2.1	0.0	**2.5**	33.3	1.0	**34.3**	1.9	3.8	**5.7**

Table 8.9 Passive stability with 10° of valgus femoral malalignment; slack-tight MCL-LCL.

	A-P Translations (mm)			I-E Rotations (°)			V-V Rotations (°)		
Knee	Anterior	Posterior	**Total**	Internal	External	**Total**	Varus	Valgus	**Total**
PC-RR	-1.2	-1.9	**-3.1**	15.4	-15.7	**-0.3**	-2.4	1.4	**-1.0**
PCRF	-4.1	-4.0	**-8.0**	16.6	-15.1	**1.5**	-2.4	1.2	**-1.2**
PC-SR	-2.6	0.1	**-2.5**	14.4	-15.5	**-1.1**	-2.2	1.1	**-1.1**
PC-SF	-1.4	0.0	**-1.0**	14.3	-21.6	**-7.4**	-1.7	1.1	**-0.6**

Table 8.10 Deviation from the neutral knee results caused by 10° valgus femoral malalignment. Positive values represent an increase in laxity.

8.3.4 Active Stability with 10° of Valgus Malalignment

Gait Kinematics:

Peak internal and external rotations increased in the rotating-bearing knees, and from the peak internal rotation position (at ~60% of the gait cycle) until the end of the gait cycle the knees were more internally rotated (see Figure 8.14). From 45% of the gait cycle onwards the fixed-bearing knees were more internally rotated compared to the neutral position; a maximum difference of ~9° was recorded at 75% of the gait cycle (see Figure 8.14).

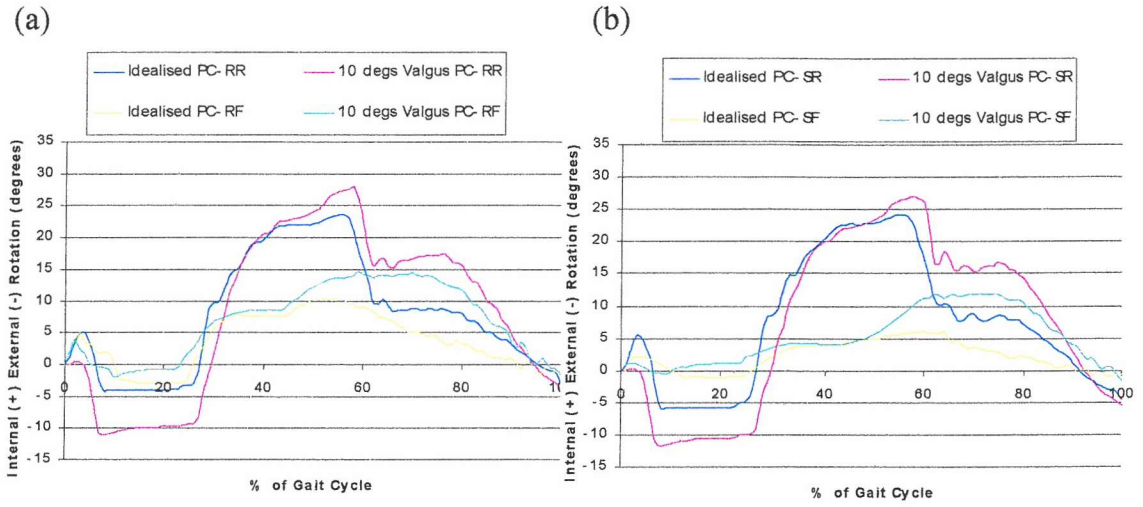

Figure 8.14 I-E rotations in the idealised and 10° valgus malaligned (a) PC-retaining and (b) PC-substituting knees during gait.

The insert rotations in the rotating-bearing knees varied from the femoral rotations during gait, and at peak internal femoral rotation the insert lagged by ~5.5° in both rotating-bearing knees (see Figure 8.15). From the peak internal rotation position until the end of the gait cycle the insert was more externally rotated compared to the femoral component. A-P stability was not significantly affected by 10° valgus malalignment.

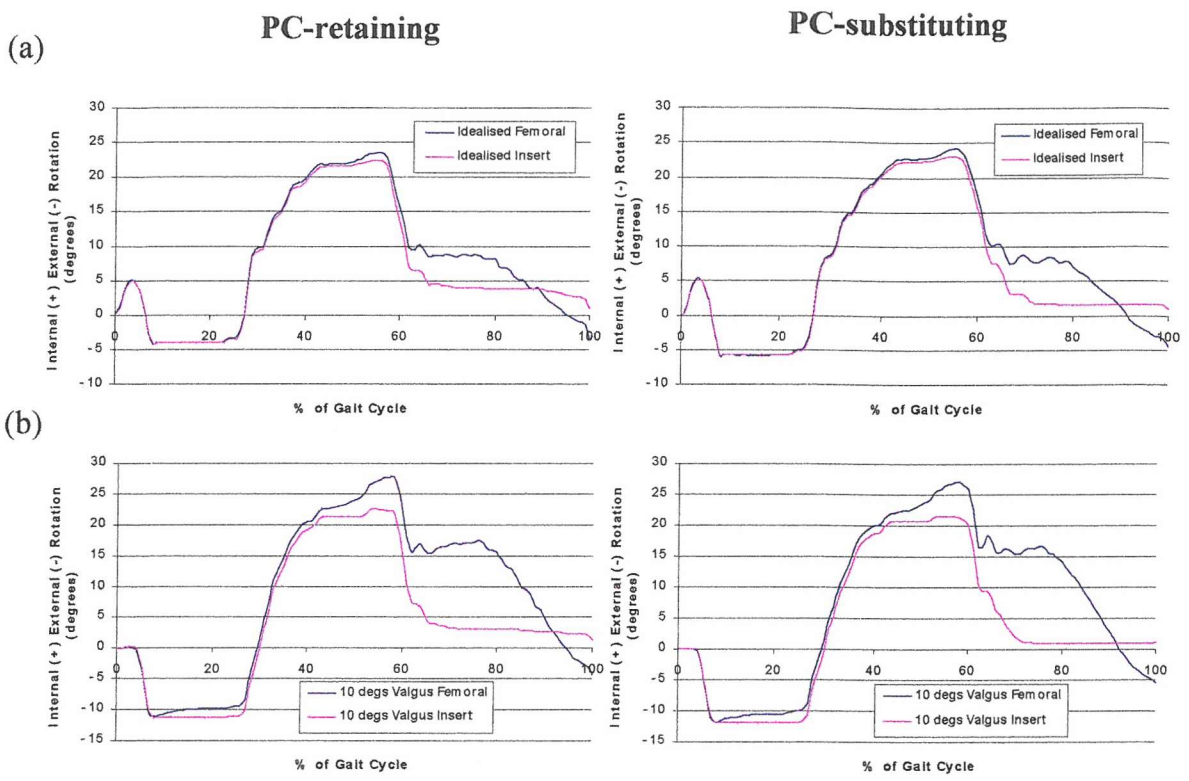

Figure 8.15 Femoral and insert rotations of the rotating-bearing knees during the gait cycle in the (a) idealised knee and with (b) 10° valgus malaligned knee.

Contact Force and Contact Pressure:

Figure 8.16 shows the medial and lateral vertical contact force distribution of the rotating- and fixed-bearing knees.

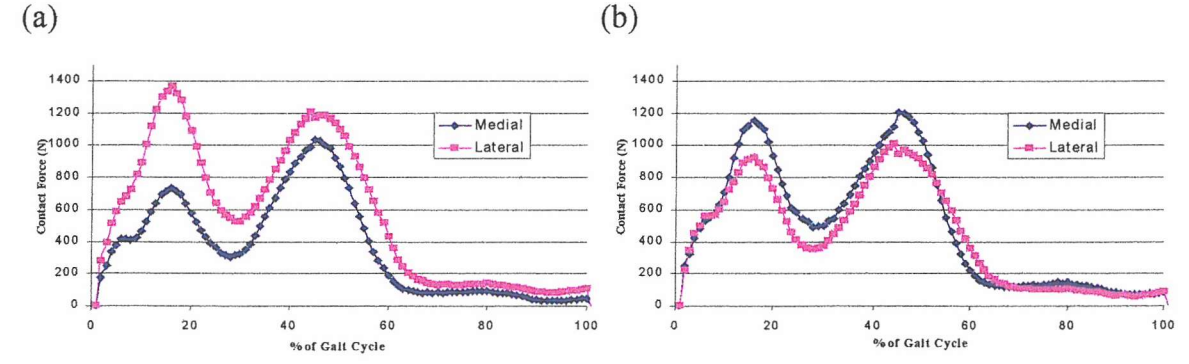

Figure 8.16 Contact force distribution due to 10° valgus malalignment in the (a) rotating-bearing and (b) fixed-bearing knee.

In the rotating-bearing knees up to 65% of the total axial force was passed through the lateral side of the knee (see Figure 8.16(a)). Medial contact forces were still larger in the fixed-bearing knees, however the medial-lateral force distribution was more even (55%-45% in the malaligned knee compared to 75%-25% in the idealised knee - see Figure 8.16 (b)).

In general contact pressures were increased on the lateral side and reduced on the medial side of the knee (see Figure 8.18). The peak lateral contact pressures increased most in the PC-RF, and least in the PC-SF (see Figure 8.17)

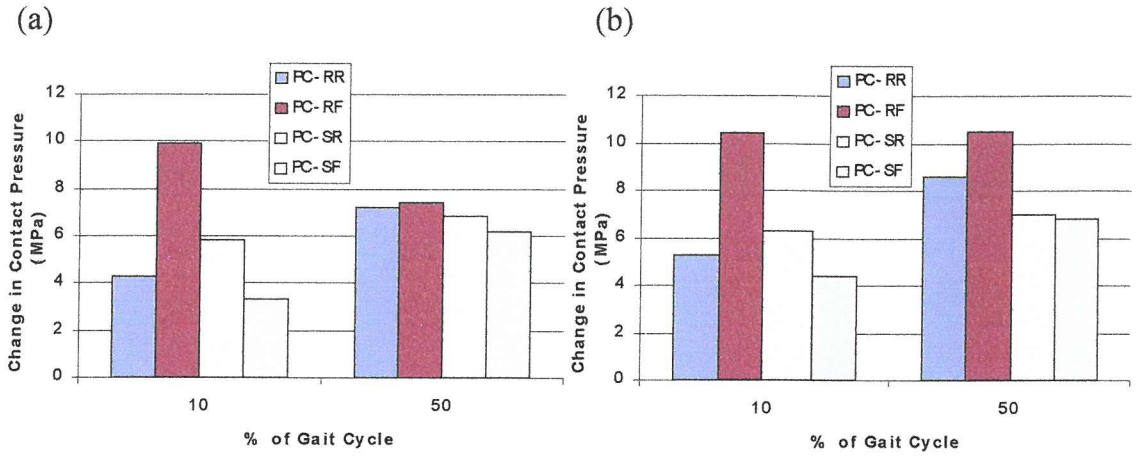

Figure 8.17 Increase in lateral contact pressure due to 10° valgus malalignment; (a) normally strained and (b) imbalanced collateral ligaments.

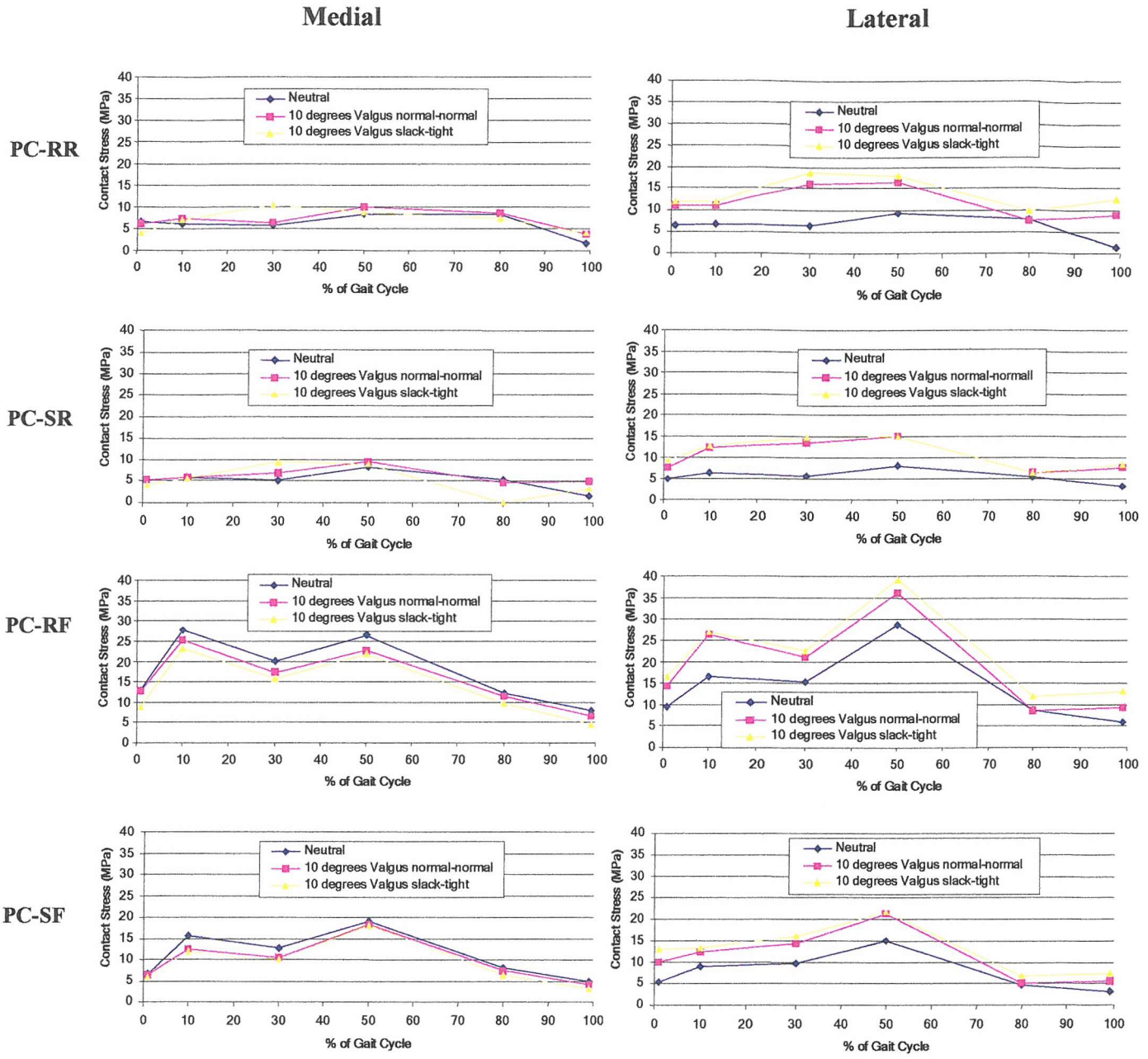

Figure 8.18 Peak contact pressures due to 10° valgus malalignment. Comparisons against the idealised knee (Neutral).

8.4 Discussion/ Summary of Chapter 8

This chapter of the thesis has compared the effects of altered ligament strains and malalignment on the motions and pressures produced in the replaced knee. Specific parameters were altered to recreate possible clinical situations, and their effects on passive and active motions were simulated through computational FE models. Chapters 5 and 7 of this thesis showed the motions and contact pressures of the idealised knee (neutral alignment, MCL-LCL normally strained); this information was used as the standard against which all other tests were compared.

The following section presents a brief discussion of the results from Chapter 8 while Chapter 9 will give a more global review of the results, discussing possible failure mechanisms (wear, loosening etc.) of the prostheses that may occur as a result of malalignment or ligament imbalance.

Effect of Altered Ligament Strains:

Imbalanced Ligaments

Passive A-P stability testing did not yield significant conclusions when assessing imbalanced ligaments; a maximum difference of 1mm was observed in all knees. With the exception of the PC-SF, internal rotations were slightly increased and external rotations were slightly reduced (by only ~2°) with a tight-slack MCL-LCL combination. The opposite was noted with a slack-tight MCL-LCL combination. The PC-SF was most sensitive to ligament imbalance at 90° flexion, where internal rotations increased by 6.2° and external rotations reduced by 6.8° for a tight-slack MCL-LCL combination. The I-E stability of the PC-SF relied on the interaction of the tibial spine and femoral component; at 90° flexion altered ligament strains affected this interaction, producing large differences in internal and external rotations. Out of the three passive stability investigations carried out, V-V rotational stability testing was the most conclusive when assessing ligament imbalance. A tight-slack MCL-LCL combination increased varus rotations (opening of the lateral side of the knee) by ~1.9°, and decreased valgus rotations (opening of the medial side of the knee) by ~1.4° in all knees. Since the V-V

rotations in the idealised knee were relatively small, an increase of 1°-2° was significant (this was equivalent to ~15%-30% of the total rotation).

The effect of imbalanced ligament strains on active motions was not significant; only minor deviations in I-E rotations and A-P translations occurred during a gait cycle. Ligament imbalance did affect the force distribution across the medial and lateral sides of the knee during gait. A maximum increase in load of ~80N passed through the tight side of the knee with imbalanced ligaments; however, during the high load positions across the gait cycle this increased axial force did not significantly affect the contact pressures on the knee. One area of concern that could be associated with an altered force distribution is intra-operative and immediate post-operative knee stability. Immediately after TKA the bone cement used to fix the knee components may not have cured 100%; if uneven forces are applied across the knee there is the potential for post-operative malalignment. During the swing phase of the gait cycle extra loading was recorded on the tight side of the knee, highlighting the fact that ligaments altered the force distribution even when no axial forces were applied.

Slack or Tight Ligaments

When both ligaments were slack, passive A-P laxity was increased more noticeably than for imbalanced ligaments; an increase of ~3.5mm was noted for all knees at 15° flexion. I-E laxity was also more significantly affected when both ligaments were slack, with increases of ~6° in all knees at 15° flexion. During V-V stability testing varus rotations increased by a maximum of ~1.6° and valgus rotations increased by a maximum of ~0.5°.

When both collateral ligaments were tight, A-P stability increased by ~4mm in the fixed-bearing knees and 1.5mm in the rotating-bearing knees at 15° flexion. I-E rotations in the rotating-bearing knees reduced by ~5.8°, and rotations reduced by 4.7° in the PC-RF. The I-E stability of the PC-SF was most sensitive to tight ligaments; reductions of 7.8° were recorded at 90° flexion. Total V-V stability was increased by ~1.5° in all knees and varus rotations were reduced by ~0.5° more than valgus rotations.

When both ligaments were slack or tight the general stability of all knees during gait was not significantly altered. Contact pressures were also not significantly affected. Any

noticeable alterations occurred during the swing phase of the gait cycle, when the peak pressures were relatively low.

In general passive stability testing could be used to assess inaccuracies in ligament strains. Ligament imbalance was best assessed with passive V-V stability testing. Over strained or lax ligaments were highlighted with all three passive stability tests. Within the strain limits assessed in the present research altered ligament strains did not significantly alter the kinematics or contact pressures across the knee during gait. However, imbalanced ligaments did alter the contact force distribution; this could affect immediate post-operative stability, possibly resulting in malalignment [87].

Effect of Malalignment:

Passive Stability

Malalignment of the prosthetic components could occur by surgical error, or by imbalanced ligaments (as mentioned above), potentially leading to catastrophic implant failure (severe insert wear/ fracture, implant loosening, dislocation). Ideally the femoral component should be placed at ~7° of valgus off the shaft axis of the femur (perpendicular to the mechanical loading axis, see Chapter 2); however, placement within a few degrees is deemed acceptable. The effect of ±3° of varus/ valgus malalignment and associated ligament imbalance was assessed in the present research.

When both collateral ligaments were normally strained 3° of varus malalignment did not have a significant effect on the passive A-P stability; a maximum change of 1.3mm was noted in all knees. During I-E stability testing with normally strained collateral ligaments, the internal rotations were reduced by over 3.5° in all knees except the PC-SF. The external rotations were increased by a similar amount in all knees. These alterations in rotations were caused by initial axial rotation of the femoral component during flexion. In the PC-SF at 90° flexion both internal and external rotations were increased (by 1.1° and 1.3° respectively). When both ligaments were normally strained passive V-V stability was not significantly affected by 3° varus malalignment.

With the exception of the PC-SF, altered ligament strains (tight-slack MCL-LCL) combined with varus malalignment did not cause a dramatic change in A-P or I-E stability. In the PC-SF internal and external rotations were reduced by 6.3° and 3.7° respectively. During V-V stability testing with imbalanced ligaments, varus rotations increased by ~1.9° and valgus rotations increased by ~1.3° in all knees. Under the same ligament condition the V-V stability with varus malalignment was similar to that in the idealised knee, showing that V-V stability was affected by ligament strains rather than varus malalignment.

When the ligaments were normally strained 3° valgus malalignment had very similar effects to varus malalignment. The only major difference was in I-E stability, where internal rotations increased by ~5.1° and external rotations reduced by ~4.8° in all knees. A slack-tight MCL-LCL combination significantly affected the I-E stability of the PC-SF only (internal rotations reduced by 0.2° and external rotations reduced by 10.0°). As with varus malalignment, V-V stability with valgus malalignment was similar to that in the idealised knee.

Active Stability

±3° coronal malalignment did not significantly affect the kinematics during gait. The medial and lateral contact force distribution was altered more significantly at positions of high axial load during the gait cycle.

3° varus malalignment increased medial loading by a maximum of ~120N and reduced lateral loading by a similar magnitude for all knees. Ligament imbalance further increased medial loading by ~70N. In general medial contact pressures increased and the lateral contact pressures reduced due to varus malalignment; a maximum increase of ~5MPa and a maximum reduction of ~6MPa were noted for all knees.

3° valgus malalignment increased lateral loading by a maximum of ~160N for all knees. Imbalanced ligaments further increased lateral loading. In the high load periods across the gait cycle lateral contact pressures increased by a maximum of ~4MPa and medial contact pressures reduced by a maximum of ~2MPa for all knees.

Extreme Malalignment:

Varus Malalignment

10° varus malalignment reduced the passive A-P translations in all knees, particularly for the PC-RF (a reduction of 6.7mm). With the exception of the PC-SF, internal rotations reduced by ~16° and external rotations increased by ~16.5° for all knees during I-E stability testing. In the PC-SF internal rotations reduced by 17.6° and external rotations increased by 11.1°. Total V-V stability was not significantly affected by varus malalignment.

For normally strained collateral ligaments, peak internal rotations were increased by ~5.5° in both rotating-bearing knees during gait, and were in a more externally rotated position until the end of the gait cycle. The fixed-bearing knees became slightly unstable at the point of peak internal rotation; the lateral contact position shifted from a more central region on the insert bearing surface (in the idealised knee) to the anterior rim (10° varus knee). In the PC-SF the insert geometry, and in particular the tibial spine increased the I-E restraint of the prosthesis. When the collateral ligaments were normally strained the gait kinematics of the PC-SF were not significantly affected, however with imbalanced ligaments the peak internal rotation increased sharply. With normally strained collateral ligaments a sharp increase in peak internal rotation (a maximum increase of ~10°) occurred in the PC-RF. For imbalanced ligaments at about 45%-50% of the gait cycle internal rotations reached such a point that anterolateral dislocation of the femoral component relative to the insert occurred in the PC-RF.

10° varus malalignment caused medial contact forces to increase by a maximum of ~450N, and lateral forces to reduce by a maximum of ~400N when the collateral ligaments were normally strained. Forces were altered by a further 100N with imbalanced ligaments. This large alteration in contact forces combined with the change in gait kinematics caused peak medial contact pressures to increase by up to 9.2MPa in the rotating-bearing knees and 17.1MPa in the fixed-bearing knees. Also in the fixed-bearing knees, lateral contact pressures increased significantly at certain positions in the gait cycle; this occurred when the contact point was shifted to the rim on the lateral side of the insert. For the PC-RF and PC-SF an increase of 59.2MPa and 42.5MPa

respectively was recorded when the collateral ligaments were normally strained; this increased to 72.6MPa in the PC-SF with imbalanced ligaments.

Valgus Malalignment

During passive stability simulations 10° valgus malalignment caused A-P translations to reduce, particularly in the PC-RF. With the exception of the PC-SF, internal rotations increased by ~15° and external rotations reduced by ~15.5° in all knees. V-V stability was not significantly affected by valgus malalignment.

When both collateral ligaments were normally strained the I-E kinematics during gait were similar for both rotating-bearing knees; peak external rotations increased by ~6° and peak internal rotations increased by ~4.3°. The I-E rotations of both fixed-bearing knees were not significantly affected for the first 45% of the gait cycle. However, from this position until the end of the gait cycle the malaligned knee remained in a more internally rotated position (a maximum deviation of ~9°).

Lateral contact forces were significantly increased and medial forces reduced due to valgus malalignment. The altered force distribution caused a maximum of ~65% of the total axial force to be passed through the lateral side of the rotating-bearing knees during gait. The distribution of medial:lateral contact forces in the fixed-bearing knees was ~55%:45%, compared to ~75%:25% in the idealised knee. This increased lateral loading caused lateral contact pressures to increase by a maximum of ~10MPa for all knees during gait. In general medial contact pressures were not significantly affected by 10° valgus malalignment.

As mentioned at the beginning of this section, altered kinematics and contact pressures could affect the long-term performance of the TKR. Increased I-E rotations could lead to increased wear and contact pressures greater than the yield strength of the polyethylene insert could cause deformation [130], [131], [132]. These situations are discussed in more detail in Chapter 9 of this thesis.

Summary

Passive stability testing was used to assess changes in ligament strains and malalignment. V-V stability testing best identified ligament imbalance, with reduced rotations on the tight side of the knee and increased rotations on the lax side. Slight malalignment was best identified by I-E stability testing, and A-P/ I-E stability testing were capable of highlighting extreme malalignment. The overall gait kinematics were not significantly affected by altered ligament strains or slight malalignment, however the force distribution across the knee was changed. Varus malalignment altered the peak contact pressures more significantly; however at positions of maximum axial force the increases were relatively small. Extreme malalignment affected the idealised knee kinematics more significantly in the fixed-bearing knees, where I-E instability was more prevalent, particularly for imbalanced ligaments. 10° varus malalignment affected the contact pressures more significantly than valgus malalignment; severe increases in lateral pressures occurred due to anterior rim contact in the fixed-bearing knees.

Chapter 9 Overall Discussion, Conclusion and Future Work

The aim of the present research was to assess the factors that alter the stability of the replaced knee, and to ascertain the importance of intra-operative stability towards post-operative stability following TKA. Loosening and instability post-operatively have been highlighted as being among the most common reasons leading to revision surgery after TKA [71], [72], [73], [74]; others include infection, patellofemoral complications and periprosthetic fractures. Correct alignment of the prosthetic components and balanced strains within the ligaments are important for stability after TKA. In the natural joint the angle between the femoral shaft axis and the mechanical axis of the lower limb is about 7° of valgus, and should be reproduced during TKA [76], [77]. Some authors believe that a small degree of malalignment may not cause serious complications [76], however others believe that an error of 5° can be significant and 10° is often catastrophic [75]. In addition, ligament imbalance has been highlighted as a cause of post-operative instability [87], with polyethylene wear and abnormal wear patterns being recorded in retrievals [83].

On this basis, the passive stability of four knee designs† was examined experimentally in the present research. Experimental testing in the sagittal, coronal and transverse plane has been reported in the literature [12], [18], [100], [101], [102], [103], [105], [107], and V-V rotational, I-E rotational and A-P translation investigations have been the most widely studied. Set flexion positions of the knee were chosen for specific stability tests; this was an important consideration as reports have stated that certain ligament groups restrain motions to a greater extent at different flexion angles [108], [109], [110].

A mechanical test rig was developed which permitted interchangeable total knee designs, and allowed the primary ligaments of the knee to be simulated. Three passive stability investigations (A-P, I-E and V-V stability testing) were achievable with the test rig, which used synthetic materials to represent the MCL and LCL. The PCL was originally simulated; however, initial testing and material behaviour issues led to its removal (see Chapter 4). From the literature it was not clear as to the exact role of the PCL after TKR, and is has been shown that knees designed to be implanted with its retention functioned normally when it was removed [7], [125], [126]. These findings suggest that testing of the PC-

† Four designs of the PFC knee system (DePuy, Leeds, UK)

retaining knees without the PCL was still valid. A comprehensive passive stability study was carried out on four different knee designs (PC-retaining fixed-bearing knee (PC-RF), PC-retaining rotating-bearing knee (PC-RR), PC-substituting fixed-bearing knee (PC-SF) and the PC-substituting rotating-bearing knee (PC-SR)). Testing was conducted in neutral and malaligned positions, and with normal and altered ligament strains.

The testing showed that the PC-SF offered the greatest stability in the sagittal and transverse planes, and that the PC-RF possessed the greatest laxity in all planes. Both rotating-bearing knees had similar I-E and V-V stabilities; however, the A-P stability of the PC-SR was greater. In general, laxity increased at greater flexion positions, and slack collateral ligaments had the greatest effect on passive stability. V-V rotational stability testing best highlighted ligament imbalance; a tight-slack MCL-LCL combination caused a maximum increase in varus rotation (opening of the lateral side of the knee) and a slack-tight combination caused a maximum increase in valgus rotation (opening of the medial side of the knee). Malalignment was best detected through I-E stability testing. Valgus malalignment generally increased internal rotations and reduced external rotations, particularly at 90° flexion, while varus malalignment reduced internal rotations and increased external rotations.

The next stage of this study aimed to identify whether there was a direct comparison between the stability of the knee under low load testing (passive stability), and active stability (normal gait). In order to assess this relationship computational models were constructed of all four knee types, and explicit finite element (FE) analysis was used to simulate the motions. The first stage of this FE study attempted to validate the computational models against the experimental results. Contact pressure measurements of the PC-RF were recorded experimentally and provided additional validation data for the computational models. In the idealised knee (neutral alignment with normally strained collateral ligaments) a good correlation was observed between the experimental and FE simulations for all knees and for all stability tests. Altered ligament strains produced comparable increases and reductions in A-P, I-E and V-V motions; however, malalignment did yield some variation between the experimental and computational results. In most cases the results were comparable, and where deviations did occur the same general trends were followed; Chapters 5 and 6 highlighted the possible experimental complications that may have accounted for these discrepancies. Overall, the

comparable stability results of all four knee designs, combined with the contact pressure measurements of the PC-RF provided confidence in the computational models.

Gait data was input into the FE models (data derived from Morrison [114]) to simulate normal gait. Testing in the present research differed from other published work as the soft tissue structures were represented as elastic-plastic structures attached to the femoral and tibial sections of the knee; in other reported studies the soft tissue structures were represented by horizontal springs [8], [112]. From these gait simulations the I-E/ A-P motions and contact pressures were recorded during one gait cycle for all knees in the idealised condition. The I-E rotations of the rotating-bearing knees were significantly larger than both fixed-bearing knees (the peak internal rotations of the rotating-bearing knees were over 50% greater than the PC-RF and 70% greater than the PC-SF). From the literature only FE simulations of fixed-bearing knees could be found; this meant the large I-E rotations noted in the present research could not be directly compared. In the natural knee rotations of this magnitude would not be expected [67], [68], [69], which implied that other restraining properties in the natural knee help increase the I-E stability of the implanted rotating-bearing knee. Indeed, the present research only simulated the MCL and LCL, and did not account for other medial and lateral soft tissue structures such as the patella, the joint capsule, and even the skin which are present in the natural joint. The fixed-bearing knees in the present research had rotations that were comparable to other published studies [8], [111], suggesting that the geometry of the inserts offered considerable restraint to I-E rotations, in particular the PC-SF. A-P translations were relatively similar in all knees, with the PC-RF possessing the greatest laxity in this plane.

The contact forces, contact pressures and contact areas varied across all knees. At positions of maximum vertical load the rotating-bearing knees had significantly larger contact areas compared to the fixed-bearing knees. This greater contact area distributed the forces across the bearing-surfaces, lowering the peak contact pressures. The PC-RF had the lowest component conformity of all the knees investigated. This resulted in the greatest contact pressures, which approached 30MPa at the high load stages across the gait cycle. The peak contact pressure of the PC-SF reached a maximum of ~20MPa. By contrast, both rotating-bearing knees had significantly lower peak contact pressures of ~9MPa. The maximum contact pressures recorded for all knees in the present study were comparable to those in the literature [9], [129]. It has been shown that a lower component

conformity can produce increased wear rates of the polyethylene component (tibial insert) [133], [134]; this is most probably due to increased contact pressures and sliding/ rolling kinematics in the lower conforming knees [130], [131], [132].

One would assume that good stability intra-operatively would translate to good stability post-operatively; however, finding direct comparisons between passive (low load conditions) and active (normal gait) stability after TKR in the literature proved problematic. Passive stability has already been discussed, therefore the next aim of the present research was to assess the effects of altered ligament strains and component alignment on active motions and contact pressures. This stage of the thesis was fully computational, using explicit finite element analysis to simulate all knee conditions.

Altered ligament strains did not have a significant effect on the kinematics or contact pressures during gait; however, the distribution of contact force across the bearing-surfaces was altered with imbalanced ligaments. An increase in contact force through the tight side of the knee was evident, and even though the contact pressures were not significantly altered the immediate post-operative effects of imbalanced ligaments could be important. It has been reported that post-operative malalignment could occur with imbalanced ligaments [87], due to an uneven bone cement thickness formed under the tibial component. Intra-operatively or immediate post-operatively the bone cement used to fix the prosthetic components to the bone may not be 100% cured, and the uneven forces associated with imbalanced ligaments could compress one side of the knee while opening up the other.

Slight malalignment in the present research did not significantly affect the gait kinematics of the knees tested. Varus malalignment caused contact pressures to increase slightly on the medial side of the knee and reduce slightly on the lateral side of the knee. The largest alterations in contact pressure occurred at positions of relatively low load across the gait cycle. The maximum increase in medial contact pressure at the high load stages of the gait cycle due to varus malalignment was ~3MPa, and the greatest reduction in lateral pressures was ~5MPa across all knees. The general effects of valgus malalignment were not as great as with varus malalignment. Normal gait kinematics were not significantly altered, and in all knees lateral contact pressures increased by ~4MPa and medial contact pressures reduced by ~2MPa at the low load stages of the gait cycle.

It had been stated that 10° malalignment could lead to catastrophic failure of the TKR [75], which may relate to severe polyethylene wear/ fracture, and implant loosening. This led to the next stage of the investigation, which assessed 10° varus/ valgus malalignment. Testing was carried out with normally strained and imbalanced collateral ligaments. Varus malalignment with a tight-slack MCL-LCL combination and valgus malalignment with a slack-tight MCL-LCL combination was adopted; this simulated a worst case scenario.

During passive stability testing it was noted that flexion was accompanied by excessive axial rotation of the femoral component in the transverse plane. Varus malalignment produced ~16° of external femoral rotation, and valgus malalignment produced ~16° of internal femoral rotation as the knee was flexed from 0° to 90°. All passive stability testing was conducted at 90° flexion. The A-P translations of all knees were reduced with varus and valgus malalignment, particularly in the PC-RF (maximum reduction of ~8mm). With the exception of the PC-SF, 10° varus malalignment reduced internal rotations by ~16° and increased external rotations by ~16.5°; the opposite was noted with 10° valgus malalignment. The I-E stability of the PC-SF was dictated by the interaction of the tibial spine and femoral component; 10° malalignment significantly altered this interaction and in turn affected the PC-SF differently to the other knee designs tested. V-V stability was not significantly affected by 10° malalignment for all knees. Intra-operatively, these passive stability findings could provide important information to the orthopaedic surgeon, highlighting possible coronal plane alignment errors. For example, if internal rotations were significantly reduced for a particular TKR, the surgeon could relate this to a large varus malalignment, therefore making appropriate alignment alterations. Table 9.1 summarises the main passive stability findings from the present research, highlighting possible surgical errors and relating them to short-term/ long-term post-operative complications.

The effect of 10° malalignment on the kinematics and contact pressures during gait was significant. 10° varus malalignment increased peak internal rotations by ~7° in both rotating-bearing knees (maximum internal rotation of ~29° for both knees). At the point of peak internal rotation, the I-E stability of both fixed-bearing knees was reduced, particularly in the PC-RF. This point of instability corresponded to a shift of lateral

contact position from the mid-bearing surface of the insert to the anterior rim (see Chapter 8, Figure 8.8). With imbalanced ligaments the PC-RF was most affected by 10° of varus malalignment; I-E dislocation occurred at the point of peak internal rotation (~50% of the gait cycle). Dislocation in itself is a major issue, and is obviously something that needs to be avoided. However, even when dislocation did not occur the increased I-E rotations were of concern. *In vitro* testing has shown that increased I-E rotations increase wear rates [131], [132], and Blunn *et al.* [135] highlighted that sliding, rather than compression or rolling dramatically increased polyethylene wear. They noted that cyclic loading alone produced minimal wear deformation; however, introducing sliding caused severe surface damage of the insert via deformation, cracking and wear (delamination). This therefore suggests that the increased I-E rotations (sliding motion) noted in the PC-RF could result in increased surface damage of the insert.

10° varus malalignment caused ~65% of the total contact force to be passed through the medial side of the rotating-bearing knees and 90% in the fixed-bearing knees during maximum loading in the gait cycle. This alteration in contact force distribution combined with the altered kinematics during gait had a significant effect on the peak contact pressures. Peak medial contact pressures increased by a maximum of 15.5MPa in the PC-RF with normally strained collateral ligaments and 17.1MPa with imbalanced ligaments up to the point of dislocation. The most significant effects were noted on the lateral bearing surfaces in the fixed-bearing knees. At most positions across the gait cycle the lateral contact pressures of the PC-RF were relatively unaltered; however, at 50% of the gait cycle when the lateral contact point was shifted onto the rim of the insert the contact pressure increased significantly. With normally strained collateral ligaments the peak lateral contact pressure increased to 88MPa (an increase of ~70%). Peak contact pressures in the PC-SF reached 57.5MPa with normally strained collateral ligaments and 87.6MPa with imbalanced ligaments. The yield strength of UHMWPE (tibial insert component) has been approximated to be 23MPa [116], [136], which therefore means that contact stresses greater than 23MPa would cause local deformation of the insert. This has been noted in retrievals [137]; however, even though other authors agree that wear and deformation of the insert increases with contact stress [130], the evidence from retrievals sometimes shows increased wear in higher conforming designs, where the contact stresses are lower [138]. A complicating factor is that highly conforming designs show

increased wear due to entrapped third body particles. This situation is beyond the scope of the present research.

The peak contact pressure of the idealised PC-RF reached ~30MPa during the gait cycle, which in itself is high enough to cause local deformation of the insert. Due to the rigid body configuration of the FE simulations no deformation was assessed in the present research, however with contact pressures reaching up to 88MPa in varus malalignment the consequences would be significant. Deformation of the anterior rim in both fixed-bearing knee designs would be certain to occur *in vivo*, leading to wear debris that could cause loosening or infection in the long-term [139]. Several types of deformation can occur in the polyethylene component. The layer of polyethylene is compressed by the metal component, causing compressive stress in a direction that is normal (perpendicular) to the surface throughout the component. The compressive stress is greatest on the surface, where the metal component is in contact with the polyethylene, and its maximum value occurs at the centre of the contact area [136]. The indentation of the metal component also causes deformation of the surface of the polyethylene component in directions that are tangential to the surface. Near the edge of the contact, the surface is stretched and tensile stresses occur in the polyethylene. In the centre of the contact area, the surface is compressed in directions tangential to the contact surface, and compressive stresses occur [136]. These tangential stresses are also greatest at the surface and vary with position along the surface and throughout the depth of the polyethylene layer. Finally, indentation of the metal component causes distortion (shearing) of the polyethylene.

In the present research the kinematic effect of 10° valgus malalignment was similar to that of 10° varus malalignment in the rotating-bearing knees. Valgus malalignment did not affect the fixed-bearing knees as significantly. In general medial contact pressures were not significantly altered by valgus malalignment; a maximum variation of 4.7MPa was noted in all knees. Lateral contact pressures increased with valgus malalignment; contact pressures in the PC-SF increased by a maximum of ~7MPa, and in all other knees by a maximum of ~12MPa during the high load periods of the gait cycle. As discussed, increased contact pressures could lead to increased wear rates of the insert [130], [131], [132].

From the results of the four knee designs assessed in the present research (the PC-RR, PC-RF, PC-SR and the PC-SF), the benefits of the rotating-bearing knee prostheses

seemed to outweigh those of the fixed-bearing knee designs. The main observation was the significantly reduced peak contact pressures across the gait cycle, due to the larger component conformity of the rotating-bearing knees. One other noticeable benefit of the rotating-bearing knees was that the kinematics and contact pressures were not significantly affected by malalignment, particularly when compared to the fixed-bearing knee designs. However, it was noted that the I-E stability of the rotating-bearing knees was lower than the fixed-bearing designs, and even though the rotations produced during gait seemed unrealistic when compared to the natural joint, it showed that the prosthesis did not provide geometric stability in the transverse plane. This indicates that the soft tissue structures around the knee will take extra load during I-E rotations; thus, if this knee design was implanted good ligamentous structures around the knee would be necessary to ensure I-E stability.

The PC-SF was more stable than the PC-RF, and during most of the testing scenarios in the present research the increased I-E and A-P stability offered by the tibial spine meant that consistent kinematics were produced during gait. However, the high geometric constraint of the PC-SF may not be totally advantageous. In normal joints, rotational loads are shared by the joint surface and the surrounding soft tissue. If the surfaces of the prosthesis carry a greater portion of the load, the portion carried by the surrounding soft tissue will be decreased. The stresses at the prosthesis-bone interface will be larger, leading to possible loosening complications [140]. The PC-RF has a lower component restraint, and therefore this problem may be avoided. However, the high contact pressures of this particular knee may yield greater wear rates and increase the probability of implant failure, either by long-term loosening or fracture of the tibial insert.

Passive Stability Test	Passive Consequence	Knee Type Affected	Possible Explanation	Active Effect	Possible Short-term/ Long-term Effect
V-V Rotational	Increase in varus laxity with a reduction in valgus laxity and vice versa	All	Slack-Tight (MCL-LCL) imbalance and vice versa	Altered vertical load distribution. Increased load on the tight side of the knee	Post-operative malalignment
I-E Rotational	Reduction in internal rotation (~4°) with an increase in external rotation (~5°) @ 90° flexion	PC-RR PC-RF PC-SR	Slight varus malalignment (3°). Normally strained ligaments	Increased medial loading (~4%) during the high load stages of the gait cycle	Minimal. Possible increased chance of loosening long-term due to progressive loading on one side of the knee.
	Increase in internal rotation (~4°) with a reduction in external rotation (~3°) @ 90° flexion	All	Slight valgus malalignment (3°). Normally strained ligaments	Increased lateral loading (~7%) during the high load stages of the gait cycle	Minimal. Possible increased chance of loosening long-term due to progressive loading on one side of the knee.
	Large reduction in internal rotation (~16°) with a large increase in external rotation (~16°) @ 90° flexion	All	Extreme varus malalignment (10°) with imbalanced ligaments (tight-slack MCL-LCL)	I-E instability in the fixed-bearing knees. Increased medial loading in all knees (~20%). Increased medial contact pressures of ~10MPa (~100% increase) in the rotating-bearing knees and 15MPa (~60% increase) in the fixed-bearing knees. Significant increase in lateral contact pressure in both fixed-bearing knees due to altered gait kinematics.	Dislocation in the fixed-bearing knees, in particular the PC-RF. Deformation of the tibial insert when the peak contact pressures were greater than the yield strength of the polyethylene. Increased wear rates, which in the long-term could lead to insert fracture, prosthesis loosening or infection.
	Large increase in internal rotation (~15°) with a large reduction in external rotation (~16°) @ 90° flexion	All	Extreme valgus malalignment (10°) with imbalanced ligaments (slack-tight MCL-LCL)	Slightly altered gait kinematics (increased peak rotations). Increased lateral loading and increased lateral contact pressures. Effects not as significant as with extreme varus malalignment.	Increased wear rates due to increased rotations and peak contact pressures. See above for further long-term effects.
A-P Translation	Reduced A-P laxity (~9mm)	PC-RF	Either extreme varus or valgus malalignment (10°)	See extreme varus and valgus malalignment effects above	See extreme varus and valgus malalignment effects above

Table 9.1 Main effects noted on passive stability; highlighting surgical possibilities and short-term/ long-term consequences.

Summary

This research has highlighted specific passive stability tests that can be used to detect possible causes of joint instability after TKR. Ligament imbalance was best detected by V-V stability testing and malalignment was best detected by I-E stability testing. The rotating-bearing knees had similar responses to passive stability testing, the PC-RF had greater laxity and the PC-SF had greater stability out of all the knees tested. The gait analysis results from the present research correlated well with other authors who suggest that varus alignment should be avoided [70]. Catastrophic outcomes were highlighted for particular knee designs with extreme malalignment, for which significantly altered kinematics, loading conditions and contact pressures were recorded. Ligament imbalance was observed to alter the force distribution across the knee, and could help explain the uneven bone cement thickness under the tibial component noted by some authors [87]. To conclude, the findings from the present research show that slightly lax or slightly tight knees under passive testing did not significantly affect the active stability of the replaced knee. Altered stability in the coronal plane could be linked to imbalanced ligaments, which in turn could be linked to altered force distribution across the knee during gait. In addition, malalignment, in particular excessive malalignment, caused passive I-E stability to be altered significantly, and was directly linked to altered gait kinematics and instability. Furthermore, it was shown that certain implant designs were more sensitive towards altered ligament strains and malalignment, and that if the soft tissue structures were not adequately strained the effects of malalignment were magnified.

The present work demonstrated the importance of correctly balanced medial and lateral soft tissue structures surrounding the knee, and correct component alignment. However, slight degrees of coronal malalignment did not significantly affect the stability of the replaced knee during gait. The findings from the present research were limited to the set conditions simulated; for example, the ligaments were strained between values of ±5% and malalignment was limited to the coronal plane (varus/ valgus). In reality the strains in the ligaments may vary somewhat, and the prosthetic components may be malaligned in different planes; however, the present research has provided a fundamental understanding into the importance of the soft tissue structures around the knee and component alignment towards joint stability.

Main Conclusions

A combined experimental/ computational FE model for passive stability testing of the replaced knee has been successfully developed. The computational FE model has been extended to allow the simulation of active motions. The assessment of passive stability was shown to be useful in determining ligament strain and alignment errors after TKR. A good correlation between the mechanical test rig in the present research and published cadaveric/ *in vivo* studies was observed; however, some limitations were evident, for example, the straining of the ligament structures and the limited number of soft tissue structures present.

The experimental results correlated well with the computational FE models, and it was shown that passive stability could be used to predict the active behaviour of the replaced knee. Using these models, the following findings have been highlighted:

- Ligament imbalance was best detected by passive V-V rotational stability testing.
- Malalignment was best detected by passive I-E rotational stability testing.
- Ligament imbalance did not significantly affect kinematics or peak contact pressures during gait; however, the vertical force distribution was altered.
- $\pm 5^{\circ}$ coronal malalignment slightly altered peak contact pressures and kinematics during gait.
- $\pm 10^{\circ}$ coronal malalignment, in particular varus malalignment, altered kinematics and contact pressures more significantly in the fixed-bearing knee designs.
- The rotating-bearing knees had significantly lower peak contact pressures, and were affected to a lesser extent by malalignment compared to the fixed-bearing knee designs.
- The posterior cruciate-retaining fixed-bearing knee had the greatest peak contact pressures during gait, and was particularly susceptible to malalignment.

Future Work

The results from the present research have provided an initial assessment of the effects of altered ligament strains and malalignment on the passive and active stability of total knee replacements. Further work in this area needs to be performed to fully understand the stability of the replaced knee and which conditions can affect its long-term survival.

Experimentally, more realistic simulations of the soft tissue structures around the knee would be beneficial; in this respect the addition of further soft tissue structures such as the patellar tendon and joint capsule would be appropriate. Using natural tissues would be ideal in terms of material properties; however, this could prove problematic due to availability, fixation to the test rig and other biological considerations. In the present research the collateral ligaments were represented by a material with similar stiffness values to the natural ligaments. If a material with additional similarities to the natural soft tissues (i.e. ultimate tensile strength, viscoelatic properties etc.) was found the test rig would provide a more realistic representation the anatomic knee.

A greater range of passive stability tests would be advantageous, for example the pivot shift test (flexion accompanied by I-E rotation) or general range of motion assessment. Furthermore, it would be useful to assess a wider range of TKR designs, or to assess different versions of a particular design (e.g. several PC-retaining rotating-bearing knee designs) to quantify a specific TKR characteristic that could contribute towards joint stability.

The same criteria can be applied to the finite element models, with for example the simulation of extra soft tissue structures and perhaps the addition of full length bones onto which the TKR can be fitted. In addition, simulating altered component position in the sagittal and transverse planes would provide a greater insight into the kinematics after TKA, as component malalignment does not take place in the coronal plane only (as simulated in the present research). Still on this issue, malalignment of the tibial component as well as the femoral component should be assessed, as this situation occurs *in vivo*.

All FE components were modelled as rigid bodies in the present research, which meant that deformation did not occur during testing. In reality the increased contact pressures noted in the present research could cause plastic deformation of the polyethylene component, and could further alter the gait kinematics and contact pressures. Modelling the polyethylene component as a solid body would provide greater deformation information. In addition, modelling as a solid body would provide internal stress information, and allow possible (delamination) wear complications to be assessed.

All gait results in the present research were obtained for one gait cycle, and although this provided kinematic information the long-term effects of altered kinematics and contact pressures could not be analysed. Simulating several, or perhaps millions of gait cycles would provide a better understanding into the effects of malalignment and altered ligament strains on the long-term behaviour of the replaced knee. Also, information on other interfaces would be beneficial: for example, the insert-tray interface or the tray-bone interface may yield important information on the stability the replaced knee. It is known that a more constrained TKR can reduce the stresses in the soft tissues and transmit greater stresses to the implant-bone interface, thus modelling/ assessing this situation would be advantageous. Simulating other scenarios such as stair climbing and impact loading activities (e.g. running etc.) may provide a more realistic analysis of the TKR. A constant amplitude walking simulation (simulated in the present research) may not be a fully realistic comparison to everyday situations that occur *in vivo*. It may be argued that implantation of TKRs in elderly patients will not be subjected to running or other high impact loading situations; however, rising from a seated position and climbing stairs are likely to occur.

These developments of the present research should allow the performance of total knees to be assessed in more detail, and perhaps allow a more accurate quantitative measurement of the long-term effects of altered gait kinematics and altered contact pressures on the survival of the TKR.

References

1. Andriacchi TP, Stanwyck ST, and Galante JO, Knee Biomechanics and Total Knee Replacement. J. Arthroplasty, 1986. 1(3): p. 211-219.
2. Nordin M and Frankel VH, Basic Biomechanics of the Skeletal System. 1980, Philadelphia: Lea & Febiger. 113-148.
3. Maquet P. Biomechanics of the Knee. 1976. New York: Springer- Verlag.
4. Kim W, Rand JA, and Chao EY, Biomechanics of the Knee, in Total Knee Arthroplastly, R. JA, Editor. 1993, Raven Press Ltd: New York. p. 9-55.
5. Quapp KM and Weiss JA, Material Characterisation of Human Medial Collateral Ligament. Journal of Biomechanical Engineering, 1998. 120(6): p. 757-763.
6. Kaufman KR, et al., Dynamic joint forces during knee isokinetic exercise. Am J Sports Med, 1991. 19: p. 305-316.
7. Straw R, et al., Posterior Cruciate Ligament at Total Knee Replacement; Essential, Beneficial or a Hindrance? J Bone Jnt. Surg, 2003. 85-B: p. 671-674.
8. DesJardins JD, et al., The use of a force-controlled dynamic knee simulator to quantify the mechanical performance of total knee replacement designs during functional activity. Journal of Biomechanics, 2000. 33: p. 1231-1242.
9. Godest AC, et al., Simulation of a knee joint replacement during a gait cycle using explicit finite element analysis. Journal of Biomechanics, 2002. 35: p. 267-275.
10. Seedhom BB, Reconstruction of the anterior cruciate ligament. Proc Instn Mech Engrs, 1992. 206: p. 15-27.
11. Butler DL, Kay MD, and Stouffe DC, Comparison of Material Properties in Fascicle-Bone Units from Human Patellar Tendon and Knee Ligaments. J of Biomech., 1986. 19(6): p. 425-432.
12. Lundberg M and Messner K, A 4-year clinical and mechanical follow-up study in 38 patients. Acta Orthopaedica Scandinavica, 1994. 65(6): p. 615-619.
13. Walker PS, Ambarek MS, and M. JR, Anterior-posterior stability in partially conforming condylar knee replacements. Clin Orthop, 1995. 310: p. 87-97.
14. Matsuda S, Hiromasa H, and Nagamine R, Changes in knee alignment after total knee arthroplasty. J Arthroplasty, 1999. 14: p. 566-570.
15. Fishkin Z, et al., Changes in human knee ligament stiffness secondary to osteoarthritis. Journal of Orthopaedic Research, 2002. 20: p. 204-207.
16. Whiteside LA and Amador DD, The effect of posterior tibial slope on knee stability after Ortholoc total knee arthroplasty. J Arthroplasty, 1988. 3: p. S51-57.
17. Anouchi YS, Whiteside LA, and Kaiser AD, The effects of axial rotational alignment of the femoral component on knee stability and patellar tracking in total knee arthroplasty demonstrated on autopsy specimens. Clin Orthop, 1993. 287: p. 170-177.
18. Shoemaker SC, et al., In vitro stability of the implanted total condylar prosthesis: Effects of joint load and sectioning the posterior cruciate ligament. J Bone Jnt. Surg, 1982. 64: p. 1201-1213.
19. Crowninshield R, Pope MH, and Johnson RJ, An analytical model of the knee. J Biomech, 1976. 9: p. 397-405.
20. Piazza SJ and Delp SL, Three-dimensional dynamic simulation of total knee replacement motion during a step-up task. J Biomech Eng, 2001. 123(6): p. 599-606.

21. Chen E, et al., A computational model of postoperative knee kinematics. Med Image Anal, 2001. 5(4): p. 317-30.
22. Dowson D, Gillis BJ, and Atkinson JR, Penetration of metallic femoral components into polymetric tibial components observed in a knee joint simulator. Am Chem Soc Symp Ser, 1985. 287: p. 215-228.
23. Walker PS, et al., A knee simulating machine for the performance evaluation of total knee replacements. J Biomech, 1997. 30(1): p. 83-89.
24. Bourne RB, Goodfellow JW, and O'Connor J, A functional analysis of various knee arthroplasties. Trans Orthop Res Soc, 1978. 24: p. 160.
25. Harris ML, et al., An Improved method for measuring tibiofemoral contact areas in total knee arthroplasty: a comparison of K-scan sensor and Fuji film. Journal of Biomechanics, 1999. 32: p. 951-958.
26. Gendle M, Holt N, and Mitchell A, The Human Knee. 1989, University of Southampton: Southampton.
27. Rigby BJ, Hirai N, and Spikes JD, The mechanical properties of rat tail tendon. Gen Physiol, 1959. 43: p. 265-289.
28. Viidik A, Functional properties of collagenous tissues. Int Rev Connect Tissue Res, 1973. 6: p. 127.
29. Diamant J, et al., Collagen: Ultrastructure and its relation to Mechanical Properties as a function of ageing. Proc R Soc Lond [Biol], 1972. 180B: p. 293-315.
30. Ham AW and Cormack DH, Histology. 8th ed. 1979, Philadelphia, J.B.: Lippincott.
31. Bailey AJ. Comprehensive Biochemistry. 1968. Amsterdam: Elsevier.
32. Mechanic GL, An Automated Scintillation counting system with high efficiency for continuous analysis: cross-links of [3H]NaBH4 reduced collagen. Anal Biochem, 1974. 61: p. 349-354.
33. Tanzer ML, Cross-linking of Collagen. Science, 1973. 180: p. 561-566.
34. Woo SL, et al., Effects of postmortem storage by freezing on ligament tensile behaviour. J Biomech, 1986. 19(5): p. 399-404.
35. Mow van C and Hayes WC, Basic Orthopaedic Biomechanics. 1991: Raven Press.
36. Bratigan OC and Voshell AF, The mechanics of the ligaments and menisci of the knee joint. J. Bone Jnt. Surg., 1941. 23: p. 44-66.
37. Piziali RL, et al., The function of the Primary ligaments of the Knee in Anterior-Posterior and Medial-Lateral motions. J Biomech, 1980. 13: p. 777-784.
38. Warren FL, Marshall JL, and Girgis F, The Prime Static Stabilizer of the medial side of the knee. J Bone Jnt. Surg, 1974. 56A: p. 665-674.
39. Jasty M, Lew WD, and Lewis JL. In vitro ligament forces in the normal knee using buckle transducers. in Transactions of the 28th Annual meeting of the Orthopaedic Research Society. 1982.
40. Hull ML, et al., Strain in the medial collateral ligament of the human knee under single and combined loads. J Biomech, 1995. 29: p. 199-206.
41. Hirokawa S, et al., Muscular co-contraction and control of knee stability. Journal of Electromyography and Kinesiology, 1991. 1: p. 199-208.
42. Harfe DT, et al., Elongation patterns of the collateral ligaments of the knee. Clinical Biomechanics, 1998. 13(3): p. 163-175.
43. Wrobe RR, et al., The role of the lateral extraarticular restraints in the anterior cruciate ligament-deficient knee. Am J Sports Med, 1993. 21: p. 257-263.

44. Markolf KL, Mensch JS, and Amstutz HC, Stiffness and Laxity of the Knee - the Contributions of the Supporting Structures. J. Bone Jnt. Surg., 1976. 58A: p. 583-593.
45. Shoemaker SC and Markolf KL, Effects of Joint load on the stiffness and laxity of ligament-deficient knees; and in vitro study of the anterior cruciate and medial collateral ligaments. J Bone Jnt. Surg, 1985. 67A: p. 136-146.
46. Noyes FR, et al. Diagnosis of Knee Ligament Injuries. in AAOS Annual Meeting. 1978. Dallas, Texas.
47. Attfield SF, et al., Soft-Tissue Balance and Recovery of Proprioception after Total Knee Replacement. J. Bone Jt Surg., 1996. 78B: p. 540-545.
48. Blankevoort L, Huiskes R, and d.L. A, Recruitment of Knee joint ligaments. J Biomech Eng, 1991. 113: p. 94-103.
49. Matyas JR, et al., Stress Governs tissue phenotype as the femoral insertion of the rabbit MCL [see comments]. J Biomech, 1995. 28(2): p. 147-57.
50. Woo SL, et al., Biomechanics of Knee Ligaments. Am J Sports Med, 1999. 27(4): p. 533-543.
51. Woo SL, et al., Mechanical properties of tendon and ligaments. 1. Quasi-static nonlinear viscoelastic properties. Biorhealogy, 1982. 19: p. 385-396.
52. Arms S, et al., Strain measurement in the medial collateral ligament of the human knee: an autopsy study. J Biomech, 1983. 7: p. 491-496.
53. Fox RJ, et al., Determination of the in situ forces in the human posterior cruciate ligament using robotic technology - a cadaveric study. Am J Sports Med, 1998. 26: p. 395-401.
54. Lange A de, et al., The application of Roentgensteroegrammetry for evaluation of knee joint kinematics in vitro, in Biomechanics: Principles and applications, Huiskes R, Campen DH van, and Wijn JR de, Editors. 1982, Martinus Nijhoff: The Hague/Boston/London. p. 177-184.
55. Noyes FR and Grood ES, The strength of the anterior cruciate ligament. Age and species-related changes. J. Bone Jt Surg, 1976. 58A: p. 1074-1082.
56. Woo SL, et al., Tensile properties of the human femur-anterior cruciate ligament-tibia complex. Am J Sports Med, 1991. 19: p. 217-224.
57. Trent PS, Walker PS, and Wolf B, Ligament length patterns, strength and rotational axes of the knee joint. Clin Orthop, 1976. 117: p. 263-270.
58. Momersteeg TJA, et al., The effect of variable relative insertion orientation of human knee bone-ligament-bone complexes on the tensile stiffness. J Biomech, 1995. 28(6): p. 745-752.
59. Brage ME, et al., Knee laxity in symptomatic osteoarthritis. Clin Orthop, 1994. 18: p. 184-9.
60. Wada M, et al., Knee laxity in patients with osteoarthritis and rheumatoid arthritis. Br J Rheumatol, 1996. 35: p. 560-3.
61. Tasker T and Waugh W, Articular changes associated with Internal Derangement of the Knee. J. Bone Jnt. Surg., 1982. 64: p. 486-488.
62. Turek SL, Orthopaedics. 1984, London: J.B. Lippincott Co.
63. Piazza SJ and Cavanagh PR, Measurement of the Screw-home motion of the Knee is sensitive to errors in axis Alignment. J Biomech, 2000. 33(8): p. 1029-1034.
64. Kettelkamp DB, et al., An Electrogoniometric study of Knee motion in Normal Gait. J. Bone Jnt. Surg., 1970. 52A: p. 775-790.
65. Lafortune MA, et al., Three-dimensional Kinematics of the Human Knee during Walking. J. Biomech, 1992. 25: p. 347-357.

66. Koh TJ, Grabiner MD, and De Swart RJ, In vivo Tracking of the Human Patella. J. Biomech, 1992. 25: p. 637-643.
67. Levens AS, Inman VT, and Blosser JA, Transverse Rotations of the Segments of the Lower Extremity in Locomotion. J. Bone Jnt. Surg., 1948(30A): p. 859-872.
68. Li XM, et al., Normal six-degree-of-freedom motions of Knee Joint during level Walking. J. Biomech. Eng., 1996. 118: p. 258-261.
69. Shiavi R, et al., Motion analysis of the Knee - II. Kinematics of uninjured and Injured Knees during Walking and Pivoting. J. Biomech., 1987. 20: p. 653-665.
70. Johnson F, Leitl S, and Waugh W, The Distribution of Load across the Knee; A Comparison of Static and Dynamic Measurements. J. Bone Jt Surg., 1980. 62B: p. 346-349.
71. Goldberg VM, Figgie MP, and F.H. III, The results of revision total knee arthroplasty. Clin Orthop. 1988. 266: p. 86-92.
72. Moreland JR, Mechanisms of failure in total knee arthroplasty. Clin Orthop, 1988. 266: p. 49-64.
73. Cameron HU and Hunter GA, Failure in Total Knee Arthroplasty: Mechanisms, Revisions, and Results. Clinical Orthopaedics and Related Research, 1982. 170: p. 141-146.
74. Friedman RJ, Hirst P, and Poss R, Results of revision total knee arthroplasty performed for aseptic loosening. Clin Orthop, 1990. 255: p. 235-241.
75. Insall JN, Surgical Technique and soft tissue release principles + Total knee replacement. Surgery of the Knee. 1984, New York: Churchill Livingstone.
76. Tew M and Waugh W, Tibiofemoral alignment and results of knee replacement. J. Bone Jnt. Surg., 1985. 67B: p. 551-556.
77. Ritter MA, Faris PM, and Keating EM, Postoperative alignment of total knee replacement: Its effect on survival. Clin Orthop, 1994. 299: p. 153-156.
78. Fehring TK and Valadine AL, Knee instability after total knee arthroplasty. Clin Orthop, 1994. 299: p. 157-162.
79. Morrison JB, The mechanics of the knee in relation to normal walking. J Biomech, 1970. 3: p. 51-61.
80. Nagamine R, White A, and McCarthy DS, Effects of rotation malposition of the femoral component on knee stability linematics after total knee arthroplasty. J Arthroplasty, 1995. 10: p. 265-270.
81. Bargren JH, Total Knee Dislocation due to Rotary Malalignment of Tibial Component. Clin Orthop, 1980. 147: p. 271-274.
82. Lecuire F and Jaffar-Bandjee Z, Posterior luxation of the tibia on total knee prosthesis: apropos of 6 cases. Rev Chir Orthop Reparatrice Appar Mot, 1994. 80(6): p. 525-31.
83. Wasielewski RC, et al., Wear patterns on retrieved polyethylene tibial inserts and there relationship to technical considerations during total knee arthroplasty. Clin. Orthop., 1994. 299: p. 31-43.
84. Coull R, Bankes MJK, and Rossouw DJ, Evaluation of tibial component angles in 79 consecutive total knee arthroplasties. The Knee, 1999. 6: p. 235-237.
85. Knutson K, et al., The Swedish Knee Arthroplasty Register: A nation-wide study of 30,003 knees 1976-1992. Acta Orthopaedica Scandinavica, 1994. 65(4): p. 375-386.
86. Reilly DT. Varus Knee Management Techniques. in State of the Art Update in Orthopaedics 2000. 2000. Whistler, BC.

87. Sambatakakis A, Wilton TJ, and Newton G, Radiographic Sign of Persistant Soft-Tissue Imbalance After Knee Replacement. J bone Jnt. Surg, 1991. 73B: p. 751-756.
88. Hsu HP, et al., Effect of knee component alignment on tibial load distribution with clinical correlation. Clin. Orthop., 1989. 248: p. 135-144.
89. Takahashi T, Wada Y, and Yamamoto H, Soft Tissue Balancing with Pressure Distribution During Total Knee Arthroplasty. J. Bone Jnt. Surg., 1997. 79B: p. 235-239.
90. Colizza WA, Insall JN, and Scuderi GR, The posterior stabilised total knee prosthesis: assessment of polyethylene damage and osteolysis after a ten-year-minimum follow-up. J Bone Jnt. Surg, 1995. 77-A: p. 1713-1720.
91. Callaghan JJ, et al., Mobile-Bearing Knee Replacement: Concepts and Results [Instructional Course Lecture]. J Bone Jnt. Surg, 2001. 82(7): p. 1020-1052.
92. Bert JM, Dislocation/subluxation of meniscal bearing elements after New Jersey Low Contact Stress knee arthroplasty. Clin Orthop, 1990. 254: p. 211-215.
93. Delp SL, Kocmond JH, and Stern SH, Tradeoffs between Motion and Stability in Posterior Substituting Knee Arthroplasty Design. J. Biomechanics, 1995. 28(10): p. 1155-1166.
94. Cloutier JM, Results of total knee arthroplasty with a non-constrained prosthesis. J Bone Jnt. Surg, 1983. 65A: p. 906-919.
95. Ewald FC, Jacobs MA, and Miegel RE et al., Kinematic total knee replacement. J Bone Jnt. Surg, 1984. 66A: p. 1032-1040.
96. Insall JN, et al., The total condylar knee prosthesis in gonarthritis. J Bone Jnt. Surg, 1983. 65A: p. 619-628.
97. Freeman MAR, Knee flexion: the cruciate ligaments and posterior stability in the flexed knee. Total arthroplasty of the knee, ed. Rand JA and Dorr LD. 1987, Aspen: Rockville. 13.
98. Stiehl JB, et al., Fluoroscopic Analysis of Kinematics after Posterior-Cruciate-Retaining Arthroplasty. J. Bone Jnt. Surg., 1995. 77-B(6): p. 884-889.
99. Dorr LD, et al., Functional comparison of posterior cruciate-retaining versus cruciate-sacrificed total knee arthroplasty. Clin Orthop, 1988. 236: p. 36-43.
100. Oliver JH and Coughlin LP, Objective knee evaluation using the Genucom knee analysis system. Am J Sports Med, 1987. 15: p. 571-8.
101. Mills OS and Hull ML, Rotational Flexibility of the human knee due to Varus/valgus and axial moments in vivo. J Biomech, 1991. 24(8): p. 673-690.
102. Mitts K, et al., Instability After Total knee arthroplasty with the Miller-Gallante II Total Knee: 5- to 7- Year follow-up. J Arthroplasty, 2001. 16(4): p. 422-427.
103. Saeki K, et al., Stability after medial collateral ligament release in total knee arthroplasty. Clin Orthop, 2001. 392: p. 184-189.
104. Whiteside LA and Amador DD, Rotational stability of a posterior stabilised total knee arthroplasty. Clin Orthop, 1989. 242: p. 241-246.
105. Whiteside LA, Kasselt MR, and Hayes DW, Varus-valgus and rotational stability in rotationally unconstrained total knee arthroplasty. Clin Orthop, 1987. 219: p. 147-157.
106. Matsuda S, et al., Knee stability in posterior cruciate ligament retaining total knee arthroplasty. Clin Orthop, 1999. 366: p. 169-173.
107. Yamakado K, et al., Influence of stability on range of motion after cruciate-retaining TKA. Arch Orthop Traumat Surg, 2002.
108. Cooper DE, Tests for posterolateral instability of the knee in normal subjects. Results of examination under anesthesia. J Bone Jnt. Surg, 1991. 73(1): p. 30-36.

109. Gollehon DL, Torzilli PA, and W. FL, The role of the posterolateral and cruciate ligaments in the stability of the human knee. A biomechanical study. J Bone Jnt. Surg, 1987. 69A: p. 232-242.
110. Grood ES, Stowers SF, and N. FR, Limits of movement in the human knee. Effect of sectioning the posterior cruciate ligament and posterolateral structures. J Bone Jnt. Surg, 1988. 70A: p. 88-97.
111. Komistek RD, et al. In vivo kinematics of PS implanted knees during gait. in 11th conference of the ESB. 1998. Toulouse, France.
112. Godest AC, et al., A computational model for the prediction of total knee replacement kinematics in the sagittal plane. Journal of Biomechanics, 2000. 33: p. 435-442.
113. Sathasivam S and Walker PS, A computer model with surface friction for the prediction of total knee kinematics. Journal of Biomechanics, 1997. 30(2): p. 177-184.
114. Morrison JB, Function of the knee joint in various activities. Bio-medical Engineering, 1969. 4: p. 537-580.
115. Markolf KL, Kochan A, and Amstutz HC, Measurement of knee stiffness and laxity in patients with documented absence of the posterior cruciate ligament. J Bone Jnt. Surg, 1984. 66A: p. 242-253.
116. Szivek JA, Cutignola L, and Volz RG, Tibiofemoral contact stress and stress distribution during total knee arthroplasty. J Arthroplasty, 1995. 10(4): p. 480-491.
117. Ateshian GA, et al., A stereophotogrammetric method for determining in situ contact areas in diarthrodial joints, and a comparison with other methods. Journal of Biomechanics, 1994. 2(1): p. 111-124.
118. Limbert G, Finite Element Modelling of Biological Connective Soft Tissues Application to the Ligaments of the Human Knee, in Bioengineering Sciences Research Group. 2001, University of Southampton: Southampton. p. 181.
119. Sathasivam S and Walker PS, Computer model to predict subsurface damage in tibial inserts of total knees. Journal of Orthopaedic Research, 1998. 16: p. 564-571.
120. Estupinan JA, Bartel DL, and Wright TM, Residual stresses in ultra-high molecular weight polyethylene loaded cyclically by a rigid moving indentor in nonconforming geometries. Journal of Orthopaedic Research, 1998. 16: p. 80-88.
121. Romero J, et al., Varus and Valgus flexion laxity of total knee alignment methods in loaded cadaveric knees. Clin Orthop, 2002. 394: p. 243-253.
122. Edwards E, Miller J, and Chan K-H, The effect of postoperative collateral ligament Laxity in total knee arthroplasty. Clin Orthop, 1988. 236: p. 44-51.
123. Insall JN, Presidential address to The Knee Society. Choices and compromises in total knee arthroplasty. Clin Orthop, 1988. 226: p. 43-48.
124. Mahoney OM, et al., Posterior Cruciate Function Following Total Knee Arthroplasty: A Biomechanical Study. J Arthroplasty, 1994. 9(6): p. 569-577.
125. Misra AN, et al., Role of the posterior cruciate ligament in total knee replacement. J Bone Jnt. Surg, 2003. 85-B: p. 389-392.
126. Pereira DS, Jaffe FF, and Ortiguera C, Posterior Cruciate-sparing Versus Posterior Cruciate-sacrificing Arthroplasty: Functional Results Using the Same Prosthesis. J Arthroplasty, 1998. 13(2): p. 138-143.
127. Colsman CS, et al., Tibiofemoral contact stress after total arthroplasty. Acta Orthopaedica Scandinavica, 2002. 73(6): p. 638-646.

128. Liau J-J, et al., The Effect of malalignment on stresses in polyethylene component of total knee prosthesis - a finite element analysis. Clinical Biomechanics, 2002. 17(2): p. 140-146.
129. Sathasivam S and Walker PS, The Conflicting requirements of laxity and conformity in total knee replacement. journal of biomechanics, 1999. 32: p. 239-247.
130. Rose RM and Goldfarb HV, On the pressure dependence of the wear of UHMWPE. Wear, 1983. 92: p. 99-111.
131. Wang A, Stark C, and Dumbleton JH, Mechanism and morphological origins of ultra-high molecular weight polyethylene wear debris in total joint replacement prostheses. Proc Instn Mech Engrs, 1996. 210: p. 141-155.
132. Kawanabe K, et al., Effects of A-P translation and rotation on the wear of UHMWPE in a total knee joint simulator. J Biomed Mater Res, 2001. 54: p. 400-406.
133. Rose RM, et al., On the true wear rate of ultrahigh molecular weight polyethylene in the total knee prosthesis. J Biomed Mater Res, 1984. 18: p. 207-224.
134. Treharne RW, Young RW, and Young SR, Wear of artificial joint materials. III. Simulation of the knee joint using a computer controlled system. j Eng Med, 1981. 10: p. 137-142.
135. Blunn GW, et al., The Dominance of Cyclic Sliding in Producing Wear in Total Knee Replacements. Clin Orthop, 1991. 273: p. 253-260.
136. Bartlet DL, et al., The effect of conformity and plastic thickness on contact stresses in metal-backed plastic implants. J Biomed Engng, 1985. 107: p. 193-199.
137. Walker PS and Hsieh HH, Comformity in condylar replacement knee prosthesis. J Bone Jnt. Surg, 1977. 59B: p. 222-228.
138. Collier JP, et al., Analysis of the failure of 122 polyethylene inserts from uncemented tibial knee components. Clin Orthop, 1991. 273: p. 232-242.
139. Bell RS, et al., A study of implant failure in the Wagner Resurfacing Arthroplasty. J Bone Jnt. Surg, 1985. 67-A: p. 1165-1175.
140. Bartel DL, et al., The Effect of Conformity, Thickness, and Material on Stresses in Ultra-High Molecular weight Components for Total Joint Replacement. J Bone Jnt. Surg, 1986. 68-A(7): p. 1041-1051.
141. Ombregt L, Bisschop L, terr Verr HJ, Van de Velde T, A System of Orthopaedic Medicine, 1995: p. 770-771.
142. Gray H, Anatomy of the Human Body. Philadelphia: Lea & Febiger, 1918; Bartleby.com, 2000

Appendix 1 – Experimental Passive Stability Testing Results

				Tibial Displacement (mm)		
PCL	**MCL**	**LCL**	**Flexion Angle (°)**	**Anterior**	**Posterior**	**Total**
No PCL	Normal	Normal	0	2.1(0.1)	2.5(0.2)	**4.6(0.2)**
	Normal	Normal	30	3.6(0.7)	3.8(0.8)	**7.4(1.1)**
	Normal	Normal	60	3.0(0.0)	4.1(0.2)	**7.1(0.2)**
	Normal	Normal	90	3.9(0.1)	7.1(1.5)	**11.0(1.5)**
	Tight	Tight	0	1.8(0.4)	2.0(0.0)	**3.8(0.4)**
	Normal	Tight	0	1.9(0.1)	2.3(0.2)	**4.2(0.2)**
	Tight	Normal	0	1.8(0.4)	2.1(0.1)	**3.9(0.4)**
	Slack	Normal	0	2.7(0.2)	2.6(0.3)	**5.3(0.4)**
	Normal	Slack	0	2.6(0.0)	2.7(0.3)	**5.3(0.3)**
	Slack	Slack	0	3.0(0.1)	2.9(0.1)	**5.9(0.1)**
	Tight	Tight	90	3.1(0.1)	5.0(0.1)	**8.1(0.1)**
	Normal	Tight	90	4.0(0.1)	4.9(0.2)	**8.9(0.2)**
	Tight	Normal	90	3.9(0.7)	5.1(0.4)	**9.0(0.8)**
	Slack	Normal	90	6.1(0.5)	8.1(0.0)	**14.2(0.5)**
	Normal	Slack	90	5.1(0.1)	7.8(0.9)	**12.9(0.9)**
	Slack	Slack	90	6.7(1.1)	9.3(0.4)	**16.0(1.2)**
Normal PCL	Normal	Normal	0	1.8(0.1)	2.2(0.1)	**4.0(0.1)**
	Normal	Normal	30	2.8(0.1)	2.5(0.0)	**5.3(0.1)**
	Normal	Normal	60	3.0(0.0)	3.7(0.4)	**6.7(0.4)**
	Normal	Normal	90	3.8(0.2)	5.4(0.2)	**9.2(0.3)**
	Tight	Tight	0	1.7(0.0)	1.9(0.2)	**3.6(0.2)**
	Normal	Tight	0	1.8(0.1)	2.0(0.0)	**3.8(0.1)**
	Tight	Normal	0	1.7(0.2)	2.0(0.1)	**3.7(0.2)**
	Slack	Normal	0	2.4(0.2)	2.6(0.0)	**5.0(0.2)**
	Normal	Slack	0	2.4(0.0)	2.6(0.2)	**5.0(0.2)**
	Slack	Slack	0	2.6(0.1)	2.8(0.1)	**5.4(0.1)**
	Tight	Tight	90	3.6(0.1)	4.0(0.3)	**7.7(0.3)**
	Normal	Tight	90	3.7(0.2)	4.5(0.2)	**8.7(0.3)**
	Tight	Normal	90	3.6(0.3)	4.5(0.2)	**8.6(0.4)**
	Slack	Normal	90	3.9(0.6)	7.2(0.1)	**11.1(0.6)**
	Normal	Slack	90	3.8(0.9)	6.6(0.2)	**10.4(0.9)**
	Slack	Slack	90	4.1(0.3)	7.9(0.8)	**12.0(0.9)**

Table 1 A-P stability results of the PC-RR in the neutral alignment position. Displacements refer to the tibial component with respect to the femoral component (± Standard deviations).

				Displacements (mm)		
Alignment	**MCL**	**LCL**	**Flexion Angle (°)**	**Anterior**	**Posterior**	**Total**
Valgus	Slack	Slack	0	3.1(0.3)	3.5(0.2)	**6.6(0.4)**
	Normal	Normal	0	2.8(0.6)	3.1(0.4)	**5.9(0.7)**
	Tight	Tight	0	2.0(0.3)	2.4(0.7)	**4.4(0.8)**
	Slack	Normal	0	3.3(0.2)	3.4(0.5)	**6.7(0.5)**
	Normal	Slack	0	3.1(0.6)	3.7(0.2)	**6.8(0.6)**
	Tight	Slack	0	2.8(0.1)	3.2(0.3)	**6.0(0.3)**
	Slack	Tight	0	2.9(0.0)	2.9(0.4)	**5.8(0.4)**
	Tight	Normal	0	2.2(0.3)	2.4(0.5)	**4.6(0.6)**
	Normal	Tight	0	2.4(0.1)	2.5(0.2)	**4.9(0.2)**
	Slack	Slack	90	4.8(0.2)	5.9(0.2)	**10.7(0.3)**
	Normal	Normal	90	4.3(0.2)	5.2(0.1)	**9.5(0.2)**
	Tight	Tight	90	3.6(0.4)	3.9(0.4)	**7.5(0.6)**
	Slack	Normal	90	4.6(0.2)	6.0(0.5)	**10.6(0.5)**
	Normal	Slack	90	4.7(0.3)	5.6(0.1)	**10.3(0.3)**
	Tight	Slack	90	4.1(0.3)	5.4(0.1)	**9.5(0.3)**
	Slack	Tight	90	4.3(0.1)	5.2(0.3)	**9.5(0.3)**
	Tight	Normal	90	3.9(0.4)	4.8(0.7)	**8.7(0.8)**
	Normal	Tight	90	3.4(0.1)	4.9(0.3)	**8.3(0.3)**
Varus	Slack	Slack	0	2.4(0.3)	3.2(0.5)	**5.6(0.6)**
	Normal	Normal	0	1.3(0.3)	2.0(0.4)	**3.3(0.5)**
	Tight	Tight	0	1.3(0.1)	1.7(0.3)	**3.0(0.3)**
	Slack	Normal	0	1.8(0.3)	2.4(0.2)	**4.2(0.4)**
	Normal	Slack	0	1.6(0.6)	2.6(0.2)	**4.2(0.6)**
	Tight	Slack	0	1.6(0.4)	2.0(0.3)	**3.6(0.5)**
	Slack	Tight	0	1.7(0.3)	1.9(0.1)	**3.6(0.3)**
	Tight	Normal	0	1.4(0.4)	2.0(0.2)	**3.4(0.4)**
	Normal	Tight	0	1.5(0.5)	1.9(0.3)	**3.4(0.6)**
	Slack	Slack	90	4.0(0.3)	6.7(0.6)	**10.7(0.6)**
	Normal	Normal	90	4.3(0.4)	4.4(0.2)	**8.7(0.4)**
	Tight	Tight	90	3.5(0.1)	4.0(0.2)	**7.5(0.2)**
	Slack	Normal	90	4.1(0.1)	5.8(0.4)	**9.9(0.4)**
	Normal	Slack	90	4.2(0.2)	5.9(0.3)	**10.1(0.4)**
	Tight	Slack	90	3.8(0.5)	5.7(0.1)	**9.5(0.5)**
	Slack	Tight	90	3.9(0.3)	6.0(0.2)	**9.9(0.4)**
	Tight	Normal	90	3.7(0.3)	4.9(0.2)	**8.6(0.4)**
	Normal	Tight	90	3.8(0.1)	5.0(0.1)	**8.8(0.1)**

Table 2 A-P stability results of the PC-RR in the malaligned position. Displacements refer to the tibial component with respect to the femoral component (± Standard deviations).

				Femoral Rotations (°)			Tibial Rotations (°)		
PCL	**MCL**	**LCL**	**Flexion Angle (°)**	**Internal**	**External**	**Total**	**Internal**	**External**	**Total**
No PCL	Normal	Normal	0	26.6(0.9)	27.5(1.4)	**54.1(1.7)**	25.9(1.1)	27(1.2)	**52.9(1.7)**
	Normal	Normal	15	26.9(1.2)	27.1(0.9)	**54.0(1.5)**	26.4(0.8)	26.7(1.3)	**53.1(1.7)**
	Normal	Normal	60	27.1(2.1)	26.1(2.1)	**54.2(3.0)**	25.1(1.7)	24.9(1.8)	**50.0(2.5)**
	Normal	Normal	90	27.9(1.1)	26.8(1.3)	**55.7(1.7)**	22.8(1.1)	20.5(1.1)	**43.3(1.6)**
	Tight	Tight	15	25.5(1.3)	26.3(2.1)	**51.8(2.5)**	25.2(1.2)	25.9(2.0)	**51.1(2.5)**
	Normal	Tight	15	26.2(2.3)	26.4(2.1)	**52.6(3.1)**	25.4(1.9)	25.3(1.8)	**50.7(2.6)**
	Tight	Normal	15	26.0(1.7)	26.4(1.1)	**52.4(2.0)**	25.2(1.8)	25.1(1.2)	**50.3(1.9)**
	Slack	Normal	15	28.9(2.5)	28.9(0.9)	**57.8(2.7)**	27.1(2.1)	27.3(0.6)	**54.4(1.3)**
	Normal	Slack	15	29.1(2.3)	28.9(2.3)	**58.0(3.3)**	28.2(1.9)	27.3(2.0)	**55.5(2.8)**
	Slack	Slack	15	30.5(2.3)	30.9(1.3)	**61.4(2.6)**	27.6(2.1)	27.9(2.2)	**55.5(3.1)**
	Tight	Tight	90	26.1(1.4)	25.4(2.7)	**51.5(3.0)**	20.4(1.1)	21.2(2.1)	**41.6(2.6)**
	Normal	Tight	90	26.6(2.1)	25.9(1.8)	**52.5(2.8)**	21.7(1.4)	21.6(1.3)	**43.3(1.9)**
	Tight	Normal	90	26.4(1.1)	25.9(1.1)	**52.3(1.6)**	20.9(0.8)	21.6(1.1)	**42.5(1.4)**
	Slack	Normal	90	29.1(1.7)	27.1(1.9)	**56.2(2.5)**	23.3(1.5)	20.4(1.6)	**43.7(2.2)**
	Normal	Slack	90	28.9(2.2)	28.8(2.3)	**57.7(3.2)**	24.8(1.9)	20.8(2.1)	**45.6(2.9)**
	Slack	Slack	90	30.1(2.2)	30.4(0.9)	**60.5(2.4)**	24.6(1.9)	21.8(0.9)	**46.4(1.6)**
Normal PCL	Normal	Normal	0	24.9(1.2)	25.1(0.9)	**50.0(1.5)**	24.3(1.3)	24.6(0.9)	**48.9(1.4)**
	Normal	Normal	15	25.8(0.9)	25.6(1.1)	**51.4(1.4)**	23.8(0.7)	24.1(1.0)	**47.9(1.1)**
	Normal	Normal	60	25.9(2.0)	25.4(1.2)	**51.3(2.3)**	23.8(1.9)	23.3(1.1)	**47.1(1.8)**
	Normal	Normal	90	26.8(0.9)	25.9(1.6)	**52.6(1.8)**	20.3(0.9)	20.4(1.4)	**40.7(1.8)**
	Tight	Tight	15	24.3(1.3)	24.0(1.1)	**48.3(1.7)**	22.9(1.1)	22.1(0.6)	**45.0(1.0)**
	Normal	Tight	15	25.0(1.5)	24.6(0.9)	**49.6(1.7)**	23.2(1.2)	22.8(0.5)	**46.0(0.9)**
	Tight	Normal	15	24.9(0.8)	24.3(1.9)	**49.2(2.1)**	23.6(0.6)	23.2(1.5)	**46.8(1.8)**
	Slack	Normal	15	27.1(1.2)	27.0(0.4)	**54.1(1.3)**	24.9(1.2)	25.2(0.6)	**50.1(1.0)**
	Normal	Slack	15	27.2(1.2)	27.5(1.5)	**54.7(1.9)**	25.2(1.1)	25.6(1.4)	**50.8(1.9)**
	Slack	Slack	15	28.8(0.9)	28.3(1.7)	**57.1(1.9)**	25.1(0.6)	24.7(1.5)	**49.8(1.8)**
	Tight	Tight	90	24.6(1.1)	24.2(1.5)	**48.8(1.9)**	23.3(0.9)	21.8(1.3)	**45.1(1.7)**
	Normal	Tight	90	24.9(2.0)	24.9(1.1)	**49.8(2.3)**	23.6(1.6)	22.9(1.2)	**46.5(1.8)**
	Tight	Normal	90	25.2(0.9)	24.9(0.4)	**51.1(1.0)**	24.6(0.9)	22.9(0.5)	**47.5(0.8)**
	Slack	Normal	90	28.5(1.3)	27.2(0.8)	**55.7(1.5)**	22.8(1.1)	20.8(0.7)	**43.6(1.1)**
	Normal	Slack	90	28.3(1.2)	27.2(1.1)	**55.5(1.6)**	22.0(1.2)	19.2(0.8)	**41.2(1.3)**
	Slack	Slack	90	29.7(1.6)	28.5(0.7)	**58.2(1.7)**	21.1(1.5)	18.8(0.4)	**39.9(0.9)**

Table 3 I-E stability results of the PC-RR in the neutral alignment position. Rotations refer to the femoral component with respect to the tibial component (± Standard deviations).

				Femoral Rotations (°)			Tibial Rotations (°)		
Alignment	**MCL**	**LCL**	**Flexion Angle (°)**	**Internal**	**External**	**Total**	**Internal**	**External**	**Total**
Valgus	Slack	Slack	15	29.7(1.6)	28.5(1.1)	**58.2(1.9)**	28.2(1.3)	24.6(1.2)	**52.8(1.8)**
	Normal	Normal	15	28.1(1.2)	28.1(1.2)	**56.2(1.7)**	27.3(1.2)	26.3(0.9)	**53.6(1.5)**
	Tight	Tight	15	27.5(0.9)	27.1(1.3)	**54.6(1.6)**	26.1(1.1)	26.5(1.0)	**52.6(1.5)**
	Slack	Normal	15	30.3(1.5)	29.7(2.1)	**60.0(2.6)**	29.4(1.9)	28.9(1.2)	**58.3(2.2)**
	Normal	Slack	15	30.8(1.8)	31.3(2.1)	**62.1(2.8)**	29.8(2.0)	27.7(1.4)	**57.5(2.4)**
	Slack	Tight	15	29.5(1.2)	29.3(1.4)	**58.8(1.8)**	28.0(1.1)	25.2(0.9)	**53.2(1.4)**
	Tight	Slack	15	30.0(1.5)	30.8(1.8)	**60.8(2.3)**	30.3(1.8)	26.8(1.3)	**57.1(2.2)**
	Slack	Slack	90	33.7(2.1)	24.3(1.8)	**58.0(2.8)**	22.0(1.9)	25.0(1.7)	**47.0(2.5)**
	Normal	Normal	90	31.7(2.1)	25.4(1.6)	**57.1(2.6)**	20.6(1.2)	25.6(1.9)	**46.2(2.2)**
	Tight	Tight	90	30.0(1.6)	24.1(1.4)	**54.1(2.1)**	24.7(1.3)	26.1(1.3)	**50.8(1.8)**
	Slack	Normal	90	33.0(1.1)	25.0(1.9)	**58.0(2.2)**	20.6(1.5)	24.9(0.9)	**45.5(1.7)**
	Normal	Slack	90	32.4(2.1)	25.0(2.2)	**57.4(3.0)**	22.9(2.1)	25.7(1.9)	**48.6(2.8)**
	Slack	Tight	90	31.0(1.9)	26.7(2.3)	**57.7(3.0)**	22.3(2.1)	24.9(1.6)	**47.2(2.6)**
	Tight	Slack	90	33.3(2.5)	25.4(2.1)	**58.7(3.3)**	20.6(1.7)	26.4(2.1)	**47.0(2.7)**
Varus	Slack	Slack	15	29.4(2.4)	28.1(1.5)	**57.5(2.8)**	27.3(2.1)	26.9(1.6)	**54.2(2.6)**
	Normal	Normal	15	28.6(1.3)	27.1(2.1)	**55.7(2.5)**	27.3(1.1)	26.6(1.8)	**53.9(2.1)**
	Tight	Tight	15	26.8(2.1)	26.0(1.6)	**52.8(2.6)**	22.7(2.0)	25.2(1.4)	**47.9(2.4)**
	Slack	Normal	15	31.1(1.4)	28.6(2.1)	**59.7(2.5)**	30.3(1.1)	28.0(1.9)	**58.3(2.2)**
	Normal	Slack	15	30.9(1.8)	29.1(2.3)	**60.0(2.9)**	27.0(1.6)	25.2(2.1)	**52.2(2.6)**
	Slack	Tight	15	31.6(1.9)	29.1(1.7)	**60.7(2.5)**	29.9(1.5)	24.8(1.7)	**54.7(2.3)**
	Tight	Slack	15	29.4(2.3)	29.8(1.6)	**59.2(2.8)**	26.1(2.1)	25.9(1.6)	**52.0(2.6)**
	Slack	Slack	90	25.1(2.3)	30.0(2.4)	**55.1(3.3)**	23.9(2.2)	21.2(2.1)	**45.1(3.0)**
	Normal	Normal	90	24.5(1.8)	28.7(0.9)	**53.2(2.0)**	23.4(1.0)	20.9(1.6)	**44.3(1.9)**
	Tight	Tight	90	25.1(1.4)	27.2(2.2)	**52.3(2.6)**	21.4(2.0)	19.1(1.3)	**40.5(2.4)**
	Slack	Normal	90	26.3(2.3)	30.3(2.7)	**56.6(3.5)**	24.6(2.5)	22.7(2.3)	**47.3(3.4)**
	Normal	Slack	90	27.4(2.4)	29.7(1.5)	**57.1(2.8)**	23.5(1.5)	20.7(2.0)	**44.2(2.5)**
	Slack	Tight	90	25.9(2.3)	30.8(2.1)	**56.7(3.1)**	26.1(1.6)	23.2(1.9)	**49.3(2.5)**
	Tight	Slack	90	27.1(2.1)	28.9(1.8)	**56.0(2.8)**	26.9(1.8)	24.5(1.8)	**51.4(2.5)**

Table 4 I-E stability results of the PC-RR in the malaligned position. Rotations refer to the femoral component with respect to the tibial component (± Standard deviations).

				Final Rotation (°)		
Alignment	**PCL**	**MCL**	**LCL**	**Varus**	**Valgus**	**Total**
Valgus	**No PCL**	Normal	Normal	5.9(0.4)	0.9(0.1)	**6.8(0.4)**
		Normal	Slack	6.5(0.6)	1.0(0.3)	**7.5(0.7)**
		Slack	Normal	5.9(0.5)	2.4(0.3)	**8.3(0.6)**
		Slack	Slack	* 6.4(0.4)	2.1(0.2)	**8.5(0.4)**
		Slack	Tight	5.0(0.2)	3.2(0.3)	**8.2(0.4)**
		Tight	Slack	* 8.1(0.6)	0.2(0.0)	**8.3(0.6)**
		Tight	Tight	5.0(0.4)	0.6(0.1)	**5.6(0.4)**
		Tight	Normal	5.9(0.5)	0.4(0.1)	**6.3(0.5)**
		Normal	Tight	5.2(0.6)	1.2(0.3)	**6.4(0.7)**
	Normal PCL	Slack	Slack	5.9(0.5)	2.0(0.4)	**7.9(0.6)**
Varus	**No PCL**	Normal	Normal	5.9(0.6)	0.1(0.0)	**6.0(0.6)**
		Normal	Slack	5.9(0.4)	0.1(0.1)	**6.0(0.4)**
		Slack	Normal	4.6(0.2)	1.2(0.2)	**5.8(0.3)**
		Slack	Slack	5.4(0.3)	0.7(0.2)	**6.1(0.4)**
		Slack	Tight	5.0(0.1)	1.6(0.2)	**6.6(0.2)**
		Tight	Slack	* 6.9(0.4)	0.0(0.0)	**6.9(0.4)**
		Tight	Tight	5.4(0.6)	0.1(0.0)	**5.5(0.6)**
		Tight	Normal	5.4(0.3)	0.0(0.0)	**5.4(0.3)**
		Normal	Tight	4.4(0.2)	0.4(0.1)	**4.8(0.2)**
	Normal PCL	Slack	Slack	5.0(0.4)	0.7(0.2)	**5.7(0.4)**

Table 5 V-V stability results of the PC-RR in the neutral alignment position. Rotations refer to the tibial component with respect to the femoral component (± Standard deviations). * indicates where the M-L limit was tripped

			Rotation (°)		
PCL	**MCL**	**LCL**	**Varus**	**Valgus**	**Total**
No PCL	Normal	Normal	4.3(0.2)	0.7(0.2)	**5.0(0.3)**
	Normal	Slack	4.5(0.4)	1.0(0.2)	**5.5(0.4)**
	Slack	Normal	4.4(0.6)	1.5(0.1)	**5.9(0.6)**
	Slack	Slack	4.9(0.9)	1.4(0.1)	**6.3(0.9)**
	Normal	Tight	3.8(0.4)	0.5(0.2)	**4.3(0.4)**
	Tight	Normal	4.0(0.3)	0.4(0.1)	**4.4(0.5)**
	Tight	Tight	3.6(0.5)	0.2(0.0)	**3.8(0.5)**
Normal PCL	Slack	Slack	4.1(1.0)	1.2(0.7)	**5.3(0.9)**

Table 6 V-V stability results of the PC-RR in the malaligned position. Rotations refer to the tibial component with respect to the femoral component (± Standard deviations).

			Tibial Displacements (mm)		
MCL	**LCL**	**Flexion Angle (°)**	**Anterior**	**Posterior**	**Total**
Normal	Normal	0	1.7(0.1)	3.3(0.0)	**5.0(0.1)**
Normal	Normal	30	3.0(0.3)	2.9(0.4)	**5.9(0.5)**
Normal	Normal	60	3.0(0.2)	3.6(0.1)	**6.6(0.2)**
Normal	Normal	90	4.2(0.2)	1.6(0.5)	**5.8(0.5)**
Tight	Tight	0	1.5(0.2)	2.4(0.2)	**3.9(0.3)**
Normal	Tight	0	1.7(0.1)	2.8(0.1)	**4.5(0.1)**
Tight	Normal	0	1.5(0.2)	2.8(0.1)	**4.3(0.2)**
Slack	Normal	0	3.0(0.3)	2.7(0.1)	**5.7(0.3)**
Normal	Slack	0	2.8(0.2)	2.8(0.1)	**5.6(0.2)**
Slack	Slack	0	3.1(0.3)	3.2(0.1)	**6.3(0.3)**
Tight	Tight	90	3.4(0.2)	1.2(0.0)	**4.6(0.2)**
Normal	Tight	90	3.8(0.3)	1.4(0.3)	**5.2(0.4)**
Tight	Normal	90	3.7(0.1)	1.3(0.1)	**5.0(0.1)**
Slack	Normal	90	4.5(0.4)	1.6(0.2)	**6.1(0.5)**
Normal	Slack	90	4.5(0.2)	1.6(0.1)	**6.1(0.2)**
Slack	Slack	90	4.9(0.2)	1.8(0.3)	**6.7(0.5)**

Table 7 A-P stability results of the PC-SR in the neutral alignment position. Displacements refer to the tibial component with respect to the femoral component (± Standard deviations).

				Tibial Displacement (mm)		
Alignment	**MCL**	**LCL**	**Flexion Angle (°)**	**Anterior**	**Posterior**	**Total**
Valgus	Slack	Slack	0	2.9(0.3)	3.0(0.3)	**5.9(0.4)**
	Normal	Normal	0	2.0(0.1)	1.9(0.1)	**3.9(0.1)**
	Tight	Tight	0	1.5(0.2)	1.3(0.0)	**2.8(0.2)**
	Slack	Normal	0	1.9(0.2)	2.7(0.3)	**4.6(0.4)**
	Normal	Slack	0	3.3(0.3)	2.5(0.1)	**5.8(0.3)**
	Tight	Slack	0	2.1(0.3)	2.7(0.2)	**4.8(0.4)**
	Slack	Tight	0	1.8(0.1)	1.9(0.1)	**3.7(0.1)**
	Tight	Normal	0	1.8(0.1)	1.6(0.2)	**3.4(0.2)**
	Normal	Tight	0	1.6(0.2)	1.4(0.0)	**3.0(0.2)**
	Slack	Slack	90	4.3(0.5)	3.2(0.2)	**7.5(0.5)**
	Normal	Normal	90	3.5(0.3)	2.1(0.2)	**5.6(0.4)**
	Tight	Tight	90	3.0(0.2)	1.7(0.1)	**4.7(0.2)**
	Slack	Normal	90	4.2(0.4)	2.3(0.2)	**6.5(0.4)**
	Normal	Slack	90	3.9(0.3)	3.1(0.4)	**7.0(0.5)**
	Tight	Slack	90	4.0(0.4)	2.5(0.2)	**6.5(0.4)**
	Slack	Tight	90	4.5(0.2)	1.7(0.0)	**6.2(0.2)**
	Tight	Normal	90	3.6(0.2)	1.8(0.2)	**5.4(0.3)**
	Normal	Tight	90	3.4(0.4)	1.9(0.1)	**5.3(0.4)**
Varus	Slack	Slack	0	2.1(0.3)	2.5(0.1)	**4.6(0.3)**
	Normal	Normal	0	2.2(0.2)	2.3(0.2)	**4.5(0.3)**
	Tight	Tight	0	1.6(0.2)	1.8(0.1)	**3.4(0.2)**
	Slack	Normal	0	1.8(0.1)	2.8(0.3)	**4.6(0.3)**
	Normal	Slack	0	2.7(0.3)	2.1(0.2)	**4.8(0.4)**
	Tight	Slack	0	2.3(0.2)	2.0(0.1)	**4.3(0.2)**
	Slack	Tight	0	3.1(0.4)	3.2(0.3)	**6.3(0.5)**
	Tight	Normal	0	1.9(0.0)	2.0(0.3)	**3.9(0.3)**
	Normal	Tight	0	1.7(0.1)	2.2(0.1)	**3.9(0.1)**
	Slack	Slack	90	4.0(0.4)	3.0(0.2)	**7.0(0.4)**
	Normal	Normal	90	4.2(0.3)	2.3(0.2)	**6.5(0.4)**
	Tight	Tight	90	3.5(0.3)	1.9(0.0)	**5.4(0.3)**
	Slack	Normal	90	4.1(0.5)	3.1(0.2)	**7.2(0.5)**
	Normal	Slack	90	4.0(0.3)	3.0(0.3)	**7.0(0.4)**
	Tight	Slack	90	3.5(0.2)	2.7(0.2)	**6.2(0.3)**
	Slack	Tight	90	5.9(0.3)	2.6(0.4)	**8.5(0.5)**
	Tight	Normal	90	3.9(0.2)	2.2(0.3)	**6.1(0.4)**
	Normal	Tight	90	4.2(0.4)	2.3(0.3)	**6.5(0.5)**

Table 8 A-P stability results of the PC-SR in the malaligned position. Displacements refer to the tibial component with respect to the femoral component (± Standard deviations).

			Femoral Rotations (°)			Tibial Rotations (°)		
MCL	**LCL**	**Flexion Angle (°)**	**Internal**	**External**	**Total**	**Internal**	**External**	**Total**
Normal	Normal	0	26.5(3.0)	26.1(2.3)	**52.6(3.8)**	25.4(2.1)	25.0(2.1)	**50.4(3.0)**
Normal	Normal	15	28.5(2.8)	32.0(2.6)	**60.5(3.8)**	27.6(2.3)	31.0(1.9)	**58.6(3.0)**
Normal	Normal	60	26.6(2.3)	29.0(1.6)	**55.6(2.8)**	22.8(1.7)	25.5(1.3)	**48.3(2.1)**
Normal	Normal	90	29.5(1.3)	28.7(1.7)	**58.2(2.1)**	24.9(0.9)	24.0(1.7)	**48.9(1.9)**
Tight	Tight	15	27.1(1.8)	30.8(0.7)	**57.9(1.8)**	26.5(1.4)	30.4(0.6)	**56.9(1.5)**
Normal	Tight	15	27.2(0.8)	31.8(2.1)	**59.0(2.2)**	26.6(0.8)	30.9(2.0)	**57.5(2.2)**
Tight	Normal	15	27.1(0.6)	30.2(0.5)	**57.3(0.8)**	26.6(0.8)	29.3(0.4)	**55.9(0.9)**
Slack	Normal	15	30.7(1.6)	33.6(0.5)	**64.3(1.6)**	28.2(1.4)	31.5(0.5)	**59.7(1.5)**
Normal	Slack	15	30.6(0.8)	33.9(2.2)	**64.5(2.3)**	28.1(0.7)	31.2(2.1)	**59.3(2.2)**
Slack	Slack	15	32.1(2.5)	35.1(0.8)	**67.2(2.5)**	30.6(1.9)	33.2(1.0)	**63.8(2.1)**
Tight	Tight	90	27.5(1.0)	28.0(1.2)	**55.5(1.6)**	20.4(1.0)	23.2(1.0)	**43.6(1.4)**
Normal	Tight	90	27.9(2.2)	28.0(2.3)	**55.9(3.1)**	23.6(1.9)	22.6(2.1)	**46.2(2.8)**
Tight	Normal	90	27.8(1.3)	28.2(1.6)	**56.0(2.1)**	23.9(1.0)	23.2(1.5)	**47.1(1.8)**
Slack	Normal	90	31.1(1.2)	32.9(1.9)	**64.0(2.2)**	24.5(1.0)	27.0(1.5)	**51.5(1.8)**
Normal	Slack	90	31.0(2.3)	33.0(2.1)	**64.0(3.1)**	23.7(2.1)	27.1(1.7)	**50.8(2.7)**
Slack	Slack	90	32.9(1.3)	34.1(1.1)	**67.0(1.7)**	23.7(1.0)	28.5(1.2)	**52.2(1.6)**

Table 9 I-E stability results of the PC-SR in the neutral alignment position. Rotations refer to the femoral component with respect to the tibial component (± Standard deviations).

				Femoral Rotation (°)			Tibial Rotation (°)		
Alignment	**MCL**	**LCL**	**Flexion Angle (°)**	**Internal**	**External**	**Total**	**Internal**	**External**	**Total**
Valgus	Slack	Slack	15	29.7(1.2)	29.5(2.0)	**59.2(2.3)**	27.1(1.1)	28.0(1.4)	**55.1(1.8)**
	Normal	Normal	15	29.3(0.9)	30.4(1.4)	**59.7(1.7)**	28.8(1.0)	29.2(1.3)	**58.0(1.6)**
	Tight	Tight	15	28.5(1.4)	28.9(1.7)	**57.4(2.2)**	27.8(1.1)	27.9(1.4)	**55.7(1.8)**
	Slack	Normal	15	29.8(2.1)	30.2(1.7)	**60.0(2.7)**	28.8(1.8)	27.8(2.0)	**56.6(2.7)**
	Normal	Slack	15	30.0(1.9)	31.4(1.1)	**61.4(2.2)**	29.1(1.2)	29.6(0.9)	**58.7(1.5)**
	Slack	Tight	15	31.2(1.2)	32.7(2.3)	**63.9(2.6)**	29.3(1.1)	28.4(2.0)	**57.7(2.3)**
	Tight	Slack	15	31.4(2.1)	30.9(2.0)	**62.3(2.9)**	29.3(1.5)	29.6(1.6)	**58.9(2.2)**
	Slack	Slack	90	31.6(1.6)	31.0(0.8)	**62.6(1.8)**	25.3(1.3)	25.4(1.0)	**50.7(1.6)**
	Normal	Normal	90	31(2.1)	28.3(1.9)	**59.3(2.8)**	24.7(1.9)	24.3(1.5)	**49.0(2.4)**
	Tight	Tight	90	26.9(0.9)	27.2(2.1)	**54.1(2.3)**	23.5(0.6)	24.1(1.9)	**47.6(2.0)**
	Slack	Normal	90	30.3(1.6)	28.9(2.3)	**59.2(2.8)**	26.9(1.4)	25.3(2.2)	**52.2(2.6)**
	Normal	Slack	90	30.1(1.9)	26.1(2.1)	**56.2(2.8)**	24.6(1.6)	24.9(1.9)	**49.5(2.5)**
	Slack	Tight	90	29.8(2.4)	28.2(1.1)	**58.0(2.6)**	24.1(2.2)	24.1(1.0)	**48.2(2.4)**
	Tight	Slack	90	29.2(2.3)	26.4(1.9)	**55.9(3.0)**	25.1(1.8)	24.2(1.6)	**49.3(2.4)**
Varus	Slack	Slack	15	29.7(0.9)	30.2(1.9)	**59.9(2.1)**	28.1(0.9)	28.2(1.5)	**56.3(1.7)**
	Normal	Normal	15	28.1(1.8)	28.9(1.5)	**57.0(2.3)**	27.1(1.6)	27.1(1.3)	**54.2(2.1)**
	Tight	Tight	15	28.0(2.1)	27.4(1.6)	**55.4(2.6)**	27.2(1.9)	26.4(1.2)	**53.6(2.2)**
	Slack	Normal	15	30.2(1.4)	30.4(2.0)	**60.6(2.4)**	28.2(1.1)	28.8(1.5)	**57.0(1.9)**
	Normal	Slack	15	29.5(1.2)	30.5(1.6)	**60.0(2.0)**	28.2(0.9)	28.4(1.2)	**56.6(1.5)**
	Slack	Tight	15	31.2(0.9)	31.5(1.8)	**62.7(2.0)**	26.1(0.5)	28.6(1.2)	**54.7(1.3)**
	Tight	Slack	15	31.7(1.6)	31.0(1.8)	**62.7(2.4)**	30.4(1.5)	29.7(1.5)	**60.1(2.1)**
	Slack	Slack	90	29.2(1.2)	33.8(2.0)	**63.0(2.3)**	24.9(1.0)	25.1(1.5)	**50.0(1.8)**
	Normal	Normal	90	26.4(0.9)	31.9(0.9)	**58.3(1.3)**	23.1(0.2)	23.3(0.9)	**46.4(0.9)**
	Tight	Tight	90	26.5(1.9)	28.2(1.2)	**54.7(2.2)**	24.2(1.5)	24.5(1.1)	**48.7(1.9)**
	Slack	Normal	90	29.8(2.0)	29.1(1.5)	**58.9(2.5)**	25.4(1.9)	26.7(1.0)	**52.1(2.1)**
	Normal	Slack	90	28.9(1.2)	27.7(0.9)	**56.6(1.5)**	25.2(1.3)	24.3(0.8)	**49.5(1.5)**
	Slack	Tight	90	28.4(1.5)	31.9(2.0)	**60.3(2.5)**	25.7(1.2)	24.9(1.5)	**50.6(1.9)**
	Tight	Slack	90	28.4(1.2)	27.8(2.1)	**56.2(2.4)**	26.4(1.0)	24.1(1.9)	**50.5(2.1)**

Table 10 I-E stability results of the PC-SR in the malaligned position. Rotations refer to the femoral component with respect to the tibial component (± Standard deviations).

			Femoral Rotation (°)		
MCL	**LCL**	**Flexion Angle (°)**	**Varus**	**Valgus**	**Total**
Normal	Normal	0	4.3(0.6)	1.6(0.2)	**5.9(0.6)**
Normal	Slack	0	5.6(0.8)	1.8(0.1)	**7.4(0.8)**
Slack	Normal	0	5.2(0.7)	1.9(0.0)	**7.1(0.7)**
Slack	Slack	0	6.5(0.8)	1.9(0.3)	**8.4(0.9)**
Normal	Tight	0	3.8(0.4)	1.7(0.4)	**5.5(0.6)**
Tight	Normal	0	4.1(0.3)	1.5(0.4)	**5.6(0.5)**
Tight	Tight	0	3.9(0.5)	1.4(0.1)	**5.3(0.5)**

Table 11 V-V stability results of the PC-SR in the neutral alignment position (± Standard deviations). Rotations refer to the tibial component with respect to the femoral component.

			Initial Rotation (°)		Final Rotation (°)		
Alignment	**MCL**	**LCL**	**Varus**	**Valgus**	**Varus**	**Valgus**	**Total**
Valgus	Normal	Normal	-	0.1(0.0)	5.4(0.6)	1.6(0.3)	**7.0(0.7)**
	Normal	Slack	-	0.1(0.1)	6.1(0.8)	1.2(0.1)	**7.3(0.8)**
	Slack	Normal	-	0.2(0.1)	5.1(0.4)	2.8(0.4)	**8.0(0.6)**
	Slack	Slack	-	0.2(0.1)	6.2(0.6)	2.3(0.4)	**8.4(0.7)**
	Slack	Tight	-	0.4(0.1)	3.9(0.4)	3.2(0.4)	**7.0(0.6)**
	Tight	Slack	0.2(0.0)	-	* 6.3(0.6)	0.6(0.1)	**6.9(0.6)**
	Tight	Tight	-	-	5.2(0.3)	0.8(0.0)	**6.0(0.3)**
	Tight	Normal	0.1(0.0)	-	6.1(0.9)	1.0(0.2)	**7.1(0.9)**
	Normal	Tight	-	0.1(0.1)	5.2(0.7)	2.0(0.3)	**7.2(0.8)**
Varus	Normal	Normal	0.1(0.1)	-	6.2(0.6)	0.6(0.2)	**6.8(0.7)**
	Normal	Slack	0.4(0.2)	-	7.8(0.9)	0.3(0.0)	**8.1(0.9)**
	Slack	Normal	0.1(0.0)	-	6.4(0.4)	1.8(0.2)	**8.2(0.5)**
	Slack	Slack	0.3(0.1)	-	* 7.8(1.0)	1.6(0.3)	**9.5(1.0)**
	Slack	Tight	-	-	5.5(0.5)	1.4(0.1)	**6.9(0.5)**
	Tight	Slack	0.9(0.2)		* 7.9(0.7)	0.2(0.1)	**8.1(0.7)**
	Tight	Tight	-	-	5.9(0.4)	0.2(0.0)	**6.1(0.4)**
	Tight	Normal	0.3(0.1)	-	6.3(0.6)	0.2(0.1)	**6.6(0.6)**
	Normal	Tight	-	-	5.7(0.6)	0.8(0.1)	**6.5(0.6)**

Table 12 V-V stability results of the PC-SR in the malaligned position (± Standard deviations). Rotations refer to the tibial component with respect to the femoral component. * indicates where the M-L limit was tripped.

				Tibial Displacements (mm)		
PCL	**MCL**	**LCL**	**Flexion Angle (°)**	**Anterior**	**Posterior**	**Total**
No PCL	Normal	Normal	0	5.9(0.4)	5.3(0.1)	**11.2(0.4)**
	Normal	Normal	30	5.5(0.3)	7.6(0.2)	**13.1(0.4)**
	Normal	Normal	60	5.1(0.6)	7.7(0.4)	**12.8(0.7)**
	Normal	Normal	90	6.4(0.6)	8.3(0.2)	**14.7(0.6)**
	Tight	Tight	0	4.8(0.0)	4.7(0.1)	**9.5(0.1)**
	Normal	Tight	0	5.1(0.1)	4.7(0.2)	**9.8(0.2)**
	Tight	Normal	0	5.2(0.1)	4.9(0.0)	**10.1(0.1)**
	Slack	Normal	0	6.1(0.2)	5.5(0.5)	**11.6(0.5)**
	Normal	Slack	0	6.0(0.2)	5.4(0.4)	**11.4(0.4)**
	Slack	Slack	0	6.4(0.1)	6.1(0.9)	**12.5(0.9)**
	Tight	Tight	90	5.1(0.2)	7.1(0.2)	**12.2(0.3)**
	Normal	Tight	90	5.5(0.3)	8.2(0.2)	**13.7(0.4)**
	Tight	Normal	90	5.5(0.1)	8.0(0.4)	**13.5(0.4)**
	Slack	Normal	90	6.7(0.5)	10.1(0.4)	**16.8(0.6)**
	Normal	Slack	90	6.6(0.1)	9.7(0.1)	**15.9(0.1)**
	Slack	Slack	90	7.4(0.2)	10.9(0.3)	**18.3(0.4)**
Normal PCL	Normal	Normal	0	5.8(0.3)	4.7(0.4)	**10.5(0.5)**
	Normal	Normal	30	5.1(0.3)	6.1(0.1)	**11.2(0.3)**
	Normal	Normal	60	4.5(0.1)	5.7(0.5)	**10.3(0.5)**
	Normal	Normal	90	5.5(0.3)	7.7(0.4)	**13.2(0.5)**
	Tight	Tight	0	5.0(0.3)	4.3(0.2)	**9.3(0.4)**
	Normal	Tight	0	5.1(0.1)	4.6(0.2)	**9.7(0.2)**
	Tight	Normal	0	5.1(0.5)	4.6(0.0)	**9.7(0.5)**
	Slack	Normal	0	5.8(0.4)	5.1(0.1)	**10.9(0.4)**
	Normal	Slack	0	5.7(0.1)	5.1(0.3)	**10.8(0.3)**
	Slack	Slack	0	6.2(0.2)	5.6(0.1)	**11.8(0.2)**
	Tight	Tight	90	5.0(0.1)	6.0(0.2)	**11.6(0.3)**
	Normal	Tight	90	5.6(0.1)	6.6(0.3)	**12.2(0.3)**
	Tight	Normal	90	5.6(0.1)	6.4(0.2)	**12.0(0.3)**
	Slack	Normal	90	6.6(0.2)	8.0(0.3)	**14.6(0.4)**
	Normal	Slack	90	6.4(0.3)	8.2(0.4)	**14.6(0.5)**
	Slack	Slack	90	7.2(0.3)	9.1(0.3)	**16.3(0.4)**

Table 13 A-P stability results of the PC-RF in the neutral alignment position (± Standard deviations). Displacements refer to the tibial component with respect to the femoral component.

				Tibial Displacement (mm)		
Alignment	**MCL**	**LCL**	**Flexion Angle (°)**	**Anterior**	**Posterior**	**Total**
Valgus	Slack	Slack	0	6.9(0.2)	6.1(0.3)	**13.0(0.4)**
	Normal	Normal	0	5.0(0.1)	5.5(0.2)	**10.5(0.2)**
	Tight	Tight	0	3.9(0.1)	5.2(0.3)	**9.1(0.3)**
	Slack	Normal	0	6.6(0.3)	5.4(0.2)	**12.0(0.4)**
	Normal	Slack	0	6.5(0.1)	5.4(0.0)	**11.9(0.1)**
	Tight	Slack	0	5.1(0.2)	5.6(0.1)	**10.7(0.2)**
	Slack	Tight	0	5.1(0.4)	5.2(0.1)	**10.3(0.4)**
	Tight	Normal	0	5.7(0.2)	5.0(0.3)	**10.7(0.4)**
	Normal	Tight	0	5.2(0.2)	4.7(0.1)	**9.9(0.2)**
	Slack	Slack	90	6.9(0.3)	9.4(0.2)	**16.3(0.4)**
	Normal	Normal	90	5.9(0.1)	6.9(0.2)	**12.8(0.2)**
	Tight	Tight	90	5.0(0.1)	6.2(0.4)	**11.2(0.4)**
	Slack	Normal	90	6.4(0.3)	7.7(0.3)	**14.1(0.4)**
	Normal	Slack	90	7.1(0.2)	9.2(0.3)	**16.3(0.4)**
	Tight	Slack	90	6.2(0.1)	6.8(0.3)	**13.0(0.3)**
	Slack	Tight	90	6.5(0.2)	7.1(0.1)	**13.6(0.2)**
	Tight	Normal	90	6.3(0.2)	6.5(0.2)	**12.8(0.3)**
	Normal	Tight	90	5.7(0.2)	5.7(0.1)	**11.4(0.2)**
Varus	Slack	Slack	0	4.7(0.0)	6.6(0.2)	**11.3(0.2)**
	Normal	Normal	0	4.6(0.1)	4.8(0.1)	**9.4(0.1)**
	Tight	Tight	0	4.3(0.2)	4.3(0.1)	**8.6(0.2)**
	Slack	Normal	0	5.1(0.3)	5.4(0.1)	**10.5(0.3)**
	Normal	Slack	0	5.2(0.2)	6.2(0.2)	**11.4(0.3)**
	Tight	Slack	0	4.8(0.1)	5.8(0.1)	**10.6(0.1)**
	Slack	Tight	0	5.1(0.1)	6.0(0.2)	**11.1(0.2)**
	Tight	Normal	0	5.2(0.2)	5.8(0.1)	**11.0(0.2)**
	Normal	Tight	0	5.1(0.2)	5.6(0.2)	**10.7(0.3)**
	Slack	Slack	90	5.6(0.2)	8.3(0.2)	**13.9(0.3)**
	Normal	Normal	90	5.5(0.1)	7.6(0.3)	**13.1(0.1)**
	Tight	Tight	90	4.9(0.3)	5.9(0.3)	**10.8(0.4)**
	Slack	Normal	90	6.0(0.1)	7.4(0.4)	**13.4(0.4)**
	Normal	Slack	90	5.6(0.1)	8.8(0.3)	**14.4(0.3)**
	Tight	Slack	90	5.4(0.2)	7.6(0.3)	**13.0(0.4)**
	Slack	Tight	90	5.1(0.1)	8.2(0.3)	**13.3(0.3)**
	Tight	Normal	90	4.9(0.0)	7.2(0.3)	**12.1(0.3)**
	Normal	Tight	90	5.1(0.2)	7.3(0.1)	**12.4(0.2)**

Table 14 A-P stability results with of the PC-RF in the malaligned position (± Standard deviations). Displacements refer to the tibial component with respect to the femoral component.

				Rotation (°)		
PCL	**MCL**	**LCL**	**Flexion Angle (°)**	**Internal**	**External)**	**Total**
No PCL	Normal	Normal	0	21.5(0.6)	22.5(1.3)	44.0(1.4)
	Normal	Normal	15	23.6(0.6)	23.6(1.2)	47.2(1.3)
	Normal	Normal	60	21.9(1.2)	21.7(0.8)	43.6(1.4)
	Normal	Normal	90	24.8(0.4)	24.8(0.9)	49.6(1.0)
	Tight	Tight	15	22.4(1.1)	22.8(1.1)	45.2(1.6)
	Normal	Tight	15	23.0(1.0)	23.3(0.4)	46.3(1.1)
	Tight	Normal	15	23.0(0.9)	22.9(0.8)	45.9(1.2)
	Slack	Normal	15	28.2(1.8)	26.7(1.2)	54.9(2.2)
	Normal	Slack	15	28.0(0.9)	26.8(1.4)	54.8(1.7)
	Slack	Slack	15	29.7(0.2)	27.8(0.9)	57.5(0.9)
	Tight	Tight	90	21.9(1.6)	22.8(0.4)	44.7(1.7)
	Normal	Tight	90	23.5(0.8)	23.6(0.4)	47.1(0.9)
	Tight	Normal	90	23.2(1.1)	23.4(0.9)	46.6(1.4)
	Slack	Normal	90	27.5(0.4)	24.6(1.0)	52.1(1.1)
	Normal	Slack	90	26.8(0.1)	25.4(0.7)	52.2(0.7)
	Slack	Slack	90	28.4(0.4)	26.8(0.2)	55.2(0.4)
Normal PCL	Normal	Normal	0	19.4(0.7)	20.1(0.3)	39.5(0.8)
	Normal	Normal	15	21.2(0.3)	19.1(0.1)	40.3(0.3)
	Normal	Normal	60	20.1(1.0)	19.9(0.4)	40.0(1.1)
	Normal	Normal	90	22.6(0.2)	22.8(0.0)	45.4(0.2)
	Tight	Tight	15	20.6(0.6)	18.3(0.5)	38.9(0.8)
	Normal	Tight	15	21.0(0.8)	18.7(0.2)	39.7(0.8)
	Tight	Normal	15	21.2(1.0)	18.9(0.4)	40.1(1.1)
	Slack	Normal	15	23.3(0.3)	22.9(0.6)	46.2(0.7)
	Normal	Slack	15	23.2(0.4)	22.9(0.5)	46.1(0.6)
	Slack	Slack	15	24.1(0.4)	23.9(0.9)	48.0(1.0)
	Tight	Tight	90	22.1(0.1)	21.2(0.3)	43.3(0.3)
	Normal	Tight	90	22.6(0.2)	22.3(0.2)	44.9(0.3)
	Tight	Normal	90	23.0(0.2)	22.2(1.3)	45.2(1.3)
	Slack	Normal	90	25.4(0.3)	26.1(0.7)	51.5(0.8)
	Normal	Slack	90	26.1(0.5)	26.4(1.0)	52.5(1.1)
	Slack	Slack	90	27.9(0.9)	27.4(1.2)	55.3(1.5)

Table 15 I-E stability results of the PC-RF in the neutral alignment position (± Standard deviations). Rotations refer to the femoral component with respect to the tibial component.

				Rotation (°)		
Alignment	**MCL**	**LCL**	**Flexion Angle (°)**	**Internal**	**External**	**Total**
Valgus	Slack	Slack	15	25.7(0.4)	23.9(0.5)	**49.6(0.6)**
	Normal	Normal	15	22.3(0.2)	20.9(0.5)	**43.2(0.5)**
	Tight	Tight	15	20.2(0.3)	20.0(0.4)	**40.2(0.5)**
	Slack	Normal	15	24.3(0.3)	20.1(0.2)	**44.4(0.4)**
	Normal	Slack	15	23.9(0.6)	19.7(0.4)	**43.6(0.7)**
	Slack	Tight	15	25.2(0.9)	24.3(0.3)	**49.5(0.9)**
	Tight	Slack	15	24.8(0.4)	20.9(0.1)	**45.7(0.4)**
	Slack	Slack	90	26.0(0.2)	21.0(0.4)	**47.0(0.4)**
	Normal	Normal	90	25.3(0.7)	20.8(0.2)	**46.1(0.7)**
	Tight	Tight	90	23.2(0.3)	19.1(0.4)	**42.3(0.5)**
	Slack	Normal	90	25.5(0.6)	21.3(0.4)	**46.8(0.7)**
	Normal	Slack	90	24.6(0.3)	20.8(0.4)	**45.4(0.5)**
	Slack	Tight	90	24.4(0.7)	21.3(0.3)	**45.7(0.8)**
	Tight	Slack	90	23.7(0.4)	20.1(0.4)	**43.8(0.6)**
Varus	Slack	Slack	15	20.7(0.3)	24.2(0.7)	**44.9(0.8)**
	Normal	Normal	15	20.7(0.5)	21.7(0.5)	**42.4(0.7)**
	Tight	Tight	15	19.0(0.4)	20.4(0.2)	**39.4(0.4)**
	Slack	Normal	15	19.6(0.4)	22.3(0.6)	**41.9(0.7)**
	Normal	Slack	15	19.4(0.4)	23.3(0.3)	**42.7(0.5)**
	Slack	Tight	15	19.6(0.3)	22.3(0.5)	**41.9(0.6)**
	Tight	Slack	15	20.3(0.3)	23.9(0.8)	**43.2(0.9)**
	Slack	Slack	90	21.5(0.3)	28.5(1.0)	**50.0(1.0)**
	Normal	Normal	90	20.3(0.2)	26.7(0.4)	**47.0(0.4)**
	Tight	Tight	90	18.1(0.3)	24.2(0.3)	**42.3(0.4)**
	Slack	Normal	90	20.9(0.4)	27.9(0.5)	**48.8(0.6)**
	Normal	Slack	90	21.2(0.3)	27.8(0.3)	**49.0(0.4)**
	Slack	Tight	90	19.6(0.3)	26.3(0.6)	**45.9(0.7)**
	Tight	Slack	90	20.7(0.7)	26.9(0.4)	**47.6(0.8)**

Table 16 I-E stability results of the PC-RF in the malaligned position (± Standard deviations). Rotations refer to the femoral component with respect to the tibial component.

				Rotation (°)		
PCL	**MCL**	**LCL**	**Flexion Angle (°)**	**Varus**	**Valgus**	**Total**
No PCL	Normal	Normal	0	*4.4(1.5)	1.3(0.5)	**6.2(1.6)**
	Normal	Slack	0	4.4(0.9)	1.9(0.3)	**6.3(0.9)**
	Slack	Normal	0	4.2(0.5)	2.2(0.4)	**6.4(0.6)**
	Slack	Slack	0	*4.8(1.0)	2.2(1.0)	**7.0(1.4)**
	Normal	Tight	0	5.1(0.7)	1.1(0.4)	**6.2(0.8)**
	Tight	Normal	0	5.3(1.0)	0.7(0.2)	**6.0(1.0)**
	Tight	Tight	0	5.1(1.2)	0.7(0.3)	**5.8(1.2)**
Normal PCL	Slack	Slack	0	4.5(0.1)	1.9(0.5)	**6.4(0.5)**

Table 17 V-V stability results of the PC-RF in the neutral alignment position (± Standard deviations). Rotations refer to the tibial component with respect to the femoral component. * indicates where M-L limit was tripped.

				Initial Rotation (°)		Final Rotation (°)		
Malrotation	**PCL**	**MCL**	**LCL**	**Varus**	**Valgus**	**Varus**	**Valgus**	**Total**
Valgus	**No PCL**	Normal	Normal	-	0.2(0.1)	3.3(0.6)	2.1(0.4)	**5.4(0.7)**
		Normal	Slack	-	-	*3.4(1.0)	1.8(0.3)	**5.2(1.0)**
		Slack	Normal	-	0.2(0.0)	*3.1(0.7)	2.9(0.6)	**6.0(0.9)**
		Slack	Slack	-	0.2(0.1)	*3.3(0.6)	2.9(0.4)	**6.2(0.7)**
		Slack	Tight	-	0.6(0.2)	*3.1(0.8)	3.1(0.5)	**6.2(0.9)**
		Tight	Slack	0.2(0.1)	-	3.6(0.8)	0.9(0.2)	**4.5(0.8)**
		Tight	Tight	-	-	3.0(0.9)	1.4(0.3)	**4.4(1.0)**
		Tight	Normal	-	-	3.3(0.6)	1.3(0.4)	**4.6(0.7)**
		Normal	Tight	-	-	3.0(0.6)	1.9(0.4)	**4.9(0.7)**
	Normal PCL	Slack	Slack	-	0.3(0.1)	*3.2(0.5)	2.1(0.5)	**5.3(0.7)**
Varus	**No PCL**	Normal	Normal	-	-	5.0(0.9)	0.8(0.1)	**5.8(0.9)**
		Normal	Slack	0.7(0.2)	-	5.3(0.9)	0.6(0.2)	**5.9(0.9)**
		Slack	Normal	-	-	4.7(0.8)	2.2(0.4)	**6.9(0.9)**
		Slack	Slack	0.3(0.0)	-	5.2(1.1)	1.7(0.3)	**6.9(1.1)**
		Slack	Tight	-	-	*3.9(0.7)	2.6(0.5)	**6.5(0.9)**
		Tight	Slack	1.2(0.2)	-	5.5(1.1)	0.5(0.1)	**6.0(1.1)**
		Tight	Tight	-	-	4.5(0.8)	0.4(0.1)	**4.9(0.8)**
		Tight	Normal	0.1(0.0)	-	5.4(0.9)	0.4(0.0)	**5.8(0.9)**
		Normal	Tight	-	-	3.6(0.5)	1.0(0.2)	**4.6(0.5)**
	Normal PCL	Slack	Slack	-	-	4.8(0.5)	1.2(0.2)	**6.0(0.5)**

Table 18 V-V stability results of the PC-RF in the malaligned position (± Standard deviations). Rotations refer to the tibial component with respect to the femoral component. * indicates where M-L limit was tripped.

			Tibial Displacements (mm)		
MCL	**LCL**	**Flexion Angle (°)**	**Anterior**	**Posterior**	**Total**
Normal	Normal	0	3.7(0.4)	3.2(0.2)	**6.9(0.4)**
Normal	Normal	30	4.2(0.2)	3.1(0.1)	**7.3(0.2)**
Normal	Normal	60	4.6(0.8)	1.3(0.2)	**5.9(0.8)**
Normal	Normal	90	3.2(0.3)	0.7(0.0)	**3.9(0.3)**
Tight	Tight	0	2.3(0.0)	1.7(0.0)	**4.0(0.0)**
Normal	Tight	0	2.9(0.6)	2.1(0.1)	**5.0(0.6)**
Tight	Normal	0	2.9(0.2)	2.1(0.1)	**5.0(0.2)**
Slack	Normal	0	4.0(0.2)	3.6(0.3)	**7.6(0.4)**
Normal	Slack	0	4.0(0.2)	3.2(0.2)	**7.2(0.3)**
Slack	Slack	0	5.0(0.2)	3.8(0.3)	**8.8(0.4)**
Tight	Tight	90	2.4(0.2)	0.7(0.1)	**3.1(0.2)**
Normal	Tight	90	2.9(0.3)	0.7(0.0)	**3.6(0.3)**
Tight	Normal	90	2.8(0.3)	0.8(0.2)	**3.6(0.4)**
Slack	Normal	90	3.4(0.2)	0.8(0.1)	**4.2(0.2)**
Normal	Slack	90	3.5(0.2)	0.7(0.1)	**4.2(0.2)**
Slack	Slack	90	4.2(0.1)	0.7(0.0)	**4.9(0.1)**

Table 19 A-P stability results of the PC-SF in the neutral alignment position (± Standard deviations). Displacements refer to the tibial component with respect to the femoral component.

				Displacement (mm)		
Alignment	**MCL**	**LCL**	**Flexion Angle (°)**	**Anterior**	**Posterior**	**Total**
Valgus	Slack	Slack	0	5.0(0.5)	4.7(0.1)	**9.7(0.5)**
	Normal	Normal	0	3.7(0.2)	3.2(0.4)	**6.9(0.5)**
	Tight	Tight	0	2.7(0.1)	2.3(0.1)	**5.0(0.1)**
	Slack	Normal	0	3.8(0.4)	3.9(0.3)	**7.7(0.5)**
	Normal	Slack	0	3.9(0.2)	4.1(0.2)	**8.0(0.3)**
	Tight	Slack	0	3.9(0.3)	3.9(0.1)	**7.8(0.3)**
	Slack	Tight	0	3.5(0.2)	3.4(0.2)	**6.9(0.3)**
	Tight	Normal	0	3.2(0.1)	2.9(0.3)	**6.1(0.3)**
	Normal	Tight	0	3.4(0.0)	2.4(0.2)	**5.8(0.2)**
	Slack	Slack	90	4.3(0.2)	0.8(0.0)	**5.1(0.2)**
	Normal	Normal	90	3.4(0.4)	1(0.3)	**4.4(0.5)**
	Tight	Tight	90	2.1(0.2)	0.7(0.0)	**2.8(0.2)**
	Slack	Normal	90	3.6(0.1)	0.7(0.1)	**4.3(0.1)**
	Normal	Slack	90	3.9(0.3)	1.0(0.1)	**4.9(0.3)**
	Tight	Slack	90	2.9(0.3)	0.7(0.0)	**3.6(0.3)**
	Slack	Tight	90	3.2(0.2)	0.7(0.1)	**3.9(0.2)**
	Tight	Normal	90	2.7(0.3)	0.7(0.0)	**3.4(0.3)**
	Normal	Tight	90	2.9(0.1)	0.8(0.1)	**3.7(0.1)**
Varus	Slack	Slack	0	4.2(0.1)	4.8(0.6)	**9.0(0.6)**
	Normal	Normal	0	3.3(0.1)	3.2(0.0)	**6.5(0.1)**
	Tight	Tight	0	2.5(0.0)	2.8(0.1)	**5.3(0.1)**
	Slack	Normal	0	3.8(0.2)	4.2(0.4)	**8.0(0.5)**
	Normal	Slack	0	3.6(0.3)	4.3(0.2)	**7.9(0.4)**
	Tight	Slack	0	3.5(0.1)	3.5(0.2)	**7.0(0.2)**
	Slack	Tight	0	3.7(0.2)	3.4(0.3)	**7.1(0.4)**
	Tight	Normal	0	3.1(0.3)	3.2(0.1)	**6.3(0.3)**
	Normal	Tight	0	2.9(0.1)	3.2(0.1)	**6.1(0.1)**
	Slack	Slack	90	4.2(0.2)	1.0(0.3)	**5.2(0.4)**
	Normal	Normal	90	3.3(0.1)	0.8(0.1)	**4.1(0.1)**
	Tight	Tight	90	2.7(0.4)	0.8(0.1)	**3.5(0.4)**
	Slack	Normal	90	3.9(0.2)	0.8(0.2)	**4.7(0.3)**
	Normal	Slack	90	4.2(0.3)	0.8(0.1)	**5.0(0.3)**
	Tight	Slack	90	3.4(0.2)	0.7(0.0)	**4.1(0.2)**
	Slack	Tight	90	3.6(0.2)	0.8(0.1)	**4.4(0.2)**
	Tight	Normal	90	3.1(0.3)	0.7(0.1)	**3.8(0.3)**
	Normal	Tight	90	2.9(0.1)	0.8(0.1)	**3.7(0.1)**

Table 20 A-P stability results of the PC-SF in the malaligned position (± Standard deviations). Displacements refer to the tibial component with respect to the femoral component.

			Rotation (°)		
MCL	**LCL**	**Flexion Angle (°)**	**Internal**	**External**	**Total**
Normal	Normal	0	13.9(0.0)	12.2(0.1)	**26.1(0.1)**
Normal	Normal	15	15.3(1.1)	16.6(0.6)	**31.9(1.3)**
Normal	Normal	60	13.8(0.1)	15.1(0.3)	**28.9(0.3)**
Normal	Normal	90	14.8(0.8)	12.8(0.1)	**27.6(0.8)**
Tight	Tight	15	14.2(0.3)	12.8(0.0)	**27.0(0.3)**
Normal	Tight	15	15.7(0.9)	14.6(0.6)	**30.3(1.1)**
Tight	Normal	15	14.3(0.1)	14.1(0.4)	**28.4(0.4)**
Slack	Normal	15	16.8(0.6)	16.6(0.4)	**33.4(0.7)**
Normal	Slack	15	17.3(0.4)	18.6(0.4)	**35.9(0.6)**
Slack	Slack	15	18.4(0.1)	18.3(0.1)	**36.7(0.1)**
Tight	Tight	90	13.1(1.0)	12.0(1.0)	**25.1(1.0)**
Normal	Tight	90	13.9(0.2)	13.0(0.4)	**26.9(0.4)**
Tight	Normal	90	13.1(0.9)	12.8(0.2)	**25.9(0.9)**
Slack	Normal	90	16.0(0.3)	14.8(1.2)	**30.8(1.2)**
Normal	Slack	90	15.9(0.4)	15.0(0.6)	**30.9(0.7)**
Slack	Slack	90	17.1(0.2)	15.8(1.5)	**32.9(1.5)**

Table 21 I-E stability results of the PC-SF in the neutral alignment position (± Standard deviations). Rotations refer to the femoral component with respect to the tibial component.

				Rotation (°)		
Alignment	**MCL**	**LCL**	**Flexion Angle (°)**	**Internal**	**External**	**Total**
Valgus	Slack	Slack	15	20.1(0.4)	17.5(0.2)	**37.6(0.5)**
	Normal	Normal	15	18.2(0.3)	16.6(0.4)	**34.8(0.5)**
	Tight	Tight	15	16.1(0.6)	15.7(0.1)	**31.8(0.6)**
	Slack	Normal	15	19.1(0.5)	17.5(0.3)	**36.6(0.6)**
	Normal	Slack	15	19.4(0.6)	16.7(0.1)	**36.1(0.6)**
	Slack	Tight	15	21.6(0.3)	16.1(0.3)	**37.7(0.4)**
	Tight	Slack	15	20.8(0.5)	17.2(0.2)	**38.0(0.5)**
	Slack	Slack	90	24.6(0.3)	17.0(0.1)	**41.6(0.3)**
	Normal	Normal	90	21.4(0.1)	16.4(0.4)	**37.8(0.4)**
	Tight	Tight	90	18.3(0.3)	14.2(0.1)	**32.5(0.3)**
	Slack	Normal	90	24.2(0.7)	17.2(0.1)	**41.4(0.7)**
	Normal	Slack	90	23.9(0.3)	17.3(0.3)	**41.2(0.4)**
	Slack	Tight	90	22.9(0.4)	17.1(0.5)	**40.0(0.6)**
	Tight	Slack	90	23.1(0.3)	16.2(0.1)	**39.3(0.3)**
Varus	Slack	Slack	15	16.1(0.3)	20.2(0.7)	**36.3(0.8)**
	Normal	Normal	15	16.3(0.1)	18.6(0.4)	**34.9(0.4)**
	Tight	Tight	15	14.6(0.1)	16.6(0.1)	**31.2(0.1)**
	Slack	Normal	15	15.7(0.2)	20.2(0.5)	**35.9(0.5)**
	Normal	Slack	15	16.7(0.3)	20.4(0.5)	**37.1(0.6)**
	Slack	Tight	15	15.2(0.4)	19.0(0.1)	**34.2(0.4)**
	Tight	Slack	15	16.9(0.2)	18.4(0.4)	**35.3(0.5)**
	Slack	Slack	90	16.1(0.1)	23.9(0.1)	**40.0(0.1)**
	Normal	Normal	90	15.8(0.5)	21.7(0.0)	**37.5(0.5)**
	Tight	Tight	90	14.8(0.3)	17.4(0.3)	**32.2(0.4)**
	Slack	Normal	90	18.6(0.3)	25.7(0.9)	**44.3(1.0)**
	Normal	Slack	90	17.0(0.1)	23.9(0.2)	**40.9(0.2)**
	Slack	Tight	90	16.1(0.2)	24.2(0.3)	**40.3(0.4)**
	Tight	Slack	90	15.5(0.2)	24.3(0.6)	**39.8(0.6)**

Table 22 I I-E stability results of the PC-SF in the malaligned position (± Standard deviations). Rotations refer to the femoral component with respect to the tibial component

		Rotations (°)		
MCL	**LCL**	**Varus**	**Valgus**	**Total**
Normal	Normal	5.3(0.9)	1.4(0.2)	**6.7(0.9)**
Normal	Slack	5.9(0.9)	1.7(0.3)	**7.6(1.0)**
Slack	Normal	5.6(0.5)	2.2(0.4)	**7.8(0.6)**
Slack	Slack	6.2(0.8)	2.3(0.2)	**8.5(0.8)**
Normal	Tight	5.0(0.6)	1.1(0.1)	**6.1(0.6)**
Tight	Normal	5.1(0.4)	0.8(0.2)	**5.9(0.5)**
Tight	Tight	4.8(1.1)	0.6(0.1)	**5.4(1.1)**

Table 23 V-V stability results of the PC-SF in the neutral alignment position (± Standard deviations). Rotations refer to the tibial component with respect to the femoral component.

			Initial Rotation (°)		Final Rotation (°)		
Malrotation	**MCL**	**LCL**	**Varus**	**Valgus**	**Varus**	**Valgus**	**Total**
Valgus	Normal	Normal	-	0.1(0.1)	5.3(0.4)	2.5(0.2)	**7.8(0.5)**
	Normal	Slack	-	-	6.3(0.6)	2.1(0.1)	**8.4(0.6)**
	Slack	Normal	-	0.3(0.0)	4.3(0.4)	4.2(0.4)	**8.5(0.6)**
	Slack	Slack	-	0.2(0.0)	5.6(0.4)	3.9(0.3)	**9.5(0.5)**
	Slack	Tight	-	0.5(0.1)	4.1(0.1)	4.6(0.3)	**8.7(0.3)**
	Tight	Slack	-	-	7.2(0.7)	0.6(0.0)	**7.8(0.7)**
	Tight	Tight	-	-	5.0(0.2)	1.6(0.2)	**6.6(0.3)**
	Tight	Normal	-	-	6.9(0.6)	0.6(0.1)	**7.5(0.6)**
	Normal	Tight	-	-	4.6(0.4)	1.8(0.3)	**6.4(0.5)**
Varus	Normal	Normal	0.1(0.0)	-	6.2(0.6)	0.5(0.1)	**6.7(0.6)**
	Normal	Slack	0.4(0.1)	-	7.1(0.7)	0.2(0.0)	**7.3(0.7)**
	Slack	Normal	-	-	5.7(0.6)	2.0(0.2)	**7.7(0.6)**
	Slack	Slack	0.1(0.0)	-	7.1(0.5)	1.2(0.2)	**8.3(0.5)**
	Slack	Tight	-	-	4.6(0.2)	2.7(0.1)	**7.3(0.2)**
	Tight	Slack	0.8(0.1)	-	*7.2(0.7)	0.2(0.0)	**7.4(0.7)**
	Tight	Tight	-	-	5.5(0.3)	0.4(0.1)	**5.9(0.3)**
	Tight	Normal	-	-	6.9(0.6)	0.4(0.2)	**7.3(0.6)**
	Normal	Tight	-	-	5.5(0.3)	0.9(0.2)	**6.4(0.4)**

Table 24 V-V stability results of the PC-SF in the malaligned position (± Standard deviations). Rotations refer to the tibial component with respect to the femoral component.

Appendix 2 – Raw Experimental Contact Pressure Results

In the raw output images the lateral condyle is shown on the right side of the image and the medial condyle on the left. The sensor pads were not large enough to cover an entire condyle, thus they were positioned so that data was recorded in the relevant areas of the bearing surfaces. An example can be seen in Figure 1; the sensors were positioned to record external femoral rotations, where the medial femoral condyles would displace anteriorly and the lateral femoral condyles would displace posteriorly during rotation. This positioning of the sensor pads gives rise to the uneven medial and lateral contact positions in the output images below.

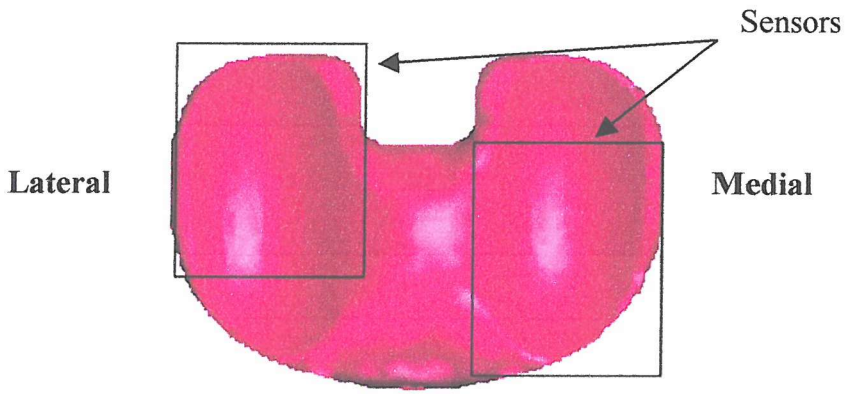

Figure 1 Visual representation of the sensor positioning for external femoral rotation testing.

Test 1
Initial

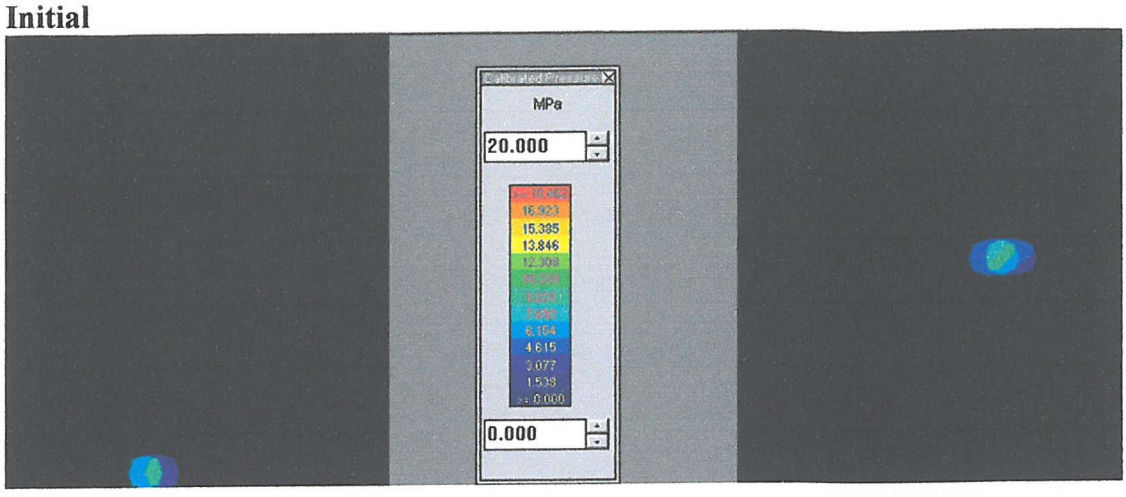

Peak Pressures

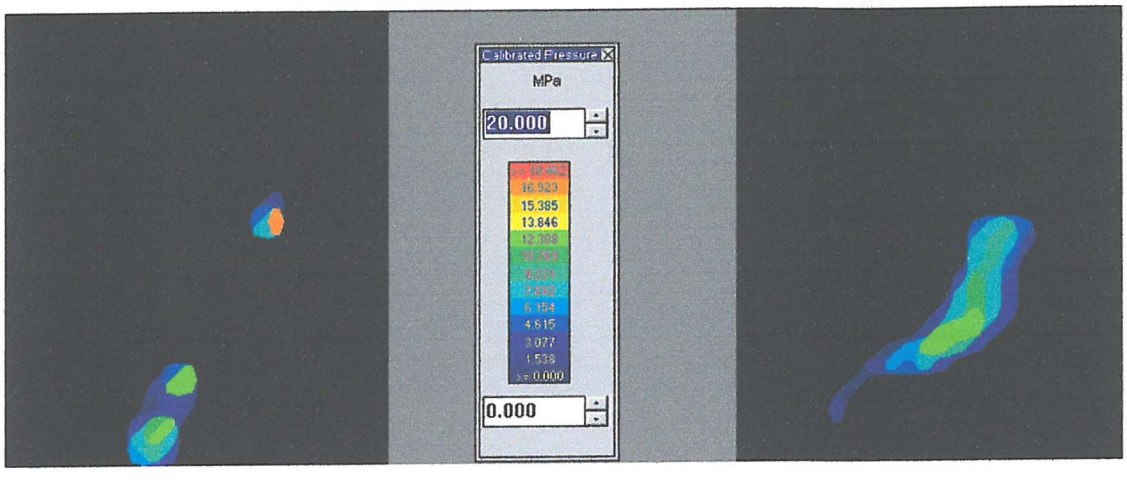

Test 2
Initial

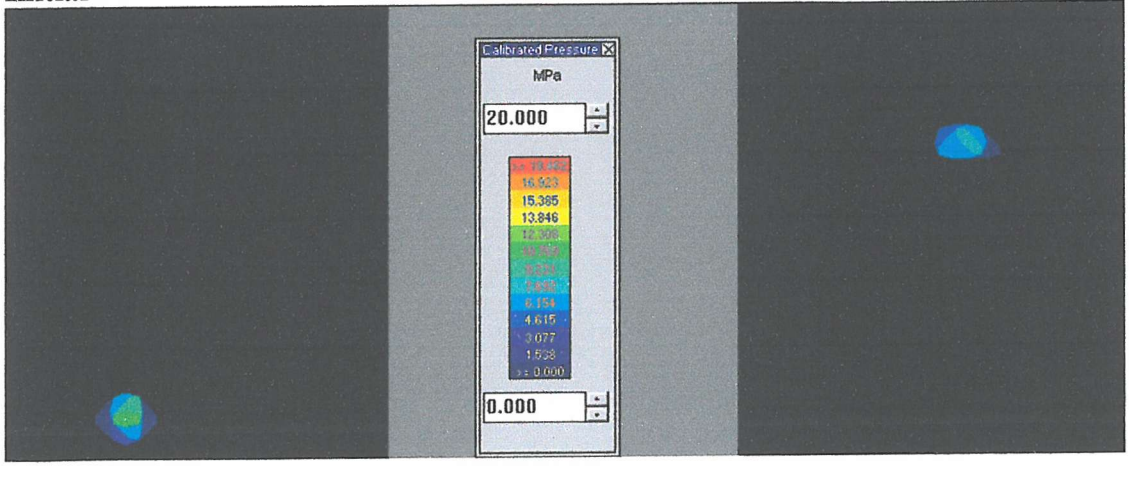

Peak Pressures

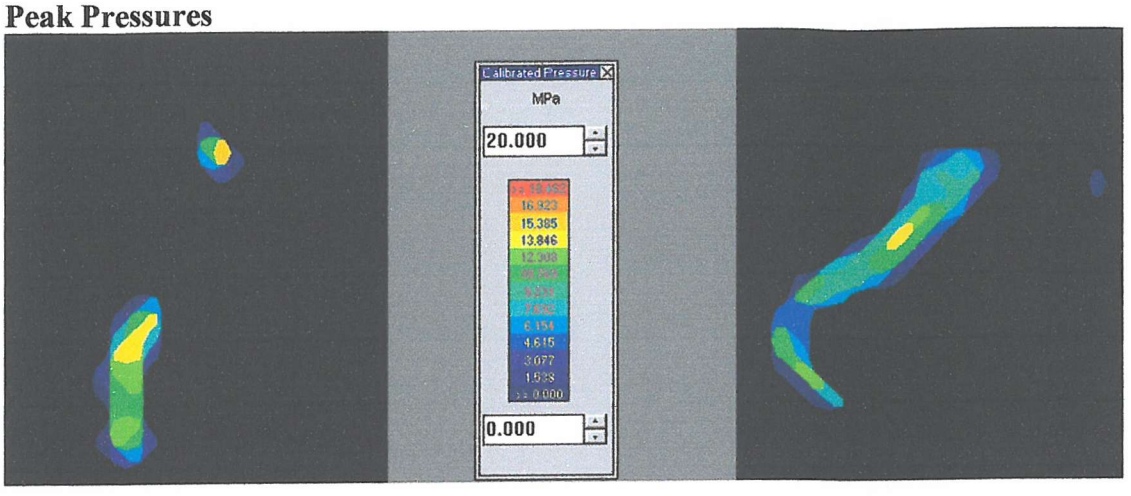

Test 3
Initial

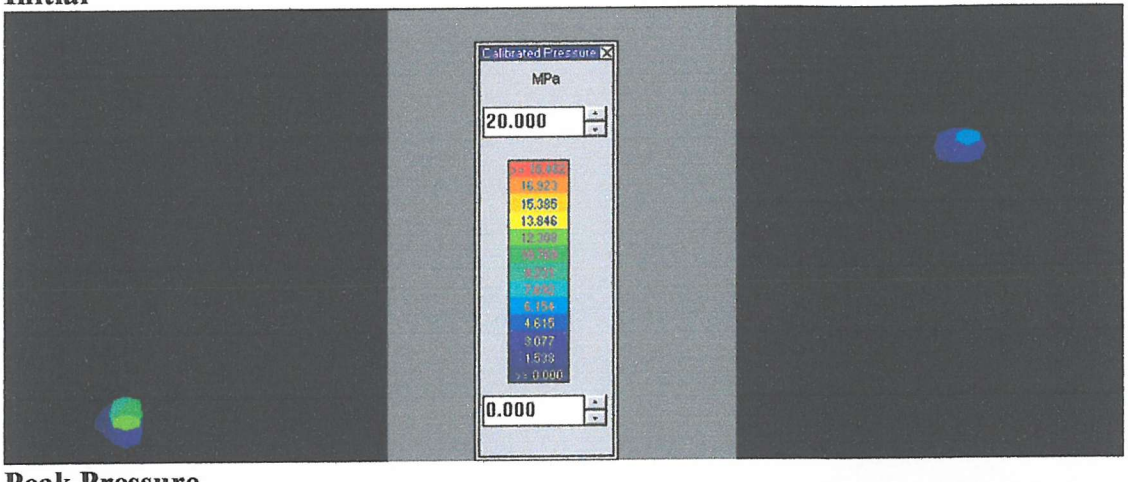

Peak Pressure

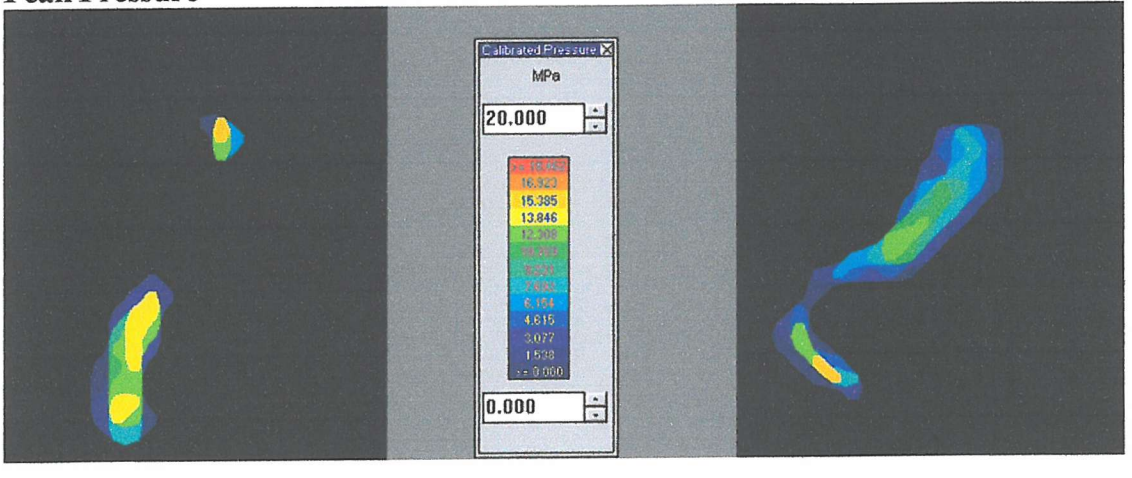

Test 4
Initial

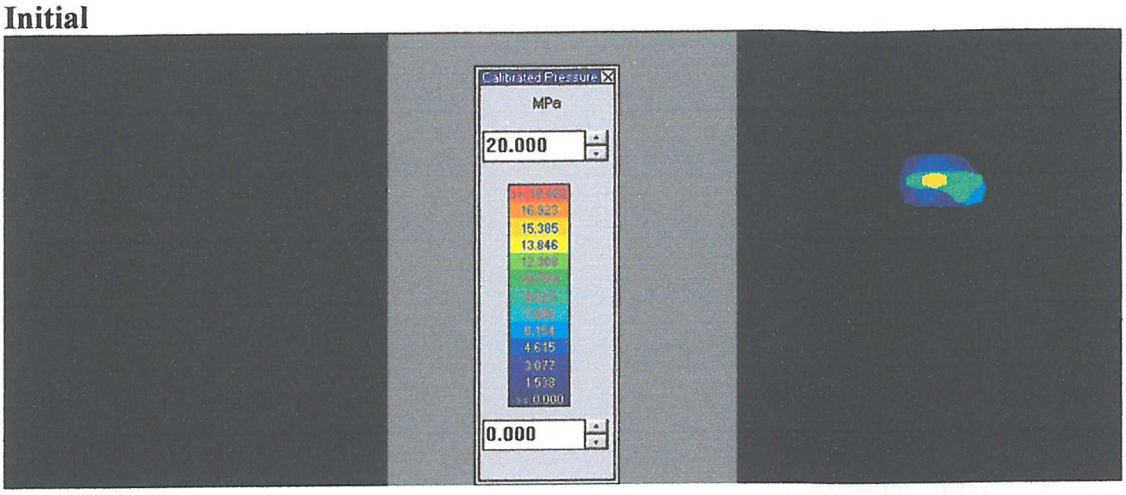

Peak Pressure

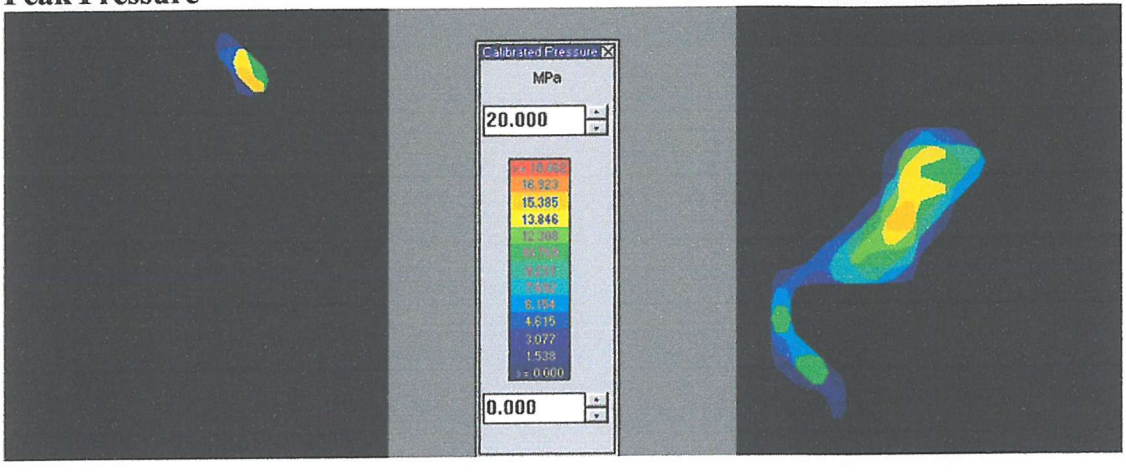

Test 5
Initial

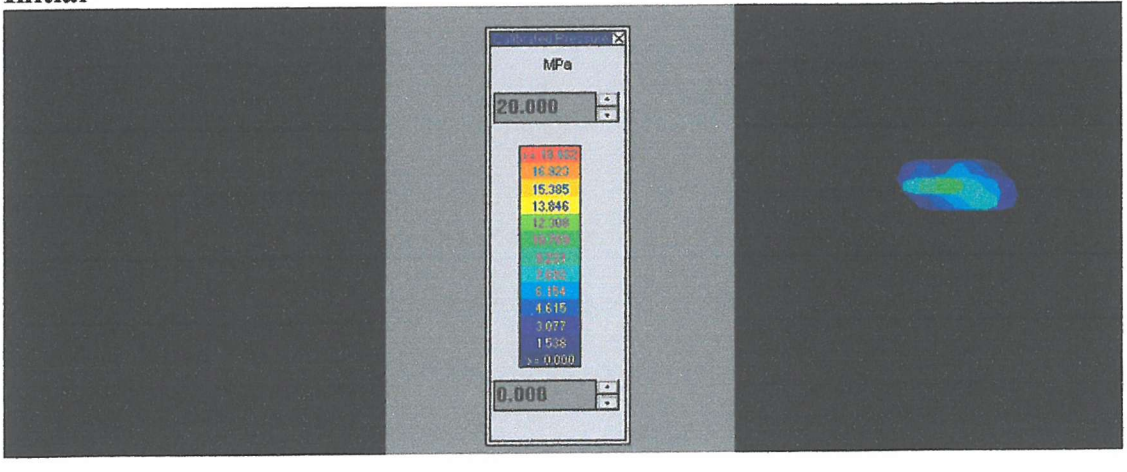

Peak Pressure

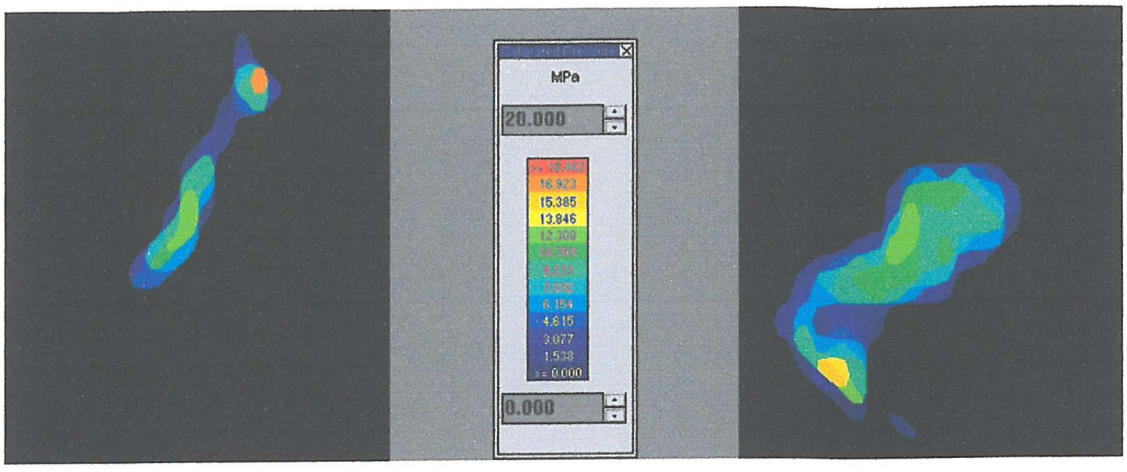

Test 6
Initial

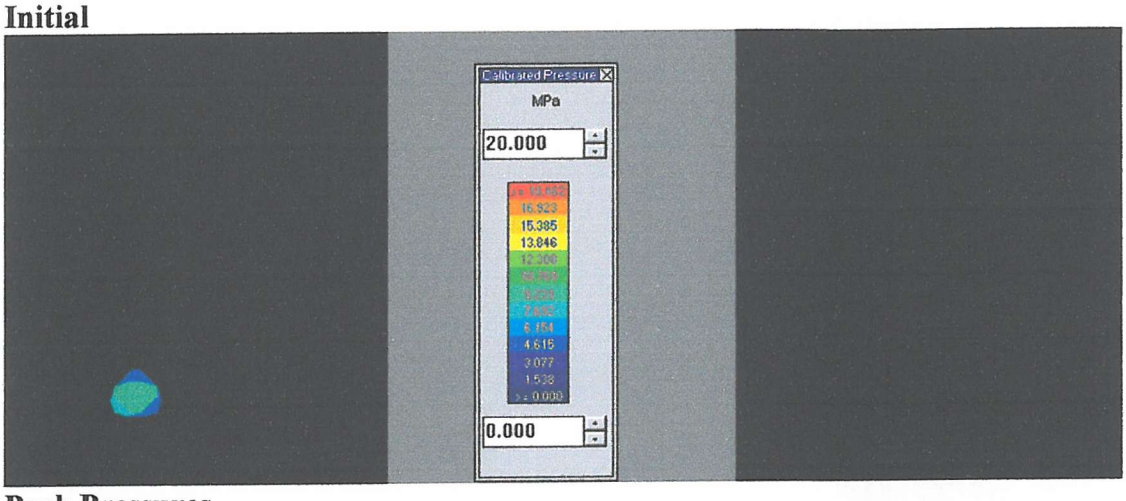

Peak Pressures

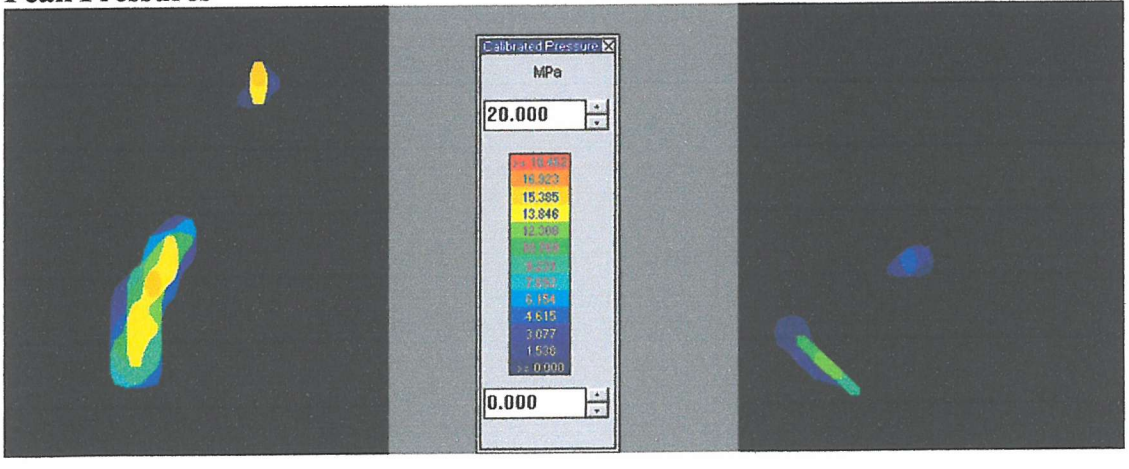

Test 7
Initial

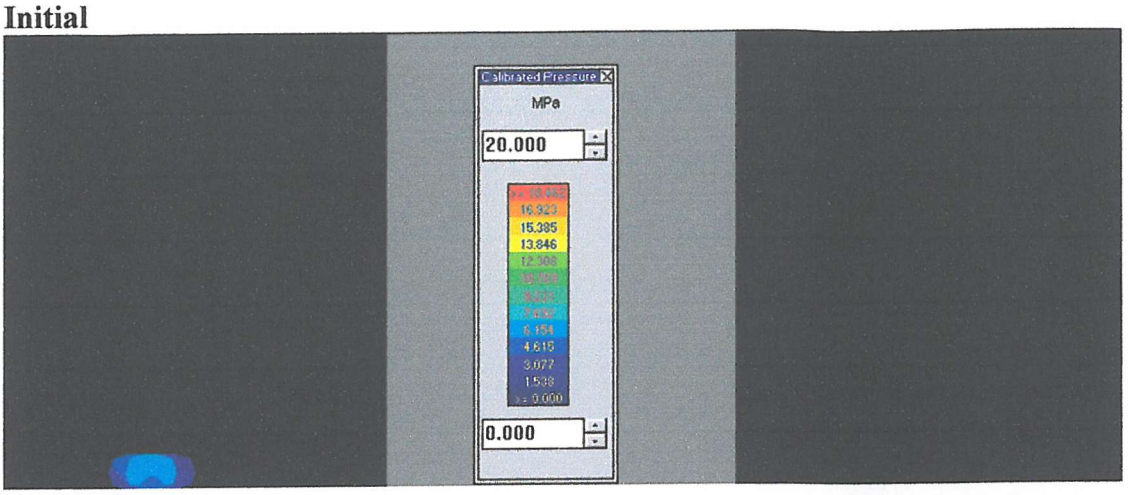

Peak Pressures

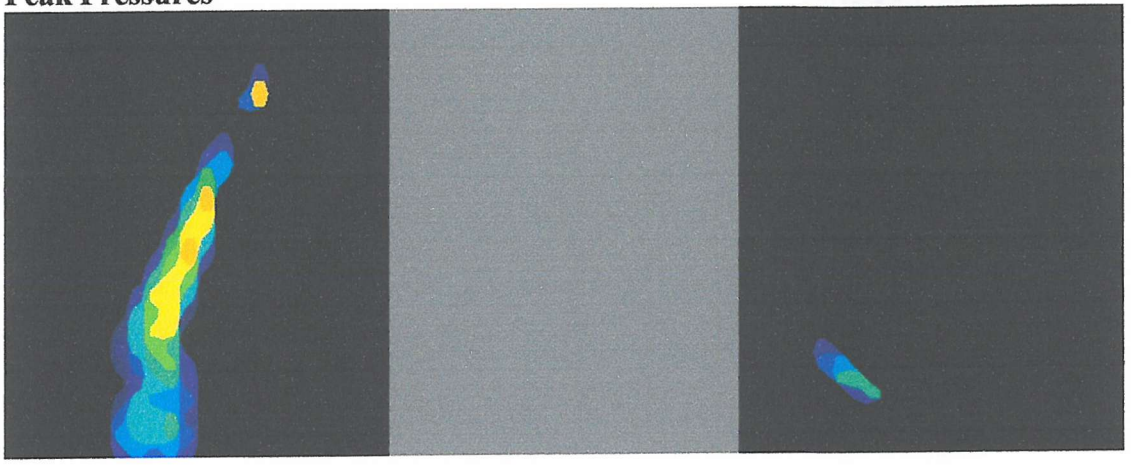

Test 8
Initial

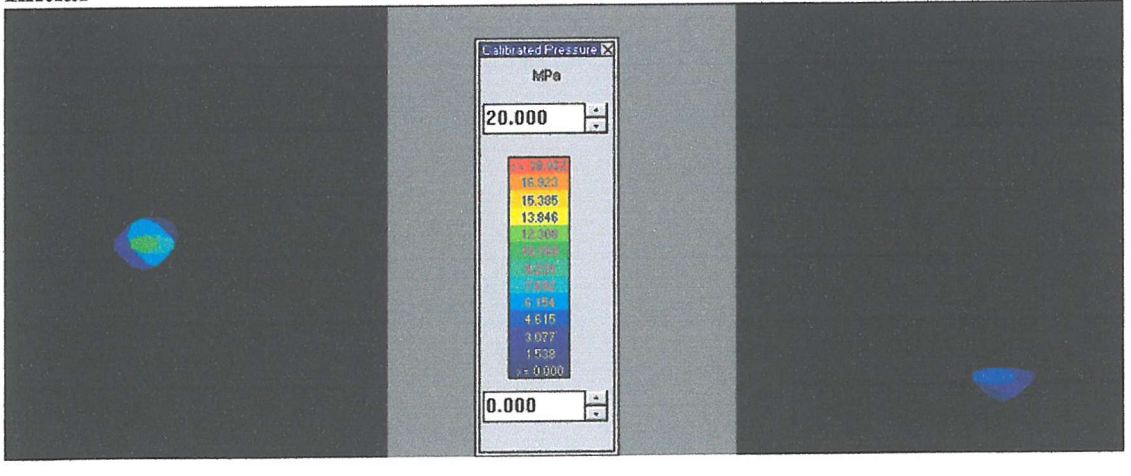

Peak Pressures

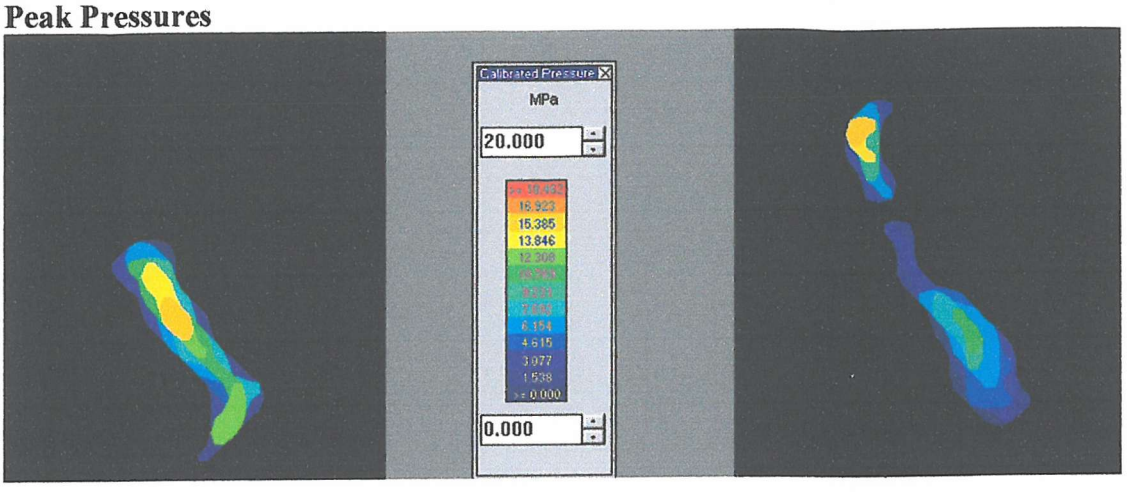

Test 9
Initial

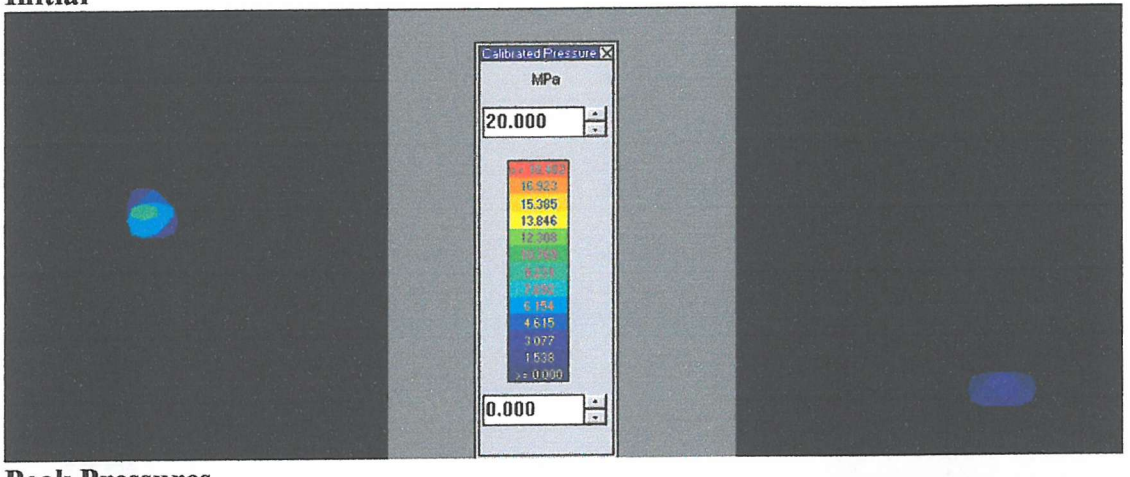

Peak Pressures

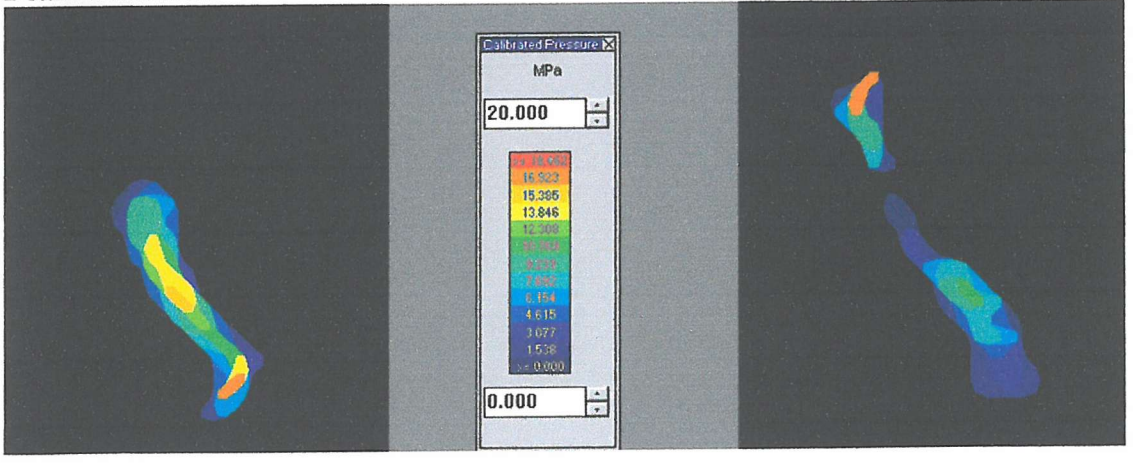

Test 10
Initial

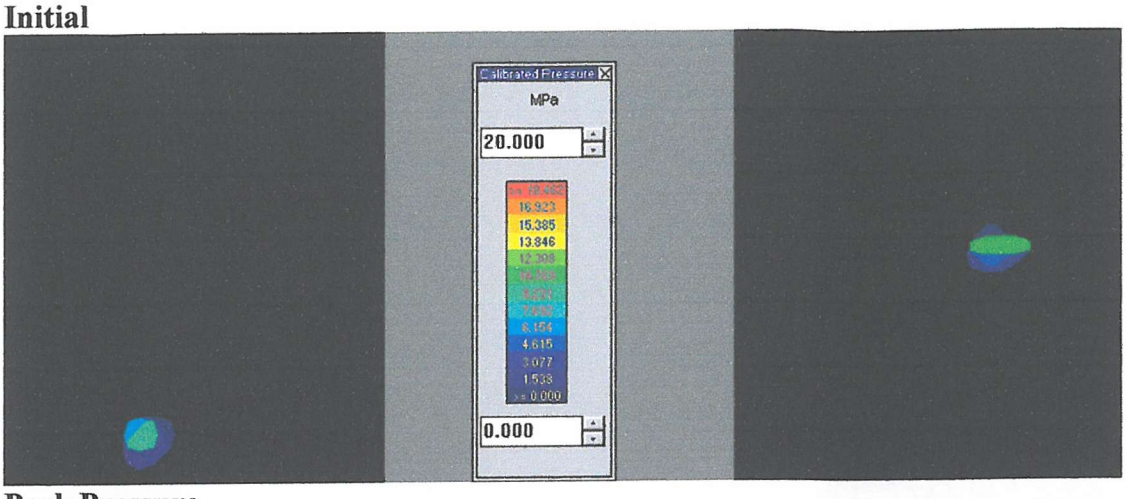

Peak Pressure

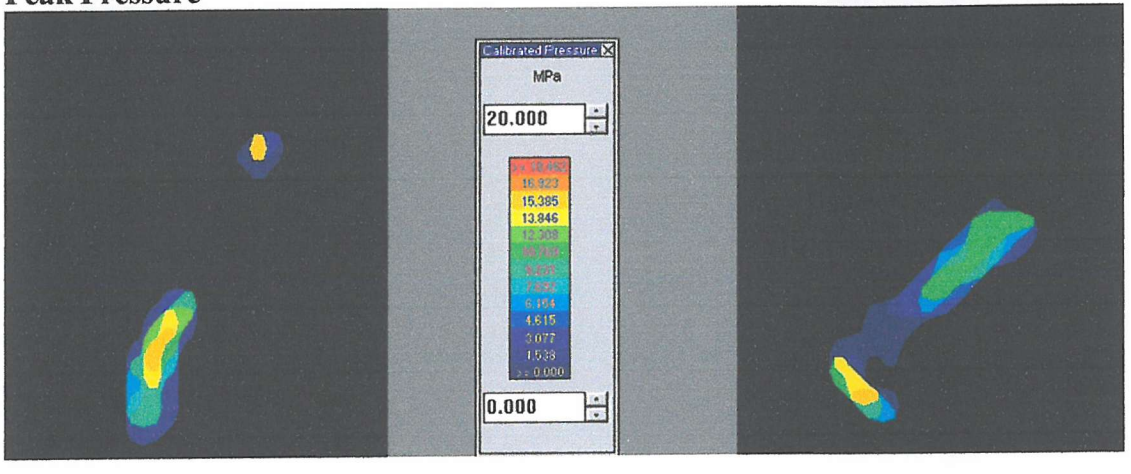

Test 11
Initial

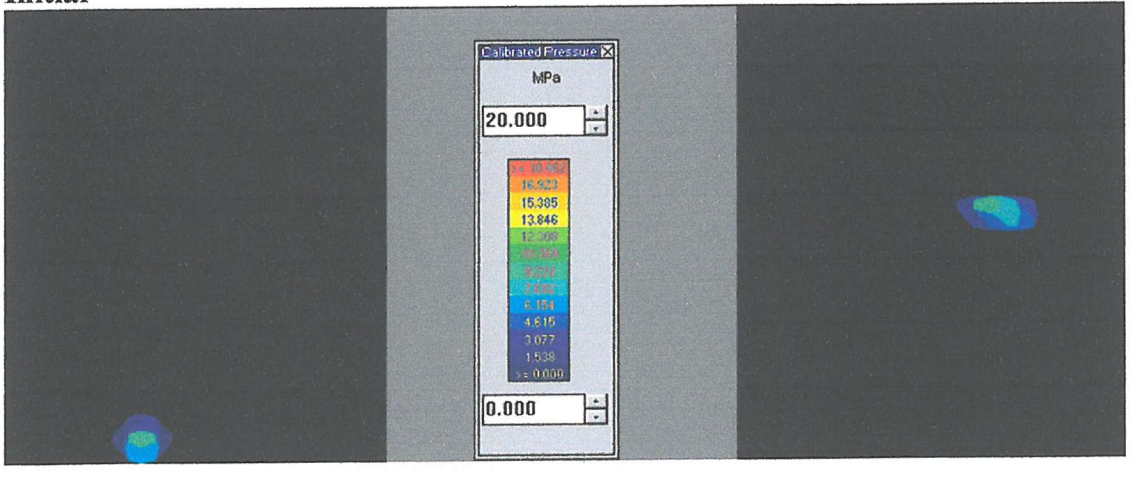

Peak Pressures

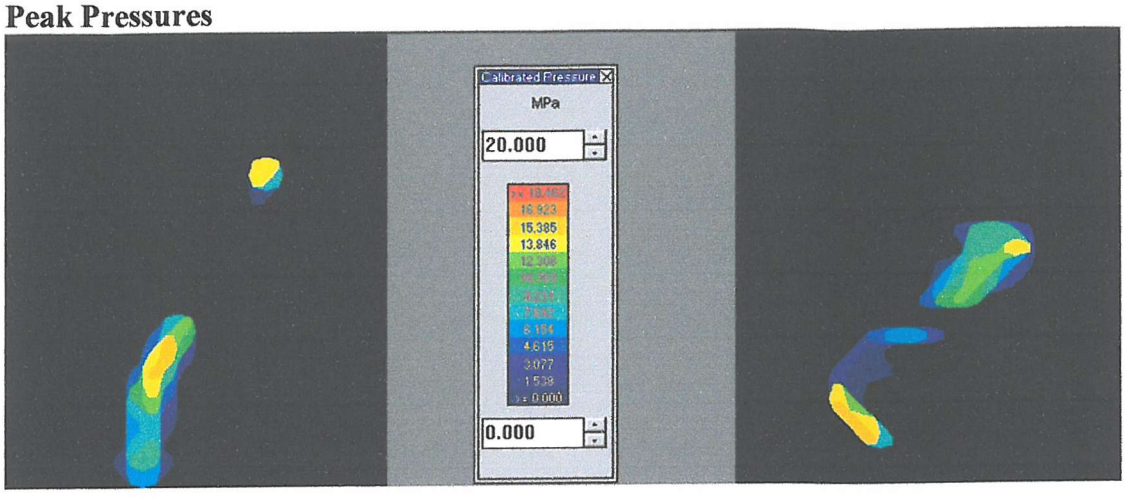

Test 12
Initial

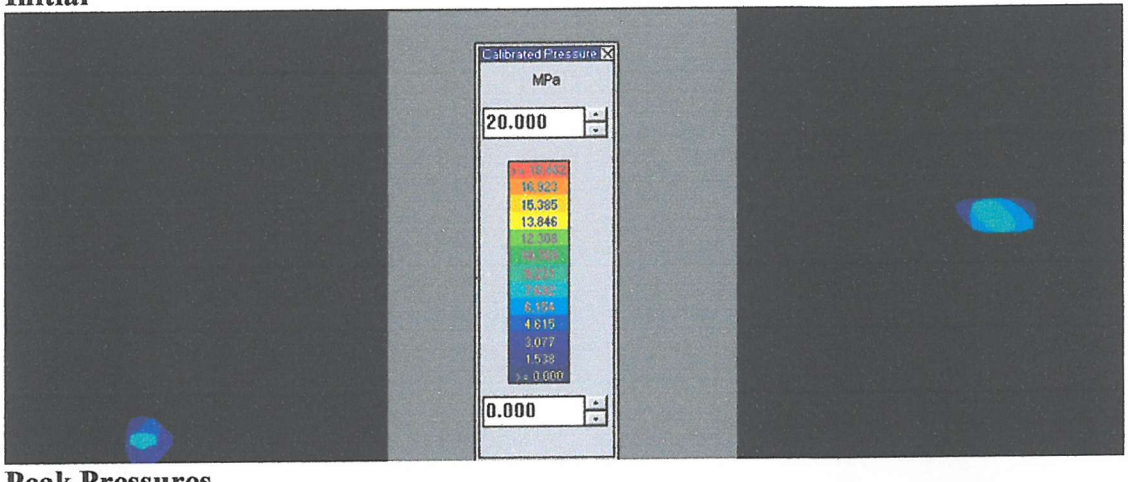

Peak Pressures

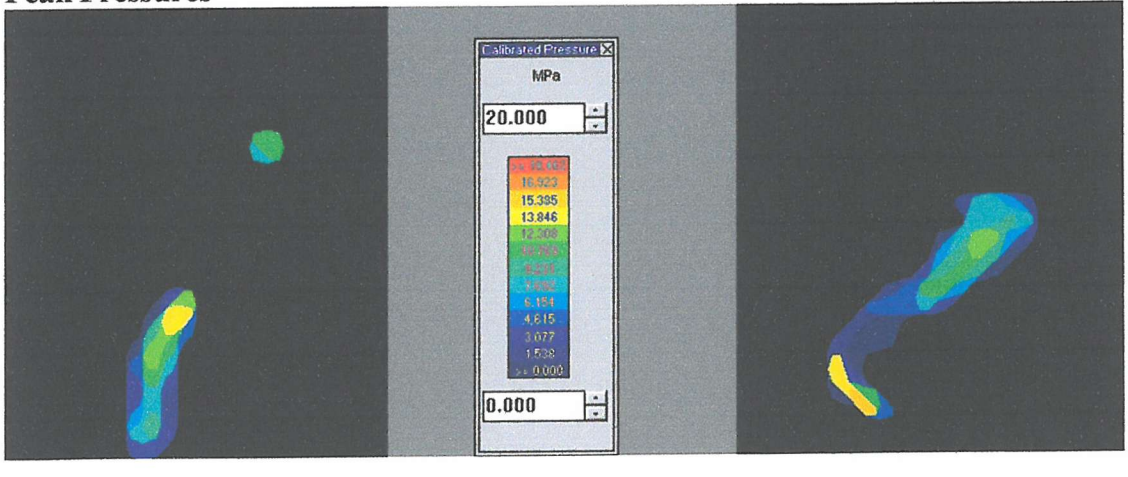

Test 13
Initial

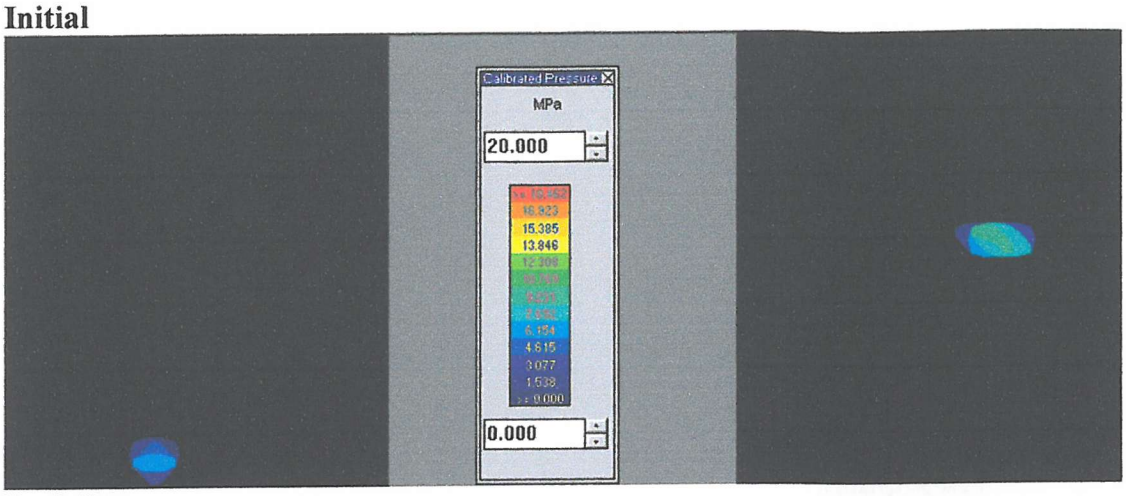

Peak Pressures

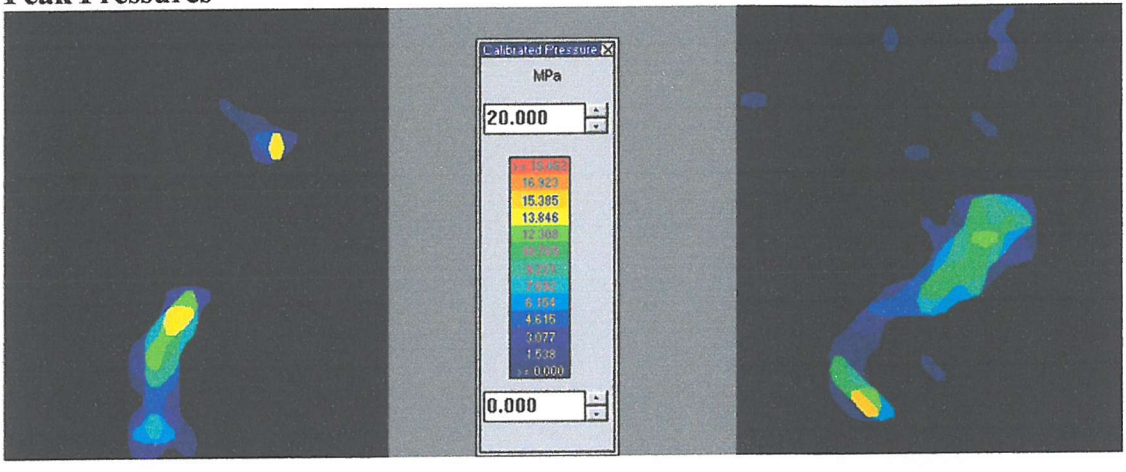

Test 14
Initial

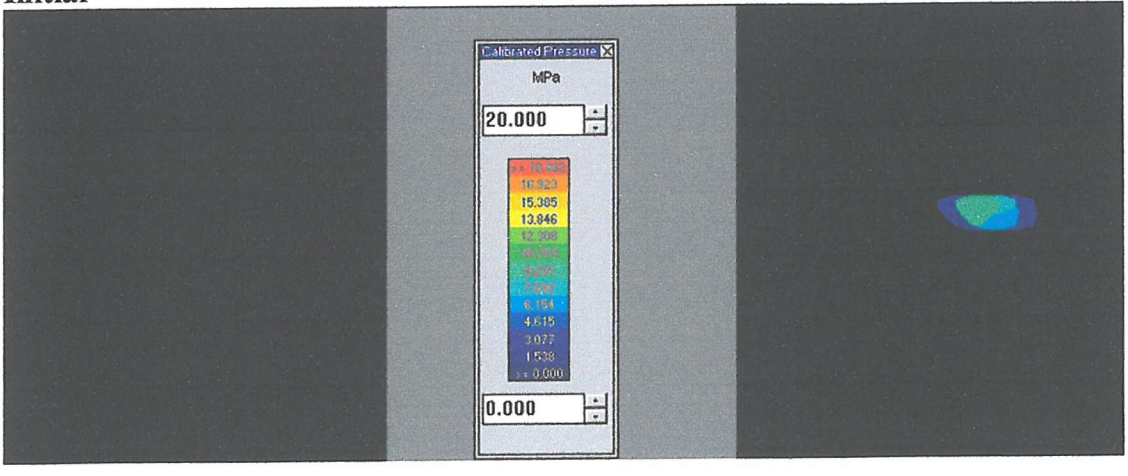

Peak Pressures

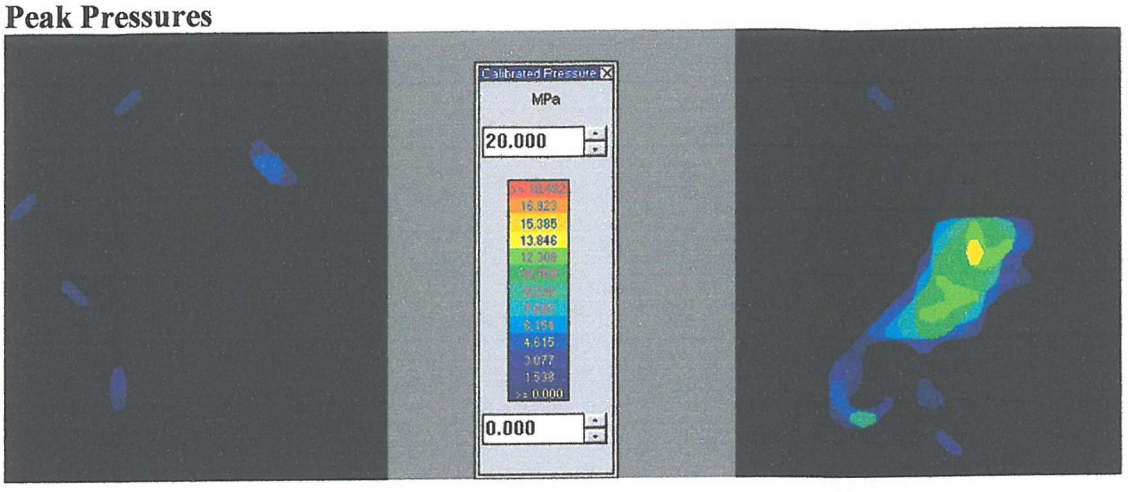

Test 15
Initial

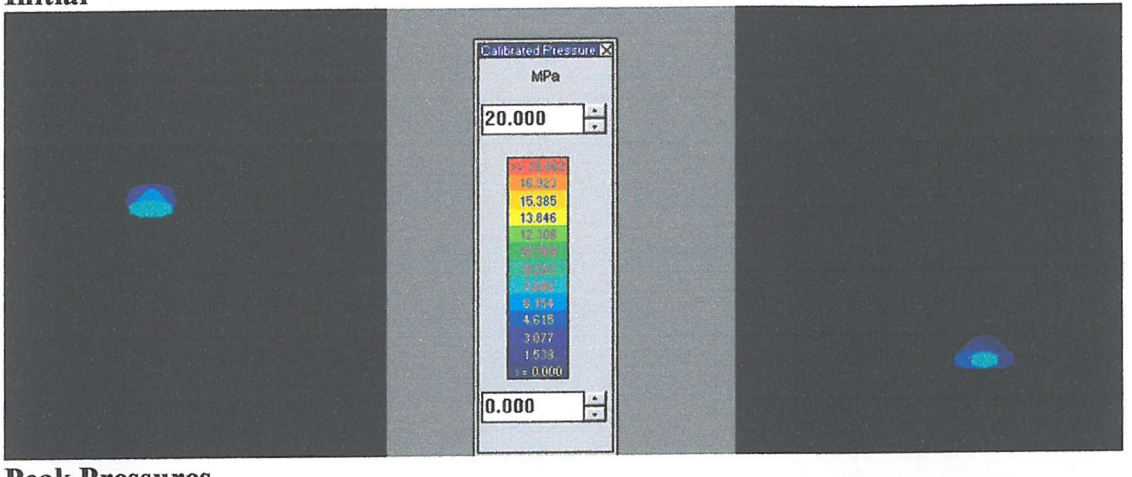

Peak Pressures

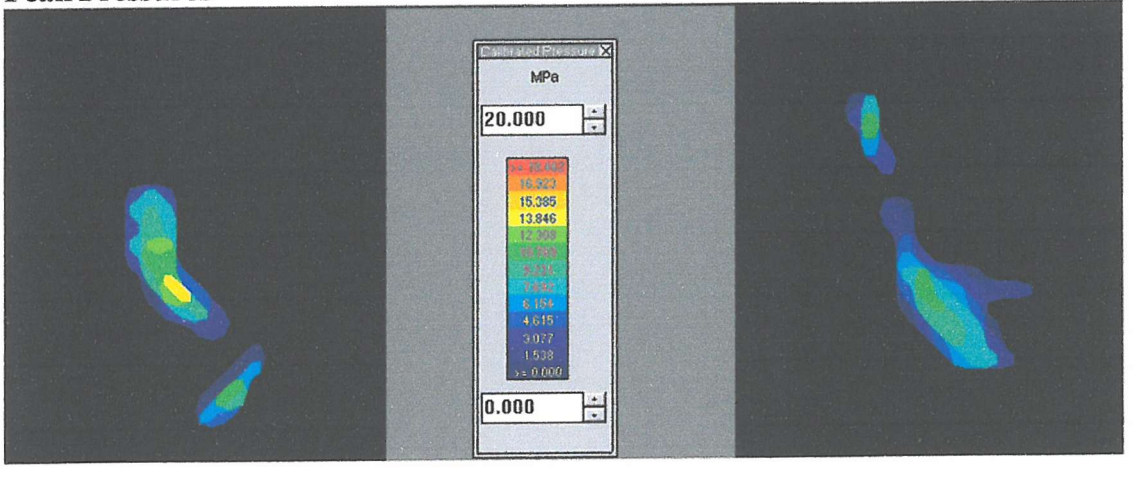

Test16
Initial

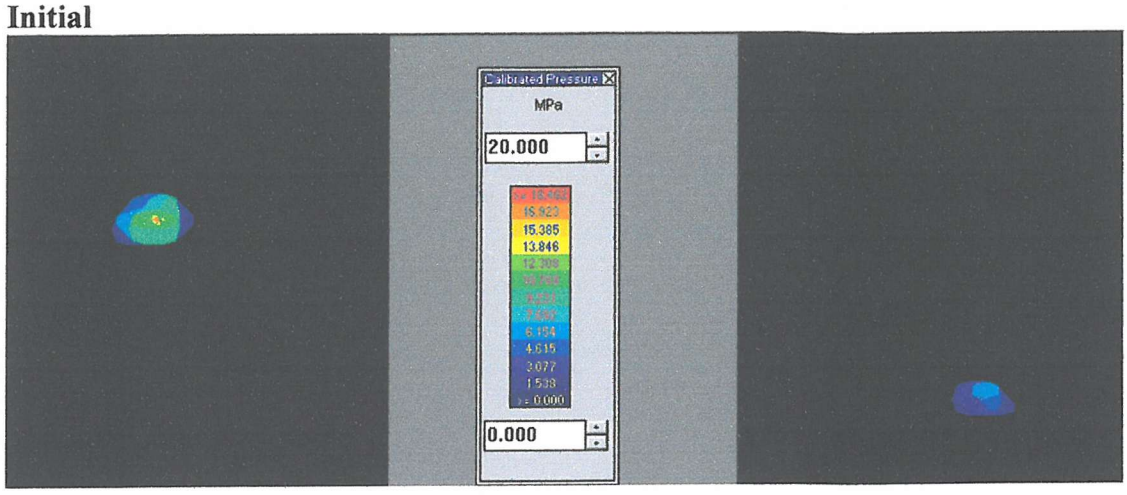

Appendix 3 – Computational Passive Stability Results

I-E stability

Ligament Strain		Flexion	Femoral Rotations (°)			Tibial Rotations (°)		
MCL	LCL	Angle (°)	Internal	External	Total	Internal	External	Total
Normal	Normal	**0**	28.8	28.8	**57.6**	27.5	28.2	**55.7**
Normal	Normal	**15**	29.5	28.4	**57.8**	28.2	28.0	**56.1**
Normal	Normal	**60**	27.4	26.4	**53.8**	22.9	23.3	**46.2**
Normal	Normal	**90**	28.3	27.3	**55.6**	23.5	25.5	**49.0**
Tight	Tight	**15**	26.0	25.8	**51.9**	25.2	25.4	**50.6**
Normal	Tight	**15**	27.2	27.3	**54.5**	26.7	26.5	**53.2**
Tight	Normal	**15**	27.9	27.0	**54.9**	26.4	26.2	**52.6**
Slack	Normal	**15**	30.4	29.7	**60.1**	29.7	28.8	**58.6**
Normal	Slack	**15**	31.1	29.4	**60.5**	29.3	28.4	**57.6**
Slack	Slack	**15**	32.5	30.5	**63.0**	30.9	29.7	**60.7**
Tight	Slack	**15**	29.3	28.0	**57.2**	26.8	26.4	**53.2**
Slack	Tight	**15**	28.1	28.1	**56.2**	27.6	26.9	**54.4**
Tight	Tight	**90**	24.8	25.2	**50.0**	21.4	22.9	**44.3**
Normal	Tight	**90**	26.8	25.7	**52.5**	23.7	22.7	**46.4**
Tight	Normal	**90**	26.1	26.6	**52.8**	20.4	24.5	**44.9**
Slack	Normal	**90**	29.8	27.8	**57.6**	25.3	24.2	**49.6**
Normal	Slack	**90**	29.4	28.8	**58.2**	22.6	26.0	**48.6**
Slack	Slack	**90**	30.8	29.6	**60.4**	25.0	26.7	**51.7**
Tight	Slack	**90**	27.5	27.8	**55.3**	19.9	24.5	**44.3**
Slack	Tight	**90**	28.0	26.0	**54.0**	24.6	21.4	**46.0**

Table 1 I-E rotations of the neutrally aligned PC-RR. Rotations refer to the femoral component with respect to the tibial component.

Ligament Strain		Flexion	Femoral Rotations (°)			Tibial Rotations (°)		
MCL	LCL	Angle (°)	Internal	External	Total	Internal	External	Total
Normal	Normal	**0**	21.4	21.7	**43.1**	-	-	-
Normal	Normal	**15**	22.2	22.9	**45.0**	-	-	-
Normal	Normal	**60**	22.1	22.0	**44.1**	-	-	-
Normal	Normal	**90**	22.5	22.3	**44.7**	-	-	-
Tight	Tight	**15**	18.2	19.3	**37.5**	-	-	-
Normal	Tight	**15**	20.1	20.2	**40.3**	-	-	-
Tight	Normal	**15**	20.5	22.0	**42.5**	-	-	-
Slack	Normal	**15**	23.6	23.5	**47.2**	-	-	-
Normal	Slack	**15**	24.2	25.2	**49.4**	-	-	-
Slack	Slack	**15**	25.6	25.9	**51.5**	-	-	-
Tight	Slack	**15**	22.6	24.2	**46.8**	-	-	-
Slack	Tight	**15**	21.7	20.9	**42.6**	-	-	-
Tight	Tight	**90**	19.7	20.3	**40.0**	-	-	-
Normal	Tight	**90**	21.3	20.5	**41.8**	-	-	-
Tight	Normal	**90**	20.9	22.2	**43.1**	-	-	-
Slack	Normal	**90**	23.8	22.2	**46.0**	-	-	-
Normal	Slack	**90**	23.3	24.3	**47.6**	-	-	-
Slack	Slack	**90**	24.4	24.4	**48.8**	-	-	-
Tight	Slack	**90**	22.2	23.7	**45.9**	-	-	-
Slack	Tight	**90**	22.8	20.5	**43.3**	-	-	-

Table 2 I-E rotations of the neutrally aligned PC-RF. Rotations refer to the femoral component with respect to the tibial component.

Ligament Strain		Flexion	Femoral Rotations (°)			Tibial Rotations (°)		
MCL	LCL	Angle (°)	Internal	External	Total	Internal	External	Total
Normal	Normal	**0**	28.7	28.8	**57.5**	27.5	28.1	**55.6**
Normal	Normal	**15**	29.3	28.5	**57.8**	28.5	27.4	**55.9**
Normal	Normal	**60**	28.9	28.8	**57.6**	25.1	25.8	**50.9**
Normal	Normal	**90**	29.7	29.6	**59.4**	25.9	26.4	**52.3**
Tight	Tight	**15**	26.1	25.9	**52.0**	25.7	25.4	**51.1**
Normal	Tight	**15**	27.0	27.5	**54.5**	26.5	26.7	**53.2**
Tight	Normal	**15**	27.7	27.3	**54.9**	26.2	25.9	**52.1**
Slack	Normal	**15**	30.2	29.6	**59.8**	29.6	26.6	**56.2**
Normal	Slack	**15**	30.8	29.7	**60.5**	28.9	27.9	**56.8**
Slack	Slack	**15**	32.1	30.8	**62.9**	30.8	29.0	**59.8**
Tight	Slack	**15**	29.0	28.3	**57.4**	26.2	26.2	**52.4**
Slack	Tight	**15**	27.9	28.3	**56.2**	26.8	26.9	**53.6**
Tight	Tight	**90**	27.2	26.4	**53.5**	23.7	23.3	**46.9**
Normal	Tight	**90**	27.4	28.8	**56.1**	23.9	25.4	**49.3**
Tight	Normal	**90**	29.3	27.4	**56.7**	26.1	23.8	**49.9**
Slack	Normal	**90**	30.0	31.3	**61.4**	26.5	27.6	**54.1**
Normal	Slack	**90**	31.9	30.5	**62.3**	28.5	26.8	**55.3**
Slack	Slack	**90**	32.2	32.2	**64.4**	28.7	27.9	**56.6**
Tight	Slack	**90**	28.5	31.1	**59.6**	25.0	28.2	**53.2**
Slack	Tight	**90**	30.7	27.6	**58.3**	27.7	23.9	**51.6**

Table 3 I-E rotations of the neutrally aligned PC-SR. Rotations refer to the femoral component with respect to the tibial component.

Ligament Strain		Flexion	Femoral Rotations (°)			Tibial Rotations (°)		
MCL	LCL	Angle (°)	Internal	External	Total	Internal	External	Total
Normal	Normal	**0**	15.8	15.1	**30.9**	-	-	-
Normal	Normal	**15**	15.7	15.2	**30.9**	-	-	-
Normal	Normal	**60**	14.9	15.4	**30.3**	-	-	-
Normal	Normal	**90**	19.1	22.6	**41.7**	-	-	-
Tight	Tight	**15**	13.9	13.7	**27.6**	-	-	-
Normal	Tight	**15**	14.3	14.6	**28.9**	-	-	-
Tight	Normal	**15**	15.2	14.6	**29.9**	-	-	-
Slack	Normal	**15**	18.0	17.6	**35.6**	-	-	-
Normal	Slack	**15**	17.6	17.0	**34.7**	-	-	-
Slack	Slack	**15**	20.2	17.7	**37.9**	-	-	-
Tight	Slack	**15**	16.4	16.8	**33.2**	-	-	-
Slack	Tight	**15**	15.6	14.6	**30.2**	-	-	-
Tight	Tight	**90**	14.7	19.3	**33.9**	-	-	-
Normal	Tight	**90**	17.8	19.1	**36.9**	-	-	-
Tight	Normal	**90**	14.4	16.3	**30.8**	-	-	-
Slack	Normal	**90**	20.5	22.3	**42.9**	-	-	-
Normal	Slack	**90**	20.3	26.4	**46.6**	-	-	-
Slack	Slack	**90**	24.2	26.0	**50.2**	-	-	-
Tight	Slack	**90**	25.3	15.8	**41.1**	-	-	-
Slack	Tight	**90**	18.7	20.8	**39.5**	-	-	-

Table 4 I-E rotations of the neutrally aligned PC-SF. Rotations refer to the femoral component with respect to the tibial component.

A-P Stability

Ligament Strain		Flexion	Tibial Translation (mm)		
MCL	LCL	Angle (°)	Anterior	Posterior	Total
Normal	Normal	**0**	4.5	2.6	**7.1**
Normal	Normal	**30**	6.2	3.7	**10**
Normal	Normal	**60**	3.6	4.6	**8.2**
Normal	Normal	**90**	4.2	5.1	**9.3**
Tight	Tight	**0**	1.4	1.9	**3.3**
Normal	Tight	**0**	3.0	2.1	**5.0**
Tight	Normal	**0**	2.8	2.4	**5.2**
Slack	Normal	**0**	5.9	3.1	**9.0**
Normal	Slack	**0**	6.0	3.3	**9.3**
Slack	Slack	**0**	7.7	3.7	**11.4**
Tight	Slack	**0**	4.2	3.0	**7.2**
Slack	Tight	**0**	4.1	2.5	**6.6**
Tight	Tight	**90**	3.2	4.0	**7.3**
Normal	Tight	**90**	3.6	4.4	**8.1**
Tight	Normal	**90**	3.8	4.5	**8.4**
Slack	Normal	**90**	4.5	5.6	**10.1**
Normal	Slack	**90**	4.8	5.8	**10.6**
Slack	Slack	**90**	4.7	6.8	**11.5**
Tight	Slack	**90**	4.8	5.0	**9.8**
Slack	Tight	**90**	4.1	4.9	**9.0**

Table 5 A-P translations of the neutrally aligned PC-RR. Displacements refer to the tibial component with respect to the femoral component.

Ligament Strain		Flexion	Tibial Translation (mm)		
MCL	LCL	Angle (°)	Anterior	Posterior	Total
Normal	Normal	**0**	5.7	7.0	**12.6**
Normal	Normal	**30**	5.6	9.4	**15.0**
Normal	Normal	**60**	6.6	8.4	**15.0**
Normal	Normal	**90**	8.3	7.5	**15.7**
Tight	Tight	**0**	5.4	6.3	**11.7**
Normal	Tight	**0**	5.5	6.6	**12.0**
Tight	Normal	**0**	5.5	6.7	**12.2**
Slack	Normal	**0**	6.7	7.5	**14.1**
Normal	Slack	**0**	6.6	7.6	**14.2**
Slack	Slack	**0**	7.8	8.1	**15.9**
Tight	Slack	**0**	5.5	7.2	**12.7**
Slack	Tight	**0**	5.6	6.9	**12.5**
Tight	Tight	**90**	6.6	6.8	**13.3**
Normal	Tight	**90**	7.3	7.2	**14.4**
Tight	Normal	**90**	7.3	7.2	**14.5**
Slack	Normal	**90**	7.9	8.6	**16.6**
Normal	Slack	**90**	8.3	8.6	**16.9**
Slack	Slack	**90**	8.3	9.6	**17.9**
Tight	Slack	**90**	7.8	7.7	**15.6**
Slack	Tight	**90**	7.6	7.7	**15.3**

Table 6 A-P translations of the neutrally aligned PC-RF. Displacements refer to the tibial component with respect to the femoral component.

Ligament Strain		Flexion	Tibial Translation (mm)		
MCL	LCL	Angle (°)	Anterior	Posterior	Total
Normal	Normal	**0**	5.2	3.4	**8.7**
Normal	Normal	**30**	5.5	4.8	**10.3**
Normal	Normal	**60**	4.8	4.1	**8.9**
Normal	Normal	**90**	6.4	0.0	**6.4**
Tight	Tight	**0**	1.9	2.6	**4.5**
Normal	Tight	**0**	3.5	2.9	**6.3**
Tight	Normal	**0**	3.4	3.2	**6.6**
Slack	Normal	**0**	6.8	3.8	**10.7**
Normal	Slack	**0**	7.0	4.2	**11.2**
Slack	Slack	**0**	8.8	4.6	**13.4**
Tight	Slack	**0**	4.8	3.2	**8.0**
Slack	Tight	**0**	4.8	3.9	**8.8**
Tight	Tight	**90**	4.3	0.0	**4.3**
Normal	Tight	**90**	5.5	0.1	**5.5**
Tight	Normal	**90**	5.2	0.1	**5.2**
Slack	Normal	**90**	7.3	0.1	**7.4**
Normal	Slack	**90**	7.6	0.1	**7.7**
Slack	Slack	**90**	8.6	0.1	**8.7**
Tight	Slack	**90**	6.1	0.1	**6.2**
Slack	Tight	**90**	6.5	0.0	**6.6**

Table 7 A-P translations of the neutrally aligned PC-SR. Displacements refer to the tibial component with respect to the femoral component.

Ligament Strain		Flexion	Tibial Translation (mm)		
MCL	LCL	Angle (°)	Anterior	Posterior	Total
Normal	Normal	**0**	5.3	4.6	**9.9**
Normal	Normal	**30**	6.8	3.9	**10.6**
Normal	Normal	**60**	6.5	0.6	**7.1**
Normal	Normal	**90**	3.5	0.0	**3.5**
Tight	Tight	**0**	4.1	3.7	**7.8**
Normal	Tight	**0**	5.0	4.0	**9.1**
Tight	Normal	**0**	5.0	4.3	**9.2**
Slack	Normal	**0**	6.1	5.0	**11.1**
Normal	Slack	**0**	6.2	5.2	**11.4**
Slack	Slack	**0**	7.4	5.6	**13.0**
Tight	Slack	**0**	5.2	4.9	**10.1**
Slack	Tight	**0**	5.3	4.4	**9.7**
Tight	Tight	**90**	1.4	0.0	**1.4**
Normal	Tight	**90**	2.4	0.0	**2.4**
Tight	Normal	**90**	2.6	0.0	**2.6**
Slack	Normal	**90**	4.5	0.0	**4.5**
Normal	Slack	**90**	4.5	0.0	**4.5**
Slack	Slack	**90**	5.3	0.1	**5.4**
Tight	Slack	**90**	3.1	0.0	**3.1**
Slack	Tight	**90**	3.5	0.0	**3.5**

Table 8 A-P translations of the neutrally aligned PC-SF. Displacements refer to the tibial component with respect to the femoral component.

V-V Stability

Ligament Strain		Flexion	V-V Rotations (°)		
MCL	LCL	Angle (°)	Varus	Valgus	Total
Normal	Normal	**0**	4.4	2.7	**7.1**
Normal	Tight	**0**	5.9	2.2	**8.1**
Tight	Normal	**0**	3.9	3.5	**7.5**
Slack	Normal	**0**	5.4	2.9	**8.3**
Normal	Slack	**0**	2.9	3.1	**6.0**
Slack	Slack	**0**	5.0	1.7	**6.7**
Tight	Slack	**0**	3.4	2.1	**5.5**
Slack	Tight	**0**	6.5	1.1	**7.6**
Tight	Tight	**0**	2.5	4.0	**6.5**

Table 9 V-V rotations of the neutrally aligned PC-RR. Rotations refer to the tibial component with respect to the femoral component.

Ligament Strain		Flexion	V-V Rotations (°)		
MCL	LCL	Angle (°)	Varus	Valgus	Total
Normal	Normal	**0**	4.5	2.1	**6.6**
Normal	Tight	**0**	6.1	1.4	**7.4**
Tight	Normal	**0**	4.1	3.0	**7.0**
Slack	Normal	**0**	5.7	2.1	**7.8**
Normal	Slack	**0**	2.9	2.7	**5.7**
Slack	Slack	**0**	5.1	1.2	**6.3**
Tight	Slack	**0**	3.5	1.7	**5.2**
Slack	Tight	**0**	6.6	0.4	**7.1**
Tight	Tight	**0**	2.5	3.5	**6.0**

Table 10 V-V rotations of the neutrally aligned PC-RF. Rotations refer to the tibial component with respect to the femoral component.

Ligament Strain		Flexion	V-V Rotations (°)		
MCL	LCL	Angle (°)	Varus	Valgus	*Total*
Normal	Normal	**0**	3.8	2.6	**6.4**
Normal	Tight	**0**	5.2	2.5	**7.6**
Tight	Normal	**0**	3.4	3.4	**6.8**
Slack	Normal	**0**	5.4	3.2	**8.5**
Normal	Slack	**0**	2.6	2.9	**5.5**
Slack	Slack	**0**	4.2	1.8	**6.0**
Tight	Slack	**0**	2.9	2.1	**5.1**
Slack	Tight	**0**	5.6	1.6	**7.2**
Tight	Tight	**0**	2.3	3.6	**5.9**

Table 11 V-V rotations of the neutrally aligned PC-SR. Rotations refer to the tibial component with respect to the femoral component.

Ligament Strain		Flexion	V-V Rotations (°)		
MCL	**LCL**	**Angle (°)**	**Varus**	**Valgus**	**Total**
Normal	Normal	**0**	4.1	2.7	**6.8**
Normal	Tight	**0**	5.4	2.3	**7.7**
Tight	Normal	**0**	3.8	3.3	**7.1**
Slack	Normal	**0**	5.2	3.0	**8.2**
Normal	Slack	**0**	2.8	2.8	**5.6**
Slack	Slack	**0**	4.3	1.7	**6.1**
Tight	Slack	**0**	3.0	2.0	**5.0**
Slack	Tight	**0**	5.7	1.5	**7.2**
Tight	Tight	**0**	2.5	3.6	**6.1**

Table 12 V-V rotations of the neutrally aligned PC-SF. Rotations refer to the tibial component with respect to the femoral component.